University of Sheffield

Mitigation of Ash Deposition, Slagging and Bed Agglomeration in Biomass-Fired Boilers: Predictive Modelling and Experimental Approaches

Nik Nor Aznizam Nik Norizam

The University of Sheffield

Faculty of Engineering

Department of Mechanical Engineering

A thesis submitted in fulfilment of the requirements for the degree of Doctor of Philosophy.

May 2024

Declaration

I, the author, confirm that the work submitted is my own work, except where work that has formed part of jointly authored publications has been included. The contribution of the candidate and the other authors to this work has been explicitly indicated below. I confirm that appropriate credit has been given within the thesis where reference has been made to the work of others. I am aware of the University's Guidance on the Use of Unfair means, cheating and plagiarism (https://www.sheffield.ac.uk/new-students/unfair-means). This work has not been previously presented for an award at this, or any other, university.

The work performed in Chapters 3 and 6 of this thesis have been published in the Journal of the Energy Institute and Fuel respectively, and the work performed in Chapter 4 is currently under review in a journal (Journal of the Energy Institute), and the work performed in Chapter 5 of this thesis is under review in a journal (Fuel).

Publications and presentations from these research outputs

Publications in scientific journals

1. Nik Norizam, N.N.A., X. Yang, D. Ingham, J. Szuhánszki, W. Yang, J. Rezende, L. Ma, and M. Pourkashanian, **An improved index to predict the slagging propensity of woody biomass on high-temperature regions in utility boilers**. Journal of the Energy Institute, 2023. **109**: p. 101272.
2. Nik Norizam, N.N.A., J. Szuhánszki, I. Ahmed, X. Yang, D. Ingham, K. Milkowski, A. Gheit, A. Heeley, L. Ma, and M. Pourkashanian, **Impact of the blending of kaolin on particulate matter (PM) emissions in a biomass field-scale 250 kW grate boiler.** Fuel, 2024. **374**: p. 132454
3. Nik Norizam, N.N.A., X. Yang, D. Ingham, N. Azri, L. Ma, and M. Pourkashanian, **An improved numerical model for early detection of bed agglomeration in fluidised bed combustion.** (Submitted to Journal of the Energy Institute, status: under review).
4. Nik Norizam, N.N.A., J. Szuhánszki, X. Yang, D. Ingham, K. Milkowski, A. Gheit, A. Heeley, W. Yang, L. Ma, and M. Pourkashanian, **Effect of kaolin on ash partitioning and slagging for the combustion of biomass fuels in a field-scale grate boiler.** (Submitted to Fuel Processing Technology, status: under review).

Poster/oral presentations at conferences

1. Nik Norizam, N.N.A., L. Ma, D. Ingham, J. Szuhánszki, and M. Pourkashanian, **A Study on the Effects of Fuel Characteristics on the Bed Agglomeration Behaviour in a Fluidized Bed.** MEC PhD Students Poster Presentations. June, 2022.
2. Nik Norizam, N.N.A., J. Szuhánszki, D. Ingham, K. Milkowski, A. Gheit, A. Heeley, L. Ma, and M. Pourkashanian, **Woody Biomass Combustion with Kaolin Injection Effects Reduction of the Fly Ash Deposits in 250 kW Pilot Scale Grate Boiler.** 2nd Feria Conference. Sheffield, UK. September, 2023.

Technical report

Nik Norizam, N.N.A., L. Ma, D. Ingham, J. Szuhánszki, and M. Pourkashanian, **A Study on the Effects of Fuel Characteristics on the Bed Agglomeration Behaviour in a Fluidized Bed,** October 2021. (Submitted to the Korea Institute of Industrial Technology, KITECH)

Acknowledgements

First and foremost, I would like to extend my deepest gratitude to my supervisors, Prof Mohamed Pourkashanian, Prof Lin Ma, Prof Derek B. Ingham, and Dr Janos Szuhánszki for their invaluable guidance and support throughout my doctoral journey. I thank Prof Mohamed Pourkashanian for providing me the opportunity to pursue this PhD and for his unwavering support in my research endeavours. I sincerely thank Prof Lin Ma for his advice on guiding my research directions in modelling work and finding solutions for the difficulties in my research. My gratitude extends to Prof Derek B. Ingham for his inspiring suggestions and patient mentorship enriched by his profound knowledge. I also thank Dr Janos Szuhánszki for his expert guidance in my experimental works. Additionally, I would like to thank Dr Xin Yang from Beijing Institute of Technology for his endless support and enriching discussions throughout my research journey.

Further, I would like to acknowledge the helps from Dr Andy Heeley, Dr Kris Milkowski, Mr Ihab Ahmed, Dr Abdulaziz Gheit for the fruitful discussions and technical assistance on the deposition probe and particulate emissions. I would also like to thank Prof Won Yang from the Korea Institute of Industrial technology (KITECH), Dr Kevin Hughes from Energy 2050, Dr Anna Foster from Chemistry department and Dr Ian Ross from department of Materials Science and Engineering of University of Sheffield for their valuable contributions to my research. Finally, but not least, my appreciation also goes to my colleagues in the Energy 2050 research group at the University of Sheffield for their support and camaraderie throughout my PhD studies.

I am thankful for the financial support provided by the Majlis Amanah Rakyat (MARA) and the University of Sheffield for funding my PhD research. Finally, I would like to express my heartfelt gratitude to my family for their love, understanding, and support during the challenging moments of my PhD journey.

Abstract

Interest in woody biomass and renewable fuel has been increasing in recent years and this has been in response to the growing need for alternative energy sources. Fluidized bed and grate furnace firing are the most utilized technologies for generating heat and power generation from biomass combustion. However, addressing the problematic ashes generated during biomass firing is critical for biomass systems, drawing substantial attention due to its adverse effects on the efficiency of the heat transfer and also exacerbating corrosion to the boiler. Ash related issues such as ash depositions, slagging and bed agglomerations have been considered as a serious problem for safe and efficient operation of biomass firing boilers. These issues must be addressed to avoid any unplanned shutdown of the boilers due to the failure in controlling the ash related issues during combustion. In this thesis, two different approaches in mitigating the biomass ash related issues in utility boiler systems has been studied through the development of predictive models and experimental work to investigate the ash behaviours in the grate boiler.

Various predictive models have been proposed to predict the ash related issues when firing different types of biomasses. However, there is no reliable general applicable method that is available for assessing biomass fuel slagging propensities and bed agglomeration tendency without carrying out extensive experimental testing. In this thesis, two predictive tools, namely the Predictive Slagging Index (I_n) and the Bed Agglomeration Index (I_a), have been developed to address ash-related issues in biomass-fired boilers. The models were developed by analysing the slagging and bed agglomeration formation of biomass firing using the thermodynamic equilibrium modelling tool FactSage together with the partial least square regression (PLSR) coupled with cross-validation. The new slagging index, I_n and bed agglomeration index, I_a have been validated and supported by experimental observations from various literatures. Both indices showed a substantially greater success rate in predicting the slagging propensity of woody biomass and bed agglomeration tendency of various biomass, in comparison to experimental observations from the literature.

In addition, numerous approaches have been proposed by the experimental works, such as the injection of chemical additives into the grate boiler to reduce the alkali species in the ash depositions and bottom ash during biomass firing. However, the impacts of the boiler condition, especially the bed behaviours of the grate boiler, has not been well understood in the past when kaolin has been added. Therefore, in this thesis, the effects of blending virgin and waste woody biomass fuels with kaolin on ash related issues in a 250 kW field scale grate

boiler has been experimentally investigated. It was found that the kaolin powder performed quite effectively as an absorbent for potassium under firing conditions due to its very small particle size and large surface area. However, severe agglomeration was observed in the combustion chamber of the grate boiler when the kaolin was added into the fuel mixtures. According to the elemental analysis by ICP-MS, the most dominant element found in the bottom ash, slag, and coarse fly ash was silica which promoted slagging and agglomeration formation. On the other hand, the alkali elements were clearly reduced in the bottom ash, slag, and coarse fly ash after adding kaolin due to the formation of alkali-aluminium silicates that reduce the release of alkali species.

Further, a comprehensive analysis of the chemical compositions of the particulate matter (PM) from the boiler has been conducted, including alkali and non-volatile species, size-fractionated mass concentrations and micromorphology images. The results showed that the PM emission levels were significantly decreased, by at least 60%, after the addition of kaolin to woody biomass fuels, which inhibited the partitioning of the alkali species into fine and ultrafine PM. On the other hand, the concentration of the non-volatile elements, Si and Al, significantly increased in the PM emissions after the addition of kaolin due to the adhesion and aggregation of particulates between airborne kaolin and the fine and ultrafine PM. These findings demonstrate the practicality of adding kaolin to mitigate aerosol emissions and their impacts in actual biomass combustion scenarios. Overall, this study provides a comprehensive understanding to the industrial users and researcher to mitigate the biomass ash deposition issues in the utility boilers.

Nomenclature

AC	Ash content
AFT	Ash Fusion Temperature
AS	Anti-scatter
BA	Bottom ash
BAI	Bed agglomeration index
BECCS	Bio-Energy with Carbon Capture and Storage
BEIS	Department for Business, Energy and Industrial Strategy
BFB	Bubbling fluidised-bed
BSED	Backscattered electron detector
CB	Cyclone Boiler
CCGT	Combined Cycle Gas Turbine
CCS	Carbon Capture and Storage
CEN	European Committee for Standardization
CFB	Circulating fluidised-bed
COSHH	Control of substances hazardous to health
Dp	Deposition propensity
d_FA	Rate of deposition of the coarse fly ash
DR	Dilution ratio
ELPI+	Dekati low pressure impactor
EDS	Energy Dispersive X-ray Spectroscopy
ESP	Electrostatic precipitator
FA	Fly ash (coarse)
FBC	Fluidised Bed Combustion
FT	Fluid temperature
FTIR	Fourier-transform infrared spectroscopy
HF	Hydrofluoric acid
HT	Hemispherical temperature
ICP-MS	Induced Coupled Plasma Mass Spectrometry
IDT	Initial Deformation Temperature
M_f	Melt fraction
MC	Moisture content
OCA	Olive-cake

OCGT	Open Cycle Gas Turbine
PBCP	Packed-Bed Combustion
PCC	Pulverized Coal Combustion
PCR	Principal component regression
PDS	Programmable divergence
PF	Pre-combustion fuel stage
PFA	Pulverised fuel ash
PLSR	Partial least squares regression
PKE	Palm kernel expeller
PM	Particulate matter
PPT	Parts per trillion
PSDs	Particle size distribution
PTFE	Polytetrafluoroethylene
QSI	Qualitative Slagging Indicator
RC	Rapeseed Cake
RMSE	Root means square error
RW	Recycle wood
S	Slag
SCR	Selective Catalytic Reduction
SED	Secondary electron detector
SEM	Scanning Electron Microscopy
ST	Softening temperature
TEM	Thermodynamic equilibrium modelling
TERC	Translational Energy Research Centre
TDT	Total defluidization temperature
TGA	Thermogravimetric analysis
VW	Virgin wood
WtE	Waste to Energy site
WWA	White-wood
XRD	X-ray diffraction

Contents

List of Figures

List of Tables

1 Introduction and Literature Review

1.1 An overview of the thermal power generation sectors

The electricity generation policy in the next decades will be driven by the increase in demand and reduction in emissions. COVID-19 has, in many ways changed the outlook of the industry globally, via the changing demand for electrical energy, the larger proportion of low-carbon generation, and the transforming nature of how electricity will be used in the future. There are numerous lessons learnt for the power field, consisting of the importance of having extra resilience as well as a smart power system to accommodate more radical modifications in the energy need. Power demand today, for example in the UK, is approximately just over 300 TWh with one-third of which being domestic use for heating. This is expected to change with a substantial increase in the demand of electricity for heating in the future. Currently, this level of power demand is met by a range of technologies. Table 1-1 is a list of the various major types of power generation technology currently employed in the UK according to GridWatch [1] which gives a general idea of the technologies used.

In the UK, biomass will continue to play a major role in the transition away from fossil fuels and decarbonisation cost-effectively the power generation sector and can sustain the economic situation as well as other industries by establishing new low carbon markets. The extent to which the biomass will be used for power generation by direct firing will depend on several constraints, in particular the availability of biomass, the technological development of increasing the fuel inventory and the cost and availability of CCS for the BECCS negative emission technology.

Table 1-1 List of the major types of power generation technologies in the UK [1][2].

Key	Description
Coal	These stations consume coal to create heat. This is utilized to heat water to generate vapor which turns a heavy steam turbine that drives a generator to produce power. Currently, one coal power plant is operational in Nottinghamshire and will remain so until September 2024. The existing Federal government strategy is to close down all coal terminals by 2025.
Nuclear	These terminals use a Uranium nuclear reaction to create heat. This is made use of to heat water to produce vapor which turns a steam turbine that drives a generator to generate electrical power. The outcome from these is much more constant than various other power generations. Variations usually indicate

	upkeep, refuelling, or problems. There are currently 8 Nuclear power terminals in the UK.
Solar	Solar is primarily used in power generation, small amounts of solar thermal are used for space and water heating. Solar generation rose 4.1 per cent to 13.9 TWh. Solar PV generation has increased rapidly since 2011 reflecting the surge in new capacity incentivised via the Feed in Tariff (FiT) support scheme. As a result, solar PV's share of renewable generation increased from just 0.7 per cent in 2011 to 10.2 per cent in 2023.
Wind	This is the power from Wind Farms and, also does not include unmetered wind turbines. The outcome of this change with the wind. As of 2024, the total number of wind turbines installed in the UK is approximately 30,000. This includes both onshore and offshore wind turbines across various wind farms throughout the country.
CCGT	Combined Cycle Gas Turbine - Generator power up by turbine that uses Natural Gas. The UK has 40 CCGT power stations.
Hydro	Hydroelectric-UK has approximately 60 Hydroelectric stations. Many are located in the Scottish and Welsh Hill regions.
Oil	These stations consume oil to generate heat. Electrical energy has been created by a steam turbine. Practically all oil stations have been decommissioned with only a few remaining.
Biomass	Bioenergy has rapidly grown over the past decade as many power stations switched from coal to plant biomass, mainly wood pellets, doubling generation. However, outages in the last two years have reduced output, with plant biomass generation at 20.8 TWh, still below the 2021 peak of 27.0 TWh.
Pumped Hydro	Pumped Storage Hydroelectric-- Pumped storage integrates 2 reservoirs. Sometimes low demand, during the evening generally, water will be pumped from the lower to the upper basin by electrical power. This water is then discharged from a reservoir or dam to generate electricity during periods of high demand, when the price of electricity is also typically higher. The UK have 4 pumped storage stations at present.
OCGT	Open Cycle Gas Turbine – The turbine that powers a generator uses gas oil, natural gas, or diesel. When necessary, these systems are costly so only run when needed. The UK have approximately 30 of these at the moment.
Other	This consists of anything not mentioned in the above**.**

1.2 Combustion of biomass

1.2.1 Biomass as fuels

Biomass consists of wood-based, energy crops, animal manure, forestry and agricultural waste, food waste and residues, etc. It can be consumed for both industrial and residential heating and electricity generation and biomass fuel has gained popularity in power stations as a boiler fuel due to its benefits of low pollution and broad supplies [3]. The people's rising concerns about energy shortages and environmental crises have led the world to pay more attention to sustainable new energy developments. Biomass, as a fuel can reduce the net CO_2 emissions as well as the sulphur and nitrogen oxides emissions so that it can be utilised as an appropriate alternative energy. Biomass fuels, however, generally present lower ash sintering temperatures [4].

Wood pellets are utilised for large-scale energy generation, but there are plans to use a more varied supply in the future for combustion. The European Committee for Standardization (CEN) test procedures have been used to measure the ash, calorific, chlorine, nitrogen, sulphur, hydrogen and carbon of various biomass pellets (wood, miscanthus, willow, wheat, rape straws and barley) in addition to test their durability, moisture content and bulk density. In terms of chemical composition, the willow or straws (i.e. wheat, rape and barley) have greater chlorine amount, nitrogen and sulphur compared to wood, and these differences could lead to boiler degradation and increased gaseous emissions. There were no significant variations in the energy contents of all the pellets, regardless of biomass type. Compared to other types of biomasses, the wood pellet's moisture content was noticeably lower, demonstrating that all these raw materials required a higher moisture content to bind [5].

The agricultural residue's nitrogen content is higher than that of the woody biomass because of the high levels of nitrogen fertiliser used in crop growth. When in the process of combustion, most nitrogen is transformed into gaseous nitrogen and nitrogen oxides (NO_x) [6]. It is known that the chlorine level of biomass is significantly higher in herbaceous than in woody biomass. Biofuels generally convert the chlorine that it contain to several gaseous by-products, including HCl, Cl_2, and alkali chlorides including NaCl and KCl. Sulphur exhibits a Cl-like behaviour during burning, with the generation of alkali salts that corrode the system being the main issue. Sulphur was found to be present in ash in quantities of 40-70% [7]. Moreover, woody biomass has less ash content compared to herbaceous biomass. High content ash in fuel underfeed stokers are not ideal because of the ash layer risk formation, which results in an abnormal airflow, resulting in incomplete combustion and escalating emissions.

1.2.2 Current status of biomass fuels

Biomass is a resource that may be a sustainable option and can provide net benefits when it comes to CO_2 emissions. This is because it can replace fossil fuels as an energy source. An important energy conversion for biomass technology is conventional combustion in thermal power plants. This can be used in huge scale power stations, such as those that were used to generate much of the electricity in the 20th century. Co-firing coal with biomass or switching coal to biomass in these plants can reduce coal consumption. Drax Power Station is one of the coal-fired power plants in the UK that has been converted to biomass located in North Yorkshire [8]. Drax has undergone a significant transformation from being primarily coal-fired to a major biomass power generator. The conversion began in earnest in the early 2010s, with Drax investing heavily in retrofitting its units to burn biomass pellets, largely sourced from sustainable forests. Drax's conversion is part of the UK's broader efforts to reduce carbon emissions and transition to cleaner energy sources. The plant now has several units that run on biomass, which has substantially reduced its carbon footprint compared to when it was solely coal-powered. Next, Lynmouth Power Station, located in North Devon, was a coal-fired power plant that underwent a significant transformation. The plant was originally built in 1954 and operated as a coal-fired facility. However, it was later converted to run-on biomass. The plant has gone through a significant modification program that has converted the 407 MWe existing coal-fired power plant to complete biomass electricity production [9]. The conversion to biomass at Lynmouth Power Station reflects the broader trend in the UK of transitioning from coal to more sustainable energy sources. This shift is part of the UK's efforts to reduce greenhouse gas emissions and improve environmental sustainability in the power sector.

Most of the biomass fuel in the UK for electricity generation is from imported pelletized wood. Nevertheless, interest in employing other resources, such as energy crops including miscanthus and coppice willow, and by-products agricultural such as olive waste and wheat straw, has arisen due to sustainability and domestic energy security concerns. Technical difficulties are presented by the variance in the characteristics of different fuels and conventional power stations need to overcome, in particular, the issues of slagging and fouling to obtain additional fuel flexibility [10]. In addition, the biomass may be utilized in an anaerobic digestion process such as food crops and grass, producing biogas that will be burnt in the heat or electricity production. This gas is processed into methane, and this is transmitted through the gas network. In general, wood pellets are currently used for large-scale electricity generation; more is proposed to be used for heating in the future. In the UK, for the longer term

a much wider range of feedstocks need to be used, including the development of energy crops such as miscanthus and short rotation coppice [11]. It is noted that plant-based generation has expanded significantly, and this is principally due to the switch from coal to biomass generation. At the same time, co-firing is diminishing due to the closure of the coal stations. In 2018, 35.6 TWh of electricity was generated from biomass in the UK. Around 68% of this came from plant biomass and 32% from waste. It is estimated that this level of biomass used can meet the expected BECCS deployment needs in 2030 and this will need to be doubled in 2040 [11].

There was a continuous demand in the growth for smaller boilers that are less than 200 kW between June 2013 and July 2015 in the commercial and industrial sectors before similar cost control systems were introduced. This has decelerated the domestic sector from going out of the market. Users who need boilers that use less than 200 kW usually chose pellet-fired boilers, and this is due to their relatively small size and easy application in low duties such as space heating. The dominant fuel choice has been for boilers with larger scales, more than 200 kW output of wood chips instead of wood pellets. This is due of the economic cost of fuel in larger boilers which work in higher duties, but, naturally, there are some anomalies to this rule. According to the widespread principle in the UK market, the bigger the boiler, the more probable it is to work on wood chips.

1.2.3 Biomass firing technologies

As of 2020, most of the biomass for electricity generation is by direct firing, either by co-firing with coal or dedicated biomass combustion. In addition, there is a small contribution from indirect combustion. Smaller boilers are used for heating, or combined heat and power. This section will focus on the direct combustion of biomass fuels.

1.2.3.1 *Cofiring technologies*

Co-firing is when two fuels are combusted in the same boiler at the same time. Co-firing of biomass is considered as a prompt solution to lower the emissions of CO_2 in power plants. This is because the co-firing implementation system is easy and cost-effective. Power plant operators have concluded that co-firing biomass fuel will reduce the capital cost and the financial uncertainty and liability compared with having a new-built stand-alone biomass power station [12]. Presently, there are three co-firing systems broadly implemented in coal plants: direct co-firing, indirect co-firing, and parallel co-firing [13].

- **Direct co-firing**: Biomass is fed straight into the boiler with coal. In this approach, biomass can be crushed alongside with the coal or independently before feeding the biomass-coal mixture into the furnace system. The difficulties associated with straight co-firing is that there is a probability of slagging and fouling, thus the limited use of various sorts of biomass [13].
- **Indirect co-firing:** Indirect co-firing sets up an independent gasifier to break down the solid biomass into syngas. Indirect co-firing has a number of advantages over direct co-firing, for example gasification cuts down gas residence time; boiler slagging is minimized because the biomass fuel is not immediately fed into the furnace; and also the indirect co-firing has the versatility to make use of the various core fuels such as coal, natural gas, and oil [13].
- **Parallel co-firing:** Parallel co-firing includes the setup of an entirely individual external biomass-fired furnace to generate steam for electricity in the coal power station. The steam produced from the biomass-fired furnace is to fulfil the coal-fired power station demands and this lowers the coal-fired power station functional risk due to the schedule of dedicated and different biomass burners working alongside the current boiler system. Parallel co-firing enhances the biomass portion throughout the co-firing of biomass as well as prevent biomass ash related issues. Nevertheless, this modern system is confirmed to be more costly than the straight co-firing strategy since the added facility is required to sustain the system [13].

The type of boilers implemented in co-firing systems normally rely on the current coal or gas-fired firing system. Common boilers utilized in a current coal-fired power station are as follows: Pulverized Coal Combustion (PCC) boiler; Packed-Bed Combustion (PBCP) boiler; Fluidised Bed Combustion (FBC) boiler; and Cyclone Boiler (CB) [14-16]. An observation between various biomass co-firing technologies is given in Table 1-2 [14-16]. The majority of plants started their involvement in co-firing with co-milling tests and then carried on developing the direct injection technology. Nonetheless, the practicality of regular co-firing relies on the transport, dealing with, and the storage of the biomass stock. A range of feedstock has been used in the UK's biomass firing plants, consisting of agriculture residues, energy crops (miscanthus), as well as forestry deposits [16].

Table 1-2: Common combustion technologies in biomass co-firing systems [14-16].

Co-Combustion System	Operation Requirements	Co-firing Percentage (% heat)	Technical Features
Pulverized Combustion	Fuel type: coal, fine shavings, and sawdust. Moisture content: <20wt% Particle size: <10-20 mm	1% to 40%	Can reduce NOx, substantially; Restricted by biomass particle dimension as well as moisture content.
Fluidised-bed combustion	Fuel type: wide range of fuels, better for woody biomass Temperature: <900^{o}C Particle size: <80 mm (BFB), <40 mm (CFB)	BFB: 80% CFB: 60% to 95.3%	The fluidised bed firing technology is one of the ideal boilers for biomass co-firing. The residue formation is troublesome, specifically in CFB.
Packed-bed combustion	Fuel type: various fuels, including coal, woody residues, straw and peat. Particle size: <30 mm	3% to 70%	Not ideal for direct co-firing.
Cyclone combustion	Ash content: >6% Volatiles: >15% Moisture content: >20% except in a dried form	10%-15% by heat input or 20%-30% by mass	Appropriate for co-firing given that very few adjustments are required for feeding and blending the coal with the biomass.

1.2.3.2 *Pulverised fuel combustion system*

With the ongoing development of large-scale power generation for biomass combustion focused on co-firing or existing coal power station conversion, pulverised fuel plants are now the most widely used power generation system for wood pellets especially in the UK [10]. In the boiler, pulverised fuel and air are fed in through a series of nozzles on the boiler's side. The burners are designed to allow air to be injected at the same time, allowing the air fuel ratio inside of the combustion chamber to be controlled. The volatile flame temperature in the primary zone of the furnace will be influenced by the air fuel ratio. Typical flame temperatures in pulverised coal furnaces range from 1700 K to 1900 K while the biomass calorific value is lower than coal which has a lower flame temperature range of 1600 K to 1800 K [17]. Achieving the maximum "burn-out" is essential for the plant's efficiency in converting fuel energy to steam and electricity [10].

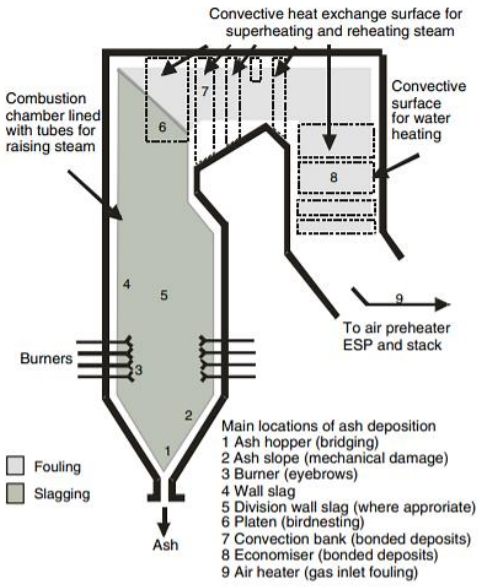

Figure 1-1 Sections of ash-linked issues in boilers [19].

Kleinhans et al. [18] covered inorganic matter combustion transformations and ash deposition mechanisms in depth. Slagging takes place in the boiler section and has a high melting point formation; fouling is located on the convective surface and has a lower temperature as shown in Figure 1-1 [19]. Slagging occurs when molten ash particles stick to the boiler surface. At lower temperatures, inorganic vapours can condense on the solid particles, coating them in a molten film. Wood ash agglomerates impact the walls or tubes, and this rearranges their structure. They lose all their kinetic energy in the process, causing the particles to stick to the surface rather than rebound. These mechanisms can entrap the solid particles in the porous deposit after the initial formation [20].

The boiler may also be at risk of corrosion due to the deposition. These agglomerates reduce the heat exchanger efficiency and cause high temperatures of the chlorine induced corrosion by forming the deposition on the tube surface [21]. All of these scenarios reduce the boiler efficiency, availability, high maintenance costs, and mechanical failures which lead to unplanned plant shutdown [22]. However, the ash deposition characteristics of burnt solid fuels are significant factors in the boiler design. For a given steam output, slagging is a significant factor in determining the size of the boiler furnaces; fouling dictates the spacing and location of the superheater and reheater tube banks in the boiler convection sections [23]. In addition, slagging regulates where and how to operate the soot blowers to maintain long-term boiler efficiency. The chemical and physical characteristics of fly ash are important factors in determining the emission control systems. As a result, ash deposition properties influence the feedstocks selection, furnace design, and combustion [24]. Figure 1-2 shows the ash deposition

regions in a conventional pulverised fuel fired boiler [25]. It is difficult to clean the slagging deposits with soot blowers because they form in the hottest regions, namely the radiation sections [19]. The surface conditions of deposits change, especially in the slagging depositions and high temperature of fouling, thus creating a layered structure. The layer that is formed on the slagging deposits is rich in Fe-bearing pyrite particles because it is dense and has a low melting temperature [26]. The initial layer of ash deposition is formed due to the vapour condensation of chemical elements. As a result, the deposit's surface temperature increases, facilitating melting and sintering to form the slag/sintered layer [22].

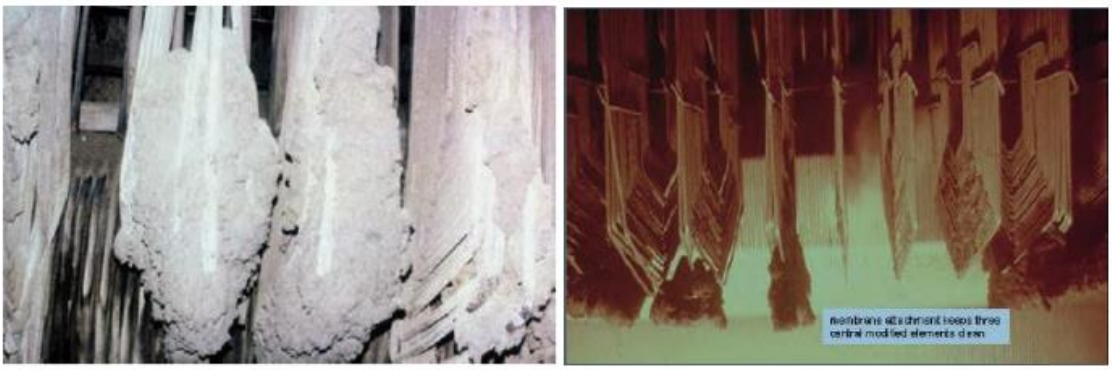

Figure 1-2: Slagging formation on a pulverised fuel boiler [25].

1.2.3.3 *Fluidised-bed combustion system (FBC)*

Fluidized bed combustion (FBC) is one of the leading systems that applies a large variety of solid fuels, including fuels of low quality but with a high amount of moisture content and mineral matter. The FBC system is a complex arrangement of nozzles that is used to keep the bed, containing fuel particles and inert material such as silica sand, in a suspended state. This suspension is maintained by recirculating the flue gases or air, which serves as the fluidizing agent. The fluidized state facilitates the efficient firing of the fuel particles in the bed. Due to the increased turbulence, constant mixing and heat transfer are enhanced which improves the firing process. The unique advantages of the FBC technology compared to the grate combustor are fuel flexibility, high efficiency of combustion and heat transfer, excellent emissions control including SO_2, and excellent system availability [27].

The fluidised bed technology can be assigned to the circulating fluidised bed (CFB) or the bubbling fluidised bed (BFB) based on the velocity of the fluidizing gas. The BFB boilers use relatively low velocities of fluidization to avoid solids elutriation while on the other hand, CFB boilers use relatively high velocities to facilitate the elutriation of solids. Overall, BFB boilers are suitable for medium-sized boilers, while CFB boilers are better suited for larger boilers [28]. One of the advantages of the FBC technology is that the process normally takes

place at minimal bed temperature (about 800-900 °C) which are known to improve the performance of the fuel which is prone to slagging and fouling [28]. However, precautions are necessary in the FBC technology due to potential ash-related issues such as bed agglomeration, slagging and corrosion which may occur regardless of the fuel quality. Deposits may build on the superheater or in the cooler region of the boiler, which may reduce the heat transfer rate and cause the flue gas to become obstructed or even blocked in the heat exchanger package. The deposits in boilers that burn low-grade fuels cause corrosion that results in lower steam temperature and less efficient power output. Fly ash melting properties are significant factors in the ash's stickiness and corrosiveness [29].

1.2.3.4 *Grate furnace combustion system*

Moving grate boilers for heat and electricity production are widely applied for solid biomass combustion on an industrial scale because they can fire different fuels of various moisture levels and require less fuel handling and preparation. Grate-fired boilers can fire practically any solid, even low-grade, fuel and are quite cheap to build. In addition, the grate normally has mechanical systems to disperse the bed fuel and to collect the ash, which enables the boiler to operate continuously. These features have made the grate-firing technology the most utilized in solid biomass combustion for large-scale boilers [30, 31]. The fuel base needs to be significantly broadened today, and the medium and small power sector needs a competitive market in affordable energy resources. Many are waste streams, e.g. forestry, agricultural, municipality or process industry. Unfortunately, the composition of ash fuel might potentially raise the potential of operational difficulties in existing plants such as particulate matter (PM) emissions, slagging and fouling [32-35]. One of the major operational challenges with ash are the production of slag on the grate. Slag production is not only determined by the amount of ash and chemical composition but also depends on the combustion technology utilised [32, 36, 37]. Figure 1-3 [38, 39] shows straw vibrating grate-fired boilers and gives an overview of the common grate-fired boiler configuration. The grate-fired boilers comprise four major elements: a fuel feeder system, a grate installation, a secondary air system and a discharge system of ash [38]. Slagging is common in grate-fired biomass boilers. The quantity of alkali is important and in particular, the high alkali level with silicone, extrinsic or inherent in the fuel may produce low-temperature alkali silicates in the fuel bed [40]. Grate combustion of high Cl content in the biomass, for example, straw may have serious deposition and corrosion issues. Deposits decrease the ability of heat transfer on the burning areas, and the overall process efficiency, while corrosion decreases the equipment lifespan. In solid fuel

burning, the solid material generated during combustion will be deposited on the heat exchanger tubes and furnace walls which may limit the heat transfer and can lead to corrosion [41]. Biomass-fired furnaces, especially straw-fired boilers, often have serious deposition and corrosion issues compared to coal-fired furnace ash as shown in Figure 1-4 [41].

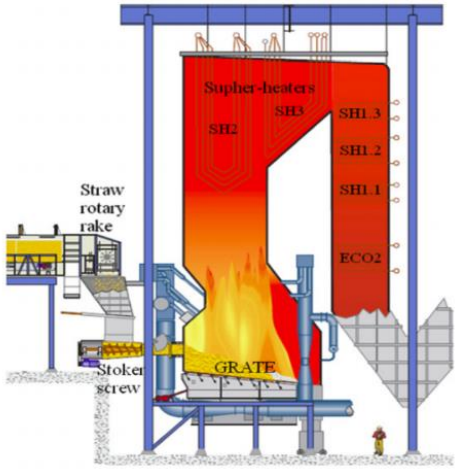

Figure 1-3: Straw vibrating grate-fired boilers layout [38, 39].

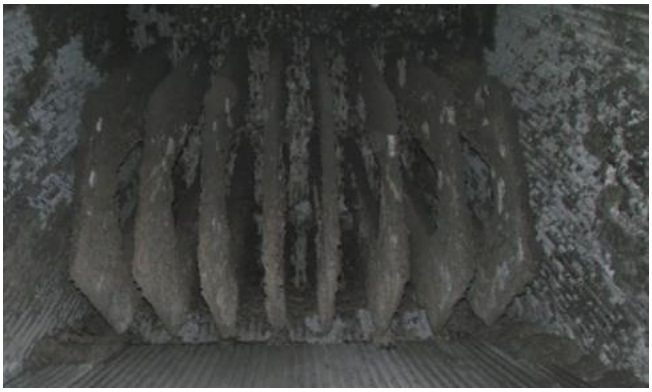

Figure 1-4: Ash deposits on superheater in top furnace during straw firing at Masnedø CHP plant [41].

1.3 Ash depositions

1.3.1 Ash sintering

Combustion is the most significant technology for heat and energy generation from biomass fuels. However, the burning of biomass fuels is typically hard because critical ash formation issues in fuel are transformed and interacted [42]. Operational issues relating to ash, for example sintering and slagging, and often these are found in biomass combustion technology. Biomass solid fuels with a high sintering propensity are generally rich in potassium, phosphorus and silica, and their interactions play a crucial role in the ash melting formation [43]. Potassium can be incorporated into complex transition reactions during

combustion in biomass fuels and partly result in potassium salts, phosphates and silicates [44-46].

Particle-to-particle agglomeration characteristics under heat treatment for ash sintering, and regularly this is used to show the densification, shrinkage, and strength development of ash. Hence, understanding the deposits development in boilers is important for ash sintering. Differences between ash fusion and ash sintering must be explained. Ash sintering is the bonding of adjacent particles due to the excess of surface tension [22]. Ash fusion indicates the melting formation during the transformation of minerals [22]. It is possible to achieve sintering in the absence of fusion. The deposits created by ash fusion and ash sintering are strong, increasing the difficulty of removing them by using soot blowers in the boilers. Furthermore, the strength development investigation caused by the ash sintering is very much desired in order to study the beginning of the sintering mechanism.

Frenkel's sintering theory asserts that particles first start to deform and come into contact with one another, causing particle-to-particle bounding, which, according to the theory, is the trigger for the pores and shrinkage of the sintered sample [47, 48]. Reduced porosity and dimension and increased strength are the result of the sintered sample from this action. To measure the onset temperature of the initial sintering (T_s), numerous techniques have been established which are the techniques used to investigate the physical characteristics of solid fuel ash samples that have experienced a sudden change. In addition, because the operating temperature of the fluidized bed firing is quite close to the initial sintering and less than the soften temperature, it has a substantial effect on the boiler process. In other words, the initial sintering temperature is used commonly to predict the amount of ash composition and in determining the firing/gasification operation temperature. The ash composition impact, the pressure, and the gas atmosphere on the initial sintering temperature are currently important to analyze [49-52]. The ash sintering and slagging reduce combustion system performance and contribute to expensive cleaning and maintenance.

1.3.2 Ash viscosity

The ash viscosity is one of the most significant aspects for high-temperature biomass ash that is used to evaluate the wet bottom combustor performance and to estimate the propensity of ash deposition. Two major techniques introduced to calculate the flow behaviours of ash or slag are as follows: [53] (i) the characteristics of the ash fusion, specifically the flow points and hemispherical areas, are measured through ash fusion testing; (ii) the slag for viscosity-temperature behaviours are investigated. Preferably, measured via a viscometer, but

this requires time, and they are generally estimated from the slag/ash composition or by comparing with the ash-fusion behaviours. A decreased viscosity of the liquid phase increases the potential for sintering or agglomeration. In addition, the fly ash's viscous behaviour has a strong influence on the tendency of the deposits' sintering and formation [54]. The deposit accumulation on the boiler walls, which have a huge surface area, can influence the heat transfer as well as promote corrosion caused by the elements forming in the running slag [55]. A deposit with high amount of viscosity will have bigger inherent strength and will be hard to remove.

A sequential ash transformation mechanism has been suggested with specific emphasis on researching the impact of the disintegrated iron-ore pellet dust on slagging in pulverised power plants. The two effects on slagging deposition between particles of coal ash and pellet dust were described as follows: (i) Enhanced melt formation; intensifying slagging deposition (ii) Decreased viscosity because of the incorporation of excessive Fe into the aluminosilicate melt. Calculations of thermochemical equilibrium have also predicted that unburnt carbon in the char can have a major impact on the formation of deposits and this is a result of enhanced melting from Fe^{3+} to Fe^{2+}. The severity of slagging deposition may depend on the ash deposit composition and, also the viscosity and temperature parameters. Another investigation by Sefidari et al. [56] was therefore aimed at determining the fuel ash composition effect on the slagging tendency of high-ranking ash composition solid fuels [56]. A Qualitative Slagging Indicator (QSI) was developed to identify new solid fuels for their possible slagging deposition propensity. The suggested QSI emphasizes the following conclusions: (i) the inverse relation of slagging deposition propensity for the solid fuels was identified with the viscosity of the estimated molten portion of the ash; (ii) as the viscosity drops (either by raising the temperature or by changing the composition of the fuel ash), stronger deposits are formed to increase the relative deposition rates. Also, low viscosity molten phases, which allow slagging, were shown to be characterised by the existence of the fluxing agents (e.g., MgO, CaO, Na_2O, K_2O, and Fe_2O_3).

1.3.3 Mechanism of ash depositions

Biomass combustion presents several technical challenges, with ash deposition being one of the most critical. This issue arises due to the significant presence of metals in biomass, particularly alkali and alkaline earth metals such as potassium (K) and calcium (Ca). Potassium is especially influential, as it can lower the melting point of ash particles, leading to increased slagging and bed agglomeration within the combustion system. These issues pose substantial

barriers to the large-scale utilization of biomass as a fuel, limiting the range of biomass types suitable for combustion. Ash deposition on heat transfer surfaces occurs through multiple mechanisms, including inertial impaction, thermophoresis, chemical reactions, turbulent eddy impaction, and condensation as illustrated in Figure 1-5 [18, 57]. Among these, inertial impaction is a key contributor, particularly for fly ash particles larger than 10 μm [57]. These particles, carried by the flue gas, have enough momentum to collide with and adhere to the heat exchanger surfaces. The extent of inertial impaction is influenced by factors such as particle size, gas velocity, and the physical properties of the ash [57, 58].

Thermophoresis is another significant mechanism, where particles migrate towards cooler regions within the furnace due to temperature gradients, resulting in finer and more uniformly distributed deposits around the heat exchanger surfaces [59]. This phenomenon is particularly important for smaller particles, which may not have sufficient inertia for impaction but are still affected by temperature-driven forces [59]. Chemical reactions also play a crucial role in ash deposition, particularly in the formation of complex compounds that contribute to the fouling of heat transfer surfaces [57, 61]. These reactions include the integration of alkali elements into silica structures, the sulphation of alkali compounds, and the decomposition of carbonates [57, 60]. These processes can lead to the formation of sticky deposits that adhere more strongly to surfaces, exacerbating deposition issues.

Turbulent eddy impaction occurs when ash particles are too light for inertial impaction and are carried by turbulent eddies close to the heat exchanger surfaces [62]. This mechanism is especially relevant for particles with a diameter of less than 10 μm and tends to occur in regions of lower temperature where gas velocities increase. In the absence of inertial impaction and thermophoresis, eddy impaction can become the dominant mechanism for ash deposition. Condensation, the final mechanism discussed, involves the deposition of inorganic vapors such as potassium chloride, KCl (g) on cooler surfaces of the heat exchanger. This process begins with the condensation of alkali compounds on clean surfaces, which provides a foundation for further deposition of coarser particles, leading to the formation of a thick, low-conductivity layer that reduces heat transfer efficiency.

The behavior of ash particles, including their tendency to adhere to surfaces, is significantly influenced by their melting characteristics under furnace conditions. The melt fraction of biomass ash can be estimated using thermochemical calculations, such as those performed with the FactSage software package. Biomass fuels rich in alkali and alkaline earth metals generally produce a higher melt fraction compared to coal at similar temperatures, resulting in increased deposition in both the radiative and convective sections of the furnace.

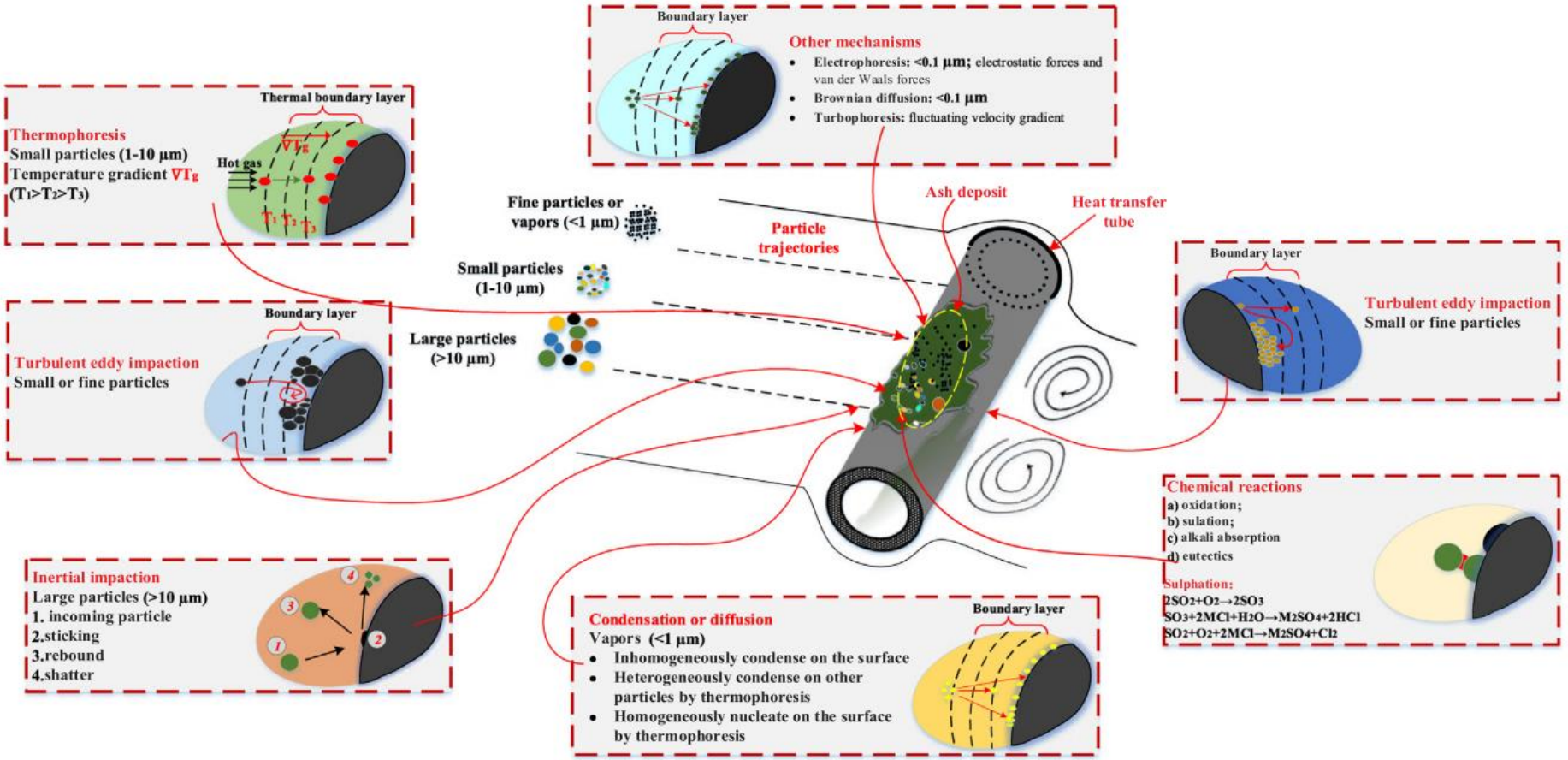

Figure 1-5 Schematic of the ash deposition formation processes on the heat transfer tube [18, 57].

The deposition characteristics of biomass can vary significantly depending on its composition. For instance, biomass with high alkali content, such as straws and grasses, tends to exhibit higher rates of slagging and fouling. However, even within similar fuel types, variations in composition such as the presence of chlorine and sulphur can lead to different corrosion behaviors on boiler surfaces. Therefore, understanding the specific properties of each biomass type is crucial for predicting and mitigating ash deposition issues. In conclusion, the complex interplay of physical and chemical processes in ash deposition makes it challenging to predict the behavior of different biomass fuels accurately. Traditional indices for predicting slagging which were developed primarily for coal, may not be applicable to biomass fuels. This highlights the need for the development of new indices tailored to the unique characteristics of biomass ash to improve the accuracy of slagging predictions.

1.3.4 Ash deposition issues

As a result of the ash deposition, the boiler is less efficient at transferring heat, which increases the risk of boiler tube corrosion and unscheduled outages. While the use of soot blowing and wall blowing are used to control deposition, deposition may occur when cleaning is ineffective due to inadequate bonding between the wall and the deposit, or because of the deposition at locations where cleaning equipment is ineffective. Constant changes in the fuel characteristics and boiler operating conditions frequently accompany deposition problems [65, 66]. Biomass is increasing in popularity for sustainable energy applications and can be obtained in various forms and from various sources. In the long term, the additional development of bioenergy has the potential to expand the use of bioenergy to meet the growing energy demands, lower carbon dioxide emissions, and combat global warming, with the benefit of disposing of urban and rural wastes [67, 68]. Now, biomass combustion is still the dominant heat and power generation technology. Even so, some biomass fuels contain potassium and other inorganic elements in addition to biomass. Ash issues during energy conversion processes result from the release and transformation of these inorganic elements [67, 69]. Operational issues related to ash significantly reduces the efficiency of combustion systems, increasing the boiler cleaning and maintenance costs as well as impeding further use of biomass as fuel [70]. There are operational problems related to the use of biomass fuels from agricultural crops, waste materials from bio-refineries, and food-processing residues that are especially prevalent during the combustion of these substances [44, 71-74].

1.3.4.1 *Slagging*

Biomass as a fuel has been gaining popularity as the demand for alternative energy sources grows. Biomass is neutral of carbon, and its use decreases the reliance on fossil fuels. Biomass combustion, on the other hand, illustrates a number of technical challenges. Ash deposits accumulate inside the furnace and on the heat exchangers such as superheater tubes. The ash build-up not only hinders the transfer of heat in the super-heat exchangers, lowering the boiler's overall thermal efficiency, but it can also cause serious slagging [19]. Slagging is a complex processes that has been studied extensively [75, 76]. Slagging is the precipitation of flying ash on the regions exposed to heat radiation. In general, there are distinct definitions of "slagging" as it pertains to different operating conditions and fuel/heat transfer regions. Slagging is usually associated with the deposit of fly ash on heat transfer surfaces or in the ‘flame exposure region' subjected to radiant heat transfer. Molten or semi-fused, dry ash, and sintered deposit comprise most of it. Because the melted and semi-liquid deposit causes stickiness, the deposited fly ash becomes adhesive when the local temperature is beyond the melting point limit for some components. In the initial stage, a thin layer of powdery deposits will form on the cool tube surfaces that face downwards. When these two deposits join with one another, a thin layer of dry porous material is formed, and this acts as an insulator. A layer of molten ash eventually forms on the surface exposed to the gas. Slag can sometimes freeze, and solidifying into a hard, glassy deposit.

In the high temperature combustion environment, alkali metals and their related compounds may form deposition on the furnace wall or enter the gas phase and deposited in the form of gas or fly ash particles on the tail heating area. Alkali and alkaline earth metals present notable difficulties and challenges; these metals have the potential to react with silica present in the ash, resulting in the formation of eutectic compounds which have lower initial melting temperatures compared to common combustion temperatures, such as potassium-sodium silicate (540 – 1170 °C) and potassium silicate (600 – 980 °C) systems [77]. The presence of these low-temperature systems can lead to the formation of molten or sticky ash particles that agglomerate which effects the issues related to ash (eg.: agglomeration, slagging and fouling) and reduces the boiler's efficiency [78-81]. Davidsson et al. [82] stated that the alkali metals, particularly potassium, are the most troublesome among the ash components, and potassium is commonly found in higher concentrations in biomass. Biomass ash also has a low melting temperature and the molten ash particles can stick the bed material together de-fluidizing the bed material. The chlorine gas in the combustion might accelerate the corrosion

in the combustion technology under the high temperature conditions [83]. Ash deposition, corrosion, and slagging formation in the biomass fuel combustion process is very harmful to the boiler operation [83-85]. As a result, of the slagging in the furnace, the boiler is less efficient at transferring heat, which increases the risk of boiler tube corrosion and unscheduled outages. To ensure biomass combustion is safe in power generation facilities, the biomass fuel slagging tendency during combustion must be predicted [86, 87]. This means that slagging can be avoided, which lowers combustion efficiency and affects the usage of biomass solid fuels [88].

Öhman et al. [89] reported that woody biomass power plants have encountered issues in the grate boiler operation mainly caused by slagging problems. Research by Fagerström et al. [33] indicated that the slag formation due to the presence of alkali elements (such as potassium and sodium) is commonly observed in the bottom ashes with low melting points. Biomass frequently contains significant quantities of bound inorganic elements that play a vital role in the growth and metabolic processes of the biomass. These elements include K, Ca, P, Fe, S, and Cl. A significant portion of these elements is emitted as vapours during combustion and then undergoes condensation, resulting in the formation of solid ash [90].

1.3.4.2 *Bed agglomeration*

Bed agglomeration and bed sintering are considered to be similar in FBC systems as the bed particles are combined through a liquified stage. Bed agglomeration can cause an unfavourable flop of the fluidized bed, which is described as defluidization. Only a few research groups have investigated bed agglomeration in fluidized bed and gasification technologies [44, 71, 91-96]. Bed agglomeration is a multiplex system where it involves both physical and chemical interactions. According to a chemical perspective, prior to the commencement of bed agglomeration, it is normal for the bed material to react towards the ash-forming matter of the energy source, which triggers the emergence of the melted phase on the bed material. The bed agglomeration that occurs in the fluidization bed firing is due to the development of a sticky glassy silicate melt, when using silica sand as the bed substance [97, 98]. In addition, it has been reported that the emergence of alkali phosphates results in bed agglomeration [91, 99]. Agglomeration is fundamentally driven by the formation of eutectic alkali silicates due to the interaction between SiO_2 in the bed material or ash and alkali species such as K_2O and Na_2O [96, 100]. The alkali silicates formation will determine the eutectic melting temperature as the primary instigator of bed agglomeration. The low melting temperature of eutectic compounds (<800 °C) will cause the bed agglomeration in the FBC due to the formation of the melt at temperature 800-900 °C [96, 101, 102].

The development of low-melting-temperature biofuel ash composites and coating layers on the exterior of the bed fragments play important roles in the beginning of the bed agglomeration system. Visser et al. [92] identified two mechanisms responsible for the agglomeration of bed particles in the FBC system which are coating-induced and melt-induced agglomeration. Melt-induced agglomeration means that straight adherence of the bed elements through relatively liquified fuel-derived cinders. The term "melt-induced agglomeration" is frequently used in FBC systems when fuel ash contains sufficient quantities of both silica and alkali metals to form eutectic melts [96]. Melt-induced agglomeration relies on larger molten ash particles colliding with the bed particles, with the molten ash acting as a viscous glue [96, 103, 104]. According to Scale et al. [103], burning char particles generate a localised hotspot which intensifies the adhesive capability of the "viscous glue". Lin et al. [105] suggested melt-induced agglomeration is when the molten char particles may serve as a foundation for the growth of agglomerates. Char fragments undergo combustion at higher temperatures than the average bed temperature and achieve almost complete melting at 900°C. Thus, the char particles will stick to the bed particles upon collision together with the viscous alkali silica melt on its surface. This has resulted in the coating of the bed particles, thereby fostering an extended propagation of adhesion among the bed particles.

However, coating-induced agglomeration has been identified as the predominant mechanism in the FBC system [96, 100]. Various researchers assessed bed particle composition and subsequently used thermodynamic calculations to identify potential melt phases. This suggests that all chemical reactions within the ash have achieved thermodynamic equilibrium corresponding to coating-induced agglomeration. The development of viscous coating surfaces on the bed molecules as an outcome of the chemical responses between the bed elements and the gaseous or fluid period ash (e.g., alkali compounds), expressed as in equations (1-1) and (1-2) [97, 106, 107] are introduced as coating-induced agglomeration:

$$SiO_2(s) + 2KCl(g) + H_2O \leftrightarrow K_2SiO_3(l) + 2HCl(g) \quad (1\text{-}1)$$

$$SiO_2(s) + 2KOH(g) \leftrightarrow K_2SiO_3(l) + H_2O(g) \quad (1\text{-}2)$$

When the techniques of coating formation is varied, the coating developing patterns also varied. The coating can possibly grow outwards onto the bed of particles, which performs as an unmoving bearer for the coating matter when the coating formation happens to be independent of the bed substance. Other than silica sand (quartz), olivine sand and porous alumina could also be used as bed materials. For example, olivine sand is usually applied in the Fluidized Bed

gasifiers because of the sand's catalytic features with regard to tar diminution in the gas maker. Applying different types of bed materials perhaps can remove the emergence of melted and glass-like silicates. Nevertheless, as the majority of the other bed materials are expensive, quartz is still mainly used as the bed material up to this date.

1.3.4.3 *Particulate emissions*

Particulate matter (PM) emissions generated from combustion sources, such as boilers, must be significantly addressed. This is due to the negative impacts of particulate matter emissions on cardiovascular and respiratory health [108]. The concentrations of alkali metals, chlorine, and sulphur in the fuel have been observed to significantly impact the formation of PM emissions during biomass combustion [109, 110]. Indeed, the release of alkali metals is recognized as a significant factor in the formation of PM in biomass combustion systems. Fine PM emissions were due to the presence of the aerosols in the flue gas [33, 111]. Previous research indicates that numerous trace metals, such as Na, K, S, and Cl, tend to accumulate in the fly ash, while elements classified as non-volatile, such as Ca, Fe, Al, Mg, Si, P, and Mn, predominantly remain in the bottom ash [112]. Trace metals present in the fine particles can substantially contribute towards their hazardous properties. Furthermore, the trace metal found in collected ashes may impose constraints on their subsequent disposal and utilization. Fagerström et al. [33] stated that the fine particles contribute to fouling on the heat exchangers causes corrosion due to the presence of the aerosols in the flue gas [111]. Generally, to reduce PM emissions, electrostatic precipitators (ESP) have been widely used in the boiler to de-dust the flue gas [113-116]. However, these particulate collectors are less efficient in eliminating intermediate particle size ranges 0.2 and 1 μm [117]. To address these problematic PM issues, various approaches have been attempted to enhance the efficiency of dust collectors, but they often come with high cost [118, 119]. On the other hand, it was reported that the use of additives able to reduce PM emissions during combustion at a lower cost [120].

1.4 Mitigation of ash depositions by the prediction model

This section aims to explain the existing methodologies employed in both industrial and research to predict ash deposition behaviour in boilers. Initially, these methods were developed with a focus on coal combustion. Over time, as the industry has shifted towards more sustainable energy sources, these predictive techniques have evolved to accommodate biomass fuels. The predictive models begin with understanding the characteristics of the coal used, including its chemical composition and mineral content. Researchers have developed empirical

formulas to estimate how these factors influence ash deposition tendencies. As the focus shifts to biomass, the complexity of combustion processes increases significantly due to the highly heterogeneous nature of biomass fuels. Unlike coal, which tends to be more uniform in composition, biomass varies widely in its ash-forming mineral content including differences in potassium, calcium, silica, and other trace elements. These variations lead to unpredictable combustion behaviours, such as ash deposition, slagging, and fouling, making biomass a more challenging fuel to manage in industrial applications. Consequently, the original coal-based formulas have been adapted and refined to better predict the behaviour of biomass ash. This adaptation involves integrating additional parameters specific to biomass, such as the potassium and chlorine content, which significantly affect the ash melting behaviour and deposition rates.

When it comes to predicting the behaviour of the ash transformation, it is imperative to find methods for predicting the degree of ash-related problems for different types of fuels. The first step in evaluating the suitability of a given fuel is through fuel ash analysis [97]. In the beginning, researchers utilised the ash's fusion temperature and fuel index to assess how the ash behaviour would change when fired with pure coal, but more recently, these techniques have been applied to estimate the ash behaviour when used in biomass and waste-derived fuel applications [28, 97, 98]. As is the case with these techniques, information is lacking regarding the mineralogy and association of the ash-forming matter [98]. In the context of determining the fuel matrix behaviour, knowing the chemical forms of the ash-forming elements is very important to estimate the characteristics of the thermal process. Although their degree of release, reactivity, and stability are all greatly affected by the mode of occurrence of these ash-forming elements in the fuel matrix, the amount and rate of release, reactivity, and stability all change in accordance with these factors.

The significance of predicting ash deposition characteristics is broadly known but the major present methods still depend on basic empirical indices obtained from the past. These indices are assumed to offer a starting point for predicting when applied to ash samples obtained from the intended blend of boiler firing. Moreover, usually the predictions are completed in the laboratory prior to firing a new fuel blend in order to anticipate any possible issues because full-scale firing is a high risk and could damage the boiler. The ash samples in the laboratory are normally prepared under controlled conditions and act differently to the actual composition of the ash [121]. In this study, the slagging and bed agglomeration indices resulted from the formation of ash and fusibility temperature correlations. Below are the explanations of the indices applied to biomass fuels.

1.4.1 Ash fusion temperatures (AFT)

The ash fusion temperature (AFT) test is the main laboratory prediction technique, and these tests consider the impacts of a high temperature on the ash condition. Over the past few years, various AFT standards have been created to cater for various kinds of coal and biomass and these are normally on a local basis. Fuel thermal decomposition in the muffle furnace is used to obtain samples of ash. Once the ash has been pressed, it can be formed into a circular cylinder, a pyramid, a cube, or a cone based on the established standard [20]. The temperature of the critical points are observed as physical changes that occur on a pyramidal or conical ash sample which is heated in oxidising or reducing environments [121]. To summarise, it is important to point out that on reducing the conditions then there is a lower number of available AFT [18] and, as a result, AFT reducing condition are not interchangeable with AFT oxidising conditions. On the other hand, the difference is sometimes small and often negligible for fuels that are relatively low in iron content [122]. The characteristic temperatures according to the American Standard Ash Fusion Test are defined as follows: Initial Deformation Temperature (IDT), Softening Temperature (ST), Hemispherical Temperature (HT), and Fluid Temperature (FT) [122]. In order to assess the AFT of biomass and solid alternative fuels, two standards have been recommended, which are the CEN/TS 15370–1 standard for the evaluation of biomass AFT and the CEN/TS 15404 standards for solid alternative fuel AFT.

According to Yu et al. [123], fuels exhibit a variety of levels of slagging when tested at the following temperatures: (i) Minor slagging occurs when the ST >1390 ℃; (ii) Slight slagging when 1250 ℃ < ST < 1390 ℃; and (iii) Serious slagging when the ST <1250 ℃. To prevent fouling in the boiler, the furnace outlet should be at a minimum temperature of 100 ℃ less than the value of the ST [124, 125] or 50 ℃ less than the IDT [125]. However, Kleinhans et al. [18] mentioned that ash particles from industrial sources will vary around 250 ℃ from the sample produced in the experimental investigations. This is because industrial boilers have distinct conditions and contain small ash particles that the laboratory specimen does not accurately represent in regard to the composition. When looking at how fast the ash sample forms inside the boiler, it is difficult to use this comparison since the laboratory ash samples have a much slower formation rate than the boiler ash [126]. AFT that have been determined experimentally, have been found to be most often utilised by plant operators [18, 124, 125]. In addition, Skrifvars et al. [127] has attempted to employ a standardized method of fuel ash testing to predict the temperature of bed agglomeration such as, the ash fusion temperature (AFT) was tested on multiple types of biomass fuels. However, the results were

unreliable, and it consistently forecasted problematic temperatures for ashes beyond the established problematic range in a fluidized bed [127].

1.4.2 Silica content (SiO_2)

Previous researchers decided that the most predominant component in slag specimens from biomass fuels is silica, which corroborates the melting composition of "sticky" silicates that produce slagging. When the relationship between the silica components in the fuel ash and the portion of fuel ash that produces slag in the furnaces is good, the silica components of the biomass will be suitable to act as a slagging measure. According to the data analysis produced by Öhman et al. [128], the essential Si content (SiO_2) is in the range of 20-25 wt% of the fuel ash. This deduction was supported by the following studies [129-131].

However, sand or soil contaminants can increase the silica levels in biomass fuels. The SiO_2 index demonstrated high possibility to create ash deposits for straws, biomass mixtures, and grasses [132]. These values of SiO_2 are in agreement with previous research [133, 134] that examined the SiO_2 levels in these kinds of biomasses and the impact on the plant's rigidness or sturdiness. In contrast, certain types of woody biomass tend to produce significant ash residues. This is often due to high Si content in the biomass, which is typically the result of external contamination [135-138]. Woody biomass should have low levels of Si without contamination, thereby preventing the creation of sticky silicates and other slagging difficulties at common firing temperatures (1000 ºC – 1100 ºC) [128]. Hence, the silica content is not suitable to apply in predicting biomass slagging behaviour because it is limited to the condition and situation of the biomass itself.

1.4.3 Chlorine content

Chlorine works as a facilitator in interactions between potassium and silica, resulting in the development of fused glassy deposits and slags at the average boiler working temperature of 800-900 ºC [139, 140]. The Table 1-3 shows the Cl (%) index to determine the slagging and fouling tendencies [141]. Overall, the ability of chlorine to make alkali vaporisation more likely is important, and alkali vapours that are not chlorinated condense more quickly [142, 143]. Research has shown that chlorine is more likely to limit the total quantity of alkali vapour that is created, and that deposit formation increases with rising vaporisation degrees [142]. Contamination from chemical preservatives or sea water can generate high amounts of chlorine in biomass fuels [144]. In addition, woody biomass tends to produce minimal ash deposits because of its low chlorine concentration, and this contradicts with the grass and straw, which

is reported to have high levels of chlorine [132, 145, 146]. Therefore, the chlorine content indicator alone is not adequate to be used in the biomass study to predict the slagging characteristics tendency due to the woody and herbaceous types are not in mutual agreement.

Table 1-3 The Cl (%) indicator to determine the slagging and fouling propensities [141].

Index Range	Slagging and fouling indicator
< 0.2	Low
0.2 – 0.3	Medium
0.3 – 0.5	High
> 0.5	Extremely high

1.4.4 Base to Acid Ratio

The base to acid ratio, $R_{b/a}$ is another common and well-used deposition indicator, where the base and acid compounds are used to describe the total weight percentages of the acidic and basic oxides as expressed in equation 1-3. The ratio is based on basic oxides fluxing effect in reducing the ash viscosity and thus increasing the slagging propensity [121]. The ash slagging tendency increases with the increase in the B/A ratio as shown in Table 1-4. In general, the rules for basic oxide compounds are to reduce the melting temperature, while acidic compounds tend to raise it. Even so, the findings by Garcia-Maraver et al. [132] mentioned that there are contradictions in the abovementioned guideline and also a divergence from the results of the previous findings, where a reduction in the B/A ratio led to an increase in HT and FT and a decrease in slag propensity. The studies by Garcia-Maraver et al. [132] stated that the majority of the biomass with extremely high tendency to slagging but some of the biomass

Table 1-4 The B/A ratio indicator for the slagging tendency [132].

B/A ratio	Indicator
B/A >1.75	Very high
1 < B/A <1.75	High
0.5 < B/A < 1	Medium
B/A < 0.5	Low

$$R_{b/a} = \frac{Fe_2O_3+CaO+MgO+K_2O+Na_2O}{SiO_2+Al_2O_3+TiO_2} \quad (1\text{-}3)$$

cases such as grass showed low B/A values. Hence, the idea to apply the B/A ratio to the biomass situation is not ideal due to many disagreements in the previous research to study the biomass propensity. Bryers et al. [137] conducted a regression analysis plotting wood-based

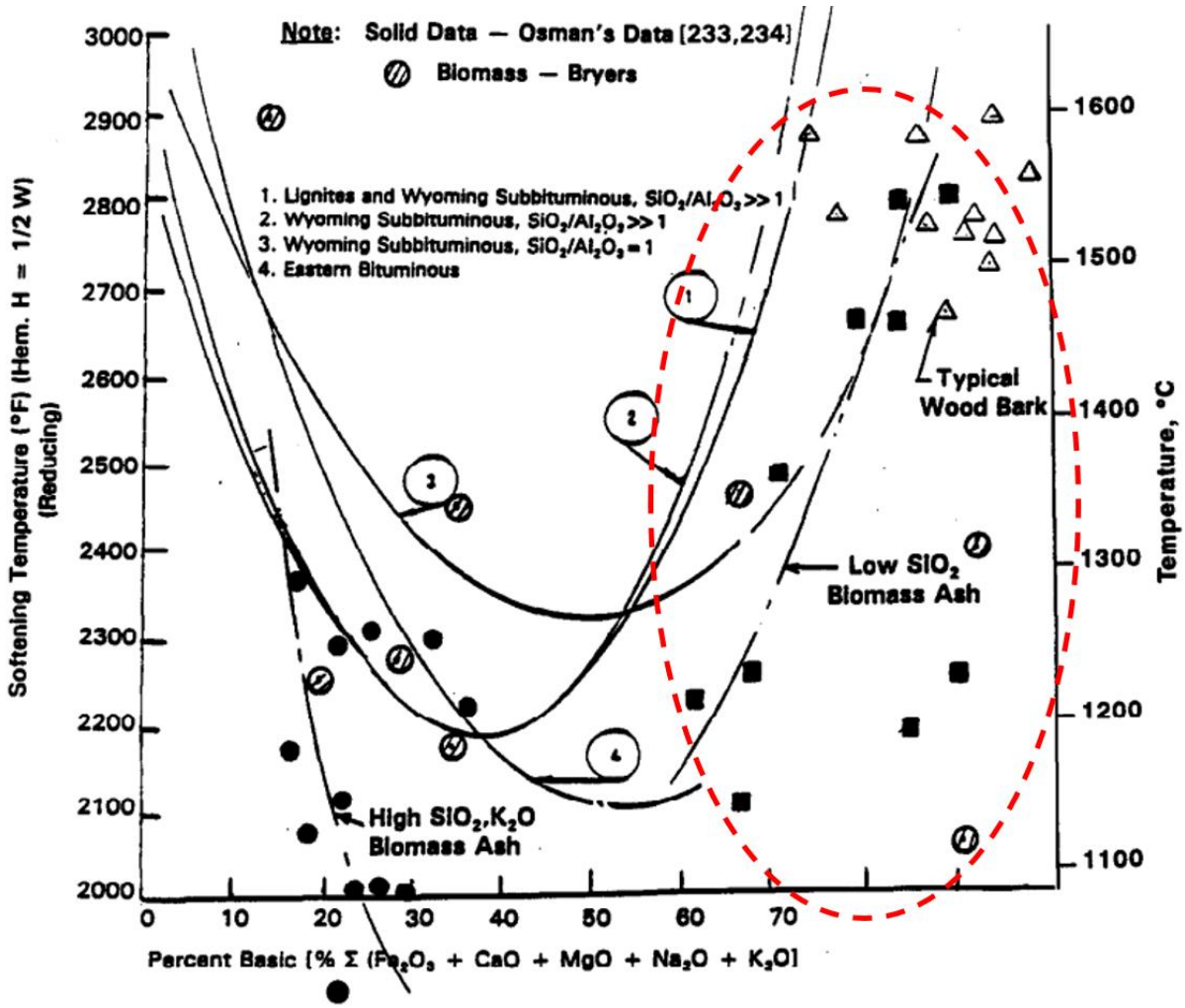

Figure 1-6 Regression analysis between percent basic for coal vs softening temperature [137].

fuels against the percentage of basic components for coal and softening temperatures. Initially, the ash from woody biomass was found to be highly basic (high in potassium and calcium, low in silica) with correspondingly high melting temperatures. However, as shown in Figure 1-6, the data points for woody biomass are scattered (red circle) across the regression analysis graph. This scattering makes it difficult to predict the combustion behaviour of woody biomass using this graph, as there is no clear trend that could indicate the behaviour of woody biomass during combustion. Furthermore, woody biomass tends to have a high B/A ratio, which would typically suggest a high slagging tendency. This is due to the fact that woody biomass generally has a higher basicity compared to acidity. However, this observation seems contradictory, as the majority of the woody biomass samples exhibit very high melting temperatures as shown in Figure 1-6, which should in theory, reduce the tendency for slagging. Therefore, this inconsistency underscores the need for a new slagging index tailored to the specific ash composition characteristics of biomass, to more accurately determine slagging tendencies.

1.4.5 Bed agglomeration index

The bed agglomeration index (BAI) was introduced (equation 1-4) to measure the operational issues in FBC technology. Low AFT can lead to bed agglomeration; therefore, higher AFT coefficient values should indicate a higher AFT. When BAI is less than 0.15, bed agglomeration occurs according to Vamvuka et al. [147]. Some publications report that silica-dominated in bed agglomerations form in fluidized bed combustors at 760-900 ºC [148, 149]. The BAI index, however, does not take this element into account when making predictions about the deposit generation. According to this indicator, biomass mixtures, woody biomass, and contaminated biomass that have higher Fe_2O_3 content are the groups that have a low potential to produce bed agglomerations. The combination of the low Fe_2O_3 in herbaceous and agricultural biomass, and their high presence of K_2O, means that this biofuel is more likely to form deposits in this kind of combustor. However, the BAI index only relies on the single indicator, which is not convincing enough to conclude the biomass product behaviours.

$$BAI = \frac{Fe_2O_3}{K_2O+Na_2O} \tag{1-4}$$

1.4.6 Babcock Index

The index of Babcock (Rs) is based on the B/A ratio, but the sulphur content is taken into consideration because prior studies linking sulphur-containing [150] biomasses with the deposits formation containing a high concentration of alkali sulphates, which are the volatiles at common firing temperatures [142]. S^d is the S percentage in dry fuel while B/A is the ratio between the acidic compounds (A) and basic compounds (B) as given in equation (1-5). Combustion of fuels containing alkali and earth alkali (K, Ca) and sulphur will produce

$$Rs = \left(\frac{B}{A}\right) \times S^d \tag{1-5}$$

sulphates, but not if they are already bound as silicates [151]. SiO_2 addition could lead to a major increase in K and Ca silicates, which would cause a significant drop in biomass ash fusion temperature [152]. In addition, another aspect that SiO_2 appears to do rather than cause problems is the prevention of sulphur-rich deposits, such as $CaSO_4$ and K_2SO_4, and this can form in unstable combustion conditions at 900 °C [142, 153]. Taking SiO_2 as a component of biomass fuel that could help minimise slagging, this statement enables the B/A index as a predictive model [132].

1.4.7 Ash Fusibility index (AFI)

Gray et al. [154] proposed the ash fusibility index, which is referred to as the HT and IDT values captured upon the ash fusion test. Equation (1-6) defines the ash fusibility index:

$$AFI = (4 \times IDT + HT)/5 \quad (1\text{-}6)$$

The index AFI is one of the most promising indices for biomass, corresponding closely to the actual fuel ash melting behaviour, ignoring any possible synergy between the ash constituents [149]. Previous research have found that the melting temperature may vary depending on the ash fusibility test's operating conditions [155]. Studies have shown that peculiar issues occur when biomass has large levels of silica, such as in herbaceous biomass [149, 156]. Garcia-Maraver et al. [132] reveal that agricultural and herbaceous biomasses have the greatest values for this index, their ashes displaying extremely high propensity to form deposits.

1.4.8 Slag Viscosity index (Sr)

This index measures the silica percentage in the ash components, excluding the alkali elements. High values of Sr indicate a high viscosity [150], and hence reduced the slagging propensity. However, based on previous researchers' findings conclude that the relationship between Sr and IDTs cannot be applied to biomass fuels. This is because by applying this equation in 1-7, it shows that the herbaceous biomass has a low tendency towards slagging which contradicts with the topic discuss in 1.4.2 on Silica Content.

$$Sr = SiO_2 \times 100/(SiO_2 + Fe_2O_3 + CaO + MgO) \quad (1\text{-}7)$$

1.4.9 Current research on ash deposition indices

Recently, the evaluation indices or criterion numbers have been prioritised as a means of solving slagging issues and specify the types of additives, co-firing fuels, and biomass fired in boilers. The alkali index refers to the proportion of a fuel's alkali content (kg kg^{-1})) to its heating value (GJ kg^{-1}) [157]. Also, the alkali index for biomass slagging uses the Na and K proportions of oxide and the high heating value (HHV) [158]:

$$AI = kg(K_2O + Na_2O)/GJ \quad (1\text{-}8)$$

The index is used to assess the slagging of coal: slagging is likely when AI is between 0.17 and 0.34 $kg.GJ^{-1}$, and slagging will definitely occur when AI is larger than 0.34 $kg.GJ^{-1}$. Vamvuka et al. [159], Oleschko et al. [160], and Diaz-Ramirez et al. [161] suggested evaluation indices:

$$(K + Na)/(Ca + Mg) \quad (1\text{-}9)$$

$$S/Cl \quad (1\text{-}10)$$

$$(Na + K + 2Mg + 2Ca)/S \quad (1\text{-}11)$$

while Jiang et al. [162] and Jenkins et al. [159] predicted biomass slagging by using the equation base-to-acid ratio. Nevertheless, Hu et al. [163] and Ye et al. [164] presented a new evaluation index, see equation (1-12), on the biomass slagging because the coal evaluation indices are not reliable for biomass. According to this new index, the value is less than 0.7 when the softening temperature (ST) is < 1000 °C, and greater than 1.7 when the ST > 1200 °C.

$$(MgO + Al_2O_3 + Fe_2O_3)/(CaO + P_2O_5) \quad (1\text{-}12)$$

Niu et al. [158] proposed two slagging equations (1-13) and (1-14) based on the effects of S, Cl, Al, K and by comparing the initial slagging behaviours of two cotton stalks. The slagging indicators of each specific ratio indices as shown in Table 1-5 [158]:

$$\mathrm{Cl_{ratio}} = (\mathrm{Cl} + \mathrm{K_2O} + \mathrm{Na_2O})/(\mathrm{SiO_2} + \mathrm{Al_2O_3}) \quad (1\text{-}13)$$

$$S_{ratio} = (S_{volatile} + K_2O + Na_2O)/(SiO_2 + Al_2O_3) \quad (1\text{-}14)$$

Table 1-5: Slagging indicators of specific indices on Cl and S ratio [158].

Ratio Index	Indicator
Cl ratio > 2.4 & S ratio >1.9	Highly prone to slagging
Cl ratio < 1.0 & S ratio >0.5	Slightly prone to slagging

The melting point of ash fuel is a significant factor in determining the boiler performance. The ash fuel melting point has been shown to be closely related to the ash oxide content. The study by Yu et al. [123] focused on analysing the biomass classification and oxide contents to estimate the biomass ash melting temperature. Yu et al. [123] proposed a biomass index for wood-based, A and herbaceous, A′:

$$\mathrm{A} = (\mathrm{CaO} + \mathrm{MgO})/(\mathrm{SiO_2} + \mathrm{Al_2O_3} + \mathrm{K_2O} + \mathrm{Fe_2O_3}) \quad (1\text{-}15)$$

$$A' = (SiO_2 + K_2O + Na_2O)/(CaO + Al_2O_3 + Fe_2O_3) \quad (1\text{-}16)$$

However, the index used to judge the property of ash slagging is not accurate for biomass because of the differences in the biomass fuel contents. The oxide element of various biomass ashes varies greatly and different oxides showed different correlations in those two types of biomass which are wood-based and herbaceous, with MgO and Na_2O showing the most

strongest evidence [123]. Öhman et al. [32] indicated that differences in the total ash and ash forming constituents of the fuel had a significant impact on the burners' performance [32]. In general, the existing indices used in the coal prediction behaviour have no relationship outcomes are incongruous when applied to predict the slagging propensity for biomass fuels. This is because the biomass ash contents are unique when compared to coal ash.

Previous research revealed that the ash fusibility test can yield varying melting temperatures depending on the operating situation [165]. Previous studies from Yu et al. [123] have shown that silica-rich biomass, such as herbaceous biomass, can cause unique problems [156, 166]. Also, some other authors have concluded that higher Sr values relate to higher IDT values are not relevant to extrapolate the indices used in coal application for biomass fuels [153]. When applied to biomass fuels, the traditional predicted coal ash coefficients give rise to mixed results. As a result, research findings that accurately and consistently predict biomass fuel on slagging should be questioned. The development of new indices should be based on real-world combustion results, taking into account not only the combustion conditions and technology, but also the biomass solid fuels heterogeneity and the characterization of physicochemical [132].

Various experimental research has attempted to employ a standardized method of fuel ash testing to predict the temperature of bed agglomeration such as, ash fusion temperature (AFT) was tested on multiple types of biomass fuels by Skrifvars et al. [127]. However, the results were unreliable, it consistently forecasted problematic temperatures for ashes beyond the established problematic range in a fluidized bed [127]. Morris et al. [96] reported that the sintering test exhibited higher accuracy but consistently underestimated problematic ash temperatures by 20–50 °C. Currently, lab and pilot-scale trials are the most reliable methods for assessing agglomeration challenges associated with a new fuel [96]. Recently, prioritizing the evaluation indices or criteria has been emphasized as a strategy for addressing bed agglomeration issues in FBC due to the low cost technique, and to obtain the chemical compositions of biomass fuel is highly convenient for researchers [167]. According to F. Scala et al. [168], the method of combination between thermodynamic equilibrium analysis and compression strength test was unable to predict the sintering tendency of biomass ash, this is due to the method not taking into consideration the interaction between ash and quartz as bed material. This also happened the same in the past when the researchers were tested the ash fusion accuracy to predict the bed agglomeration temperatures. Therefore, it was concluded that the ex-situ method failed to predict the bed agglomeration behaviours [168]. Over the years, researchers have proposed various empirical indices for bed agglomeration in the FBC

system. The alkali index is generally effective in predicting agglomeration, however, its accuracy diminishes when considering factors such as alternative bed materials or additives, as noted by various researchers [148, 169, 170]. Fernández Llorente and Carrasco García [171] determined that the ratio of alkaline earth oxides to alkaline oxides is a weak indicator of ash sintering likelihood and severity. Moreover, the bed agglomeration index (BAI) was introduced to measure the operational issues in FBC technology. Bed agglomeration is formed when BAI is less than 0.15 according to Vamvuka and Zografos [172]. Several publications report that silica-dominated in bed agglomerations form in fluidized bed combustors at 760-900 ºC [148, 149]. The BAI index, however, does not take this element into account when making predictions about deposit generation.

1.5 Mitigation of ash depositions by aluminosilicate additives

Biomass combustion involves complex physical and chemical processes. The experimental works help to give a better understanding on the operation of biomass combustion systems. By studying combustion under different conditions, researchers can identify the most efficient and environmentally friendly methods of burning biomass by reducing the potential of ash deposition issues in the boiler. In addition, understanding the particulate emissions and environmental impact of biomass combustion is also crucial for developing sustainable energy solutions. For many years, there has been much research on the possible additives for minimizing the issues linked to biomass ash. Additives can be organized based on the contained reactive substances, such as Al-silicates, sulphur, phosphorous, and calcium, etc. based additives. Additives with high reaction capacities and high chemical adsorption can reduce K-linked ash problems in the biomass firing process. The effective system of a chemical reaction is related, approximately, to the K-Ca-P, K-Al-Si, and K-Ca-Si mechanism. The capabilities of the additives to decrease ash-associated issues are highly affected by the mass/molar ratios of the relevant reactive elements of the additives and the biomass ash, the atmosphere of the reaction, as well as the firing technology [45]. Therefore, the experimental investigation on the impact of addition aluminosilicates additives with woody biomass in the pilot scale boiler is significant to address important issues such as chemical compositions and combustion behaviour in the boiler.

Various additives, including bauxite, diatomaceous earth, calcium oxide, and kaolin, have been recommended to concurrently mitigate both the formation of deposits and the emissions of particulate matter [173-175]. Previous studies have been reported on additives utilization in solid fuel [71, 174, 176, 177] as a strategy of changing the ash deposition

produced. Additives improve the characteristics and deposition rate by diluting the problematic ash groups and increasing the ash melting temperature [45]. Aluminosilicate (Al-Si) additives have the capability to transform the liquid phase and vapour, $KSiO_3$, and KCl to potassium aluminium silicates of a higher melting temperature [178] and binding the potassium among the ash. This ultimately decreases the existence of KCl and KOH in the flue gas, and thus protecting against the generation of alkali chlorides via interactions with HCl and the following corrosion in the presence of oxidation. Generally, these reactions take place surrounding the combustion region, and minimizing the development of fine substances and water-soluble alkali of metal salts [178]. In addition, the regenerative procedure can avoid gaseous chlorine by preventing volatilization of alkali metal during early firing.

One problem that occurs by using additives in biomass firing is the high cost related to getting the additives. Additives that have been suggested to being efficient in the literature, such as limestone or kaolin, are always difficult to reach the power plants and need to be outsourced. As coal pulverised fuel ash (PFA) is easily available in converted power plants with a low cost, there will be a high possibility of using PFA as an additive within the industrial market. Although coal ash depositions can vary and importantly depend on the coal type, some coal ash depositions may have significant SiO_2 and Al_2O_3 concentrations and have potential as aluminosilicate-based additives [90]. The reductions of sodium, potassium, sulphur and chlorine were observed in the aerosols when adding coal fly ash into a pulverised wood fuel combustor. However, Nowak et al. [179] reported that the usage of coal fly ash as an additive will be restricted in the future due to the decision by the European Union to discontinue the usage of coal combustion for power generation [179]. Therefore, the growing research interest in kaolin has emerged compared to coal fly ash due to its better sorption capacity, and it is considered the most viable option for future industrial use [120].

Kaolin has been presented in enhancing the ash deposition properties of problematical biomass, forming potassium aluminosilicates from volatile potassium. Lab-scale investigations have been carried out in screening two biomass fuels with high-potassium ashes, namely, white-wood (WWA), and olive-cake (OCA), and adding kaolin powder at a mass fraction of 5% [180]. By continually using these additives can increase the flow temperatures based on the ash fusion testing results. For WWA, kaolin was investigated to lower the deformation temperatures and boost up the flow temperatures over the firing temperature levels. Testing of the sinter strength indicated that the additive used dramatically improves the composition of the OCA properties, preventing the KCl precipitation and development of deposits that are not well removed when using a sootblower. In addition, kaolin is used to remove sintering at all

temperatures. Both additives had negative impacts during the sintering of WWA, indicating that the use of Al-Si additives should be limited to biomass with high Cl and high K content. Viscometry of OCA at high temperatures combined with thermodynamic modelling, showed that the viscosity at the firing temperature was significantly lower than at lower temperatures. This decrease in viscosity is attributed to the formation of silicates and the high concentration of Mg. Kaolin at 5% mass portion was estimated to improve this characteristic, creating favourable viscosity with aluminosilicate formation. The outcomes show that the addition of kaolin can make high K and Cl biomass, such as OCA, suitable for pulverised-fuel types of combustion [90].

The findings by Davidsson et al. [82] conclude that kaolin is a successful absorbent for potassium during the firing of the boiler. In general, kaolin possesses a small particle size which results in a large surface area, and this is significant for the adsorption of gaseous substances from the flue gas [82]. Research has demonstrated that both physical adsorption and chemical reaction mechanisms are involved in the capture of potassium by kaolin [181-184]. When potassium reacts with kaolin, the potassium aluminium silicates and muscovite will be formed, which possess higher melting points compared to potassium silicate. Previous combustion experiments have been carried out by Clery et al. [185] with the addition of kaolin to the straw and this produced a positive outcome with reduction of the potassium released in the biomass ash. Another investigation demonstrated that the ash fusion temperatures were significantly increased when peat was blended with kaolin and lime during combustion [89]. The results from previous work [89] have shown that the addition of kaolin in the high silica fuel will slightly reduce the slagging issues in the commercial 10-15 kW boiler while blending kaolin with the low silica fuel has a negative impact on the slagging tendency in the pellet burner. According to Rebbling et al. [186], the function of kaolin to capture the alkali elements relies on the temperature. The transformation of kaolin when it is heated can be expressed as follows [187-189]:

$$Al_2Si_2O_5(OH)_4\ (kaolinite) \rightarrow Al_2O_3 \times 2SiO_2\ (metakaolin) + 2H_2O\ (g) \sim 450\ °C \quad (1\text{-}18)$$

$$Al_2O_3 \times 2SiO_2 \rightarrow SiAl_2O_4\ (spinel) + SiO_2\ (amorphous) \sim 980\ °C \quad (1\text{-}19)$$

$$3(Al_2O_3 \times 2SiO_2) + 3SiO_2\ (amorphous) \rightarrow 3Al_2O_3 \times 2SiO_2\ (mullite) + 4SiO_2 \sim 1100\ °C \quad (1\text{-}20)$$

The metakaolin is transformed into spinel and SiO_2 (amorphous) and the alkali capturing capability is significantly reduced at temperatures above 980 °C. The main new phases formed are kalsilite and leucite when metakaolin reacts with K, according to eqs 1-21 and 1-22 [188]:

$$Al_2O_3 \times 2SiO_2\,(metakaolin) + 2KOH \rightarrow 2KAlSiO_4\,(kalsilite/kaliophilite) + H_2O \quad (1\text{-}21)$$

$$Al_2O_3 \times 2SiO_2\,(metakaolin) + 2SiO_2 + 2KOH \rightarrow 2\,KAlSi_2O_6\,(leucite) + 2\,H_2O \quad (1\text{-}22)$$

1.6 Thesis proposal

In this section, the discussion focuses on identifying the existing research gaps within the field of ash deposition in biomass combustion. From the analysis of these research gaps, the author has proposed 4 research novelties to fill the gaps left by previous researcher in the combustion of the biomass field.

1.6.1 Research gaps

Based on the critical review of the literature in the biomass combustion sector, several important issues need to be much better understood. The research gaps left by the previous researchers must be filled so that the industry is able to better sustain the electricity production with less ash related issues, unplanned shutdowns, and reduce the maintenance costs in the power plants. The study to develop new formulae for predicting biomass ash deposition has become a hot topic among the researchers. Several attempts on this research topic have introduced new equations for biomass fuel but the outcomes are not able to satisfy the objectives. Previous studies have proposed various indices and coefficients to estimate the biomass ash deposition propensities. The indices and coefficients have been applied to various types of biomasses with different origins to help determine which indices and coefficients will work best. However, when considering a wide range biomass fuels, the findings show no relationship as well as no predictive trend. The contradictory findings show that much more research and real observation testing is required to validate all these indices. To the best of the authors' knowledge, a number of research investigations have been performed in the past to develop empirical slagging and bed agglomeration prediction indices in the fixed bed and fluidised bed combustor, respectively, however, the applicability of the existing indices across different types of biomass to estimate the slagging and bed agglomeration tendency remains limited. This is because the researches are mostly based on the fuel and ash composition but do not consider the thermal chemical condition of the ash itself and thus there is a lack of understanding of the biomass ash chemistry.

Furthermore, limited research has been reported on the impact of the kaolin injection towards the agglomeration and slagging formation in the grate boiler. Most of the studies were focused on the impact of the kaolin to minimize the alkali species release during combustion. Recent studies [190] mentioned that most of the researches were focused on the testing of

different types of additives to capture the K upon firing the fuels. The reduction of deposit formation is closely linked to the reduction in the release of alkali from the fuel bed [34, 191]. This can be accomplished by capturing the alkali in the bottom ash where it forms as stable compounds, then this can be effectively managed and removed by the ash removal systems such as the bottom ash bin. However, it must be noted that, capturing the alkali in the bottom ash also will cause the potential of the formation of severe agglomeration and slagging especially in the grate boiler. This is because the presence of the eutectic compounds, which have low-temperature systems, has a high potential to cause the formation of sticky ash particles that agglomerate on the moving grate of the boiler. Therefore, the studies on the grate boiler condition, especially the agglomeration and slagging condition after the injection of additives must be addressed to avoid any unplanned shutdown of the grate boiler due to the failure to maintain and control the agglomeration and slagging behaviour during combustion.

Next, numerous studies have been conducted to investigate the impact of kaolin on the PM emissions during biomass firing in a small scale <100 kW, however, it is not certain whether the same is valid for biomass firing with kaolin addition in a field scale >100 kW *(scale characterization based on BEIS report)* [192]. This is because, in a field scale furnace, biomass and mineral particles may experience significantly higher heating rates, reaching higher temperatures and more vigorous fragmentation compared to bench-scale reactors, leading to increased mineral matter being released into the fly ash [120]. Moreover, the feed rate in the field scale will be much higher compared to the lab scale. As a result, more mineral matter such as non-volatile elements, alkali and alkali earth elements are released from the biomass during combustion. These elements become part of the fly ash, which is the fine particulate residue that is carried along within the flue gas. At the present, there is limited research with the focus on well-defined chemical elements partitioning in the PM emissions especially on the silica content. Most of the research publications have discussed the silica content in coarse fly ash (>10μm), while data of the silica content in aerosols form (PM <10μm) have not been well understand due to the lack of appropriate analysis methods in determining the silica. It has been confirmed that the silica and its partitioning play a critical role in the ash deposition issues in the biomass boiler [167, 193]. Therefore, it is very important to understand how kaolin additives affect the silica partitioning in the PM emissions of field scale combustor. Moreover, the kaolin consists of high amount of silica content and adding the kaolin may increase the excess of silica in the biomass boiler. To the best of the author knowledge, five papers on the control of particulate matter emissions from biomass combustion by adding

kaolin have been published in the past 5 years. A comparison of the main content and research gaps of these literatures is listed in Table 1-6.

Table 1-6 A comparison of main content of five papers published within the past five years.

Authors	Main content and research gaps
Gehrig et al. [194]	A set of pelletized of spruce mixtures blended with kaolin to investigate the PM reduction (potassium mainly) in a 12 kw biomass boiler. It was mentioned that Si and Al were increased in the boiler ash due to the kaolin, however, there was limited quantitative analysis on the chemical partitioning of Si, Na, Ca, Mg in PM emissions.
Nowak et al. [195]	Investigation of the impact of the alkali upon capture efficiency in a 6 kW electric heated furnace where beech wood was co-fired with kaolin. There was only limited observations on the chemical elements partitioning in ultrafine PM.
Wang et al. [190]	To conduct a quantitative testing of the reaction between kaolin and coal fly ash and volatile K-salt species, which are produced during the combustion of biomass in an entrained flow reactor. Lack of analysis and discussion on the chemical compositions in ultrafine PM.
Höfer et al. [196]	$CaHPO_4$ and kaolin were used to investigate the PM reduction (focus on potassium) of wood straw blend in 8 kW boiler. Lack of explanation of chemical elements partitioning consist of non-volatile (Si & Al), alkali earth metals (Ca & Mg) and sodium.
Rebbling et al. [186]	The kaolin reduces the volatile alkali species which is K and Na in a 40 kW grate boiler of woody biomass combustion. Limited explanation on the silica formation in the PM emissions.

1.6.2 Research aims and novelty

Biomass will still be one of the primary demands for energy sources globally in the near future. This is because biomass provides low carbon emission, reduce the dependency on fossil fuels such as coal and is widely accessible. Biomass plays a significant role in meeting the power generation worldwide and especially in developing countries. However, biomass combustion showed a number of technical challenges in the combustion industry, especially

ash deposition issues. The biomass ash is complex and unique due to the different types of biomasses having different behaviours of the chemical compositions, and especially the new batch of fuels. It is vital for more research work to be performed to provide a better understanding of the ash deposition behaviour of the new fuels. This is to maintain the long-term efficient operation of the boilers and minimize the maintenance costs for the industry.

At the present, the application of thermodynamic equilibrium modelling (TEM) has become extensive in the industry as a tool to predict the ash transformation behaviour and the chemical and physical characteristics of ash in various ash-related processes, such as issues with ash deposition, slag formation in furnaces, bed agglomeration in fluidised-beds, heat transfer surfaces corrosion, and smelt bed behaviour patterns in boilers. The thermodynamic equilibrium design proved to be a reliable approach to estimate ash related issues in the boilers, by measuring the melt fraction in deposited salts generated during the flue gas condensation on heat-transfer surfaces [197]. Therefore, developing a reliable ash deposition index is still essential for understanding the ash deposition tendencies of new biomass fuels for boilers. Furthermore, the ash deposition propensity predictions are demanded by the industry, as there is a need to design a simple and easy-to-use method that can make predictions on the ash composition. Hence, it is very important to create a reliable and good index of the ash deposition to predict the ash composition propensity of any new solid fuels that are used in boilers.

Additionally, fuel treatment by adding aluminosilicate additives to the feedstocks is one option to mitigate ash deposition issues such as slagging, bed agglomeration and particulate matter emission in the boiler. The formation of ash deposition is more complex in boilers for the combustion of solid fuel. The temperature profile, fuel feeding rate, and number of processes (heat transfer, combustion, particle movement, deposition growth, particle sticking and impaction, etc.) need to be taken into consideration to assess the ash deposition in the boiler. Experimental work provides a much better understanding to the power generation industry user and researcher in this field by applying the state-of-the-art equipment to mitigate the ash deposition issues. These experimental approaches are critical as they help validate theoretical models and provide empirical data that can be used to refine strategies for the ash management. As such, this work not only contributes to academic knowledge but also offers practical solutions that enhance the efficiency and sustainability of power generation systems. Furthermore, the application of advanced technologies and equipment in the Translational Energy Research Centre facility allows for the precise analysis and better control over the combustion process of biomass with the addition of the additives, leading to optimized

operational conditions and improved environmental performance. Therefore, this research has two different approaches in mitigating the ash deposition which is the development of tools to predict the ash depositions by TEM and experimental work to investigate the ash deposition behaviours in more industrial and in-situ condition tests.

The novelty of this study is as follows:

1) A new numerical model has been developed to predict the slagging propensity of woody biomass on the high-temperature regions in utility boilers and the TEM is validated by the experimental datasets available in the literature. A new index, I_n has been developed by partial least squares regression (PLSR) coupled with cross-validation to introduce an indicator that represents the severity in the slagging of the biomass. The indicator is significant in guiding the users, especially power plant operators of the energy power generation in determining the wood-based biomass fuel slagging behaviours.
2) An improved index has been successfully developed to predict the bed agglomeration in fluidised bed combustion of biomass fuels. This model has been modified and accomplished to extend the TEM-PLSR coupled with cross validation method for different applications. The bed agglomeration index, I_a has been formulated based on the melt fraction in the FBC application using quartz as the bed material. The I_a model has been validated with the experimental observations from the literature with a 90% accuracy.
3) An investigation has been performed to study the impacts of aluminosilicates additives (kaolin) with biomass fuels towards the ash related issues in a field scale 250 kW grate boiler. The ash related issues focus on mitigating the agglomeration in the boiler, slagging tendency, rate of reduction of fly ash, and partitioning of chemical compositions in the combustion chambers. A comprehensive analysis has been carried out to illustrate the chemical fractionation from the fuel prior to combustion and post combustion stage. A detailed explanation on the impacts of the combustor behaviour after the addition of kaolin has been highlighted in this research chapter and this has not been reported in the literature previously. This is useful and important for the researchers to better understand the behaviour of the kaolin reaction with biomass by using field scale equipment.
4) An assessment of the effects of blending kaolin with biomass towards the reaction of formation and emission of particulate matter (PM) in a biomass fired pilot scale grate boiler. This research has focused on analysing the alkali element, alkali earth metal and non-volatile elements and especially silica. This is because the silica content in aerosols

form (PM <10 μm) have not been well understand in the past due to the lack of appropriate analysis methods in determining the silica. It has been confirmed that the silica and its partitioning play a critical role in the ash deposition issues in the biomass boiler. These findings have not been previously presented in the literature, and it is very important to address this issue to the industrial users/researchers when adding kaolin to the biomass in the furnace. Moreover, this study has contributed valuable new findings to optimize the kaolin dosage when added to woody biomass, thus paving the way for future studies. The detailed discussion on this topic have enabled an understanding to be provided that will benefit industrial users and researchers of the new optimization and improvement in the performance of biomass fired boilers.

1.6.3 Scope of the thesis

The objectives of this thesis can be divided into several research milestones:

- In Chapter 2, a detailed description of the chemical composition data for the ash deposition prediction model, experimental facilities and laboratory are discussed in the following chapters.
- In Chapter 3, the numerical model to predict the slagging propensity of woody biomass in the high temperature region is presented. Also, a detailed discussion on the melting fraction predicted by the thermodynamic equilibrium model is discussed.
- In Chapter 4, an improved numerical model to predict the bed agglomeration behaviour in the fluidized bed boiler was developed. A detailed development of the model which considers the quartz as the bed material and sensitivity of the model is presented.
- In Chapter 5, an experimental investigation to study the effects of adding aluminosilicate additives into the biomass fuels on the partitioning of chemical elements in the 250 kW grate boiler is presented. A detailed discussion on the chemical composition, temperature profile, gas composition, X-ray diffraction analysis are illustrated. In addition, the deposition propensity on the ceramic coupon is presented.
- In Chapter 6, the impact of the kaolin addition on the formation and emission of particulate matter (PM) in the biomass fired plot scale grate boiler is explained. A detailed discussion on the chemical composition partitioning, especially the non-volatile elements, alkali elements, and alkali earth metal are presented.
- In Chapter 7, the key findings and conclusion are discussed followed by some recommendations for the possible future research of this study are presented.

2 Methodology

Summary

This chapter introduces the data used to develop and validate the models to predict the slagging propensities and bed agglomeration tendency of biomass firing in a fixed bed and fluidized bed technology, respectively, as described in Section 2.1-2.3. In addition, the experimental facilities, laboratory analysis and methodology will be discussed in detail to analyse and mitigate the bottom ash, slag, coarse fly ash and emission of particulate matter, as described in Section 2.4-2.7.

2.1 Thermodynamic equilibrium model

Generally, to predict the ash formation during the firing of the biomasses and biofuels, the thermodynamic equilibrium and experimental techniques must be applied. Both the experimental work and thermodynamic computation are unable to produce precise data in biomass boilers regarding the combustion chemistry by itself in multiplex and multicomponent problems. Nonetheless, ash analysis systems and thermodynamic computations appear to show a more accurate forecast of the ash conversion activity. There is one outstanding predictive technique, namely the FactSage thermochemical software and database, which has been widely applied in biomass firing analysis for computing the equilibrium, multiphase multicomponent, and multiplex stage diagrams, which have the function of composition, atmospheric and temperature settings. In 2001, Factsage was established and developed together by both FACT-Win/F*A*C*T and ChemSage/SOLGASMIX thermochemical collection which originated more than 28 years ago. One is allowed to obtain and operate pure matters and solution databases when choosing Factsage as it includes a large amount of information, calculations, databases and manipulation modules. FactSage is very beneficial in the chemistry community as it is a very important software, which helps one to execute a broad range of thermochemical computations. This software delivers data on the stages developed, proportions and compositions, the single chemical elements activities and the thermodynamic characteristics for all pressures, compositions and temperatures. This application builds upon the Gibbs power reduction and includes huge databases for oxide or silicate and salt composition structures. Unmixed compounds and solution stages are included in the databases. The unmixed compound (pure compound) is composed of a stoichiometric element composition, whereas there are optimized frameworks for the solution stages in the solution databases. The techniques applied to initiate the thermodynamic database have been thoroughly analysed by

Lindberg et al. [198]. The databases include all solution phases and pure compounds. The databases of the solution phase and pure compound contain enhanced parameters and stoichiometric substance properties, respectively.

Factsage has a notable influence on coal globally, such as in the Netherlands, North Dakota, South Korea and Japan. This software is popular for the composition of step-change technologies in the assessment and assortment of coal for entrained flow coal gasification and discharge furnace iron creation by researchers throughout the globe. In the FactSage software, the significant characteristics are the huge assessed multi-component solution databases which have the thermodynamic features that work for the temperature and composition. The databases include 15 components of oxides or glass solutions, ceramic solutions aqueous solutions and many more. All the databases have been produced by analytical assessment and optimization of all the available information through all the relevant solution samples. As a result, the collaboration between FactSage with X-ray diffraction (XRD) can be applied to estimate the responses that occurs between minerals and the mineral conversion and slag development. In addition, it may be a suitable method to assist in obtaining a better understanding of the liquefying features of mineral substances in coal and aid in aggregating the slag development in gasifier activity.

The ash-forming characteristics at high temperatures can be evaluated by using FactSage [199]. Chemical stability estimations can be made to the molten phase fraction in the ash and the phase adjustments related to the ash fusion temperature, which can be associated with the phase equilibria thermodynamic modelling. Recently, with the assistance of the computerized thermodynamic model, there are few academic works on the forecasting of the ash fusion temperature (AFT). Huggins et al. [156] linked the AFT of coal ashes to the liquidus temperatures in the ternary equilibrium phase diagrams of SiO_2–Al_2O_3–XO (where X = Fe, Ca or K). Jak et al. [200] estimated the ash fusion for the coal behaviour by utilizing the multicomponent structure Al–Ca–Fe–O–Si with the assistance of the FACT thermodynamic computer sets. The Equilib mode, as illustrated in Figure 2-1, often highlighted in FactSage software as one of the core functions for thermochemical equilibrium calculations. The Equilib mode is used to calculate the equilibrium state of a system based on the given conditions, such as composition, pressure and temperature. First, the selection of appropriate thermochemical databases which contain the thermodynamic data for the substances involved in the system is important before starting a calculation. Second, computes the input conditions (reactants) which consist of the temperature, pressure, and initial amounts in grams or moles of each component present in the system as shown in Figure 2-2. Third, the condition of the system

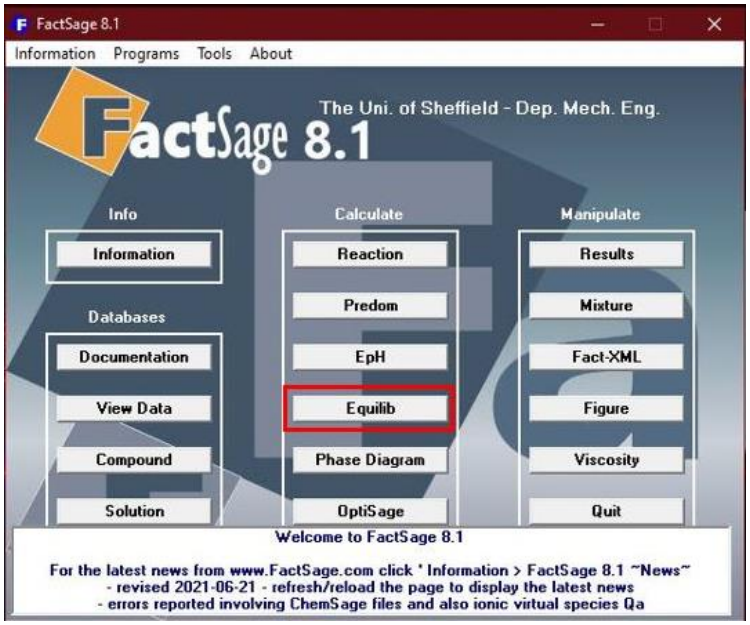

Figure 2-1 Equilibrium mode in the FactSage 8.1 interface.

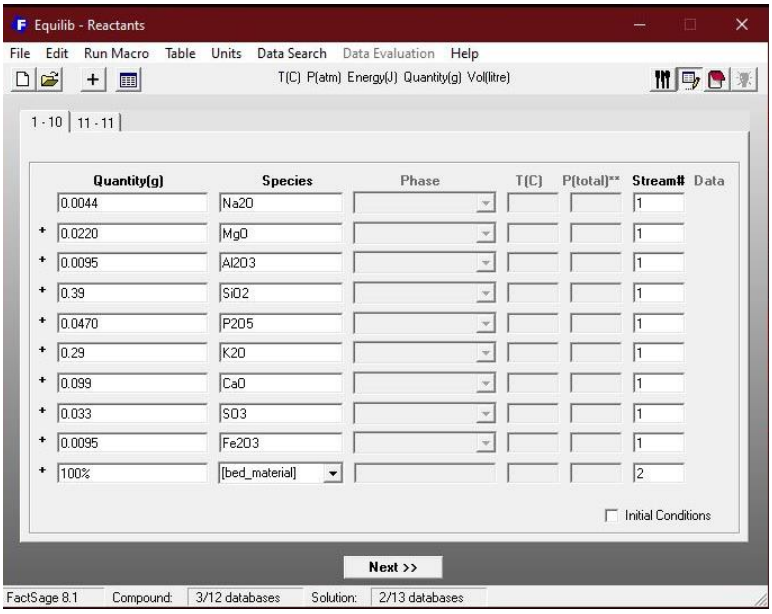

Figure 2-2 Reactants input settings in the FactSage 8.1.

will be specified based on pressure, volume, isothermal, adiabatic, etc. Figure 2-3 illustrates the database settings to select the chemical elements and compounds that are potentially formed in the equilibrium calculation and the phases (gas, liquid, solid). Next, the calculation will be executed based on the equilibrium systems that minimize the total Gibbs free energy. FactSage will provide the results which consist of the amount of each phase, chemical compositions, enthalpy, entropy, etc upon completion of the calculation. Overall, Equilib mode provide a better understanding in thermodynamic properties for research in the combustion process, metallurgy, process engineering, materials science, etc.

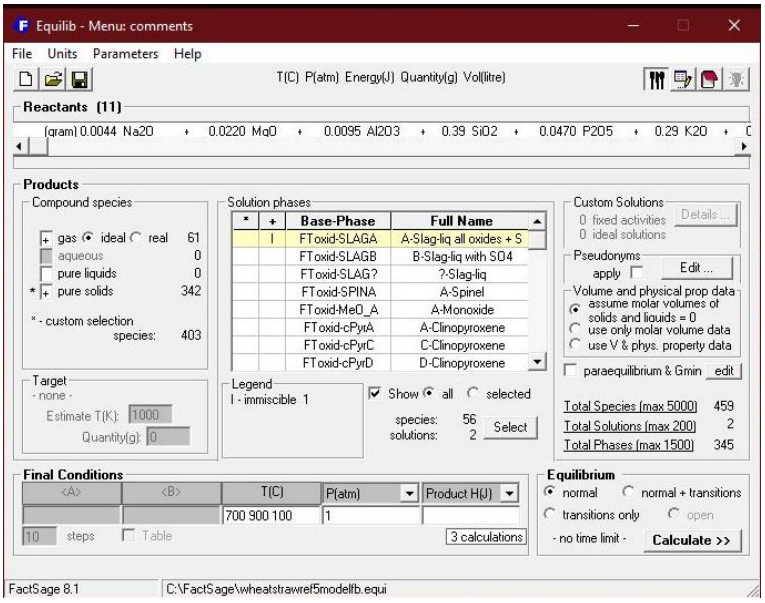

Figure 2-3 Databases settings in the FactSage 8.1.

2.2 Partial least square regression (PLSR) and cross validation

The mathematical approach PLSR associate features and generalises the multivariate regression and analysis of the principal component analysis [201]. It can analyse larger data, and multivariate systems with a high degree of correlation and is better than the multiple regression method [202]. PLSR generally increases the correlation between *X* and *Y* and their convergence system to a minimum and the residual error is always obtained with smaller factors than using principal component regression (PCR) [203]. Figure 2-4 shows the graphical illustration [203] of the technique of the Partial Least Squares Regression (PLSR) which is a statistical method used to correlate the relations between two matrices (*X* and *Y*) by forecasting

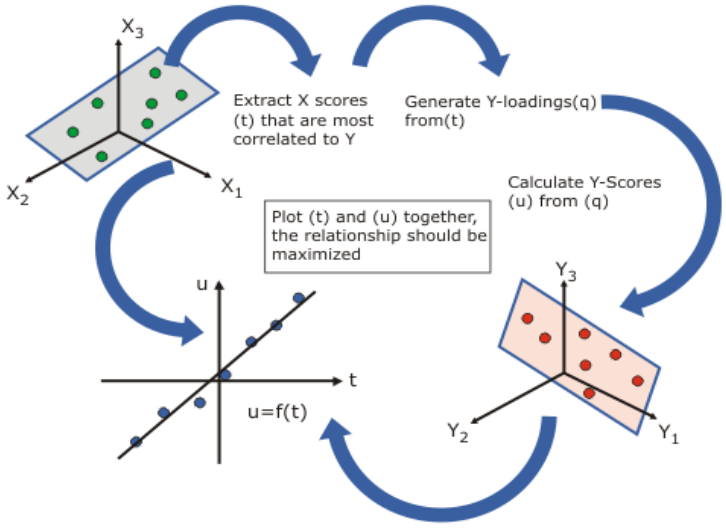

Figure 2-4: PLS Regression graphical illustration of procedure [203].
**Remarks: The t- and u-scores represent the correlation between X and Y on a particular model component.*

the *Y* variables from the *X* variables. It is used when the predictor variables, *X* are many and highly collinear. The process begins with the matrix of predictor variables, *X* which involves finding a linear combination of the *X* variables that explains the variation in the response matrix, *Y* by extracting *X*-scores*, t* that are most correlated with it. First, generate the loadings, *q* for *Y* by using the *X*-scores, *t*. This step involves creating a linear regression model where the *X*-scores, *t* used to predict the *Y* matrix. The loadings, *q* represent the direction of the relationship between the *X*-scores, *t* and the *Y* variables. Second, calculate the *Y*-scores, *u* from loadings, *q*. These *Y*-scores, *u* are the projections of the *Y* variables onto the space defined by the *X*-scores, *t*. Third, plot *t* and *u* together after calculating the *X*-scores, *t* and *Y*-scores, *u*. Ideally, the relationship between these two sets of scores should be maximized which means that the variation explained by the scores in *X* also captures the maximum variation in *Y*. Lastly, the final relationship of a function, *f* shows how the *Y*-scores, *u* relies on the *X*-scores, *t*. In the PLSR method, this function is to predict Y from X. This method is frequently used to identify both the stopping criterion and the total amount of the latent variables while performing cross-validation with only a single observation at a time [202, 204, 205]. PLSR is particularly suitable for problems where fewer observation data are available such as those in the biomass slagging propensity analysis. For more information on the PLSR and the cross-validation technique, please refer to [201, 202, 204, 206-208]. Regression coefficients contained in the PLSR summarise all the predictor-response relationships. The coefficients in the PLS regression can be implemented for any of the components. The original model equation for the raw coefficients can be expressed as follows:

$$Y = B_0 + B_1X_1 + B_2X_2 + \ldots \tag{2-1}$$

The equation 2-1 provided is the general form of a multiple linear regression model, which is used to describe the relationship between a dependent variable, *Y*, and one or more independent variables, $X_1, X_2 \ldots X_\infty$. *Y* is the dependent variable or the predicted outcome variable and B_0 is the intercept term. It represents the forecasted mean value of *Y* when all *X* variables are zero. $X_1, X_2 \ldots X_\infty$ are the independent variables or predictors which are the factors that influence the dependent variable. $B_1, B_2 \ldots B_\infty$ are the coefficients for the independent variables $X_1, X_2 \ldots X_\infty$. These coefficients represent the change in the dependent variable *Y* for a one-unit change in the corresponding independent variable which holds all other independent variables constant. The equation models the work by assuming a linear relationship between the dependent variable and each of the independent variables.

2.3 Ash deposition data of biomass combustion in fixed bed and fluidized bed boilers

2.3.1 Case study i: Fixed bed technology combustor

A total of 28 biomass ash composition datasets were collected from the literature, as shown in Table 2-1 [63, 89, 209-214], which consists of ash compositions, ash content (%) and experimental slagging observations. 8 major ash compositions (MgO, Al_2O_3, SiO_2, K_2O, CaO, Fe_2O_3, Na_2O, P_2O_5) were included in the simulations; however, TiO_2 and SO_3 were excluded due to their low amount in the ash. The first 13 datasets (numbers 1-13) are experimental ash composition data and have been considered as training datasets and the last 15 (numbers 14-28) will be used as testing datasets. The training datasets 1-13 consist of experimental ashes from 13 types of pure wood-based biomass that were chosen due to the availability in the literature of the experimental observation data for the biomass slagging behaviour to determine the slagging propensities of biomass fuels in the combustion. The remaining 15 testing datasets (numbers 14-28) consisting of pure woody biomass were selected based on the fuel and ash analysis carried out by the previous researchers. The experimental observations were visually classified according to a four-graded scale described by Öhman et al. [32]. In addition, the slag quantity was also described as the "fraction of fuel ash that forms slag" (wt%), calculated by dividing the total slag collected from the burner by the entire amount of incoming fuel ash.

2.3.2 Case study ii: Fluidised bed technology combustor

A total of 22 datasets containing biomass ash compositions were gathered from relevant literature sources [215-221], as illustrated in Table 2-2, which consists of the ash compositions, ash content (%) and experimental observations of bed agglomeration in the FBC boiler. 9 major ash compositions (Na_2O, MgO, Al_2O_3, SiO_2, P_2O_5, K_2O, CaO, SO_3, Fe_2O_3) and quartz as a bed material were included in the model, however, TiO_2 was excluded due to its low content in the ash. The initial 10 datasets (1-10) represent the experimental ash composition data and have been designated as training datasets, while the subsequent 12 datasets (11-22) will serve as testing datasets. The experimental observations have been performed in the past by monitoring the bed's behaviour over time at various temperatures. By gradually increasing the temperature in a controlled experimental setup, the temperature at which the bed material stops to behave as a fluidized bed (defluidization temperature) is identified. This temperature is a critical indicator of the onset of severe agglomeration. Furthermore, the samples of the formed agglomerates were collected and conducted for the sintering degree tests. This method helps in understanding the physical characteristics of the agglomerates formed in the FBC combustor.

Table 2-1 Case study i: chemical ash composition for various types of wood-based biomass [63, 89, 209-214].

No.	Biomass	MgO	Al_2O_3	SiO_2	K_2O	CaO	Fe_2O_3	Na_2O	P_2O_5	Ash content (%)	Experimental Observation
1	Pine chips	10.90	4.02	5.49	11.31	45.42	0.95	0.05	7.14	0.25	Low
2	Stemwood II	12.83	1.86	8.67	19.98	47.96	1.05	0.05	7.60	0.31	Low
3	Oak chips	8.13	2.83	1.32	31.94	24.83	0.38	3.64	10.33	0.55	Low
4	Softwood sawdust	5.40	5.10	28.59	14.89	33.17	5.05	1.78	6.02	0.50	Low
5	Sawdust	10.00	10.14	12.91	7.27	28.14	9.58	8.13	13.83	0.2	Low
6	Bark-spruce	4.71	3.23	15.18	10.56	60.73	0.66	0.45	4.49	3.6	Moderate
7	Bark-pine	4.96	11.76	21.88	12.32	46.23	1.80	1.06	5.13	1.9	Moderate
8	Bark	5.08	9.15	31.33	10.67	33.36	3.90	1.84	4.68	4.4	Moderate
9	Scots pine II	5.93	0	50.04	15.25	23.10	0	0	5.68	0.5	Moderate
10	Scots pine III	4.96	0	50.72	17.45	20.27	0	0	6.59	1.1	Moderate
11	Logging residues II	5.84	3.26	31.99	11.95	34.65	1.62	2.33	8.36	2.7	Moderate
12	Wood II	5.50	1.25	48.51	15.18	22.32	1.16	0.72	5.37	0.76	High
13	Bark II	4.69	4.54	28.70	11.39	41.37	2.19	1.64	5.49	3.6	High
14	Stemwood	7.33	0	7.88	19.53	61.87	0	0	3.38	0.2	Low
15	Wood	9.60	2.40	10.12	22.07	48.94	1.55	1.04	4.28	0.30	Low
16	Scots pine	8.88	6.09	25.08	8.33	37.85	2.44	6.60	4.72	0.45	Low
17	Oak sawdust	7.46	2.39	15.80	9.32	39.23	2.48	2.88	2.03	0.82	Low
18	Energy wood	6.87	2.32	11.82	16.64	52.18	1.97	1.86	6.33	1.0	Low

19	Eucalyptus chips	14.11	1.58	4.86	18.83	25.85	0.49	4.04	16.30	0.33	Low
20	Pine sawdust	13.55	4.51	9.72	11.53	39.14	4.87	0.47	3.54	0.53	Low
21	Pulpwood	12.34	0	4.34	29.35	53.97	0	0	5.84	0.7	Low
22	Wood pellets	10.21	8.58	21.09	25.04	28.77	2.69	3.62	4.30	0.57	Low
23	Softwood sawdust II	4.71	6.06	37.58	12.07	27.15	4.93	2.88	4.62	0.7	Moderate
24	Logging residues III	5.16	3.29	32.71	11.51	36.25	1.45	1.19	8.45	2.5	Moderate
25	Pinecone chips	11.03	4.55	9.12	40.03	13.62	0.24	4.09	6.44	1.21	Moderate
26	Scots pine IV	5.17	0	53.85	15.55	25.43	0	0	6.88	1.3	Moderate
27	Logging residues	1.41	11.31	70.47	4.05	6.34	3.80	2.63	1.36	6.4	High
28	Bark III	2.41	9.73	52.19	5.77	20.27	5.09	2.47	2.07	8.6	High

Table 2-2 Case study ii: chemical ash compositions for various types of biomass [215-221].

No.	Biomass	Na_2O	MgO	Al_2O_3	SiO_2	P_2O_5	K_2O	CaO	SO_3	Fe_2O_3	M_f	Ash content (%)	Experimental Observation
1	Logging residues	0.96	5.16	3.08	31.63	5.37	10.44	36.38	5.22	1.75	0.27	2.4	Low
2	Bark I	1.50	3.69	5.08	37.16	2.95	7.95	36.12	3.47	2.09	0.28	3.7	Low
3	Wheat straw	0.85	3.47	0.21	35.86	6.24	31.55	11.73	9.94	0.15	1.00	5.7	High
4	Rapeseed meal	0.20	9.95	0.24	2.16	32.29	17.83	11.31	25.48	0.55	0.40	7.4	Low
5	DDGS-logging residues	0.43	6.68	0.99	12.06	22.15	17.14	12.77	27.08	0.69	0.50	3.2	Low
6	DDGS-wheat straw	0.48	5.64	0.12	17.25	19.71	24.82	6.27	25.50	0.20	0.79	5.05	High

7	Logging residues-PA	0.95	4.99	3.03	31.12	7.82	10.27	35.09	5.01	1.72	0.28	2.4	Low
8	RM	0.19	9.91	0.23	2.38	32.16	17.74	11.47	25.33	0.60	0.43	6	Low
9	Rice straw	0.51	6.74	2.44	24.56	0	7.54	26.72	0	4.46	0.19	n/a	n/a
10	Corncob	2.29	7.24	3.65	32.39	0	15.36	3.67	0	5.40	0.70	n/a	n/a
11	DDGS	0.20	6.99	0.03	3.27	28.65	19.35	2.31	38.98	0.22	0.70	4.4	High
12	DDGS-willow	0.37	6.67	0.38	5.06	25.35	19.69	10.73	31.39	0.36	0.55	3.3	High
13	Logging residues-PA 2	0.89	4.71	2.86	29.36	13.01	9.69	33.11	4.73	1.50	0.39	2.4	Low
14	Rapeseed mean-bark	0.86	7.41	2.15	17.30	19.51	13.59	22.03	15.94	1.22	0.40	4.8	Low
15	Rapeseed cake	7.32	8.41	0.20	1.29	35.69	18.32	13.35	15.07	0.35	0.70	7.5	High
16	Bark II	1.72	4.23	5.36	31.41	3.66	8.46	42.87	0	1.30	0.18	4.9	Low
17	Forest residues	1.22	6.14	2.46	17.93	6.40	15.99	42.02	5.23	2.00	0.16	n/a	Low
18	Wheat straw 2	0.44	2.20	0.95	39.00	4.70	29.00	9.90	3.30	0.95	1.11	7.3	High
19	Thistle	7.70	3.30	2.30	12.00	1.40	9.10	29.00	0	0.87	0.35	8.9	High
20	Almond shell	0.49	2.60	0.49	3.50	2.40	31.00	16.00	0	0.27	0.65	0.94	High
21	Brassica	0.72	2.20	1.30	8.10	3.80	16.00	25.00	0	0.53	0.27	7.7	Low
22	Cotton stalk	3.67	9.00	3.30	6.33	7.33	32.67	17.33	0	1.57	0.67	1.75	High

a) All chemical compositions of ash were measured in wt%.

b) M_f: Melt fraction obtained from the FBC model.

2.4 The 250 kW grate combustor

The combustion testing was conducted at the Waste to Energy site (WtE) in the Translational Energy Research Centre (TERC) using a 250 kW moving step grate boiler (MAGNO-VR) [222]. These types of boilers are specifically intended for the combustion of biomass fuels, and capable of handling high residual water content (up to ~60%). The fuel was fed into the grate by a transfer auger that was connected to the feeding system from the biomass fuel silo to the combustion furnace. The kaolin feeding system line was installed directly to the transfer auger line to ensure the fuel will mix homogeneously with the kaolin powder as shown in Figure 2-5. A hydraulic cylinder is employed to ensure the robust control of the moving

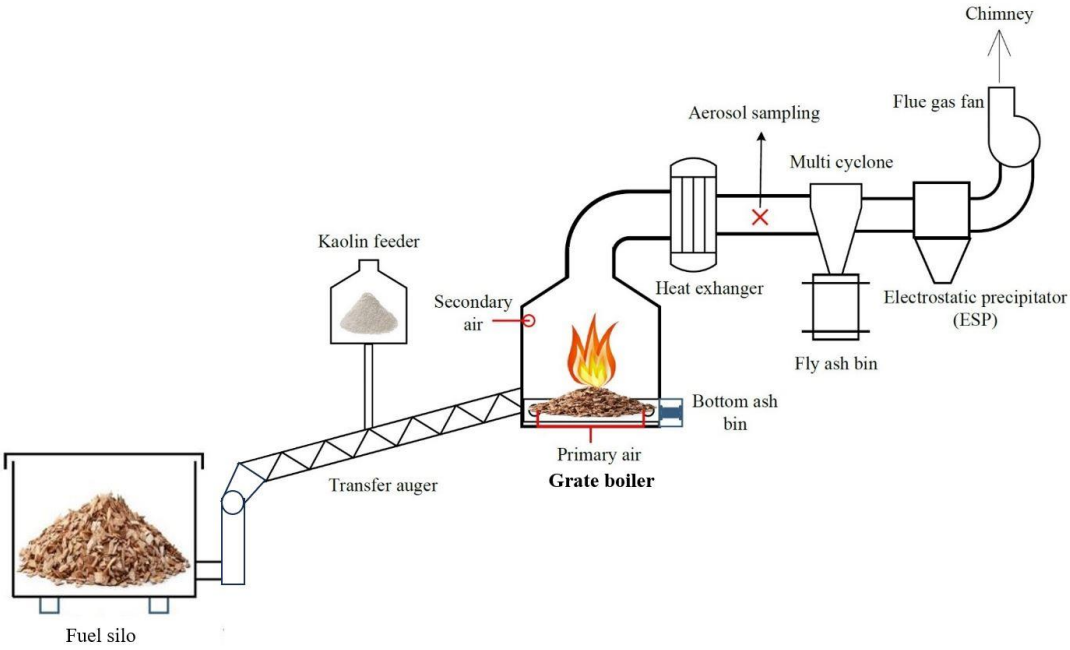

Figure 2-5 Conceptual sketch of the grate boiler combustion system in the TERC facilities.

grate. The grate boiler has dual-walled steel housing design to preheat the combustion air and radiation vault with high-temperature refractory bricks. The combustion air consists of primary air which is blown in from under the grate (Figure 2-6, num. 5) to initiate the firing of the fuels and the secondary air located above the grate, at the top of the side walls (Figure 2-6, num. 6) to complete the combustion process. The distribution of air between these can be modulated. Control of the combustion air is very important in grate boiler firing systems to maintain an optimum bed temperature and combustion process. The bottom ash is automatically discharged at the end of the grate and picked up by the auger to transfer to the bottom ash bin. The flue gas from the combustion chamber is directed to the chimney through the inner tubes of the heat exchanger. Sampling of particles and emissions take place after the heat exchanger. In addition,

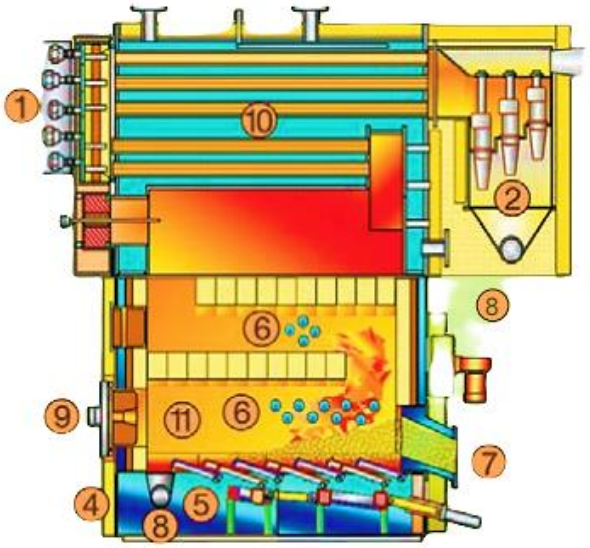

Figure 2-6 Diagram inside of 250 kW Grate boiler by Hargassner [222].

Table 2-3 Detailed description of parts in the 250 kW grate boiler [222].

No.	Parts	Description
1	Automatic heat exchange cleaning	This mechanism is designed to regularly clean the surfaces of the heat exchanger to maintain the efficiency of heat transfer from the combustion gases to the water being heated.
2	Multi cyclone	After combustion, the flue gases contain dust and fly ash particles that need to be removed before the gases are vented.
3	Flue gas fan	This fan is used to channel the flue gases through the boiler and out through the chimney. It ensures the constant flow of flue gases which helps in maintaining an efficient combustion process and in preventing the build-up of gases within the system.
4	Insulation	The boiler is insulated to retain heat, maximize the energy efficiency, and protect the equipment from the high temperatures generated within the combustion chamber.
5	Primary air	Primary air is necessary for the initial combustion process to ignite and stabilize the fire. It is blown in from under the grate to the combustion chamber where the fuel is located.
6	Secondary air	This air is supplied to the combustion process, which is located above the grate, at the top of the side walls. Secondary air provides additional oxygen to completely burn unburned char, fuels, gases and particulates.
7	Fuel stoking	The mechanism automatically feeding the fuels to the grate by the stoker auger which connected the feeding line to the

		grate boiler. It ensures a continuous fuel supply for the combustion process.
8	Automatic ash removal in 50/240-litre ash box	As the fuel burns, fly ash is produced as a byproduct. This system automatically collects the fly ash into the fly ash bin.
9	Combustion chamber door	This door provides access to the combustion chamber for maintenance and inspection such as grate blockage, removal of the slag and bottom ash at the side of the wall of the furnace and on the grate, replace thermocouples and clean the combustion chamber.
10	Heat exchanger	A heat exchanger is the component where the heat from the burning fuel inside the combustion chamber is transferred to the water. The hot gases from the combustion chamber pass through the heat exchanger which usually contains tubes with the water to transfer the heat. It also responsible to maintain the water flow below 85 °C to prevent overheating in the main boiler systems and buffer tank that supply the water.
11	Combustion chamber	The combustion chamber is where the fuel is burned to generate heat. It is where the bottom ash, slags and unburned char formed on the grate.

the flue gas composition (O_2, CO_2, CO, SO_2 and NO_x) was monitored during the testing using the Fourier-transform infrared spectroscopy (FTIR). Next, the fly ash that is captured by the multi cyclone drops down to the fly ash bin (as shown in Figure 2-5). The electrostatic precipitator was installed after the multi cyclone to remove and collect all the fine particles in the flue gas before being discharged through the chimney by the flue gas fan. The operation of the grate boiler must strictly follow the standard operating procedure (SOP_GB01) which is prepared by the site supervisor. Table 2-3 provided a detailed description of the parts involved in the 250 kW moving step grate boiler by Hargassner [222].

2.5 Feedstocks and additive

Table 2-4 shows the composition of two types of feedstocks used in this study which are virgin wood (VW) and waste wood grade A recycled wood (RW) together with kaolin as an additive. The sample of the feedstocks were sent to the Socotec laboratory to carry out the analysis of biofuel (EN-068574). Virgin wood has a slightly higher volatile matter indicating that it may have more compounds that can be vaporized at higher temperature compared to

Table 2-4 Chemical compositions of the feedstocks and additive.

Content	Unit	Virgin wood, VW	Recycled wood, RW	Kaolin, K	Standard
Volatile matter	%	74.60	69.70	-	EN ISO 18123:2015
Fixed carbon	%	13.30	12.30	-	
Moisture content	%	10.90	16.40	-	EN ISO 18134-1:2015
Ash content	%	1.20	1.60	-	EN ISO 18122:2015
C	%	45.33	41.24	-	EN ISO 16948:2015
H	%	5.63	5.18	-	EN ISO 16948:2015
O	%	47.72	51.71	-	
N	%	0.11	0.25	-	EN ISO 16948:2015
S	%	< 0.02	0.02	-	EN ISO 16994:2015
Cl	%	0.05	0.01	-	EN ISO 16994:2015
SiO_2	%	33.00	23.30	48.00	
Al_2O_3	%	2.40	7.30	36.50	
Fe_2O_3	%	3.10	4.20	0.02	
TiO_2	%	3.30	0.50	0.68	
CaO	%	22.20	23.30	0.07	
MgO	%	3.10	4.30	0.30	
Na_2O	%	4.10	2.60	0.10	
K_2O	%	5.80	9.00	1.65	
P_2O_5	%	1.20	2.00	-	
SO_3	%	1.80	10.10	-	
Net calorific value	kj/kg	15253	15013	-	EN 14198:2009

**All values in the Table 2-4 are based on as received basis.*

recycled wood. The SiO_2 amount in the VW is higher compared to the RW which is 33% and 23.3%, respectively. This is potentially due to few reasons: i) the loss of silica oxide components during the use and recycling process of recycled wood, and ii) the high external contamination might be observed in the virgin wood. On the other hand, the K_2O and SO_3 amounts were about 1.5 and 5.5 times, respectively higher in the RW compared to the VW. Therefore, there is high potential that the RW fuel is problematic in the combustion compared to VW. The kaolin employed in this study was fine milled powder (70% of particles <1 μm and 4% of the particles at 8 μm). Kaolin (K) was blended with two woody biomass fuels, virgin

wood and waste wood (grade A recycled wood), at two different dosages (1.55 wt% & 2.5 wt%) based on the fuel compositions as received basis. This process resulted in the creation of 6 fuel mixtures, i.e. VW (pure virgin wood); VWK1.55 (VW + 1.55 wt% K); VWK2.5 (VW + 2.5 wt% K); RW (pure recycled wood); RWK1.55 (RW + 1.55 wt% K); and RWK2.5 (RW + 2.5 wt% K). The ratios of kaolin were selected based on the work by Nowak et al. [179], who suggested that the ratio between the kaolin additive and the fuel should be lower than the ratio used with coal fly ash (< 3.22 wt%). In this study, the minimum ratio of the kaolin addition was set at 1.55 wt%, as this corresponded to the lowest feed rate capability of the screw feeder. The composition of the two different types of fuels and kaolin are shown in Table 2-4. The kaolin additive is made up of mostly silica (48%) and alumina (36.5%). It also contains potassium, however about 3 and 5 times less than the virgin wood and recycle wood, respectively.

Ash Fusion Temperature (AFT) is significant in combustion processes as it indicates the temperatures at which ash will affect the operation of boilers and other combustion systems. The AFT can be categorized into 4 different temperatures which are Initial Deformation Temperature (IDT), Softening Temperature (ST), Hemisphere Temperature (HT) and Fluid Temperature (FT) [122]. The IDT is a temperature at which the ash first begins to deform. It indicates when the ash starts to soften and change shape, which is important to understand how the ash will react as the temperatures increase in a combustion system. ST is the point where the ash becomes semi-solid and is no longer a solid shape. This behaviour is critical because it marks the transition of ash into a state that could potentially cause clinkers or slag in the combustion equipment. HT is a temperature when the ash has deformed into a hemisphere shape. This temperature provides an important indicator of the behaviour of the ash viscosity during the combustion process. FT is a temperature at which the ash becomes fluid-like and flows [122]. It is the highest temperature in AFT and is critical because when ash reaches this point, it can result in the formation of fouling where ash sticks to surfaces and causes blockages or inefficiencies in the system. AFT was analysed in the Socotec laboratory by using ISO 540:2008 standard.

Virgin wood has an initial deformation and softening temperature of 1410 °C, a hemisphere temperature of 1420 °C, and a flow temperature of 1430 °C as shown in Table 2-5. When kaolin is added to virgin wood, the temperatures at IDT and ST were significantly lower which were 1320 °C for IDT and 1350 °C for ST. This is due to the kaolin causing the ash to become reactive at lower temperatures. However, the hemisphere temperature and flow temperature are reduced to a lesser extent from 1420 °C and 1430 °C to 1370 °C and 1380 °C,

respectively. For the RW case, the IDT is 1310 °C, lower than the virgin wood. The ST is slightly higher than its IDT at 1340 °C, with HT and FT being at 1380 °C and 1410 °C, respectively. Similar to virgin wood, adding kaolin to recycled wood also lowers the AFT. The IDT and ST are at 1310 °C and 1320 °C, respectively, with the HT and FT at 1330 °C and 1340 °C. This shows that kaolin has a consistent effect on lowering the ash fusion temperatures which will increase the risk of slagging and fouling in the combustion system.

Table 2-5 Results of Ash Fusion Temperature on two different types of fuels mixed at a ratio 1.55% of kaolin.

Ash fusion temperature (AFT), T °C	Virgin wood, VW	VW + kaolin	Recycle wood, RW	RW + kaolin
Initial deformation temperature, IDT	1410	1320	1310	1310
Softening temperature, ST	1410	1350	1340	1320
Hemisphere temperature, HT	1420	1370	1380	1330
Fluid temperature, FT	1430	1380	1410	1340

2.6 Ash deposits sampling

In this sub-section, the explanation will involve the sample collection of the ash deposits which consists of bottom ash (BA), slag (S), coarse fly ash (FA), the rate of deposition of the coarse fly ash (d_FA) in the primary overpass zone (before heat transfer region) and the particulate matter sampling (PM). There are 3 types of experiments were carried out to mitigate the ash deposit sampling: a collection of bottom ash and slag from the bottom ash bin and on top of the grate, particulate matter emissions sampling and deposit mass uptake of coarse fly ash. A total of about 40 experimental matrices were designed to investigate the impact of kaolin on the formation of ash depositions in a 250 kW grate boiler when firing two types of fuel which are virgin wood and recycled wood with a constant feed rate of 50.2 kg/hr as shown in Table 2-6. The limitation of this study was missing a full-scale mass collection of bottom ash and slag during virgin wood firing due to the continuous requirements of the facility where the flue gas generated by the grate boiler must be channelled to the carbon capture plant facility, preventing shutting down the boiler's operation for sampling purposes. However, representative samples (small-scale collection) for the bottom ash and slag were obtained from the bottom ash (*bottom ash and slag sampling can be done while the furnace is in operation by following the standard of procedure*) bin for the analysis of chemical elements.

Table 2-6 Experimental matrix conducted in the 250 kW grate boiler.

No.	Fuel	Ash deposits sampling	Kaolin dosage (based on fuel mass), %	Fuel ash + kaolin feeding rate (kg/hr)	Run time (min)
1	Virgin wood	d_FA	0	0.60	205
2	Virgin wood	d_FA	0	0.60	500
3	Virgin wood	d_FA	0	0.60	300
4	Virgin wood	d_FA	0	0.60	500
5	Virgin wood	PM	0	0.60	120
6	Virgin wood	PM	0	0.60	120
7	Virgin wood	PM	0	0.60	120
8	Virgin wood	d_FA	1.55	1.38	120
9	Virgin wood	d_FA	1.55	1.38	290
10	Virgin wood	d_FA	1.55	1.38	400
11	Virgin wood	d_FA	1.55	1.38	290
12	Virgin wood	PM	1.55	1.38	120
13	Virgin wood	PM	1.55	1.38	120
14	Virgin wood	PM	2.5	1.86	120
15	Virgin wood	PM	2.5	1.86	120
16	Recycle wood	BA, S, FA	0	0.80	600
17	Recycle wood	BA, S, FA	0	0.80	600
18	Recycle wood	BA, S, FA	0	0.80	600
19	Recycle wood	d_FA	0	0.80	210
20	Recycle wood	d_FA	0	0.80	115
21	Recycle wood	d_FA	0	0.80	300
22	Recycle wood	d_FA	0	0.80	210
23	Recycle wood	PM	0	0.80	120
24	Recycle wood	PM	0	0.80	120
25	Recycle wood	PM	0	0.80	120
26	Recycle wood	BA, S, FA	1.55	1.58	420
27	Recycle wood	BA, S, FA	1.55	1.58	420
28	Recycle wood	d_FA	1.55	1.58	115
29	Recycle wood	d_FA	1.55	1.58	90
30	Recycle wood	d_FA	1.55	1.58	115
31	Recycle wood	d_FA	1.55	1.58	310
32	Recycle wood	PM	1.55	1.58	120
33	Recycle wood	PM	1.55	1.58	120
34	Recycle wood	BA, S, FA	2.5	2.06	420
35	Recycle wood	BA, S, FA	2.5	2.06	420
36	Recycle wood	d_FA	2.5	2.06	180
37	Recycle wood	d_FA	2.5	2.06	80
38	Recycle wood	d_FA	2.5	2.06	250
39	Recycle wood	PM	2.5	2.06	120
40	Recycle wood	PM	2.5	2.06	120

2.6.1 Bottom ash and slag

The bottom ash and slag in a 250 kW grate boiler are by-products of the combustion of biomass fuels. Bottom ash includes unburnt carbon and inert materials and can be found on top of the grate of the boiler. On the other hand, slag is formed when ash components melt and then re-solidify which causes operational challenges such as grate blockage, agglomeration on the grate, reduced efficiency of the heat transfer and high risk of needs a force shutdown of the boiler. These issues have been common in the power generation industry, various studies have been performed in the past to mitigate these issues, and one of them is to mitigate the formation of the bottom ash and slag in the combustion chamber of the grate boiler [83, 89]. The author has explored the effectiveness of blending kaolin with two different feedstocks at varying ratios to address the challenges posed by the formation of bottom ash and slag in the 250 kW grate boiler.

The method begins by collecting the bottom ash and slag from the bottom ash bin and on top of the grate after each completed experiment. Then, the bottom ash (< 3 mm) and slag (> 3 mm) particles were defined by using a circular 200 mm diameter of sieve with a mesh of 3 mm. These sample are weighed to obtain the mass of ash produced during each test performed and some of the representative samples were sent to the micro-preparation lab for sample preparation. This process will be explained in detail in Section 2.7, Laboratory Analysis. The collected ashes (bottom ash and slag) from the combustion experiments were classified visually as shown in Figure 2-7 according to the classification by Öhman et al. [32, 223] as follows:

Category 1: non-sintered ash residue

Category 2: partly sintered ash

Category 3: totally sintered ash (smaller blocks)

Category 4: totally sintered ash (larger blocks)

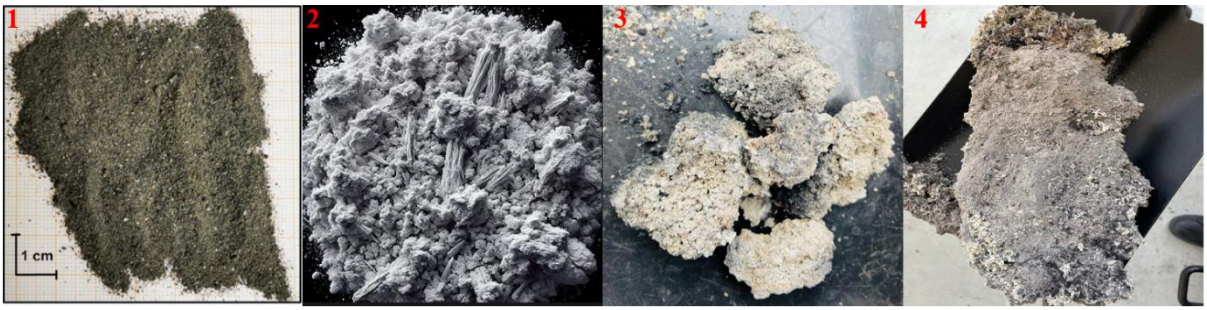

Figure 2-7 Sintering degree classification. The number represented is the explanation by Ohman et al. [29].

2.6.2 Coarse fly ash

The combustion of biomass generates the coarse fly ash (>10 µm) which is carried away with the flue gases. Coarse fly ash is removed from the gas stream using a multi cyclone as illustrated in Figure 2-6. These systems capture the coarse fly ash particles from the flue gases before they are channelled out through the chimney. The coarse fly ash captured by these systems is then conveyed to a multi cyclone fly ash bin ash shown in the Figure 2-8. The multi cyclone bin acts as a repository for the ash collected from the combustion process. It is crucial for mitigating ash deposition issues within the boiler as this coarse fly ash can adhere to the walls in the heat transfer regions, leading to inefficiency of the furnace. Therefore, further analysis needed to understand the behaviour of the coarse fly ash generated from virgin wood and waste wood with the addition of kaolin by analysing the metal elements associated with the fly ash. The sample collection of the coarse fly ash can be obtained from the multi-cyclone bin when the boiler is not in operational mode. The multi-cyclone fly ash bin must be detached

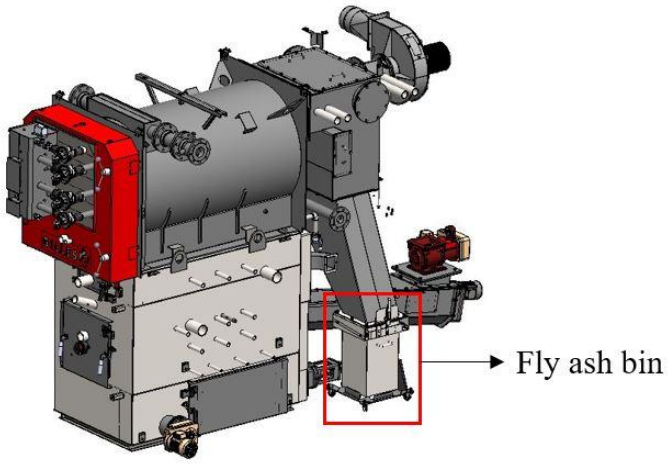

Figure 2-8 Multi cyclone fly ash bin (red square) in a schematic diagram of the 250 kW grate boiler.

from the housing before collected the coarse fly ash sample. This samples then will prepared in micro-preparation lab for further analysis. Detailed explanation on the sample preparation will be explained in detailed in Section 2.7, Laboratory Analysis.

In addition, it is important to analyse the deposition propensity from the firing of both virgin wood (VW) and recycled wood (RW) to observe trends and understand the behaviour of fly ash within the boiler system. Moreover, the addition of kaolin into the VW and RW will provide a better understanding of the impacts of the deposition propensity in the 250 kW grate boiler. Figure 2-9 shows the process involves a device known as an air-cooled probe which is used to collect the fly ash deposits in a 250 kW grate. The probe is made of stainless steel and

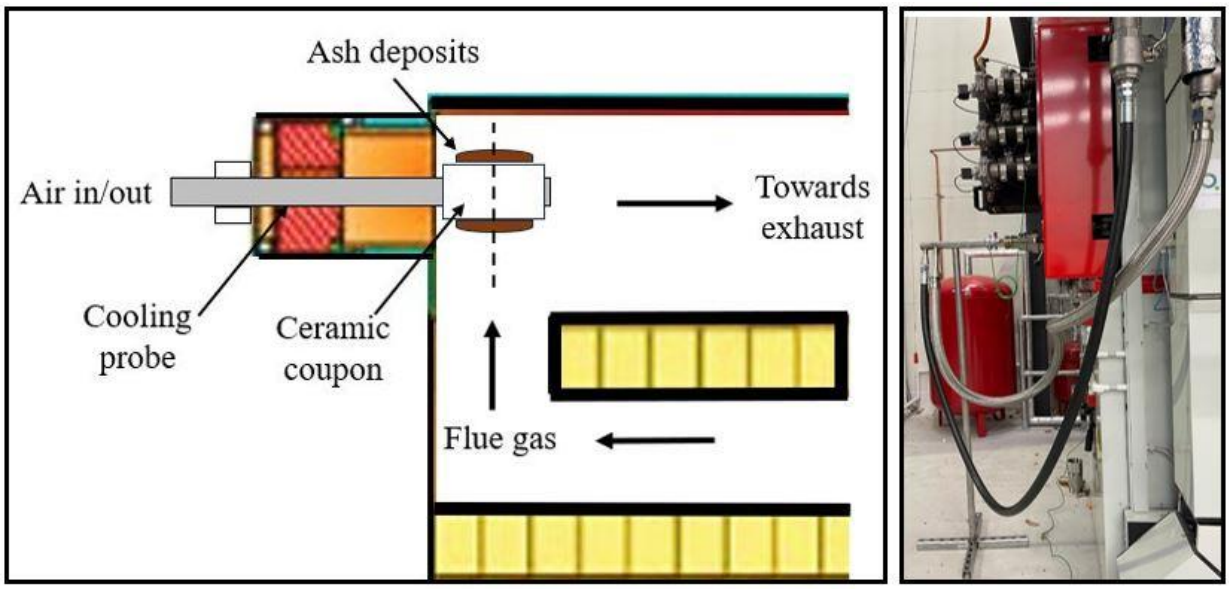

Figure 2-9 Stainless steel probe insertion into the primary overpass region of the grate boiler (area before heat transfer region). left image: Schematic diagram of the probe insertion; right image: side view of the probe installation.

Figure 2-10 A ceramic coupon is installed at the tip of the stainless-steel probe.

equipped with a ceramic coupon at the tip, is designed to withstand high temperatures of approximately 700-750 °C. The process of the probe installation and operation must strictly follow the standard operating procedure (SOP_GB17) which is prepared by the author and approved by the site supervisor. The probe is inserted into the primary overpass zone of the 250 kW boiler which is the area before the heat transfer region where the flue gas path of a boiler. The probe's length is 1.5 m which allows it to reach into the chamber far enough to collect the ash samples directly from the gas stream. The ceramic coupon (37 mm (OD) x 30 mm (ID) x 150 mm (L)) at the tip of the probe as illustrated in Figure 2-10 is exposed to the fly ash in the gas stream. The fly ash particles will adhere or stick to the ceramic coupon's surface as the flue gas passes through the coupon. The air-cooled system was designed to cool down the stainless-steel probe from being overheated due to exposure at a very high temperature of 700-750 °C in the primary overpass zone of the boiler. The piping was designed to supply the air flow rate at 120 m^3/hr with 2 bars of pressure to maintain the temperature of the stainless-steel probe below 90 °C. The probe is removed from the primary overpass zone of the boiler after a specific time of exposure for the fly ash collection. The collected fly ash

on the ceramic coupon will be cooled down for a certain period before weighing the coupon to record the weight difference. This process will be repeated at least 3 times to determine the trend and the relationship of the weight of the fly ash on the coupon with the period time exposure of the coupon in the primary overpass zone of the grate boiler. Then, the process is repeated by using different mixtures of fuel. This study is critical in understanding the behaviour of fly ash in combustion systems especially to observe the deposition propensity of the fly ash when kaolin was added into the different feedstocks.

2.6.3 Particulate matter (PM) emissions sampling

Particulate matter (PM) emissions may have significant impacts on environment and health. This is due to the presence of aerosols in the flue gas which is not efficiently captured by dust collector system such as electrostatic precipitators (ESP). It was confirmed that alkali metals play an important role in the formation of PM emissions [224, 225]. Thus, it is important to mitigate the issues that occurred in the PM emissions due to the release of inorganic elements within the flue gas produced by biomass firing. In this study, the PM emissions was investigated by collecting the sample of PM emissions. At the start of each experiment, the grate boiler was operated for 3 hours to preheat the furnace and establish a stable operating condition before commencing the sampling. The VW and RW firing measurements were replicated 3 times, while those for VWK1.55, VWK2.5, RWK1.55 and RWK2.5 were repeated two times due to the fuel availability. The PM sampling consisted of a PM_{10} cyclone, a Dekati ediluter, a Dekati low pressure impactor (ELPI+), a pressure gauge, and a vacuum pump. The sampling setup can be seen in the Figure 2-11. The flue gas flow rate of 10 L/min was drawn from the central part of the flue duct using a stainless-steel probe with a diameter of 10 mm and directed through a PM_{10} cyclone to remove particles with aerodynamic diameters larger than 10 µm. Next, the

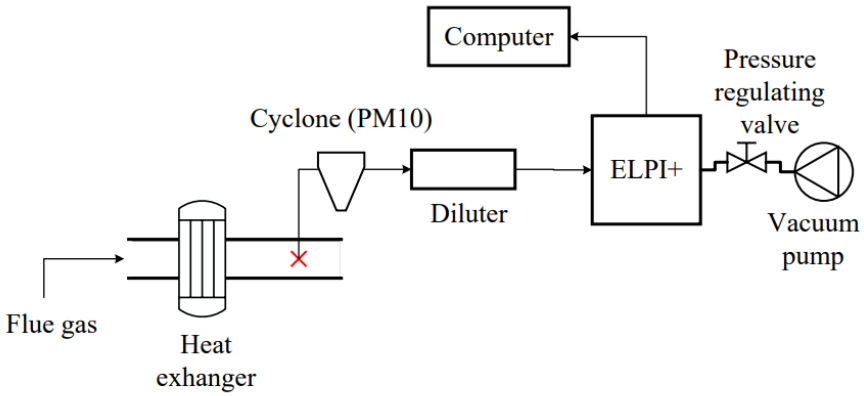

Figure 2-11 Schematic diagram for the PM (aerosols) setup using Dekati instruments.

Figure 2-12 Particulate analyzer: Dekati low pressure impactor (ELPI+).

samples were diluted using an ejection diluter (Dekati® eDiluter™) to provide a homogeneous and stable sample flow throughout the entire measurement system. The total dilution ratio (DR) used was 25. The flue gas was sampled through the ELPI+ as illustrated in Figure 2-12 to determine the number and mass concentrations of particles based on discrete size distributions. The device operates on the principle of inertial separation and consists series of 14 stages (with size ranges of 10 nm – 10 μm) of collection plates. As the aerosol stream passes through each stage, the particulates experience inertial forces due to the change in direction of the flow as it goes through the nozzles. At each stage, particles with a larger aerodynamic diameter are unable to make the turn through the nozzles due to their high inertia and impact on the collection surface while smaller particles remain airborne and proceed to the next stage. Each stage of the impactor has a collection plate where particles of a certain size range are captured. The stages are designed so that each subsequent stage collects smaller particles, allowing for a size distribution to be determined. This is because smaller particles remain in the airstream and pass on to the next stage whereas larger particles are deposited on the plates.

Figure 2-13 shows a set of polycarbonate membrane filters from a Dekati® ELPI+ after collecting ultrafine fly ash particles from biomass combustion. Each filter has captured particles from a different size range as particles passes through it. The polycarbonate filters then will be analysed to determine the elements associated within the PM emissions. This can involve by examining their morphology using Scanning Electron Microscopy and Energy Dispersive X-ray Spectroscopy (SEM-EDS) and assessing particulate matter's chemical composition by Induced Coupled Plasma Mass Spectrometry (ICP-MS).

Figure 2-13 Ultrafine fly ash samples on polycarbonate foil with apiezon-H grease.

The black spots on the filters indicate where the particles have been collected and their distribution of the particulates on the polycarbonate membrane filters. The aerosol particles were collected through a polycarbonate membrane treated with a high vacuum grease (Apiezon-H) which can stand at high temperatures. A tiny layer of grease is applied to the surface of the polycarbonate membrane filter before sampling. The grease acts as a sticky surface to ensure that particles adhere to the polycarbonate membrane filter. This is useful for ultrafine particles that might otherwise not be collected efficiently. In addition, Apiezon-H grease offers an effective seal to prevent air leaks in the sampling apparatus which is to prevent inaccuracies in the measurement of particle concentrations. It is chemically inert and does not react with the particulates being collected. Next, the samples were grouped based on PM_{10} (1 µm < PM_{10} ≤ 10 µm), PM_1 (0.1 µm < PM_1 ≤ 1 µm) and $PM_{0.1}$ (≤ 0.1 µm). To prevent the condensation of acidic gases and agglomeration of wet particles, the sampling probe, cyclone, ELPI+, and the connecting tubes were all heated to a temperature of 180°C. The duration of each measurement lasted for at least two hours to collect a representative quantity of the PM samples.

2.7 Laboratory analysis

This sub-section provides a comprehensive overview of laboratory analysis conducted to analyze samples collected for bottom ash, slag, coarse fly ash and ultrafine fly ash (PM emissions). The steps involve sample preparation to analytical measurement to determine the chemical composition, morphology, characteristics, and behaviour of the samples.

2.7.1 Sample preparation

Sample preparation is the process of selecting representative samples and preparing them according to the standards required for analytical testing. This process adheres to establish protocols to ensure that the samples accurately reflect the composition of the material being analyzed. Proper sample preparation is critical as it directly influences the accuracy and reliability of the test results. The preparation steps might include grinding, milling, sieving, mixing, and drying to meet the specific requirements of the analytical methods employed. By following these guidelines, the author can minimize potential errors and obtain data that is both valid and reproducible.

2.7.1.1 Milling and grinding

Figure 2-14 illustrates the equipment that uses mechanical forces such as compression, shear, friction, and impact to reduce particle sizes of any substances called a TEMA mill machine. The working principle of this machine is aligned with the operation of a ball mill or any similar milling type of equipment available in the market. Figure 2-14 (1) shows a puck and ring grinding vessel used to grind and mill the hard and powder samples to a very fine powder in the least amount of time. The vessels are made of hardened steel, tungsten carbide and zirconia ceramic for maximum strength with minimal weight. The bottom ash, slag and coarse fly ash is placed in the vessel individually as shown in Figure 2-14 (2) to avoid the

Figure 2-14 Procedure to mill the bottom ash and slag samples using a puck and ring grinding vessel.

mixtures and cross-contamination between them. Then, the vessel is closed with a lid with and 'O' ring seal to ensure no samples escape out from the vessel during the grinding and milling process. The vessel then is placed in the clamping mechanism with a self-locking and easy-release mechanism for the grinding and milling process for 90 seconds. Figure 2-14 (3) shows the slag samples have been grinding and milling to the ultrafine powder (~20 μm). The process

is important to prepare samples with the requirement of particle sizes less than 100 µm. Usually, this is essential for the analytical analysis such as chemical elements to ensure samples dissolve or react completely with the solvent.

2.7.2 Sieving and mixing

The process of sieving and mixing ash using a riffle box involves dividing a bulk sample into smaller which are more manageable portions for testing, ensuring that the sub-samples are representative of the whole. First, sieving is required to separate the ash particles after completion of the grinding and milling process. The ash is passed through two sieves with mesh sizes of 50 µm and 20 µm, respectively. After sieving, a riffle box is used to mix the sample and reduce its quantity for testing while maintaining its representativeness. The riffle box (sample splitter) consists of a series of chutes which divide the sample into two halves as the material is poured into the hopper at the top. This ensures that each half is approximately equal and representative of the original sample. The sample can be reduced and prepared based on the requirements for the laboratory analysis by repeatedly passing the sample through the riffle box. The riffle box process is considered economical due to the simplicity of the equipment and the efficiency of the process. For the best results, it is important to use a riffle box with chute widths about 2.5 to 3 times larger than the largest particle in the sample to prevent blockages and ensure the free flow of the material. This method is widely recognized in the industry and when done correctly, can provide a high degree of accuracy, making it a fundamental technique in material testing and quality control.

2.7.3 Moisture and ash content

The moisture content of biomass significantly impacts the combustion efficiency of biomass. High moisture levels require more energy to vaporize the water content, which reduces the net energy output from the biomass fuel [226]. This makes the combustion process less efficient since part of the energy from the fuel is used just to dry it out during combustion. The moisture content of biomass inversely affects its calorific value. The drier the biomass, the higher its energy content per unit mass, making it a more efficient fuel. On the other hand, the ash content is the material that remains after the complete combustion of the biomass. It is primarily composed of incombustible minerals present in the fuel. High ash content can lead to slagging, fouling, and corrosion in the boiler which will affect the performance and increase the frequency of maintenance of the furnace.

Figure 2-15 shows a process to determine the moisture and ash content using standards of EN 18134-1:2015 and EN 18122:2015, respectively in the virgin wood, recycled wood and the mixture of kaolin with both of the feedstocks. This method involves drying and firing the samples using an oven and muffle furnace, respectively. The process of measuring the moisture and ash content can be done simultaneously. First, at least 3 empty crucibles with labels have

Figure 2-15 Representative sample of ash in the crucible for moisture and ash content analysis. Top image (1): Ash before firing in the muffle furnace. Bottom image (2): Ash after firing in the muffle furnace.

measured the weight, w_1 by using a measuring scale. Second, the ash samples are placed in the 3 different crucibles with labels and recorded the weight. This weight can be considered as the wet mass, w_2 (initial weight). Third, the crucibles contained ash samples then is dried in the drying oven at a temperature of 105 °C for 24 hours. The samples are dried until they reach a constant weight, ensuring that all moisture is removed. Fourth, the samples is placed in the desiccator for at least 15 minutes to cool down to room temperature before measuring theirweight after the drying process. This weight is called the dry weight, w_3. The moisture content can be obtained based on the equation 2-2 as follows:

$$Moisture\ content, MC = \frac{w_2 - w_3}{w_2} \times 100\% \quad (2\text{-}2)$$

The drying process is important in obtaining the ash content because the moisture content can significantly affect the weight of the samples, resulting in inaccurate measurements of the ash content. Initially, the ash samples are fired in a muffle furnace at 550 °C after the drying process. The muffle furnace setting was set at 3 hours for the dwell time and 1.5 hours

for the cooling period. The samples were placed in a desiccator for at least 30 minutes to cool down before weighing the samples, w_4 after completing the firing process in the muffle furnace. The ash content can be determined by applying the equation 2-3 as follows:

$$Ash\ content, AC = \frac{w_4 - w_1}{w_3 - w_1} \times 100\% \quad (2\text{-}3)$$

Table 2-7 presents the analysis of the moisture content and ash content of the fuels (VW & RW) with the addition of kaolin. The moisture content in the woodchips was decreased in line with the kaolin addition at 1.55% and 2.5%, from 10.90% to 10.23% and 9.02%, respectively. This trend was also observed in the recycled wood case. However, the ash content increased for both cases (woodchips & recycled wood) when blending with kaolin. The ash content for the woodchips is 1.2% and this increases to 2.54% and 3.62% when adding 1.55% and 2.5% kaolin, respectively. The ash content in the recycled wood was 1.6%, which increased to 2.96% and 4.16% after mixing in the kaolin, respectively. The results obtained from the ash content indicated an increased slagging tendency and the possibility of a high amount of bottom ash formation during the testing.

Table 2-7 Moisture and ash content analysis.

Fuel mixture	Moisture content (%)	Ash content (%)
Virgin wood (VW)	10.90 ± n.a.	1.20 ± n.a.
VWK1.55	10.23 ± 0.05	2.54 ± 0.05
VWK2.5	9.02 ± 0.05	3.62 ± 0.09
Recycled wood (RW)	16.40 ± n.a.	1.60 ± n.a.
RWK1.55	10.60 ± 0.19	2.96 ± 0.13
RWK2.5	9.72 ± 0.07	4.16 ± 0.11

2.7.4 Chemical Elements Analysis

The analysis of the chemical elements in the ash produced from biomass firing is essential in the combustion research area. This will help the researcher to have a better understanding of the inorganic element's behaviour in mitigating the ash compositions of any particular biomass fuel. Inductively Coupled Plasma Mass Spectrometry (ICP-MS) is an analytical method used for detecting inorganic elements of biomass ash at very low concentrations [227, 228]. It is a highly sensitive technique that can measure trace elements in various types of samples up to parts per trillion (ppt). In this sub-section, a detailed explanation of the digestion method used to analyse the bottom ash, slag, coarse fly ash and ultrafine fly

ash by ICP-MS. The sample preparation for the digestion method of bottom ash, slag, and coarse fly ash, described in Section 2.7.4.1-2.7.4.2 was carried out by the laboratory of the School of Chemical and Process Engineering, University of Leeds as part of their analytical services. The digestion method for ultrafine fly ash in Section 2.7.4.3 was performed by the analytical laboratory of the Chemistry Department, University of Sheffield.

2.7.4.1 Bottom ash, slag, coarse fly ash digestion method

First, the ash samples were weighed approximately 0.4 g in the 60 ml polypropylene beaker. Then, the beaker was placed in the fume cupboard. Second, 2 ml of distilled water was added to the beaker, then swirl the distilled water before adding 10 ml of Hydrofluoric (HF) acid. Third, place the beaker that contained the solutions into the steam bath to evaporate the HF acid. It must be noted that Hydrofluoric acid is an extremely corrosive and toxic substance. This procedure must strictly follow the control of substances hazardous to health (COSHH) and risk assessment provided by the laboratory officer. In addition, HF acid handling only can be done by the professional trained officer. Fourth, the polypropylene beaker was placed again in the steam bath for 10 minutes to dry the residue of 10 ml HF acid. Fifth, the beaker was taken out from the steam bath and 30 ml of distilled water was poured into the beaker and allowed it to cool. Sixth, the contents of the beaker is washed and rinsed using 400 ml Pyrex beaker, then the Pyrex beaker is placed on the hot plate to dry the residues. Seventh, the Pyrex beaker was removed from the hot plate and allow it to cool before adding 3 ml of H_2SO_4 and place it back on the hot plate. The final stage of this solution preparation required care as the residue must not be allowed to dry. White sulphuric acid fumes must persist for at least 5 minutes. Eighth, the Pyrex beaker was removed and allowed to cool before carefully adding approximately 200 ml of distilled water, then place the Pyrex beaker back on the hotplate for 30 minutes. Last, the Pyrex beaker was removed from the hot plate and allowed to cool down before transferring the solutions to a 250 ml volumetric flask. The solutions was stored in 50 ml plastic bottles for the ICP-MS analysis to obtain P_2O_5, Al_2O_3, CaO, Fe_2O_3, K_2O, MgO, and Na_2O.

2.7.4.2 Silica by colorimetry

The process of analyzing silica by colorimetry is designed to quantify the amount of silica (SiO_2) in a biomass ash sample. Colorimetry is a technique that measures the intensity of the colours in a solution, which can be correlated with the concentration of SiO_2. When analyzing silica, this involves a reaction that produces a coloured compound proportional to

the silica content. The first step involves preparing the sample so that the silica is in a form that can react with the reagents used in the colorimetric analysis. The reagents needed were Ammonium molybdate, a 10% of the concentration of Tartaric acid, and a reducing solution. The first step required to pipette 10 ml of solution A, 10 ml of each standard solution, and a blank solution into separate 100 ml volumetric flasks. Then, 50 to 60 ml of water is mixed and diluted to each of the 100 ml volumetric flasks. Next, 1.5 ml of ammonium molybdate solution was added by using a measuring pipette, then mixed and allowed to stand for 10 minutes. Last, the tartaric acid solution was pipette at 4 ml followed immediately by 1 ml reducing solution into the first 100 ml volumetric flask and mixed the solutions, then the contents of this volumetric flask must be diluted immediately to the specific level of the volumetric flask or "mark" and stirred them before proceeding to the next 100 ml volumetric flasks. The solutions are allowed to stand for one hour before determining its absorbance at 650 nm using the blank solution as a reference.

For solution A, initially, the sodium hydroxide was weighed for 1.5 g in a nickel crucible covered with a nickel lid and heated to melt the sodium hydroxide by using a burner. Second, the ash sample was weighed approximately 0.05 g before being transferred to the sodium hydroxide that had been cooled down. Third, the crucible that contained the ash samples and cold sodium hydroxide was heated and gently swirled to ensure no particles of the ash samples floated on the surface of the melted sodium hydroxide. The process was continued to heat the crucible with the sample for about 5 minutes at a dull red heat, and then remove the crucible from the flame. Last, the melted sample was gently swirled or rotated around the sides of the crucible and allowed to cool. This technique ensures that the entire volume of the sample is evenly exposed to the cooling process. Please refer to equation 2-4 to calculate the percentage of SiO_2 as follows:

$$SiO_2(\%) = \frac{A1 \times C \times V1 \times V3 \times d}{A2 \times W \times 10^4 \times V2} \quad (2\text{-}4)$$

Where:

A1 = absorbance of sample

A2 = absorbance of standard

C = concentration of standard mg/L

V1 = aliquot of standard

V2 = aliquot of sample

V3 = original volume

W = weight in g

d = 10

2.7.4.3 Polycarbonate membrane (ultrafine fly ash ≤ 10µm) digestion method by HNO_3-H_2O_2 with microwave digestion.

Working principle of the microwave digestor, Ethos X:

The Ethos X system is designed to use microwave energy to rapidly heat samples in a controlled manner to break down complex matrices using strong acids or reagents which prepare the samples for elemental analysis. A rotating platform that ensures uniform exposure of all samples to the microwave energy. The tall cylinder is a microwave-transparent vessel designed to withstand high pressures and temperatures that occur during digestion as shown in Figure 2-16. Samples and reagents are sealed within these vessels. The vessel is placed into the microwave digestion system. The microwave energy heats the samples uniformly, causing the solvent or acid to react with the sample and leading to its dissolution. After the digestion is complete, the vessels are cooled with excess pressure and is safely released. The digested sample is transferred to a container for ICP-MS analysis. The microwave digestion method is favoured because of its speed, efficiency, and ability to digest difficult samples that might not dissolve easily with other methods. It's also advantageous because it can minimize the loss of volatile elements and the risk of contamination during the digestion process.

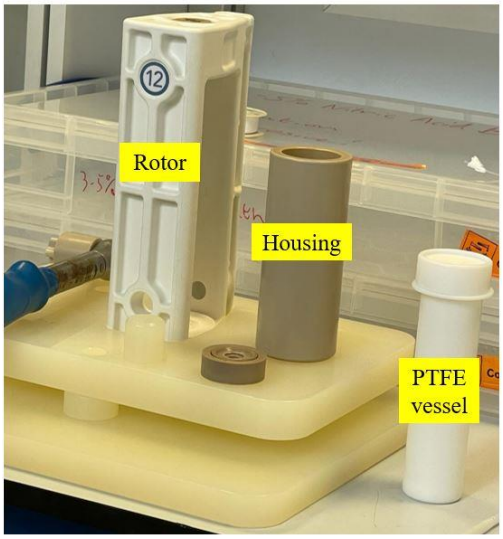

Figure 2-16 Microwave digestion vessels and accessories for sample preparation.

Digestion method:

The PM samples collected by the polycarbonate membrane filter were digested with a microwave, assisted with 69% concentration of HNO_3 and 30% concentration of H_2O_2, and analysed with the inductively coupled plasma mass spectrometry (ICP-MS) to investigate the

concentration of the element compositions which were SiO_2, Al_2O_3, CaO, K_2O, MgO and Na_2O. To ensure data consistency, the average of a minimum of three samples, including one from each of the 3 repetitions for each fuel mixture was ascertained to determine the elemental concentrations via ICP-MS. To begin with, the polycarbonate membrane filter contained the particulate samples as shown in Figure 2-13 was weighed accurately to 4 decimal places and it has been transferred to the PTFE vessels as illustrated in Figure 2-16. PTFE vessels then was placed in a fume cupboard. Second, 9 ml of 69% HNO_3 and 1 ml of 30% H_2O_2 were added into the PTFE vessels containing PM samples by using a measuring pipette. Third, closed and secured the PTFE vessels with the lid and the PTFE vessel was placed into the rotor as shown in Figure 2-16 using the tools provided. Then, the rotor was placed in the microwave digestor, Ethos X as illustrated in Figure 2-17. The microwave digestion program for the temperature was set at 210˚C with the ramp rate at 210˚C/20 minutes, the dwell temperature at 210˚C/40 minutes, and the cooling period for 15 mins. This is the optimum setting found by the author for the digestion of the polycarbonate membrane (fly ash $\leq$ 10 µm). Upon completion of the microwave digestor, the rotor was transferred to the fume cupboard together with the tools needed to open the pressurised PTFE vessels. It must be noted that some nitric oxide gas will be diffused out from the PTFE vessels during the opening of the PTFE vessels. It is required to ensure to open the fume cupboard with the shield as low as possible. Next, the digestion solution from the PTFE vessel was transferred into the 50 ml centrifuge tube that contains

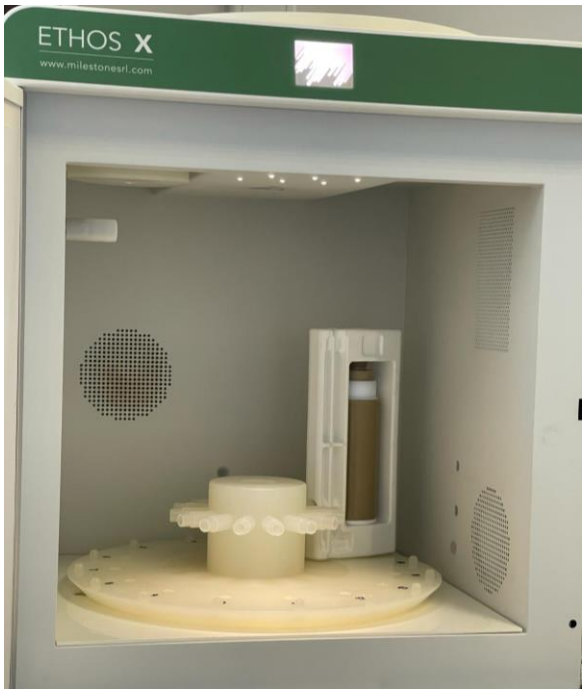

Figure 2-17 A laboratory microwave digestion system, Ethos X.

10 ml of 1% of the concentration of HNO_3. The rinse process took place to clean any residues in the PTFE vessel with 1% concentration of HNO_3 with 3 times repetition. Then, the digestion solution was diluted by adding 1% HNO_3 into the 50 ml centrifuge tube up to the 50 ml line. Last, the centrifugal tube was closed with the lid and inverted the tube to ensure the digestion solution was mixed well in the tube. The 50 ml centrifuge tube containing the digestion solution may require placing in the ultrasonic bath for 48 hours to dissolve any residues left. The sample was then sent to the ICP-MS lab *(details of ICP-MS calibration can be found in the Appendix)* for the analysis of SiO_2, Al_2O_3, CaO, K_2O, MgO and Na_2O. It was compulsory to wear chemical-resistant gloves and safety goggles all the time and all the preparations and acid handling must take place in the fume cupboard to ensure safety in the chemical lab.

2.7.5 X-ray diffraction (XRD)

X-ray diffraction (XRD) is a technique used to study the structure of crystalline materials. XRD analysis plays a critical role in understanding the ashes produced from the combustion of biomass which have undergone the chemical transformations to form crystalline structures at high temperatures [229]. Understanding the mineralogical composition of biomass ash through XRD analysis is vital for predicting its behaviour in combustion systems. This information is crucial in assessing the ash's reactivity and melting temperature as it impacts the possibility of clinker and slag formation which can adhere to boiler surfaces and reducing heat transfer efficiency and potentially leading to operational issues. Additionally, the identification of specific mineral phase compounds that may form during combustion is important as these compounds may significantly affect boiler operation by promoting slagging.

The working principle of XRD [230] is when the crystalline structure causes a beam of incident X-rays to diffract into many specific directions. By measuring the angles and intensities of these diffracted beams, a crystallographer can produce a three-dimensional picture of the density of electrons within the crystal. The mean positions of the atoms in the crystal can be determined, as well as their disorder, chemical bonds, and various other information from the electron density. The X-ray beam penetrated directly into the samples which caused the atoms in the samples to be scattered when hit by the X-ray. As the wavelength of X-rays is similar in scale to the distance between the atoms in the crystal, they can be diffracted in a coherent pattern. As the scattered waves interfere with one another, constructive interference (amplification) occurs at specific angles for specific spacings of atoms within the crystal. This is described by Bragg's law in the equation 2-5 [231] as follows:

$$n\lambda = 2d \sin\theta \quad (2\text{-}5)$$

where λ is the wavelength of the X-rays, d is the distance between atomic layers in the crystal, θ is the angle of incidence, and n is an integer representing the order of the diffracted beam. The diffracted X-rays are then detected, processed, and counted. A detector measures the number of photons at each diffraction angle, and the data are converted into a diffraction pattern, which is a graph of the intensity of the diffracted X-rays versus the angle of diffraction. The resulting pattern of peaks can be analyzed to determine various properties of the material (ash). Each material will have a characteristic pattern of diffraction, which can be used to identify the phases present in the samples of the crystalline structure.

Figure 2-18 shows a set of powder samples for XRD analysis. These samples were prepared by grinding the material to a fine powder as explained in Section 2.7.1. The powder is then pressed evenly into a sample holder ring with a flat surface to ensure that the X-rays can penetrate the samples uniformly. The standard sample holder ring's internal diameter is 16 mm and the thickness is 2.4 mm. Next, these samples was placed in an instrument called the PANalytical X'Pert Powder system, which is an X-ray diffraction (XRD) system using the source of Cu radiation as illustrated in Figure 2-19. The PANalytical X'Pert Powder system is used for phase identification and quantification, phase transitions, crystallography, and structure. The samples were placed inside the machine, where it was exposed to an X-ray beam. The X-rays interact with the samples producing a diffraction pattern, which can be detected and recorded. The standard operating value of this X-ray equipment is 45 kV and 40 mA. The equipment was set to the reflection mode by using the settings of Reflection-Transmission

Figure 2-18 Six sample holders for mounting specimens (ash) for XRD analysis.

Figure 2-19 PANalytical X'Pert^3 Powder machine for XRD analysis in Royce Discovery Centre (RDC), University of Sheffield.

spinner PW3064/60. The start and stop angle (degree 2Theta) were set at 5° and 70°, respectively. The aperture size of the programmable divergence (PDS) was set at 1/8° while anti-scatter (AS) slits were set at 1/4°. The specific pattern of diffraction (peaks at certain angles with specific intensities) is unique to the crystal structure of the material in the sample, allowing for precise identification and analysis. This model comes with software that allows for sophisticated data analysis, which could include comparing the diffraction data to known standards or running full pattern fitting to identify the crystalline structures present in the sample.

2.7.6 SEM-EDS

Scanning Electron Microscopy (SEM) is a type of electron microscope that produces images of a sample by scanning the surface with a focused beam of electrons. The electrons interact with atoms in the sample, producing various signals that can be detected and translated into high-resolution images [232]. This allows for the detailed observation of the surface topography and morphology of the bottom ash, slag and coarse fly ash. Figure 2-20 shows the Hitachi TM3030 Plus, which is a model of a table top Scanning Electron Microscope (SEM). It is equipped to handle a variety of samples with minimal preparation. It can provide high-magnification images with a depth of field and resolution that far exceed what's possible with

Figure 2-20 Hitachi TM3030 Plus model of Tabletop Scanning Electron Microscope (SEM).

optical microscopes. This SEM can accommodate a range of sample types and sizes, often without the need for extensive preparation. It typically includes a backscattered electron detector (BSED) for compositional contrast imaging and a secondary electron detector (SED) for detailed topographic imaging. Energy Dispersive X-ray Spectroscopy (EDS) is an analytical technique used for elemental analysis or chemical characterization of a sample. When the electron beam interacts with the sample in SEM, it can eject inner-shell electrons from the atoms in the sample. As the atoms return to their ground state, they emit X-rays at energies characteristic of their specific elements. EDS systems detect these X-rays and quantify the elemental composition of the material under study. By analyzing the energy and intensity of the emitted X-ray signals, EDS can determine the elements present in the sample and their relative abundance. In this thesis, the author used 3 different techniques to analyse the biomass ash samples under SEM.

Carbon adhesive tape

Figure 2-21 shows a powder sample that has been mounted on carbon tape for scanning electron microscopy (SEM) analysis. A double-sided adhesive carbon tape is used to secure the powder sample to the sample holder or stub. Carbon tape is used for its electrical conductivity, which is important for SEM imaging to prevent charging effects on the sample. Powders can be challenging to analyze due to their tendency to scatter electrons and charge under the electron beam. Attaching the powder to carbon tape helps to stabilize the sample and provides

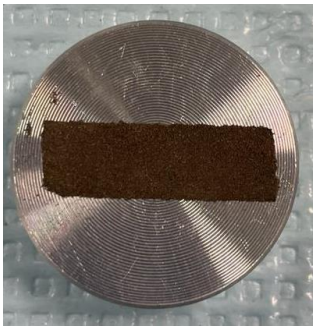

Figure 2-21 Bottom ash samples on the carbon adhesive tape for SEM-EDS analysis.

a conductive path for electrons to the ground by reducing electrical charging effects [233]. In SEM, a focused beam of electrons is scanned across the sample. The electrons interact with the atoms in the sample, producing various signals that can be collected to form images with nanometre-scale resolution. The same electron interactions that produce the SEM image also emit X-rays characteristic of the elements present in the sample. The sample on the carbon tape was placed in the SEM's vacuum chamber. As the SEM scans the sample, it produces detailed images of the powder's surface topography. This preparation method is vital for getting clear images, especially for powders that may not be inherently conductive.

Cold mounting by epoxy resin

The process of cold mounting with epoxy resin is commonly used in materials science to encapsulate a sample for microscopy. It is useful for delicate or brittle materials such as the solid slag byproduct from biomass combustion, as the process doesn’t involve the application of heat which could change the sample's structure. Initially, the granular slag sample is cleaned to remove any loose particles or contaminants and then placed into a blue mounting cup as shown in Figure 2-22. Two parts of epoxy resin which consists of a resin and a hardener were mixed in the 2:1 ratio. The mixture needs to be stirred thoroughly to ensure a uniform blend and avoid any air bubbles. The mixed epoxy is carefully poured into the mould covering the slag sample. It's important to pour slowly and in one spot, allowing the epoxy to envelop the sample and further prevent air bubbles. The mould with the epoxy will be placed in a vacuum chamber to remove any trapped air bubbles as shown in Figure 2-22 (right image). Next, the filled mould is left to cure at room temperature for 24 hours. Once the epoxy has fully cured and hardened, the mount is removed from the mould which contains the slag sample completely encapsulated in a block of epoxy as illustrated in Figure 2-23. The mounted sample is often trimmed to remove any excess resin and then polished. Polishing should be done carefully to reveal a flat, smooth surface of the sample for examination without introducing scratches.

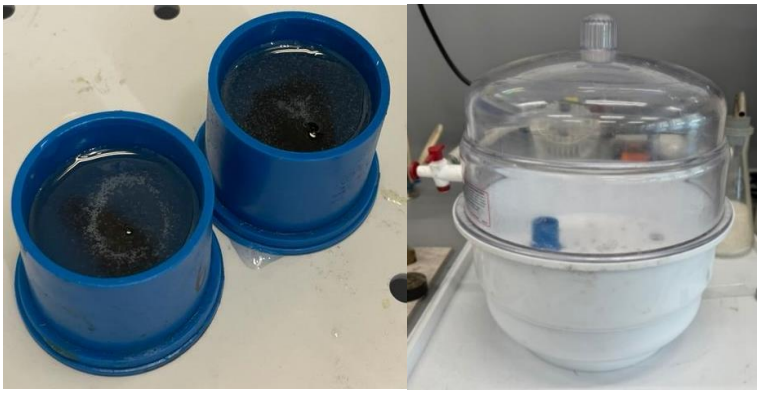

Figure 2-22 Left image: slag samples mount in epoxy resin. Right image: the vacuum chamber to remove air bubbles in the epoxy resin.

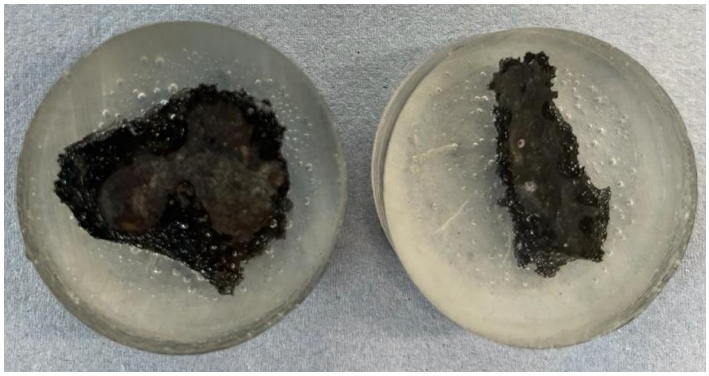

Figure 2-23 Slag sample finishing in cold mounting by epoxy resin.

Figure 2-24 Buehler AutoMet 250 for grinding and polishing specimens.

Buehler AutoMet 250 is an automatic grinding and polishing machine as shown in Figure 2-24. This is a machine designed for grinding and polishing materials in preparation for microscopic testing. The machine's grinding feature involves using progressively finer abrasive grits to remove material from the sample surface. This was to create a flat, even surface that

can be analyzed. After grinding, the sample surface was polished to produce a highly reflective surface free of scratches and deformities. This was done using fine abrasive particles in a liquid medium. The machine has a water supply to keep the sample cool during grinding and polishing and to help remove any remaining debris or abrasive from the sample surface. The Buehler AutoMet 250 also allows the user to set parameters such as the speed of the plate, the force applied to the sample, and the duration of grinding and polishing based on the guidance provided in the Buehler manual catalogue. The finely polished surface is then examined under SEM to observe the morphology and behaviour of the slags.

Gold coating

Two particulate matter emission samples from polycarbonate membrane filters were mounted on stubs and coated with a thin layer of gold as presented by Figure 2-25. The gold coating serves to make the sample conductive, thus preventing the accumulation of electrical charge when it is bombarded with electrons in the SEM. Gold is a common choice because it is highly conductive, does not oxidize, and produces an even coating [234]. In addition, the gold coating was used in this procedure due to the very light sample behaviour. It was almost impossible to observe the ultrafine fly ash samples on a polycarbonate membrane filter without mounting or attaching the filter with any mechanism. This is because high risk that ultrafine fly ash will be blown away during the suction of the vacuum pump in the SEM machine. Thus, mounting the samples with the gold coating technique is the best solution.

The samples were placed on two stubs individually, which are small platforms that can be inserted into the SEM. The samples on the stub were placed inside the chamber of a sputter coater which is a device used to apply the coating. The air inside the sputter coater chamber is pumped out to create a vacuum. This reduces the possibility of interference from other gases during the coating process. Inert argon gas is then introduced into the chamber at a controlled low pressure. Argon is used because it is an inert gas and will not react with the gold or the samples. An electric field is applied to ionize the argon gas, creating positively charged argon ions. The charged ions are accelerated towards a piece of gold. Upon making contact with the gold, the high energy of the accelerated ions is sufficient to dislodge atoms from the gold itself. These atoms travel through the chamber and uniformly coated the samples.

The amount of gold deposited is monitored to achieve a coating thickness between 2 and 20 nm, depending on the requirements of the SEM-EDS analysis. After the coating reaches the desired thickness, the inflow of argon gas is stopped, and the vacuum is broken by slowly venting the chamber with air. The gold-coated samples were transferred to the SEM-EDS

Figure 2-25 Specimen samples of ultrafine fly ash (<10µm) with gold coating for SEM-EDS analysis.

analysis equipment. The conductive coating allows for better imaging and analysis because it prevents the accumulation of static charge on the sample surface. The coating must be thin to avoid masking the sample's features but thick enough to allow for conductivity. In EDS analysis, which detects X-rays emitted by the sample as a result of being hit by the electron beam, the coating must be accounted for in the analysis, as it will contribute to the X-ray signal detected. The gold layer's atomic number is high, which means it can significantly affect the detection of lighter elements and this is considered when interpreting EDS results. The gold coating ensures that the SEM-EDS analysis yields clear images and accurate compositional data.

2.7.7 Thermogravimetric analysis (TGA)

Thermogravimetric Analysis (TGA) is a method used to determine the thermal stability, composition and characterization of biomass ash which consists of bottom ash, slag and coarse fly ash [235]. TGA measures the mass of a substance as it is heated, cooled, or held at a constant temperature. It's useful for studying the combustion and thermal decomposition of biomass. Figure 2-26 shows the TGA machines (model: TA Q50) that have been used to analyze the thermal stability and behaviour of byproducts of biomass firing. First, about 10 mg amount of biomass ash is prepared and placed in the TGA instrument's sample pan. Second, the sample pan is placed in a furnace where the pure oxygen gas will be used to burn the sample at 1000 °C. The heating ramp was programmed to increase at a rate of 20 °C/10 minutes and dwell time of 10 minutes once the target temperature of 1000 °C was reached. As the temperature increases, the TGA instrument continuously measures the mass of the biomass ash sample. Any change in mass which might be due to loss of moisture, combustion, or decomposition of various constituents is recorded. Several pieces of information on biomass ash combustion behaviour can be determined through TGA, such as moisture content, volatile matter content, ash content and the thermal decomposition profile. For biomass ash analysis, TGA can provide

an understanding of the temperature at which various components of the ash will decompose or react, which is crucial for managing ash-related issues in biomass combustion systems.

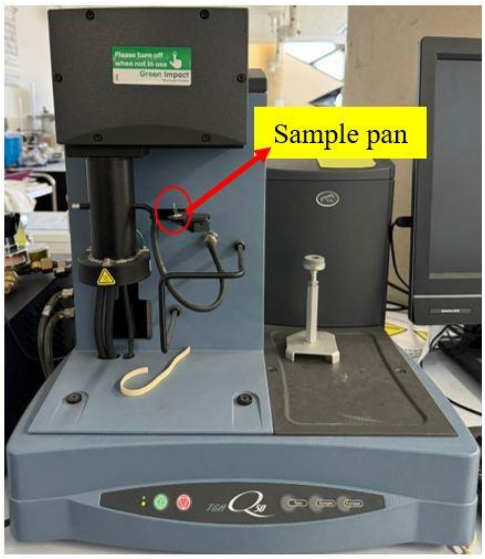

Figure 2-26 TGA machine TA Q50 used in Diamond facilities, University of Sheffield.

2.8 Summary

Overall, the methodology of this thesis is to address the challenges of ash deposition, slagging and bed agglomeration in biomass-fired boilers. This is structured into several key stages that combine theoretical modelling, comprehensive literature review and experimental works. The development of a thermodynamic equilibrium model with the integration of partial least square regression (PLSR) coupled with cross-validations provides a deeper understanding of the impacts of the chemical compositions of biomass on combustion behaviour in boilers. The work has been based on desktop literature reviews of published documents, such as research papers published in journals and conferences to gather all the data required to develop predictive modelling in Chapters 3 & 4. For experimental approaches, the methodology integrates both experimental investigation and analytical assessment in a 250 kW grate boiler system to evaluate the impact of kaolin addition on the combustion characteristics of biomass fuels. This includes fuel preparation which consists of virgin and recycled wood with a mixture of kaolin at ratios of 1.55% and 2.5%. Next, the boiler is fired with each fuel mixture under controlled conditions to maintain the consistency of the experimental trials. The operating parameters such as temperature, airflow, and feed rate are monitored and kept constant to ensure the comparability of results. During the firing process, observations are made regarding the behaviour of the fuels and the formation of ash deposits. Samples of ash deposits are collected for each fuel mixture after completing the firing. The collected bottom ash, slag,

coarse fly ash and ultra-fine fly ash samples were analyzed for their physical and chemical properties. Despite the limitations during the experiment, the author successfully carried out the testing to mitigate the ash deposition issues in the boiler by ensuring comprehensive data collection without necessarily disturbing the boiler's operation. The methodology employed in the thesis is designed to provide a thorough understanding of the mitigation of ash deposition, slagging and beg agglomeration in biomass-fired boilers through prediction model and experimental approaches.

3 An improved index to predict the slagging propensity of woody biomass on high-temperature regions in utility boilers.

3.1 Introduction

Ash deposition-related issues adversely affect the thermal transfer and cause corrosion to biomass fired utility boilers. To ensure that biomass combustion is safe in power generation boilers due to the slagging formation, the slagging tendency of biomass combustion must be predicted [86, 87] so that measures can be taken to reduce the slagging if necessary [84, 88, 201]. There has been gaining a lot of interest among the researchers to investigate the slagging formation issues in the boiler. Recently, the evaluation indices or criterion numbers have been prioritised as a means of solving slagging issues in the biomass boiler. The widely used method at the moment is to carry out the predictive analysis on the biomass ash compositions on the slagging formation. This is because these methods are low cost, and it is very convenient for the researchers to obtain the chemical compositions of the biomass fuel. The significance of predicting slagging characteristics is broadly known but the major present methods still depend on basic empirical indices obtained from the past [137]. These indices are assumed to offer accurate predictions when implemented to ash samples obtained from the intended blend of boiler firing. Moreover, usually, the predictions are completed in the laboratory prior to firing a new fuel blend in order to anticipate any possible issues because full-scale firing is high risk and could damage the boiler [121].

Various models have been proposed to estimate the slagging propensities for firing biomass fuels of different origins. However, there is no reliable general applicable method that is available for assessing biomass fuel slagging propensities without carrying out extensive experimental testing. In addition, empirical correlations developed for coal produce large inaccuracies when applied to biomass. Therefore, a new semi-empirical index based on chemical equilibrium calculation, ash composition and ash content is developed to predict the slagging behaviours of biomass combustion in fixed-bed combustor technology. The current research is focused on predicting the woody biomass slagging propensities. Wood pellets are currently mainly used for large-scale electricity generation; more of these wood pellets are proposed to be used for heating and combined heat and power in the future. The thermodynamic equilibrium modelling (TEM) has been employed to determine the melt fraction of biomass fuels. Then the partial least square regression (PLSR) coupled with cross-validation has been used to develop a new formula to predict the slagging index based on the experimental ash composition and the melt fraction from TEM. The results obtained with the designed index

show a substantially greater success rate in predicting the biomass ash slagging propensity when compared with the experimental observations from the literature. The predictive tool developed is able to assist the users in determining biomass characteristics and behaviours during firing in the fixed-bed boiler.

3.2 Model setup

In this section, the explanation will focus on the data used to develop the prediction method to estimate the slagging propensities of biomass. A total of 28 biomass ash composition datasets were collected from the literature, as shown in Table 2-1, which consists of the ash compositions, ash content (%) and experimental slagging observations. 8 major ash compositions (MgO, Al_2O_3, SiO_2, K_2O, CaO, Fe_2O_3, Na_2O, P_2O_5) were included in the simulations; however, TiO_2 and SO_3 were excluded due to their low amount in the ash. The first 13 datasets (numbers 1-13) are experimental ash composition data and have been considered as training datasets and the last 15 (numbers 14-28) will be used as testing datasets. The training and testing datasets will be computed using thermodynamic equilibrium modelling to predict the value of the melting fraction formed based on the ash compositions. The melting fraction formed will then be multiplied by the ash content of the fuel to create a FactSage slagging index, I_f. The results obtained will be used in the PLS regression analysis to create a new formula, I_n, to predict the slagging propensity. Finally, I_n will be validated with the experimental slagging observations.

The training datasets 1-13 consist of experimental ashes from 13 types of pure wood-based biomass that were chosen due to the availability in the literature [63, 89, 209-213] of the experimental observation data for the biomass slagging behaviour to determine the slagging propensities of biomass fuels in the combustion. The remaining 15 testing datasets (number 14-28) consisting of pure woody biomass were selected based on the fuel and ash analysis carried out by the previous researchers [63, 89, 209-213]. This data will be used to validate the model equation developed using PLS regression and to show the capability of the expression formed to predict the slagging observation without the need to conduct combustion tests. The FactSage 8.1 thermodynamic software was used in this chapter to predict the biomass melting fraction for the fuels (1-13) listed in Table 2-1. The model was set up as follows:

i. The model is set up assuming equilibrium conditions with the databases FACTPS, FTsalt and FToxid.
ii. Table 2-1 consists of 8 major ash compositions (MgO, Al_2O_3, SiO_2, K_2O, CaO, Fe_2O_3, Na_2O, P_2O_5) from experimental ash composition were normalised and oxygen was

applied as the input to the model.

iii. The temperature for the equilibrium simulations was set to be in the range of 1150 – 1250 °C. This temperature has been benchmarked based on the common biomass fixed-bed boiler operating temperature [210].

iv. The "SLAGA" model, with two-phase immiscibility, was used in the calculations as the solution species [236].

v. Record the average reading of the slagging weight formed for each fuel resulting from the equilibrium simulation.

vi. The slagging weight formed from the equilibrium simulation will be fractioned with 1g of the ash to obtain melt fraction. The melt fraction will be multiplied with the ash content for each fuel to obtain the Factsage slagging index I_f.

3.3 Results and Discussion

3.3.1 Melting fraction predicted by using thermodynamic equilibrium calculations

The melt fraction is defined by the weight ratio of the slag liquid formed based on 1 gram of the fuel ash by thermodynamic equilibrium calculations. Theoretically, the maximum value of the melt fraction must be 1.0 where the total of 1g of ash is fully melt into the slag-liquid. The melt fraction idea was introduced by Isaak et al. [237] and they stated that more liquid will be present in the deposit as the temperatures increase. It was experimentally reported that the stickiness of deposits will increase with the increase in deposit temperature [237]. Therefore, the temperature indirectly impacts on the deposit stickiness by affecting the amount of liquid phase in the deposit. Zhou et al. [238] presented a sample melting curve that illustrates the particle melt fraction with respect to the particle temperature, which clearly shows that the melt fraction of the ash increases with an increase in temperature. The melting fraction concept became popular in forecasting the biomass ash deposition [19, 238, 239]. Beckmann et al. [240] illustrated the melting curve of Middleburg coal ash by using FactSage 6.1. Figure 3-1 shows the melt fraction (SLAG-liq, red line) graph of Oak chips (3) and it is clearly illustrates that the degree of melt increases with an increase in the temperature. Based on the Figure 3-1, the Oak chips start to melt at 750 °C where the melt fraction is 0.05 and increase linearly to the degree of melt (0.46) at 1150 °C. It must be noted that the different biomass fuel will have different degree of melting behavior due to the difference in its ash compositions. For example, Oak chips give a melt fraction of 0.46 while Bark spruce (please refer to Table 3-1) indicate its melt fraction of 0.56 at 1150-1250 °C. Thus, the degree of melt presented in our Factsage simulation

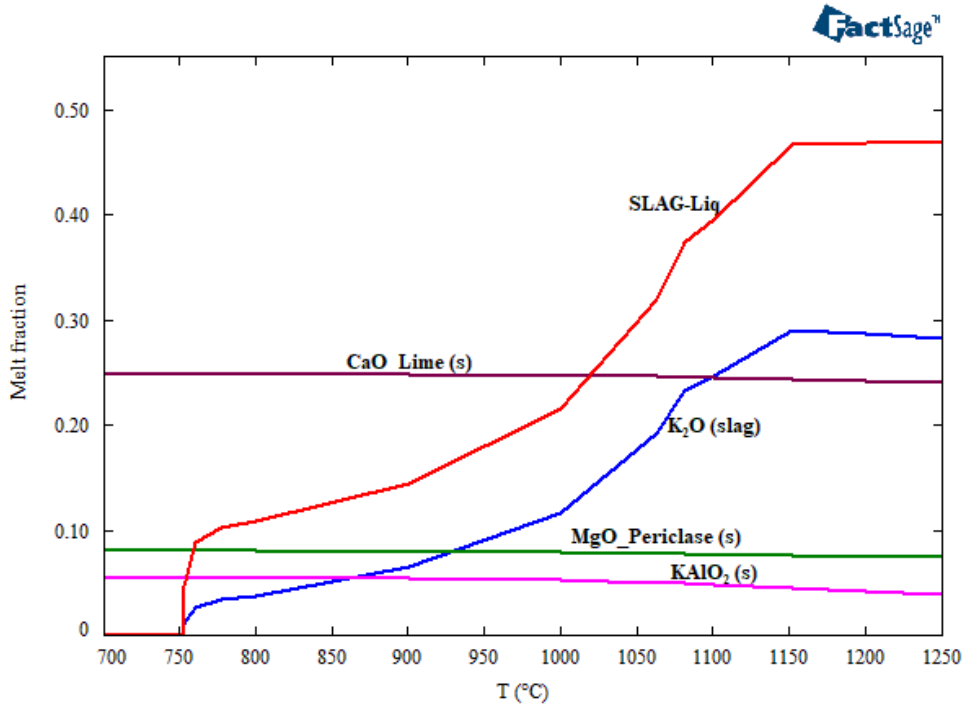

Figure 3-1 Solid-liquid phase for Oak chips (3) obtained by the FactSage equilibrium simulation

agrees with the typical melting curve presented by Zhou et al. [238] and melting curve of Middleburg coal by Beckmann et al. [240]. In this chapter, the study is focused on the determination of the melt fraction in the high-temperature regions (1150-1250 °C) only. The melting fraction has been obtained from the FactSage thermodynamic equilibrium model for the 13 woody biomass fuels (training datasets). Then, the melting fraction was multiplied by the ash content to introduce the Factsage slagging index, I_f. The I_f value will be represented as the proportion of the actual slag in the fuel with respect to the ash content. This is because, the I_f value will be considered as a quantitative measurement of the slag for the biomass fuel ash and will be compared with the experimental observation which is the qualitative measurement (low, moderate, high). Please refer to [211, 212, 214] for a detailed explanation of the experimental observation's classifications. Table 3-1 shows the melt fraction based on 1g of fuel ash input and the I_f value with respect to the ash content and experimental observation for each fuel in the training datasets.

Table 3-1 Melting fraction data of the biomass obtained from the FactSage 8.1 model.

Num.	Biomass	Melt fraction	I_f	Experiment observation [94, 216-222]	Ash content (%)
1	Pine chips	0.48	0.12	Low	0.25
2	Stemwood II	0.51	0.16	Low	0.31

3	Oak chips	0.46	0.25	Low	0.55
4	Softwood sawdust	0.76	0.38	Low	0.50
5	Sawdust	0.82	0.16	Low	0.20
6	Bark-spruce	0.56	2.09	Moderate	3.60
7	Bark pine	0.60	1.14	Moderate	1.90
8	Bark	0.61	2.68	Moderate	4.40
9	Scots pine II	0.90	0.45	Moderate	0.50
10	Scots pine III	0.86	0.95	Moderate	1.10
11	Logging residues II	0.81	2.20	Moderate	2.70
12	Wood II	1.00	0.76	High	0.76
13	Bark II	0.80	2.88	High	3.60

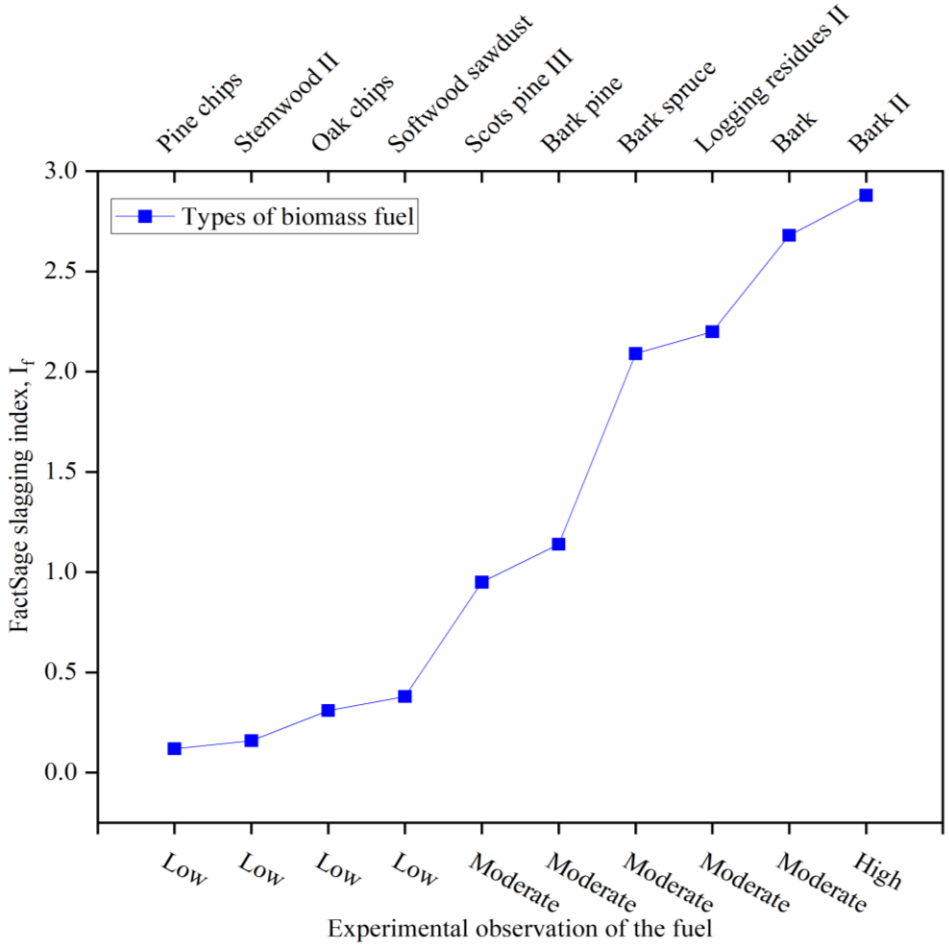

Figure 3-2 Relationship between the FactSage slagging index, I_f and experimental observations of the slagging of biomass fuels.

Figure 3-2 shows the positive trend on the relationship between the FactSage slagging index, I_f and experimental observation. This indicates that the value of the slagging index from FactSage will increase corresponding to the experimental observations moving from low to moderate and high of the biomass fuel slagging propensities. The ash content of the fuel is very important in determining the values of the Factsage slagging index, I_f as shown in Table 3-1. For example, the melt fraction of biomass fuel Oak chips (3) and bark-spruce (6) in Table 3-1

are 0.46 and 0.56, respectively. However, the experiment's observation [63, 210] stated that the slagging severity for the two fuels are low and moderate, respectively. This is due to the difference in the ash content for the two fuels. Oak chips (3) has low ash content which is 0.55% compared to the 3.60% in Bark-spruce (6). The experimental observation is consistent with the predicted I_f, which are 0.25 for Oak chips (3) and 2.09 for bark-spruce (6). Hence, the ash content will influence the slagging severity level. It is noted that, according to the method of the ternary diagram proposed by Näzelius et al. [214], both Oak chips (3) and Bark-spruce (6) are in the low slagging area. This indicates that the method by Näzelius et al. [214] fails to correctly evaluate the slagging potential for Bark-spruce (6). This is because the method did not take into consideration ash content. However, this is not the case for Wood II (12). The equilibrium model predicts a high melting fraction, yet Öhman et al. [89] reported a low ash content of 0.76%. Consequently, the index of slagging tendency, I_n is 0.76, categorizing it as moderate. This contradicts the literature [89], which indicated a high slagging tendency for Wood II (12). The discrepancy is particularly concerning given the reported low ash content, which is unexpected for a problematic fuel. Typically, problematic fuels have higher ash content, often 3% or above. This raises questions about the accuracy of the reported ash content for Wood II (12) and its implications for slagging behaviour. Therefore, one should be cautious when using the method to predict the slagging potential of fuels with significant differences in ash content. A comparison of the slagging index between with and without ash content will be explained in Section 3.3.3, Figure 3-4.

3.3.2 New Predictive Indices, I_n

The method to predict the slagging propensities of biomass can help the power plant operator predict the quality of the fuel before firing the biomass. The aim of this section is to develop a new predictive index formula that can be used to forecast the slagging propensity of woody biomass based on the fuel ash composition only, without performing a thermodynamic equilibrium calculation process, since the FactSage software is not widely used among power plant operators. The new predictive index formula, I_n, is developed based on I_f as shown in Table 3-1, by using the PLS regression analysis coupled with cross-validation together with chemical ash compositions (training datasets 1-13) from Table 2-1. After performing the PLSR coupled with the cross-validation method, the root means square error (RMSE), R^2, and slope for the training data were 0.006, 0.998 and 0.996, respectively. These indicate a good model fit [241]. The expression for I_n is obtained as follows:

$$I_n = |[0.43 - 2.476 \times 10^{-1}\ (MgO + CaO) + 7.147 \times 10^{-1}\ SiO_2 + 3.674 \times 10^{-1}\ (K_2O + Na_2O) + 18.875 \times 10^{-1}\ Fe_2O_3 + 11.306 \times 10^{-1}\ P_2O_5]| \times \text{Ash content (\%)} \quad (3\text{-}1)$$

**Condition applying eq 3-1:*

a. *The **mass fractions** of the ash compositions must be applied for the oxide parameters (non-normalized) in the Equation 3-1.*
b. *The **I_n index** will always a **positive value** due to the lowest value of melt fraction is 0.18.*

It is noted from Equation (3-1) that the MgO+CaO has a negative coefficient, which implies that the predicted slagging index, I_n will decrease with an increase in the values of MgO+CaO. On the other hand, the parameters (SiO_2, K_2O+Na_2O, Fe_2O_3 and P_2O_5) related to the slagging formation of biomass fuel are found to have a positive coefficient which means that the predicted slagging index, I_n will be high with an increased value of these four parameters. These elements with positive coefficients are highly prone to slagging formation and silica is the most common component of the biomass slag [129-131]. The regression coefficient of potassium combined with sodium is the smallest value among the positive coefficients, which is +0.3674. This indicates that the potassium element can be considered to have a low impact on the biomass slagging behaviour when the content of silica oxide is low, especially for wood-based biomass. For example, Oak chips (3) was observed to have a high amount of K_2O (31.94 wt%) among the training datasets (1-13), a low SiO_2 (1.32 wt%) and a significant amount of CaO (24.83 wt%) and this has resulted in 0.25 in the FactSage slagging index, I_f based on Table 3-1. Experiments carried out by [63] showed that the Oak chips (3) has low slagging propensities. Hence, the presence of a high amount of potassium ~32 wt.% does not produce a big impact on the slag formation of Oak chips (3). This is because the Oak chips (3) has low silica oxide and high content of calcium oxide as well as a low ash content, which is 0.55%. It was suspected that the potassium is not able to accelerate the slagging formation with a small amount of silica oxide present in the fuel (3). Figure 3-1 shows the solid-liquid phase equilibrium composition from the FactSage simulation for Oak chips (3) fuel. The graph shows a low value of potassium (K_2O-liq) formed in all the slag phase (slag-liq) which is about 0.29 g based on 1 g input of fuel ash. A small amount of potassium appears in the solid phase, such as $KAlO_2$. Another example that can be observed is logging residues (27) from Table 2-1, the potassium content is the lowest among the datasets which is 4.05 wt%, a very high SiO_2 (70.47 wt%) and low value of CaO (6.34 wt%). The experiment carried out by [210] indicated that the logging residues is observed as severe slag. This showed that the amount of potassium is not significant in the formation of slagging without the presence of high silica and low calcium contents.

3.3.3 Analysis and application of the new predictive indices, I_n

This section mainly focuses on the validation of the new predictive indices, I_n, against the testing datasets (14-28) in Table 2-1 by using the fuel ash analysis from the literature [63, 89, 209-214]. The range of ash compositions and ash content used to validate the slagging index, I_n are illustrated in Table 3-2. Table 3-3 shows the comparison of the biomass slagging tendency between the experimental observations and predicted indices of the testing fuels. The logging residues (27) and Bark III (28) were observed to have severe slagging in the experimental observation [210, 211]. This can be related to the high value of silica oxide and the low amount of calcium oxide content compared to other types of pure woody biomass fuels based on their chemical ash compositions. In addition, the total ash content for the logging residues (27) and Bark III (28) are 6.40% and 8.60%, respectively. The predicted index value for the logging residues (27) is 6.50, while for the Bark III (28) is 7.7 and both fuels (27 & 28) are considered to have a high value of the index. On the other hand, the clean wood fuel (Stemwood, Scots pine, Energy wood, Eucalyptus chips, Pulpwood, Wood pellets) and wood sawdust (Oak sawdust & Pine sawdust) are low in slagging behaviour based on the experimental observation. This is because the clean wood fuel and wood sawdust have a low amount of SiO_2 and a high amount of calcium oxide content as shown in Table 2-1. Their predictive indices, using I_n equation 3-1, are ranging from 0.08 to 0.52, respectively, and all the I_n values found to have low index values. The Softwood sawdust II, Logging residues III, Pinecone chips and Scots pine IV were observed as moderate slagging, with the predictive index values being 0.57, 1.83, 0.80 and 1.10, respectively. Overall, it can be concluded that the pure woody biomass with silica-rich fuel tends to have a high slagging tendency while the biomass fuels with a high amount of calcium have a low slagging potential. In the absence of soil contamination, the clean wood chips and sawdust pellets have a low intrinsic silica concentration and this results in them being low slag fuel sources [63].

Table 3-2 Range of ash composition used for slagging index, I_n validation

Ash compositions	Minimum (wt %)	Maximum (wt %)
MgO	1.41	14.11
Al_2O_3	0	11.31
SiO_2	4.34	70.47
K_2O	4.05	40.03
CaO	6.34	61.87
Fe_2O_3	0	5.09

Na_2O	0	6.60
P_2O_5	1.36	16.30
Ash content (%)	0.20	8.6

Table 3-3 Comparison of the biomass slagging tendency between the experimental observation and prediction indices of the testing data (woody biomass).

Num.	Type of biomass	Prediction Indices, I_n	Experimental observation [60, 86, 205-210]
14	Stemwood	0.08	Low
15	Wood	0.16	Low
16	Scots pine	0.29	Low
17	Oak sawdust	0.44	Low
18	Energy wood	0.52	Low
19	Eucalyptus chips	0.20	Low
20	Pine sawdust	0.30	Low
21	Pulpwood	0.30	Low
22	Wood pellets	0.40	Low
23	Softwood sawdust II	0.57	Moderate
24	Logging residues III	1.83	Moderate
25	Pinecone chips	0.80	Moderate
26	Scots pine IV	1.10	Moderate
27	Logging residues	6.50	High
28	Bark III	7.70	High

Figure **3-3** shows the correlation between the FactSage slagging index, I_f (blue line) and predictive slagging index, I_n (red line). As we know that the predictive slagging index, I_n was developed based on the FactSage slagging index by using the PLSR method coupled with the cross-validation method. The testing data were simulated using the FactSage equilibrium calculation to obtain the melting fraction and multiply it with the ash contents to create I_f. We can clearly see that both indices which are I_f and I_n are in mutual agreement and have the same trend as the calculated slagging index. Figure 3-4 shows the comparison of the performance of the slagging indicator with and without ash content. It is observed that the trend (without ash content) in the red colour line does not agree with the slagging observation increasing from

low to moderate while the trend in the green colour line agrees with the observation. This may indicate that the ash content cannot be ignored in determining the severity of the slagging for the biomass fuels.

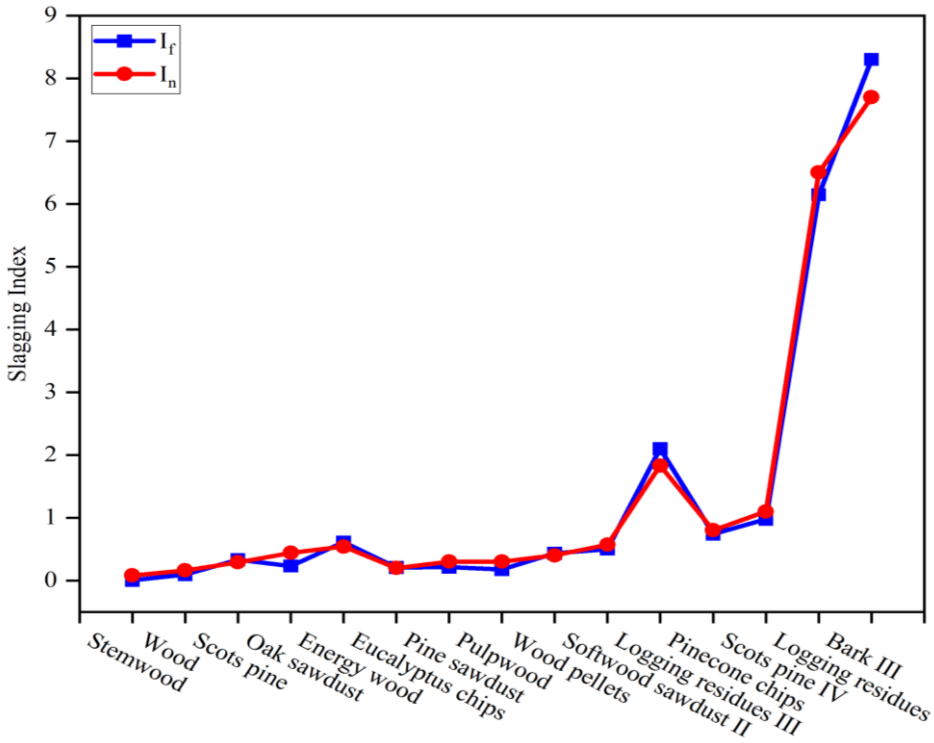

Figure 3-3 Comparison between the FactSage slagging index, I_f (blue line) and predictive slagging index, I_n (red line).

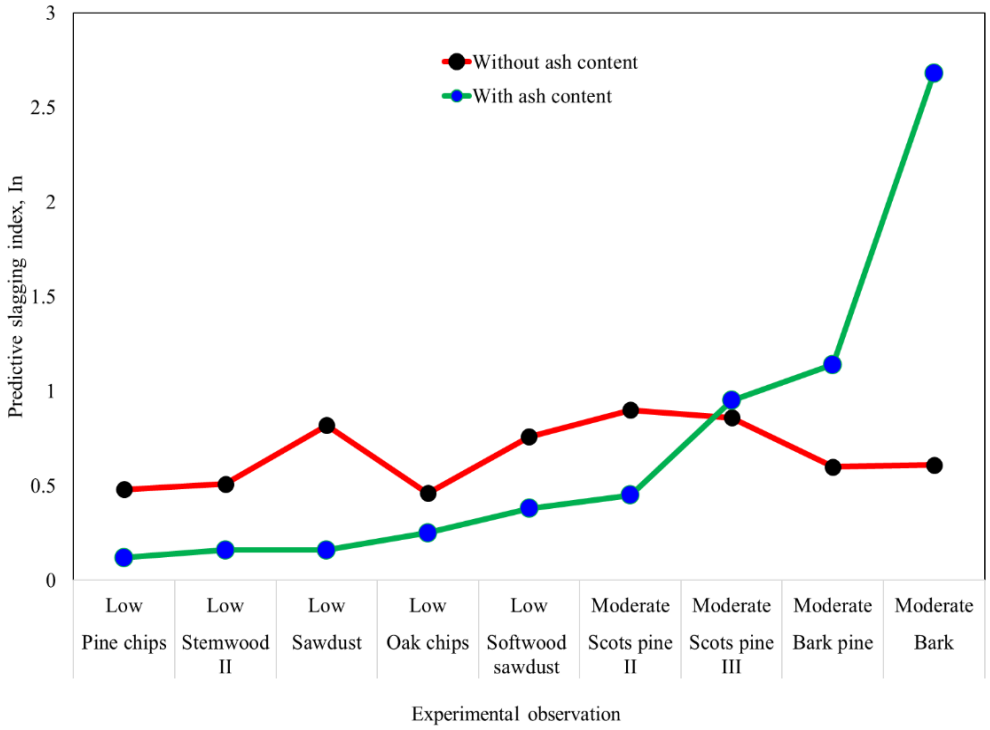

Figure 3-4: Comparison of the performance of the slagging index with and without ash content.

3.3.4 Slagging boundary indicator

The slagging boundary indicator represents the severity in the slagging of the biomass. The indicator is significant in guiding the users, especially power plant operators of energy power generation in determining the wood-based biomass fuel slagging behaviours. Figure 3-5 illustrates the graph showing the relations between the experimental observation and predictive slagging index, I_n. It can be clearly observed that the predictive slagging index is positively correlated with the experimental observations for most fuels. According to Figure 3-5, the boundary value between low and moderate slagging regions may be 0.55 (please refer to the green dotted line in Figure 3-5). This value has been decided based on the median interval between the lowest value of I_n for the moderate experimental observation and the highest value for the low slagging observation. The boundary number between moderate and high slagging may be 2.10 (please see the red dotted line in Figure 3-5). This is because the moderate observation fuel shows a consistently linear increase of the index value, I_n which is from 0.57 to 1.99 while the predictive index value, I_n for the high-slagging fuel starts from 2.17 to 7.70.

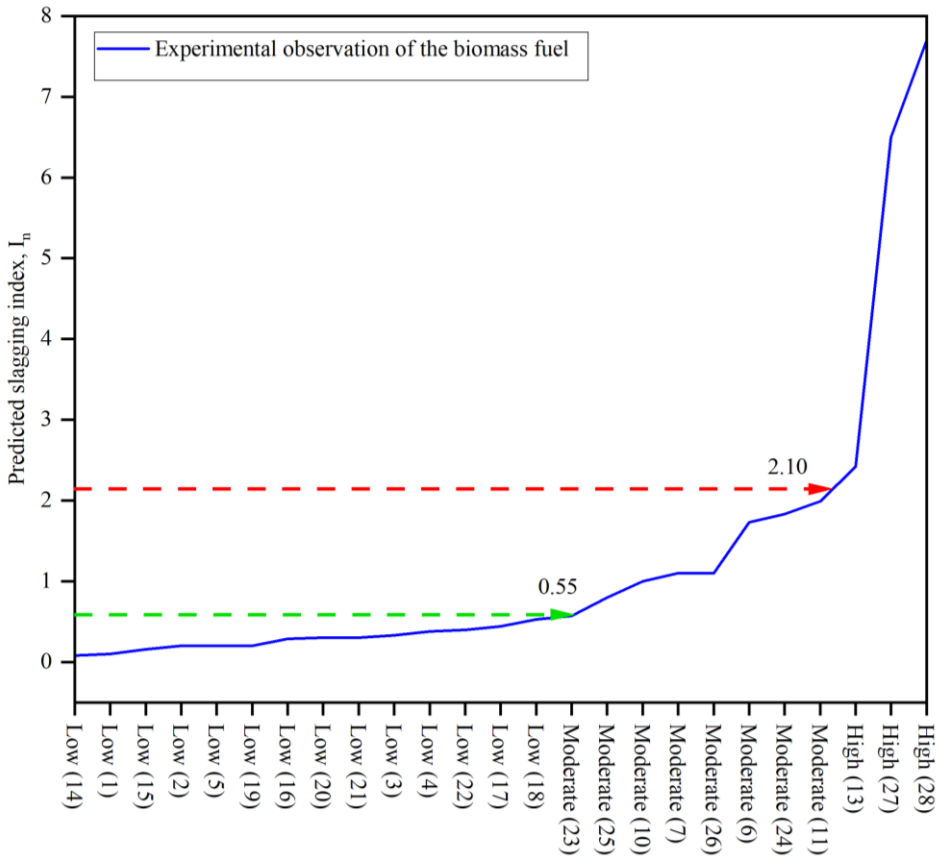

Figure 3-5 Correlation between the predictive slagging index, I_n and the experimental observations of the biomass fuel. (The x-axis represents the fuel number based on the list in Table 2-1).

This value has been determined by applying the median interval method between moderate and high slag propensity. The availability of experimental observations for high-slagging fuel is really needed in order to improve and determine the boundary of the slagging behaviour between moderate and high in the future. Large datasets may be required in the future to fine-tune and improve more on the boundary values. Currently, it has been classifying the indicator of the slagging predictive index into 3 main groups: low slagging ≤ 0.55; $0.55 <$ moderate slagging < 2.10; high slagging ≥ 2.10 as shown in Table 3-4.

Table 3-4 Slagging predictive index, I_n indicator.

Slagging index boundary	Slagging predictive index, I_n
Low	≤ 0.55
Moderate	0.56 – 2.09
High	≥ 2.10

3.3.5 Comparison of the new biomass slagging predictive indices, I_n with the 5 different types of existing expressions.

The performance of the new predictive equation for I_n is compared with the 5 different types of existing indices equations. These 5 different types of expression are developed to predict the coal ash behaviour but were also used to compare the biomass ash slagging, for example by Garcia-Maraver et al. [132]. Figure 3-6 illustrates the number of predicted samples out of the 15 testing fuels that match the experimental observations [63, 123] for each index.

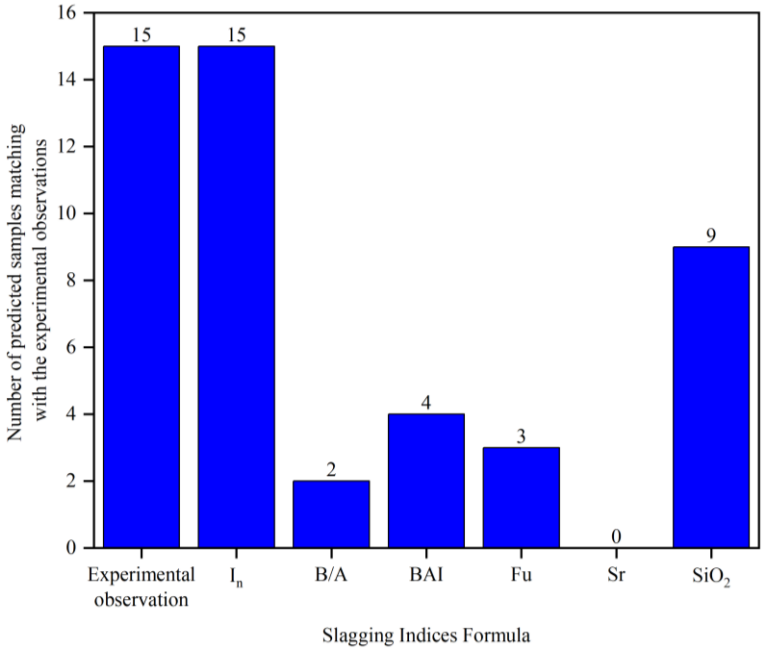

Figure 3-6 Comparison of the number of predicted samples matching with the experimental observations between I_n and 5 existing indices [63, 123].

The new index proposed in this chapter shows that I_n successfully predicted all the samples matching with the experimental observations. On the other hand, the 4 existing indices (B/A, BAI, Fu, Sr) were only able to predict the maximum 4 samples correctly while the use of SiO_2 content was able to accurately predict 9 samples (out of 15) showing that SiO_2 is indeed one of the dominating species in the slagging formation for these fuels.

3.4 Performance of the indices, I_n for woody biomass with peat addition

3.4.1 Woody biomass with peat addition

The experimental data presented by Näzelius et al. [212], which consists of 12 blends of Sawdust and Energy crops with various amounts of Peat: Sawdust 100%; Sawdust + Peat A & B (with ratios 0-30 wt %); Energy wood 100%; Energy wood + Peat A & B (0-30 wt %), is used in this study. There is an increasing demand for Peat as a new material in the solid recovered fuel industry [212]. However, Peat is known to have high ash content, which is

potentially problematic in the combustion compared to stem wood. The biomass datasets of Näzelius et al. [33] are divided into two groups, which are Case 1 (Sawdust + Peat A/B) and Case 2 (Energy wood + Peat A/B). In the experiments by Näzelius et al. [212], two types of Peat (Peat A and Peat B) were pelletized into stem wood sawdust and energy wood at three different ratios (5 - 30 wt%), respectively. Peat A is the traditional Scandinavian fuel peat that has higher levels of ash and silica (carex), and Peat B has lower levels of ash and a higher Ca/Si ratio [212]. Please refer to the Table 3-5 for the ash contents of the raw materials used by Nazelius et al. [212]. The experiment was carried out in a P-labelled and underfed commercial pellet burner (15kW) [212].

Table 3-5 Ash content for 4 different types of biomass [212].

Fuel type	Sawdust (wt%)	Energy wood (wt%)	Peat A (wt%)	Peat B (wt%)
Ash (%)	0.20	1.00	5.30	1.10

i. ***Case 1 (Sawdust + Peat A/B)***

Figure 3-7 [212] shows the average elemental ash compositions of the sawdust and blends of sawdust with Peat A/B. Silica compositions were the lowest in the pure sawdust (red column) while were the highest with the addition of Peat A into the sawdust. It can be clearly seen that the influence of the Peat addition on the sawdust resulted in a gradually increasing amount of silica in the blending compositions between Peat A/B and sawdust at ratios of 5-30 wt%. Another major effects of Peat A addition on the sawdust that can be observed in Figure 3-7 are the amount of calcium and magnesium formed. The pure sawdust without the addition of Peat A has a high amount of CaO+MgO which is 41.49 wt%, however, after the addition of Peat A with ratios of 5 and 30 wt%, the amount of CaO+MgO significantly decreases from 25 wt% to 17.28 wt% respectively. The mixture between sawdust and Peat B with ratios of 5 and 30 wt% generally increase the amount of CaO+MgO from 45.30 wt% to 52.47 wt% and no significant changes in the Si level for both ratios. This was expected due to the high Ca/Si ratio in Peat B.

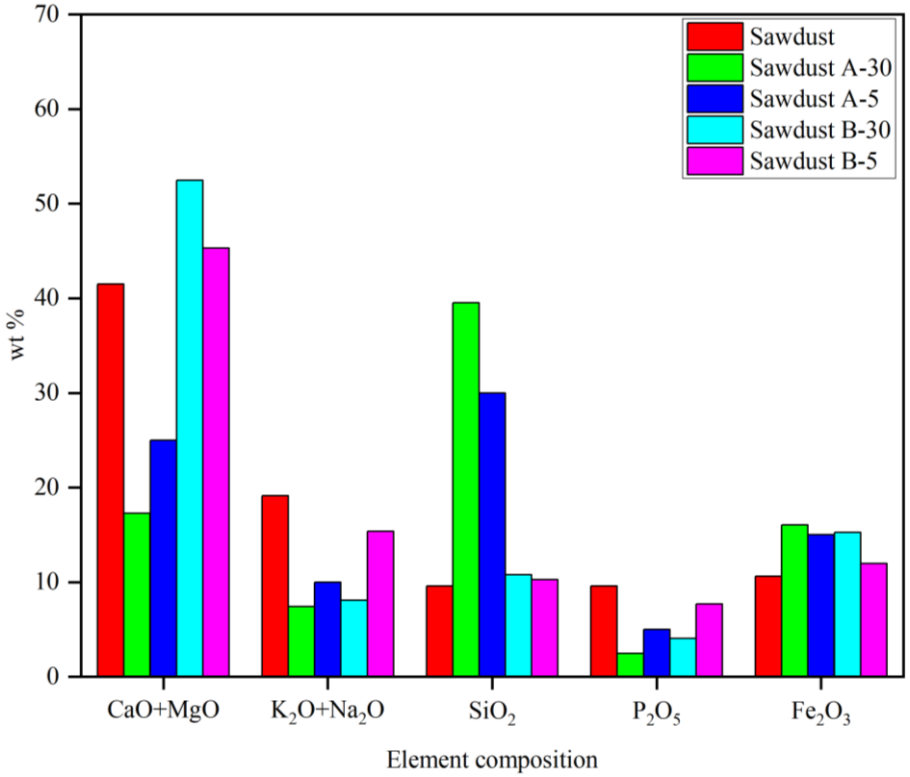

Figure 3-7 Elemental fuel ash compositions of the Sawdust and blends of Sawdust with Peat A/B [208].

Table 3-6 Comparison of the biomass slagging tendency between the experimental observation and prediction indices for Case 1.

Type of biomass	Prediction Indices, I_n	Prediction observation indicator for slagging	Experimental observation [212]
Sawdust	0.16	Low	None
Sawdust A-30	2.49	High	High
Sawdust A-5	0.60	Moderate	Moderate
Sawdust B-30	0.43	Low	Moderate
Sawdust B-5	0.32	Low	Low

Table 3-6 presents a comparison of the slagging between the predictions using I_n and the experimental observations from Näzelius et al. [212]. The predicted indices, I_n for Sawdust A-30 is 2.49 and was observed as severe slagging in the experimental result [212]. The I_n of Sawdust B-5 was 0.32, which can be ranked as low slagging, which was consistent with the experimental observation. The pure sawdust value of I_n forecasted was relatively small which is 0.16 while Näzelius et al. [212] mentioned that there was no slagging observed during the experiment. This is due to the high CaO+MgO and low silica in the ash although the content

of K_2O+Na_2O is relatively high. The I_n estimated for Sawdust A-5 and Sawdust B-30 were 0.60 and 0.43, respectively, and these were shown as moderate slagging (experimental observation). Overall, only Sawdust B-30 failed to satisfy the experimental observation as the predicted I_n was categorized as low slagging propensity while it was observed as moderate slagging in the experiment.

ii. ***Case 2 (Energy wood + Peat A/B)***

Figure 3-8 [212] presents the bar graph of ash compositions of pure Energy wood with the addition of Peat A & B. Pure Energy wood has a low silica content and high content of CaO+MgO. In addition, we can clearly see that the major effect of Peat A addition to the Energy wood is the drastic decrease in the calcium and magnesium values. The silica will continue to increase with the addition of Peat. Table 3-7 shows the comparison of slagging between the predictions and the experimental observations for blends of Energy wood with Peat A/B. Pure Energy wood has high value of CaO+MgO elements and the predicted slagging index, I_n value was 0.52 which is ranked as low slagging. Näzelius et al. mentioned that there was no slagging observed during the firing of the pure energy wood [212]. The EW A-30 and EW A-15 predicted by I_n were 3.01 and 2.17, respectively, while the experimental observation considered them as being severe slagging due to the burner needing to be shut down during firing [212]. This is suspected to be due to the high amount of SiO_2 and the low amount of CaO+MgO in their fuel compositions. The predictive indices, I_n for EW A-5 was forecasted to be 0.88, while it was observed to be moderate slagging in the experimental observation [212]. In addition, the slagging observation based on an experiment conducted by Näzelius et al. [212] indicated that all the blended ratios for Peat B 5-30 wt% with energy wood have low slagging formation while the I_n indices prediction were 0.53, 0.54 and 0.55, respectively. Overall, the predictive index, I_n developed is able to predict up to 80% accuracy for the mixture of biomass between Sawdust, Energy wood and Peat A/B.

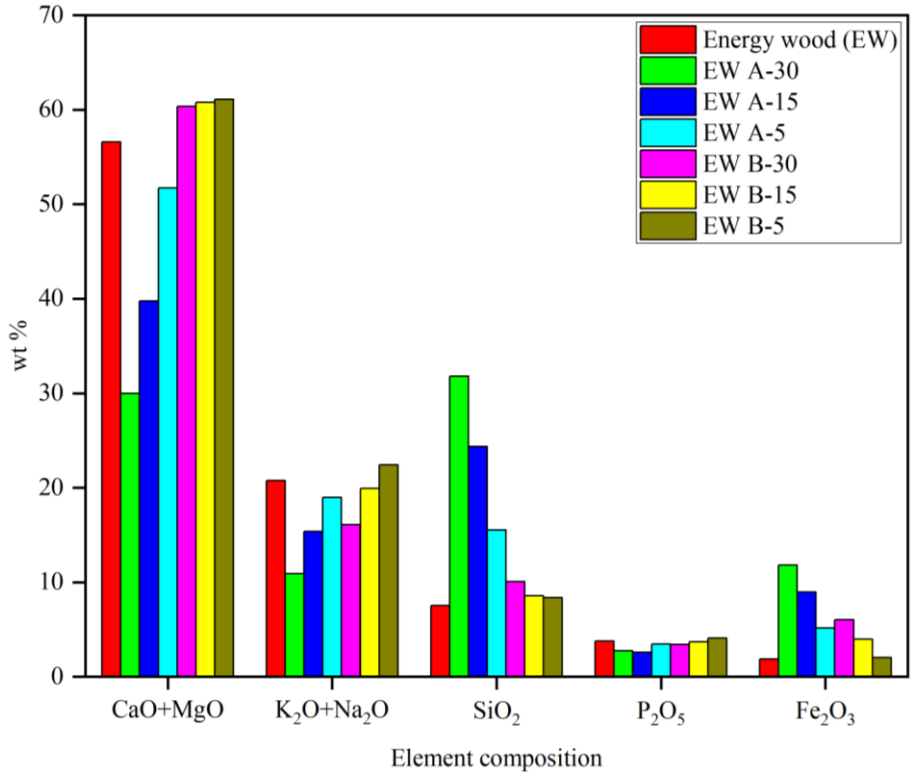

Figure 3-8 Elemental fuel ash compositions of the Energy wood and blends of Energy wood with Peat A/B [208].

Table 3-7 Comparison of the biomass slagging tendency between the experimental observation and prediction indices for Case 2.

Type of biomass	Prediction Indices, I_n	Prediction observation indicator for slagging	Experimental observation [212]
Energy wood (EW)	0.52	Low	None
EW A-30	3.01	High	High
EW A-15	2.17	High	High
EW A-5	0.88	Moderate	Moderate
EW B-30	0.55	Low	Low
EW B-15	0.54	Low	Low
EW B-5	0.53	Low	Low

3.4.2 Residues biomass

The experimental data illustrated by Weber et al. [242, 243] which consists of 6 types of herbaceous biomass which are Mixed wood, Poplar, Palm kernel expeller (PKE), Switchgrass II, Grain residue and Fermentation residue. The biomasses were fired to investigate the issues of deposits formed at high-temperature regions (950-1200 °C). Figure 3-9 presented the fuel ash composition of 6 types of herbaceous biomass [242, 243] determined by X-ray fluorescence. Mixed wood has an extremely high amount of CaO+MgO and the

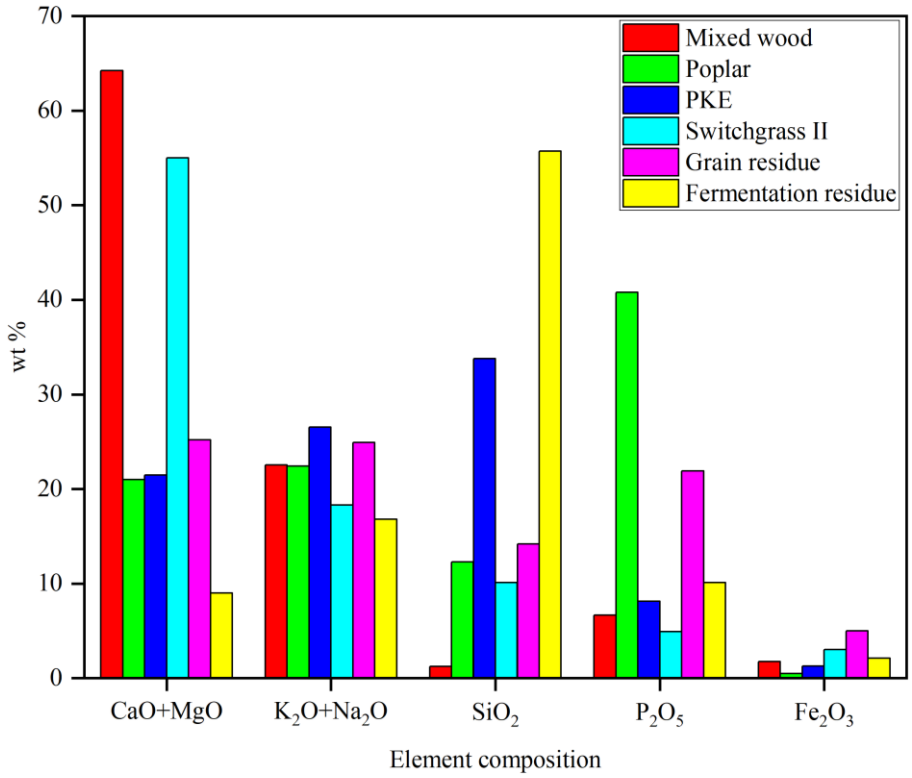

Figure 3-9 Fuel ash compositions of the 6 types of herbaceous [242, 243].

Table 3-8 Comparison of the biomass slagging tendency between the deposited mass versus ash and prediction indices, I_n.

Num.	Type of biomass	Prediction Indices, I_n	Ranking of the biomass slagging propensity from low to high [242, 243]
1	Mixed wood	0.93	1
2	Poplar	1.70	2
3	PKE	3.70	3
4	Switchgrass II	4.88	4
5	Grain residue	6.33	5
6	Fermentation residue	6.59	6

lowest amount of silica among others. Fuel ash composition in Fermentation residue is contradicted from Mixed wood which is the lowest amount of CaO+MgO and the highest value of SiO_2. Poplar has the highest amount of phosphorus which is approximately 41 wt%. The I_n was employed to determine the slagging indices of every single biomass from Figure 3-9. The results later will be compared between the prediction indices, I_n and the rank of the biomass (Mixed wood, Poplar, Palm kernel expeller (PKE), Switchgrass II, Grain residue and Fermentation residue) slagging propensity from low to high. The slagging propensity rank was determined by analysing the deposited mass versus ash input after 2 hours of deposits collected on high-temperature surfaces (>1000°C) [243]. The rank of the 6 various types of biomasses

can be illustrated in Table 3-8. Based on, the prediction indices, I_n successfully predicted the slagging propensity for all biomass with respect to the biomass slagging propensity ranking provided by the literature [243]. However, it must be noted that the main objective of this chapter is to develop the slagging propensity for woody biomasses only. The author strongly suggested always taking a precaution when applying the herbaceous biomass to the I_n formula. This is because the ash composition for herbaceous biomass is more exotic compared to woody biomass. This can be clearly seen in the distribution of ash composition for herbaceous biomass in Figure 3-9.

3.5 Conclusion

This research chapter has demonstrated that it is practical to employ thermodynamical equilibrium modelling together with PLSR with cross-validation to accurately predict the slagging propensity of firing biomass in utility boilers. The new slagging index, I_n was developed by analysing the melting fraction predicted by the FactSage software taking into consideration the ash content of the fuels and using the numerical PLS regression coupled with a cross-validation technique. The proposed method has been validated against the experimental observations from the literature on wood-based biomass in fixed bed and grate type of combustors. The findings show that the slagging propensity index may be classifiable into 3 main groups: low slagging when $I_n \leq 0.55$; $0.55 <$ moderate slagging < 2.10; and high slagging when $I_n \geq 2.10$.

For the tested woody biomass fuels, the new index, I_n shows a substantially greater success rate than 5 existing indices in assessing the boiler slagging potential. Furthermore, the predictive index, I_n has been extended to herbaceous biomass and blended applications between woody biomass and Peat. The result shows that the I_n expression is able to predict the slagging potential with high accuracy. It can be confirmed that the main element that contributes to the slagging formation in the biomass firing a fixed-bed is silica oxides. Woody biomass with higher values of calcium elements will have a low tendency to slag while those with a higher value of silica oxides will have a high probability of slagging.

It should be noted that the new predictive slagging index, I_n has taken into consideration the level of the ash contents of the biomass fuels. The index must be applied in high-temperature regions of the fixed bed and grate-type boilers operation. The new predictive index, I_n is based on wood-based biomass with high SiO_2 and CaO contents. Therefore, care should be taken when extending the predicted indices I_n developed in this chapter to other types

of biomass fuels, in particular very high potassium fuels. The author strongly recommends that future experimental studies at industrial/full scales should be performed to obtain a large dataset of experimental observations in real applications. This will improve and increase the accuracy of the predictive indices to accurately predict the biomass slagging propensities.

4 An improved index to predict the tendency of bed agglomeration in fluidised bed combustion of biomass fuels.

4.1 Introduction

Quartz is still mainly used as the bed material in FBC up to this date because the majority of the other bed materials are expensive [244, 245]. Thus, it is crucial to predict the bed agglomeration tendency of fluidised quartz bed combustion of biomass firing to guarantee the safety of FBC technology in power generation. This allows for the pre-emptive measure to mitigate the bed agglomeration formation if required. Over the years, researchers have proposed various empirical indices for bed agglomeration in the FBC system. However, the applicability of the existing indices across different types of biomass to estimate the bed agglomeration tendency remains limited. This is due to the different characteristics of chemical compositions such as herbaceous and woody types of biomass fuel. Moreover, previous studies have mainly focused on the melting temperature when it is associated with the bed agglomeration in the FBC system, but do not take into account the effects of different ash compositions from various types of biomasses that will affect the eutectic melting temperature. This is due to the lack of understanding of the behaviour of the chemical composition of biomass ash among researchers in biomass fuels [167]. Also, this can be supported by Morris et al. [96], who recommended determining bed agglomeration behaviour influenced by the fuel ash composition. Additionally, this study extends the work of Nik Norizam et al. [167] who originally developed an index for predicting slagging propensity in fixed bed combustors as discussed in Chapter 3. In this chapter, an improved semi-empirical index based on the thermodynamic equilibrium model (TEM) is developed to predict the bed agglomeration tendency, I_a of biomass combustion in FBC technology.

The current research is focused on forecasting the bed agglomeration which considers the chemical ash compositions in FBC biomass technology. The TEM has been employed to determine the melting degree of biomass fuels with the presence of SiO_2 (quartz) as bed material. Then the partial least square regression (PLSR) coupled with cross-validation has been employed to create a new numerical model, I_a to estimate the bed agglomeration index based on the experimental ash composition and the degree of melt from TEM. The results obtained with the new formula, I_a demonstrate a significantly greater success rate in forecasting the tendency of bed agglomeration as compared to experimental observations from the existing literature. The developed predictive tool is essential for enabling users to assess biomass behaviours and anticipate bed agglomeration conditions during combustion in FBC technology.

4.2 Model setup

In this section, the discussion focuses on the datasets employed to develop an improved index to predict the bed agglomeration tendency of biomass. A total of 22 datasets containing biomass ash compositions were gathered from the relevant literature sources [215-221], as illustrated in Table 2-2, which consists of ash compositions, ash content (%) and experimental observations of bed agglomeration in the FBC boiler. 9 major ash compositions (Na_2O, MgO, Al_2O_3, SiO_2, P_2O_5, K_2O, CaO, SO_3, Fe_2O_3) and quartz (SiO_2) as a bed material were included in the model, however, TiO_2 was excluded due to its low content in the ash. The initial 10 datasets (1-10) represent the experimental ash composition data and have been designated as training datasets, while the subsequent 12 datasets (11-22) serve as testing datasets. The training and testing datasets are analysed through thermodynamic equilibrium modelling to predict the melting fraction based on the ash compositions. The obtained results are utilized in the PLS regression analysis and are formulated in a new equation, denoted as I_a, for predicting the bed agglomeration behaviour without the necessity for conducting combustion tests in the future. Subsequently, the effectiveness of I_a is validated against the experimental observations of bed agglomeration in the FBC system. In this research chapter, the bed material was introduced in the model (iii) to simulate the melt fraction mechanism in the FBC boiler, and the setting of the TEM is as follows:

i. The model is configured under the assumption of equilibrium conditions, utilizing the FACTPS, FTsalt, and FToxid databases.
ii. Table 2-2 incorporates 9 ash compositions (MgO, Al_2O_3, SiO_2, K_2O, CaO, Fe_2O_3, Na_2O, P_2O_5, SO_3) derived from experimental ash composition were normalised and oxygen designated as input-stream 1 in the model.
iii. Quartz (SiO_2) was introduced into the system as input-stream 2. The temperature range for the equilibrium simulations was set between 700 and 900 °C. This temperature range has been chosen based on the typical operating conditions of biomass FB boilers [96].
iv. The simulations utilized the "FToxid-SLAGA" and "FTsalt-SALTF" model, incorporating two-phase immiscibility as the solution database [200].
v. Record the weight range of the solid-liquid phase formed for each fuel as a result of the equilibrium simulation.
vi. The solid-liquid phase formed during the equilibrium calculation is fractioned by 1g of the ash to calculate the melt fraction, M_f.

4.3 Results and discussion

4.3.1 Comparison melt fraction with and without the presence of SiO_2 (quartz) predicted by TEM.

The idea of the melting fraction has gained popularity in predicting the deposition of biomass ash [19, 238, 239]. Recently, Nik Norizam et al. [167] successfully developed a model to predict the slagging propensity in a fixed bed boiler of woody biomass in the high temperature region by employing the melting fraction concept obtained from the Factsage 8.1 equilibrium model. The present work enhanced the fixed bed model introduced by Nik Norizam et al. [167] to suit the application of the FBC technology. Based on the Figure 4-1, the melt fraction was compared between the current FBC (with bed material) and the fixed bed model (without bed material). The motivation was to show the sensitivity of the melt fraction model with and without the presence of the bed material (quartz). The presence of bed material (rigid lines) has higher melt fractions compared to without the presence of the quartz (dash lines). This proves that the presence of SiO_2 (quartz) as bed material actively reacts with the fuel ash compositions and produced a significant amount of agglomerates in FBC by the coating-induced mechanism.

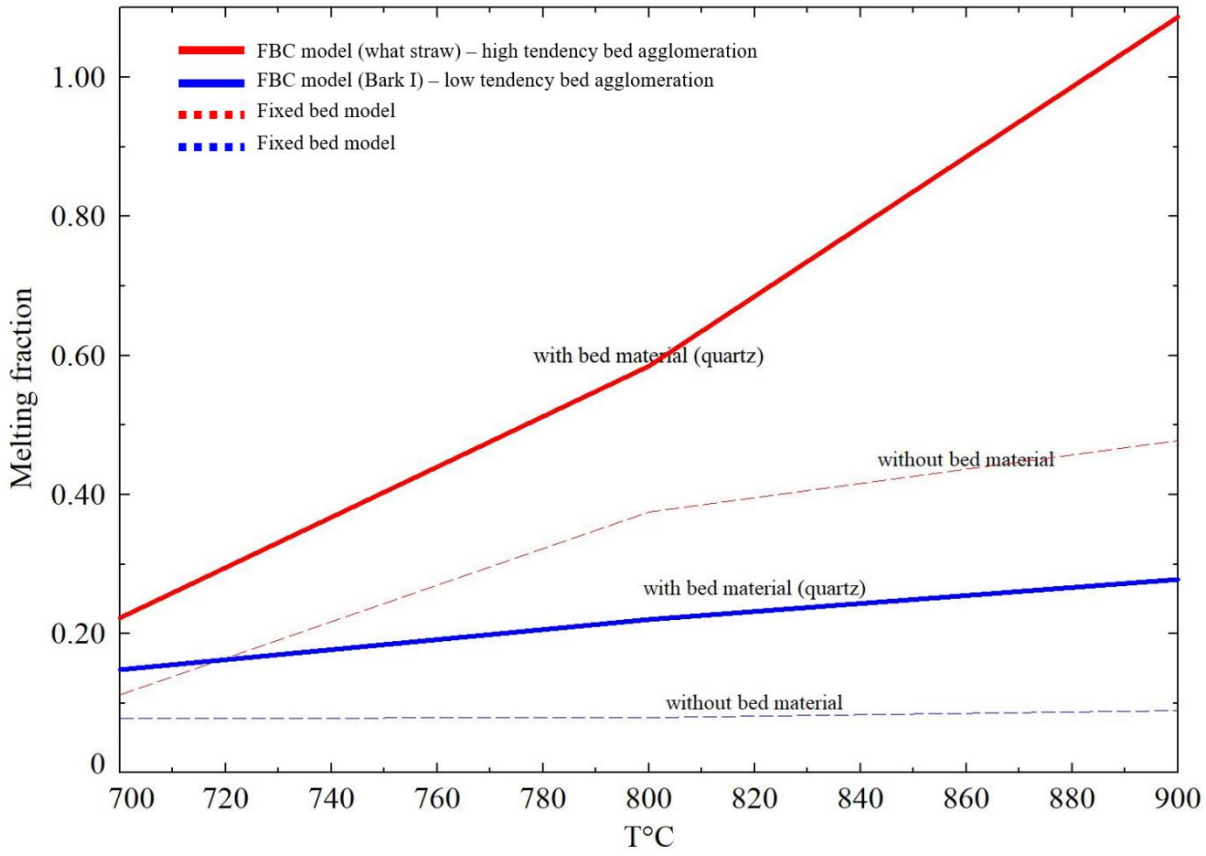

Figure 4-1 Comparison of the melt fraction between the FBC model with bed material and the fixed-bed model without bed material.

Figure 4-1 demonstrates that Wheat straw (red line) exhibits a higher melting fraction than Bark I (blue line). Experimentally, it was observed that Wheat straw tends to have a high propensity of bed agglomeration, whereas Bark I exhibits a low tendency for bed agglomeration. This is because Wheat straw has a high ratio of K_2O/CaO compared to the Bark I. The analysis of the chemical compositions of ash will be further explained in Section 4.3.2. In addition, Figure 4-1 clearly illustrates the melting degree increases with an increase in the temperature. Thus, the melting degree illustrated in the authors TEM simulation is in agreement with the common melting curve demonstrated by Zhou et al. [238] and the melting fraction of woody biomass in a fixed bed boiler by Nik Norizam et al. [167]. This paper concentrates on determining the melt fraction exclusively in the low-temperature range of 700-900 °C based on typical FBC operating conditions [96].

4.3.2 Analysis and application of an improved BAI, I_a

Predicting the bed agglomeration tendency in FBC can assist power plant operators in anticipating the fuel quality before the biomass firing. The objective of this section is to create an improved formula for the bed agglomeration index, I_a. This formula is intended for predicting the bed agglomeration behaviour of biomass based on the fuel ash composition, thus eliminating the need for a thermodynamic equilibrium calculation process. This is particularly relevant as the FactSage software is not extensively utilized among power plant operators. The development of the new bed agglomeration index, I_a is based on the melting fraction, M_f and chemical ash compositions (training datasets 1-10) as shown in Table 2-2 by applying the method of the PLS regression (PLSR) analysis, coupled with cross-validation. The root means square error (RMSE), R^2, and slope for the training data were 0.027, 0.991 and 0.991, respectively which suggested a good fit of the model [246]. The expression for I_a is acquired as follows:

$$I_a = |[0.20 - 1.3599(MgO + CaO) + 2.024(K_2O + Na_2O) + 1.1614SiO_2 + 3.126 \times 10^{-1}(SO_3 + P_2O_5)] \quad (4\text{-}1)$$

**Condition applying eq 4-1:*
*The **mass fractions** of the ash compositions must be applied for the oxide parameters (non-normalized) in the Equation 4-1.*

The negative coefficient in Equation (4-1) for MgO+CaO indicates that an increase in the values of MgO+CaO will result in a decrease in the predicted value of BAI, I_a. Conversely, the parameters (SiO_2, K_2O+Na_2O, SO_3+P_2O_5) associated with the bed agglomeration tendencies

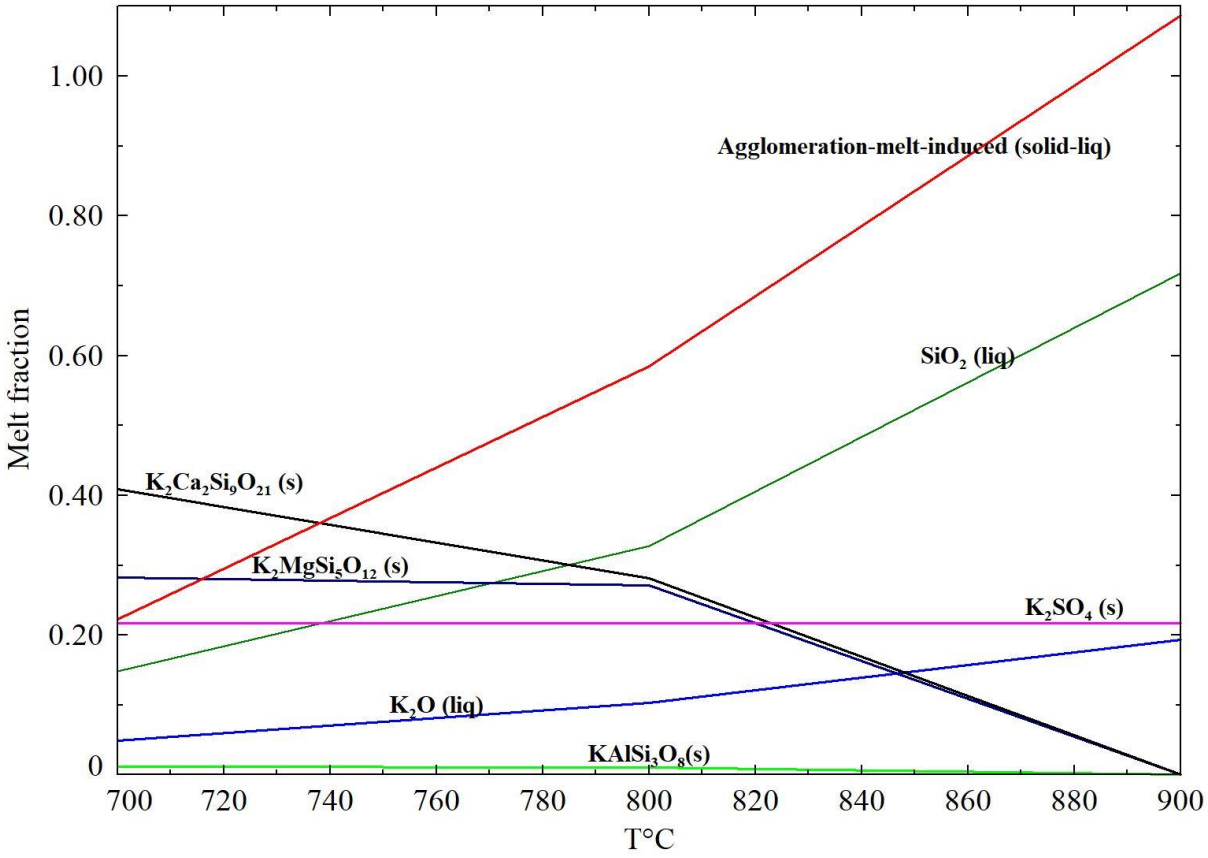

Figure 4-2 Solid-liquid phase for Wheat straw (3) obtained by the FactSage equilibrium simulation.

of biomass fuel exhibit positive coefficients. This implies that an increased value of these three parameters will result in a higher predicted number of BAI, I_a. Elements exhibiting positive coefficients are highly prone to the formation of bed agglomeration, with potassium being the most prevalent component in the agglomerates [91, 96, 97, 105, 216, 220]. Among the positive coefficients, the highest value is +2.024, and this corresponds to the regression coefficient of potassium combined with sodium. This suggests that the presence of the potassium element significantly influences the bed agglomeration behaviour. Morris et al. [96] explained that agglomeration caused by the melt-induced mechanism occurs when there is an sufficient content of silica and alkali metal in the fuel ash. Lin et al. [215] found that high potassium content in straw leads to the development of agglomerates and defluidization. According to Grimm et al. [219], the wheat straw (potassium rich fuel) showed a high tendency of bed agglomeration upon firing in 5 kW bubbling fluidized bed reactor. Figure 4-2 illustrates the solid-liquid phase for wheat straw obtained by the TEM simulation, it is clearly shown that most of the compounds containing potassium which consists of $K_2Ca_2Si_9O_{21}$, $K_2MgSi_5O_{12}$, K_2SO_4, and $KAlSi_3O_8$.This is in agreement with the study by Lin et al. [215] who suggested that compounds containing potassium have a tendency to persist in the bed and create

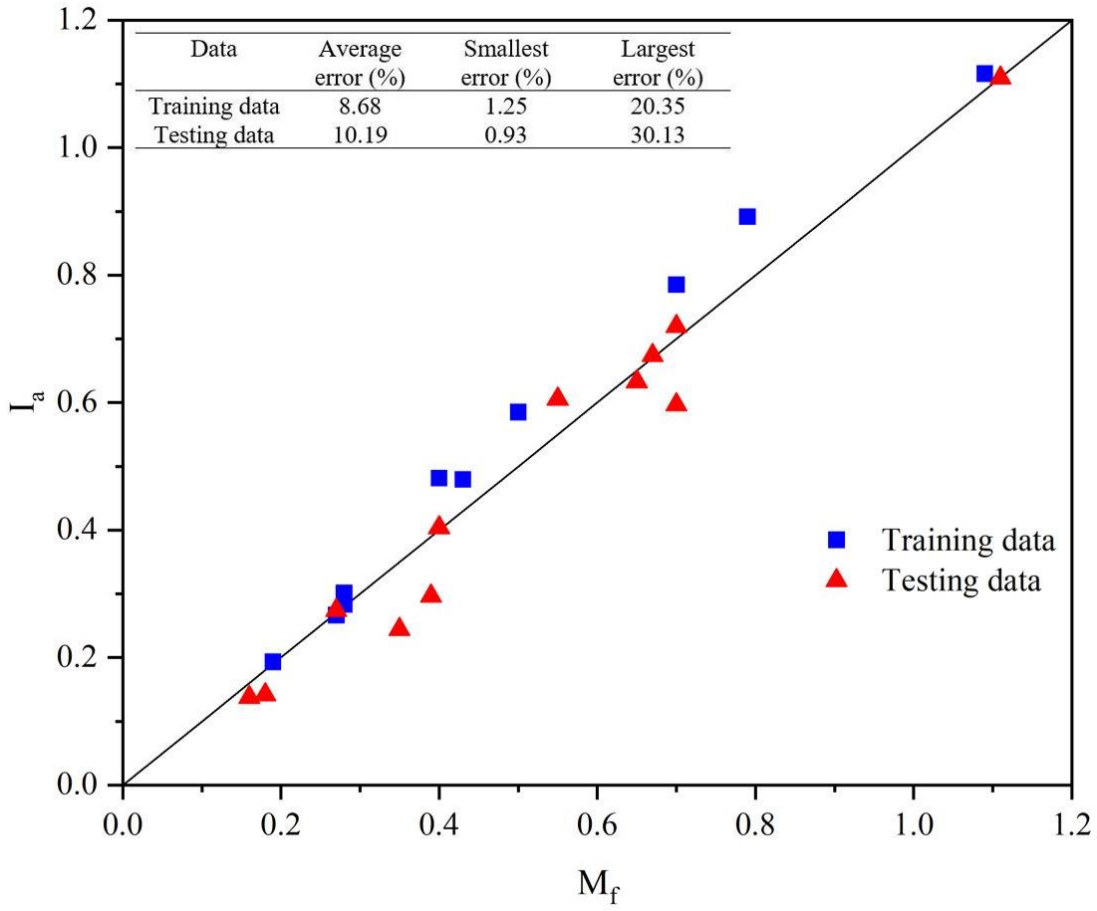

Figure 4-3 Comparison between melt fraction by TEM, M_f and predictive BAI index, I_a.

potassium-rich ash with a low melting point during the combustion process. Moreover, the experimental observations from Table 2-2 shows that about 95% of high bed agglomeration tendency was observed when the potassium value is higher than 18 wt%.

Figure 4-3 demonstrates a comparison between the melt fraction values, M_f and the predicted agglomeration index, I_a and the estimated error. The melt fraction for the 10 biomass fuels (training datasets) were determined using the TEM. The M_f value serves as a quantitative measure of the bed agglomeration behaviour and will be compared with the qualitative measurement (low and high) based on experimental observations. As explained in Section 4.3.1, the value of the melt fraction, M_f increases, and this corresponds to the experimental observations of bed agglomeration from low to high tendency. For a comprehensive explanation of the classifications of the experimental observations, please refer to the Table 4-1 [91, 105, 216-218, 220, 221]. It can be observed that the predicted index, I_a closely matches the melt fraction, M_f for both the training and testing datasets. It was found that the average error for the prediction of the bed agglomeration index, I_a is 10.19%, which indicates that both of the indices M_f and I_a are in agreement with each other and exhibit the same trend as the calculated agglomeration index.

Table 4-1 A comprehensive explanation of the classification for the bed agglomeration tendency by experimental observations.

Authors	Technique used to determine the bed agglomeration in FBC
Grimm et al. [91]	The study evaluates the bed agglomeration tendency based on the formation and characteristics of coating layers on bed particles, as well as the temperature at which agglomeration leads to defluidization.
Lin et al. [105]	The paper uses defluidization time as the primary metric to assess the agglomeration tendency in FBC, with temperature being a critical factor influencing this behavior. The shorter the time before defluidization occurs, the higher the agglomeration tendency.
Yu et al. [215]	The study is to determine the tendency of agglomeration in FBC of biomass by measuring the slip resistance between particles. An increase in slip resistance between particles will correspond to the defluidization and high tendency to bed agglomeration.
Llorente et al. [216]	The sintering degree of agglomerates of bed material was determined visually and the assessment of ash disintegration in the agglomerates and deposits.
Liu et al. [217]	The bed agglomeration tendency was measured by monitoring the chemical composition changes, observing the physical changes in the bed material particles, and correlating these with the operational stability of the CFB during the experiments.
Piotrowska et al. [219]	The bed agglomeration tendency was concluded by analysing the temperature and pressure to determine the initial and total defluidization temperature. The initial defluidization temperature indicated the growth of agglomerates. The bed agglomeration tendency will reduced with an increased in defluidization temperature.

Figure 4-4 shows the predicted value of the new improved agglomeration index, I_a versus the 12 datasets (Table 2-2, numbers 11-22) of experimental observations from the literature [215-221]. The range of ash compositions used to validate the bed agglomeration index, I_a is illustrated in Table 4-2. It was discovered that the I_a index values fall below 0.5 when the bed agglomeration tendency is low according to the experimental observations. For example, Forest residues (17) and Brassica (21) were observed to have a low tendency of bedagglomeration in the experimental observation [217, 220]. This is due to the low ratio of K_2O/CaO. On the other hand, the I_a value predicted for the high tendency of bed agglomeration

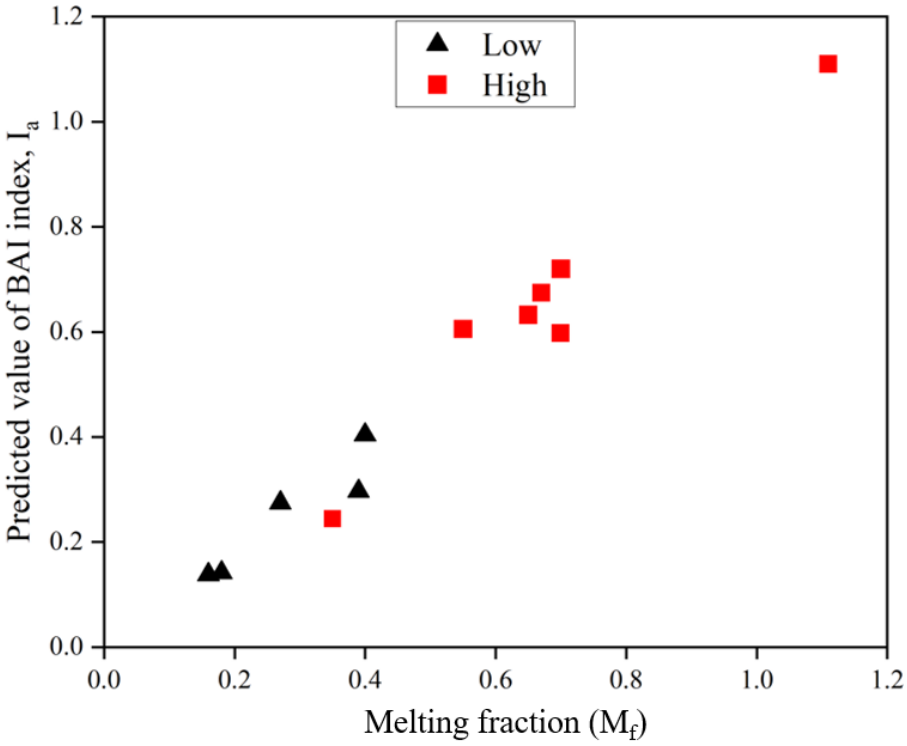

Figure 4-4 The predicted values of the proposed index, I_a versus melting fraction by Factsage of the bed agglomeration tendency. The colour code (red square and black triangle) shown in the graph represents the experimental observations.

Table 4-2 Range of ash composition used for bed agglomeration index, I_a validation

Ash compositions	Minimum (wt %)	Maximum (wt %)
Na_2O	0.20	7.70
MgO	2.20	9.00
Al_2O_3	0.03	5.36
SiO_2	1.29	39.00
P_2O_5	1.40	35.69
K_2O	8.46	32.67
CaO	2.31	42.87
SO_3	0	38.98
Fe_2O_3	0.22	2.00

in biomass firing is more than 0.5. Most of the biomass fuels that were observed to exhibit high bed agglomeration have a high K_2O/CaO ratio. For example, Wheat straw II (18) and Cotton stalk (22) have high amount of potassium which are 29 wt% and 32.67 wt%, respectively while the amount of calcium for both fuels are lower than the potassium content. However, one of the testing datasets, which is Thistle (19), failed to satisfy the experimental observations as the

predicted value of I_a is below 0.5 while it was observed to have a high tendency of bed agglomeration during the testing [217]. This is potentially due to a few reasons: i) The Thistle has high calcium content and low potassium values which were 29 wt% and 9.10 wt%, respectively, and this willdecrease the index value based on the coefficients in the Eq 4-1. ii) There is missing SO_3 content in the experimental analysis which also affected the calculation of I_a. iii) According to Llorente et al. [217], the agglomerates of Thistle exhibit a weak sintering degree, which could raise questions regarding the classification process of biomass fuel agglomerations. Therefore, caution should be exercised when applying the predictive method, I_a, to bed agglomeration in biomass fuels with significantly difference in the chemical ash compositions, especially the potassium to calcium ratio. Additionally, proper observations during the experiments are necessary to avoid any confusion to the researchers who developed the predictive model for the combustor units. In summary, it can be concluded that biomass with a potassium-rich ash compositions tend to exhibit high bed agglomeration tendency whereas the biomass fuels with a high amount of calcium content have low bed agglomeration potential in the fluidised-quartz bed combustor.

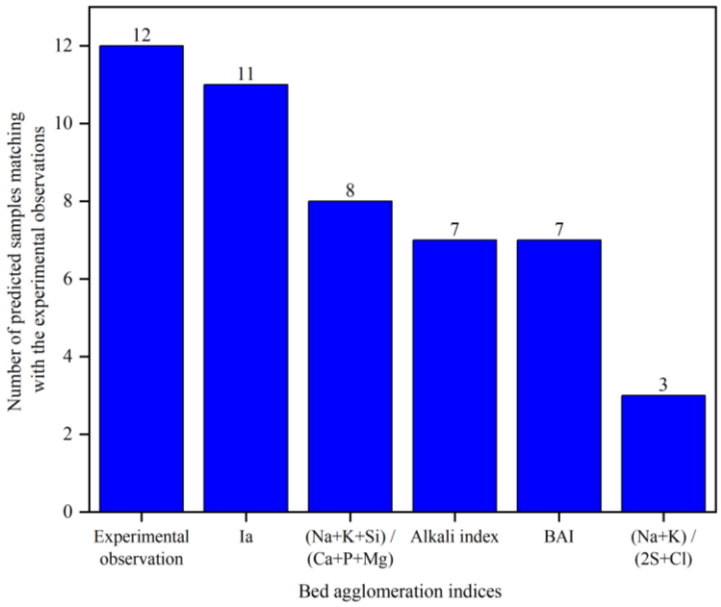

Figure 4-5 Comparison of the number of predicted samples matching with the experimental observations between I_a and 4 existing indices [142, 169, 170, 172, 247].

Figure 4-5 shows the performance of the newly improved model equation for I_a compared with the four different existing index equations [142, 169, 170, 172, 247]. These four distinct expressions are created for predicting the bed agglomeration behaviour in the FBC technology [96]. Figure 4-5 illustrates the number of predicted samples, out of the 12 testing fuels (11-22), that correspond to the experimental observations for each index. It is observed that the ranking for the accuracy in the prediction performance, arranged from high to low, is

as follows: I_a > I2 = (Na + K + Si) / (Ca + P + Mg) > Alkali index, AI = BAI > I1 = (Na + K) / (2S + Cl). The new improved index, I_a, successfully predicted a total of 11 out of 12 samples in accordance with the experimental observations. On the other hand, the four existing indices (I2, Alkali index, BAI, I1) could only accurately predict a maximum of 66% of the total samples.

4.3.3 Performance of the index, I_a on the total defluidization temperature (TDT).

Alkali metals play a crucial role in the formation of agglomerates, however, phosphorus also has been focused on recently due to its potential to aggravate the formation of bed agglomeration [91, 248-250]. Therefore, the influence of adding phosphorus-rich fuels that show the effects on the total defluidization temperature (TDT) was investigated to test the sensitivity of the I_a index. TDT denotes the temperature where no fluidization is observed [251], specifically defined when the first temperature at which the pressures curve reaches its lowest point. The performance of I_a was evaluated using 7 datasets as illustrated in Figure 4-6 [220], where the Ca/P ratio varied by blending Rapeseed cake (phosphorus-rich) with Bark II (calcium-rich) at ratios ranging from 10 to 70 wt%.

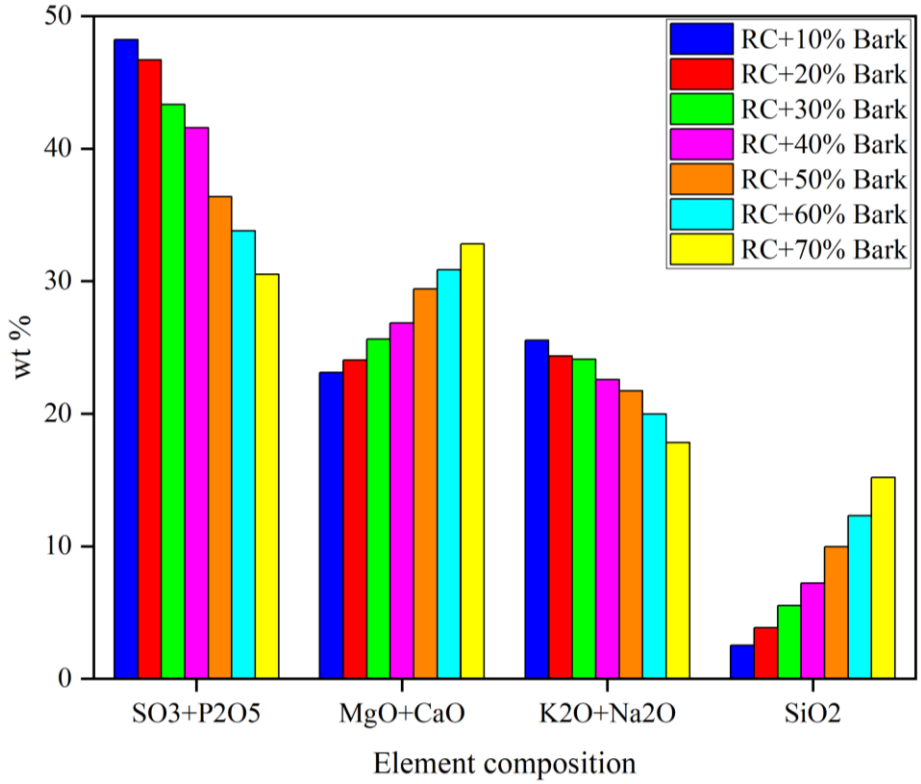

Figure 4-6 Elemental fuel ash compositions of the blends of Rapeseed Cake (RC) with Bark [220].

Figure 4-7 illustrates the I_a prediction with respect to the ratio of bark in the fuel blend between rapeseed cake and agglomeration tendency determined by TDT [220]. The I_a was

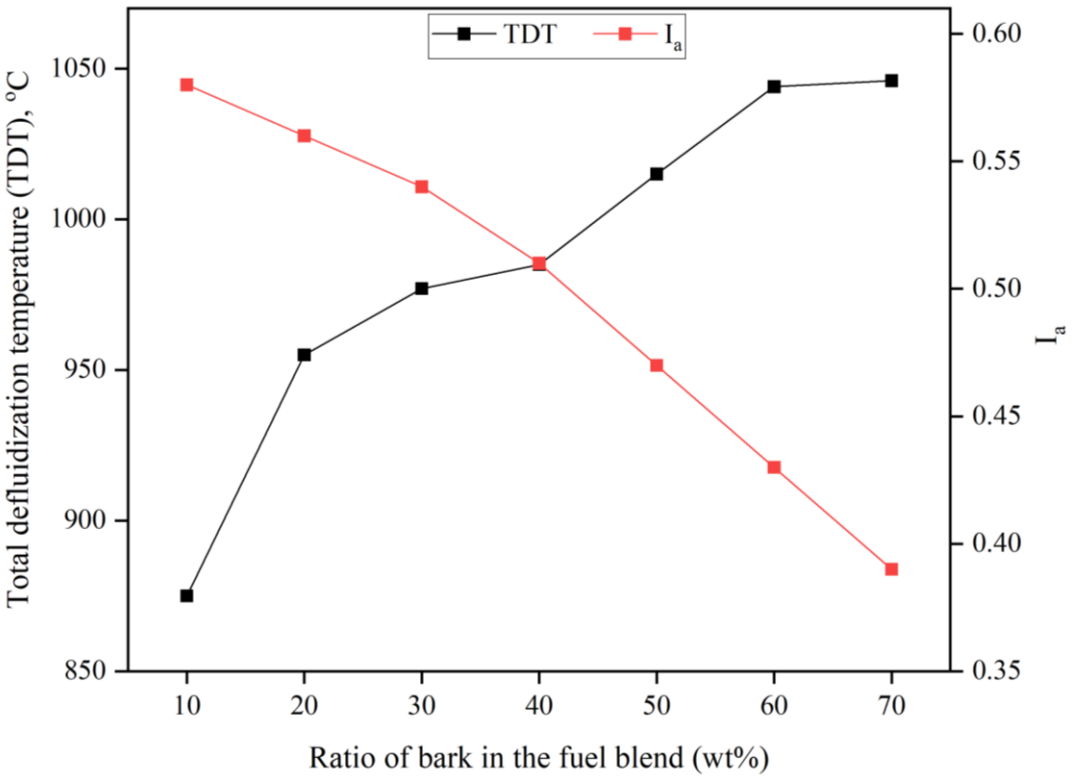

Figure 4-7 Comparison between the new predictive index, I_a and TDT by experimental observations [220] versus the ratio of bark in the fuel blends with rapeseed.

observed to decrease linearly with the increasing proportion of bark in the fuel mixtures. This suggested that the tendency of agglomeration is reduced from high to low. On the other hand, the TDT was found to increase when the ratio of bark in the fuel blend is increased from 10 to 70 wt%. This trend indicates that an increase in TDT will decrease the agglomeration tendency from high to low. Thus, this agrees with the I_a prediction and TDT by experimental observation. This is because the increase in the Ca content in a Ca-K-P system can cause a shift in the melting temperature above 1000 °C [73], which is aligns with a TDT at 1045 °C for fuel mixtures containing over 60 wt%. Piotrowska et al. [250] discovered that, in the co-combustion of wood and rapeseed cake, low-melting potassium silicates can form on the bed material grain surfaces. This process is followed by the adhesion of phosphorus-rich molten ash particles, potentially leading to agglomerate formation during fluidized bed combustion at 850 °C. Grimm et al. [219] conducted a study on bed agglomeration behaviours in the FBC of phosphorus-rich biomass and found that the dominant process involves the direct adhesion of partially molten ash particles containing K−Mg−P and Ca−K−Mg−P to the bed material grains. Piotrowska et al. [220] suggested the impact of phosphorus on the agglomeration severity is highly dependent on the Ca/P ratio.

4.4 Conclusions

This study has successfully developed an improved semi-empirical index to predict the tendency of bed agglomeration through the melt fraction mechanism. The index, I_a takes into account the chemical ash compositions when biomass is fired in fluidized bed combustors. The predictive tool created is capable of assisting industrial users in determining bed agglomeration behaviours when firing various types of biomass in FBC boilers. The newly improved bed agglomeration index, I_a was created by analysing the predicted melting fraction through TEM, considering the quartz as the bed material used in the FBC system and chemical compositions of fuel ash, by employing the numerical PLS regression coupled with a cross-validation. The presented method has been verified using experimental observations from existing literature on biomass in the FBC technology. The results indicate that the BAI propensity index, I_a can be categorized into two primary groups: low bed agglomeration tendency when $I_a \leq 0.50$ and high bed agglomeration propensity when $I_a > 0.50$. In addition, the I_a demonstrates a significantly higher success rate compared to four existing indices in evaluating the tendency of bed agglomeration in fluidized bed type of boiler.

It can be confirmed that the primary element contributing to bed agglomeration formation is K_2O, while a high value of CaO will reduce the tendency of bed agglomeration in FBC. It should be noted that P_2O_5 can accelerate the formation of bed agglomeration, but a high Ca/P ratio will drop the bed agglomeration as confirmed by TDT and I_a prediction. The index should be utilized during the low-temperature (700-900°C) operation of fluidized bed boilers. In addition, the I_a index is developed based on fluidized quartz bed combustion, therefore, caution should be exercised when extending the predicted indices, I_a in this paper to other types of bed material used in FBC technology. The author strongly recommends obtaining more extensive datasets of experimental observations by conducting tests at an industrial or full scale to improve the accuracy of the predictive indices in forecasting the tendency of bed agglomeration of FBC.

5 Effect of kaolin with biomass fuels on ash partitioning, slagging and combustion behaviour in a 250 kW grate boiler.

5.1 Introduction

Moving grate boilers for heat and electricity production are widely applied for solid biomass combustion on an industrial scale because they can fire different fuels of various moisture levels and require less fuel handling and preparation. Grate-fired boilers can fire practically any solid, even low-grade, fuels and are cheap to build. In addition, the grate normally has mechanical systems to disperse the bed fuel and collect the ash, which enables the boiler to operate continuously. These features have made the grate-firing technology the most utilized in solid biomass combustion for large-scale boilers [30, 31, 252]. Unfortunately, the composition of ash in the fuel might potentially raise operational difficulties in existing plants because of agglomeration on the grate, and slagging [32-35]. Slagging is common in grate-fired biomass boilers. In biomass combustion, the solid material generated during firing will be deposited on heat exchanger tubes and furnace walls which may limit heat transfer and can lead to corrosion [181]. These scenarios will reduce the boiler efficiency, availability, high maintenance costs, and mechanical failures which lead to unplanned plant shutdown [48].

The potential for agglomeration and the formation of severe deposits can be reduced if the potassium is trapped in the bed as compounds with high melting points. Additives have been known as an alternative to mitigate ash-related issues, especially alkali species during combustion. Additives hold great potential in industrial applications for addressing ash-related challenges, as it effectively traps the troublesome ash components, such as gaseous KCl and KOH through adsorption while also enhancing the ash fusion properties [78, 253]. Various methods have been proposed, such as the injection of kaolin into the grate boiler to reduce the slag and ash depositions in the heat transfer region during combustion. This can be accomplished by capturing the alkali in the bottom ash where it forms as stable compounds, then this can be effectively managed and removed by the ash removal systems such as the bottom ash bin. However, it must be noted that capturing the alkali in bottom ash also will cause the potential for the formation of severe agglomeration and slagging, especially in the grate boiler. This is because the presence of the eutectic compounds which have low-temperature systems has a high potential to cause the formation of sticky ash particles that agglomerate on the moving grate of the boiler. Therefore, the studies on the grate boiler condition, especially agglomeration and slagging condition after the injection of additives must

be addressed to avoid any unplanned shutdown of the grate boiler due to the failure to maintain and control the agglomeration and slagging behaviour during combustion.

Therefore, the aim of this work is to investigate, both experimentally and theoretically, the effects of blending biomass fuels with kaolin on ash-related issues in a 250kW field-scale grate boiler. This work will focus on mitigating the agglomeration, slagging tendency, partitioning of chemical elements of ash composition and deposition propensity when adding the kaolin to the feedstocks. One of the primary causes that dictate the partitioning of the elements between the various ash streams generated is the volatility of the elements present in the fuel. The partitioning and relative distributions of the chemical ash compositions with a particular focus on the changes in the non-volatile, alkali and alkaline earth species from the pre-combustion fuel stage (PF) to the post-firing stage; bottom ash (BA), slag, and coarse fly ash (FA). In addition, the thermodynamic equilibrium model (TEM) has been employed to determine the degree of melting of the slagging and the crystalline structures formed after the addition of kaolin into the woody biomass fuels. Overall, this study provides a much better understanding to the researchers and power generation operators in mitigating the ash related issues such as ash depositions in the furnace and optimizing biomass combustion for energy production.

5.2 Results and Discussions

This section will discuss the findings of an experimental investigation on the combustion of biomass fuels with kaolin addition in a 250 kW grate boiler. The outcome of this field experiment will provide a comprehensive analysis of the impacts observed in Sections 5.2.1 - 5.2.2. These consist of the slagging tendency of the virgin wood and waste wood grade A recycled wood with the mixtures of kaolin at the ratio of 1.55% and 2.5%, deposition propensity on the ceramic coupon, temperature profile throughout the combustion process and gas composition analysis. Laboratory analysis which included the chemical elements by Induced Coupled Plasma Mass Spectroscopy (ICP-MS), crystalline structure identification analysis by X-ray diffraction (XRD), morphology images by Scanning Electron Microscopy (SEM), and thermal stability by Thermogravimetric analysis (TGA) of bottom ash, slag and coarse fly ash will be discussed in detailed in Sections 5.2.4 - 5.2.7. By exploring these aspects, a comprehensive understanding of the agglomeration, slagging behaviour, ash partitioning, deposition propensity, and transformations of non-volatile and alkali species can be achieved throughout the combustion process in the grate boiler. By comprehensively studying these

aspects, researchers and power plant operators can gain valuable insights into the combustion behaviour of different fuels and increase the efficiency of the operation of biomass boilers.

5.2.1 Combustion analysis and observations

5.2.1.1 Gas Composition Analysis

In this experiment, the CO_2, O_2 and pollutant emission levels in the flue gas of virgin wood blended with kaolin were assessed and the results are illustrated in Figure 5-1 (a) and (b). The gas compositions were analysed by using Fourier Transform Infrared Spectroscopy (FTIR) at the inlet of the flue gas exhaust. Figure 5-1 shows the comparison between the experimental results (Exp) and the prediction made by an equilibrium model by Nik Norizam et al. [167]. This comparison aims to validate the prediction model (equilibrium) against the real experimental data obtained from the field. The data was taken during the stable condition of the operation in the grate boiler, this is to reduce the fluctuation readings of the gas compositions which led to the error. Figure 5-1 (a) is divided into two sections by a vertical black dash which indicates the different conditions of the experiment. In this experiment, the VW indicate the baseline of the study which is pure virgin wood without the addition of the kaolin while VWK1.55 is the conditions when 1.55% of kaolin was added to the fuel. The observation of CO_2 and O_2 levels were stable in the virgin wood without kaolin. The oxygen was increased by about 13% while CO_2 dropped ~15% in the flue gas after one hour of blended kaolin with the virgin wood (VWK1.55), as shown in Figure 5-1 (a). This phenomenon occurred because the kaolin consists of octahedral hydroxide and tetrahedral silicate sheets with a ratio of 1:1 [254, 255]. Hence, it can act as a promising CO_2 adsorbent due to its affordability, abundant availability in nature, and strong mechanical and chemical stability [256]. The equilibrium model's predictions for CO_2 and O_2 concentrations align closely with the experimental values. Specifically, for VW, the model's forecast for O_2 in the flue gas is 12.7 %, which is in line with the experimental range of 11.8–12.5 %. In the case of VWK1.55, the discrepancy between the model's predictions and the experimental findings is a mere 0.2 %, indicating the model's reliable performance in estimating O_2 concentrations in the flue gas. On the other hand, the CO_2 predicted by the equilibrium model highly corresponds with the experimental data for both the VW and VWK cases.

Figure 5-1 (b) illustrates the comparison involves assessing the average emissions of pollutants, such as SO_2, NO_x and CO between the experimental data and the predicted equilibrium modelling. The content of SO_2 decreased to ~32% after the addition of kaolin at 1.55% of dosages. In the presence of kaolin, the SO_2 emission was lower which is 2.48 g/MJ

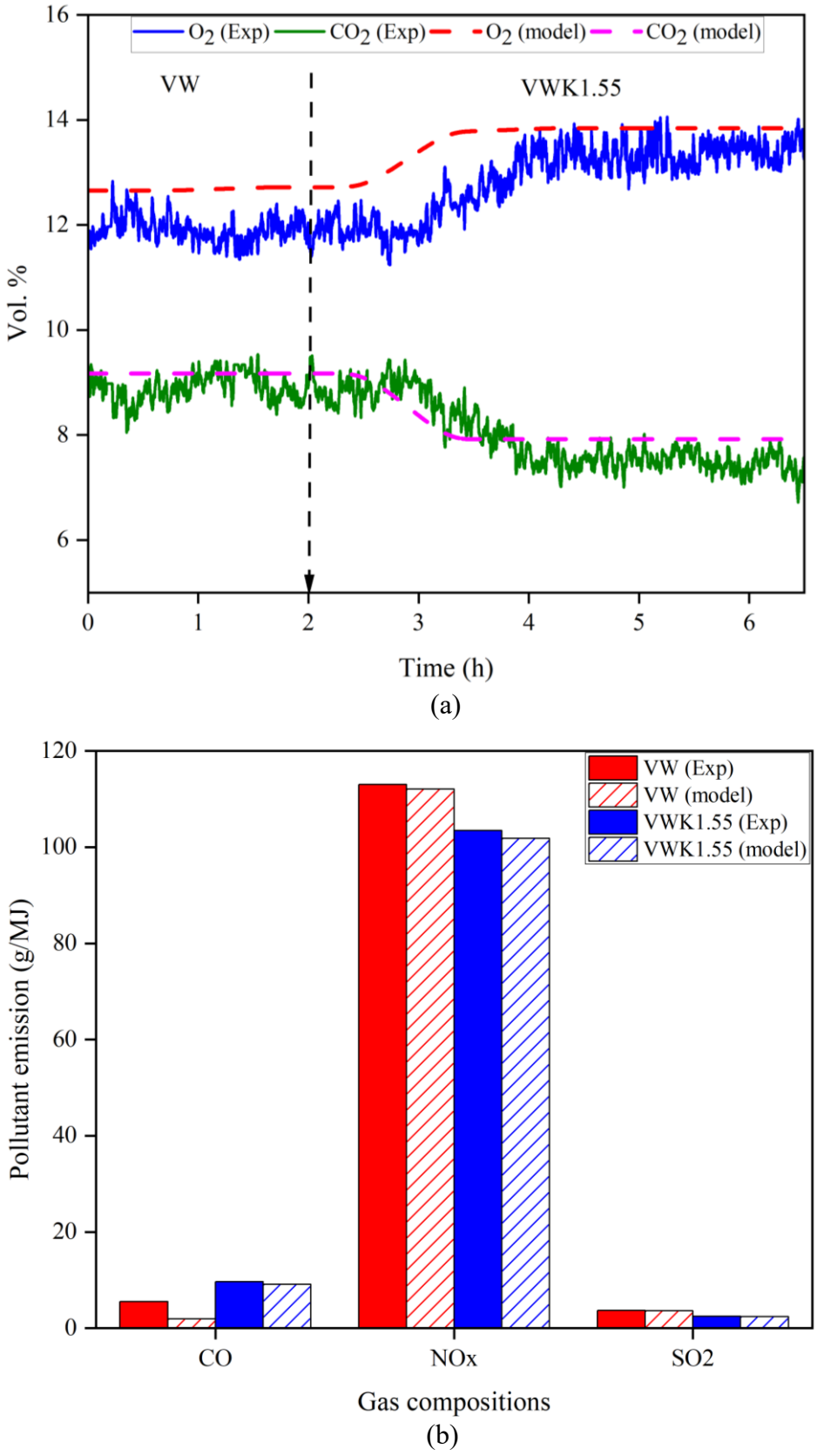

Figure 5-1 Comparison between the experimental and predicted model. a) Gas composition of O_2 and CO_2 in the flue gas by FTIR analysis. b) pollutant emissions level of CO, NO_x, and SO_2.

for VWK1.55 compared to without kaolin which is 3.68 g/MJ. This may be due to the KCl, KOH and potassium in the gas phase being captured by kaolin based on the reaction of chemical sulfation [257-259]. The predicted value of SO_2 is 3.61 g/MJ and 2.39 g/MJ for VW and VWK1.55, respectively. This indicates that the equilibrium model is able to predict 95% accurately. The CO emissions were found to increase from 9.66 g/MJ to 13.54 g/MJ after blending kaolin with VW at 1.55% of kaolin concentrations. This may be suspected to be due to the excessive amount of kaolin mixed with the virgin wood, which temporarily resulted in incomplete combustion on the grate. When the addition of kaolin to virgin wood was fired at more than 450°C in the combustion chamber, its moisture was released through the de-hydroxylation reaction, which may cause a temporary increase in the CO levels. The predicted value for CO concentration in the VW shows about 35% discrepancy while the predicted value of CO in the VWK1.55 is comparable. The NO_x emissions were found to reduce during the combustion of fuels with the addition of kaolin. This corresponds with the outcomes from the predictive model, which displays a trend that is identical to the experimental data. In this experiment, it was discovered that the virgin wood fired with kaolin addition reduced the temperature of the grate boiler during firing. This is due to the formation of NO_x being temperature-dependent in the combustion processes. Generally, the concentration of NO_x emissions tends to increase with higher combustion temperatures. This is because the high temperatures supply the required energy for nitrogen and oxygen in the air to undergo reactions, resulting in the formation of NO_x compounds. However, emissions of NO_x are influenced by a range of operational factors, including the type of fuel used, the ratio of the excess oxidants, and the methods of operation. Thus, additional research is required to enhance our understanding of NO_x emissions when kaolin is introduced into the biomass firing system.

5.2.1.2 Temperature profile

Figure 5-2 and 5-3 illustrate the temperature profile of the combustion of virgin wood and recycled wood cases, respectively. The temperature profile represents the variation in temperature at a primary overpass region which is nearest to the heat transfer area region inside the grate boiler during the combustion process as shown in Figure 2-9. The temperature profile is critical for understanding the efficiency and overall performance of the combustion process, especially for observing the impact of adding kaolin to the fuels. In this study, the temperature profile was monitored and recorded for 512 minutes for all the fuel mixtures. For the virgin wood case, the kaolin addition (VWK1.55) shows a notable high-temperature difference throughout the entire duration compared to the VW. During the kaolin addition, the temperature

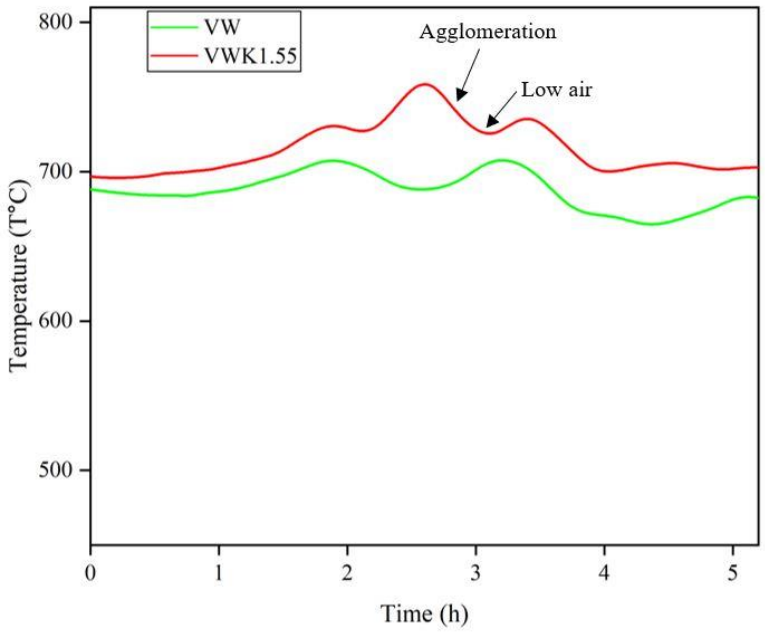

Figure 5-2 Temperature profile for VW cases with kaolin addition in a primary overpass region.

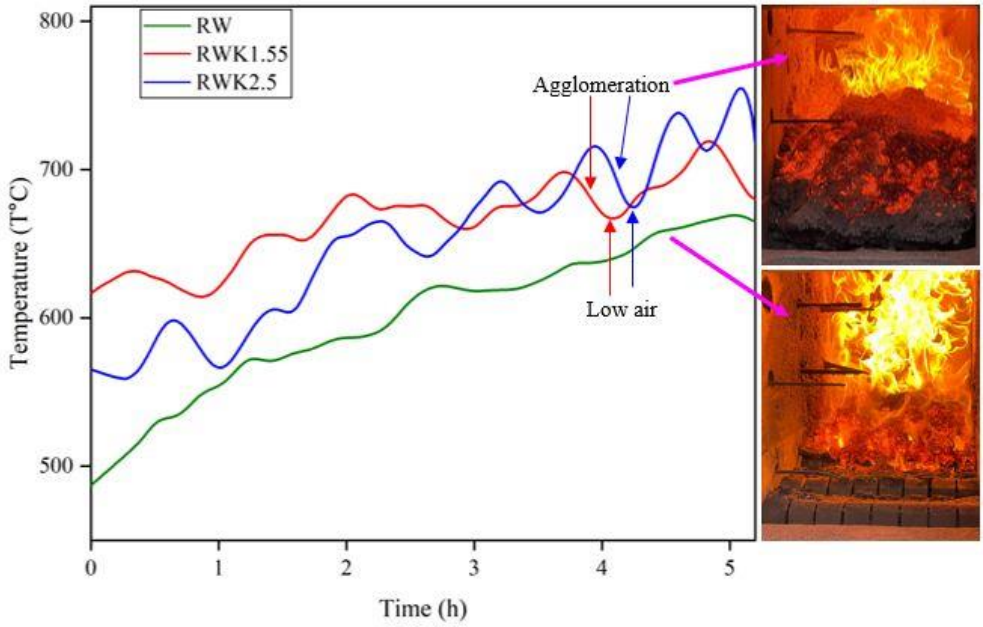

Figure 5-3 Temperature profile for RW cases with kaolin addition in a primary overpass region.

of the boiler increased significantly after adding kaolin, however, it was observed that the temperature profile of VWK1.55 shows a significant fluctuation in the temperature from a period hour of 2 to 3.3. Based on Figure 5-2, approximately at 160 minutes, the VWK1.55 temperature is the highest which is at 760 °C, however, the temperature dropped to 725 °C after 25 minutes. This is due to the burning fuels being agglomerated on the grate which blocked the primary air source from underneath of the grate boiler. Therefore, the temperature trend will

drop due to the lack of incoming air to the burning fuels as shown in Figure 5-2. This can be explained clearly in Figure 5-4 by the working principle of the grate boiler the mechanism of the formation of agglomeration on the bed and the combustion system in the grate boiler. On the other hand, the trend of the temperature profile of VW shows the fluctuation at 110 and 190 minutes with both maximum temperatures reaching 705 °C. The range of the temperatures recorded in VW is from 665 °C to 705 °C which indicated 40 °C temperature variations compared to 65 °C temperature difference in the VWK1.55. The addition of kaolin was found to increase the melting point of aluminosilicate compounds, consistent with findings from Boström et al. [260], but it also increased the tendency of slag formation on the grate due to fuel agglomeration.

For the recycled wood case, the temperature profile demonstrated a consistent and increased linearly with temperatures steadily rising from 490°C to 690°C for 512 minutes. The temperature of RW in the primary overpass region of the grate boiler is lower compared to the VW. This observation aligns with the ash fusion temperature (AFT) data presented in Table 2-5, where the AFT value for VW is significantly higher than that for recycled wood RW.In Figure 5-3, the fuel mixtures with kaolin blending show the distortion of the temperature profile for both scenarios. During the initial 175 minutes, the temperature profile of RWK1.55 was recorded to be higher than that of RWK2.5. However, from 175 to 512 minutes, the situation reversed with RWK2.5 exhibiting higher temperatures compared to RWK1.55. This aligns with the expectations that an increase in the kaolin ratio would lead to a corresponding rise in the temperature. Throughout this latter period, both fuel mixtures experienced significant temperature fluctuations, which were erratic and beyond control. This phenomenon is attributed to the formation of severe agglomerations on top of the grate in both fuel mixtures. Figure 5-4 clearly explains the detail on the working principle and the mechanism of the grate boiler during the firing of the fuel.

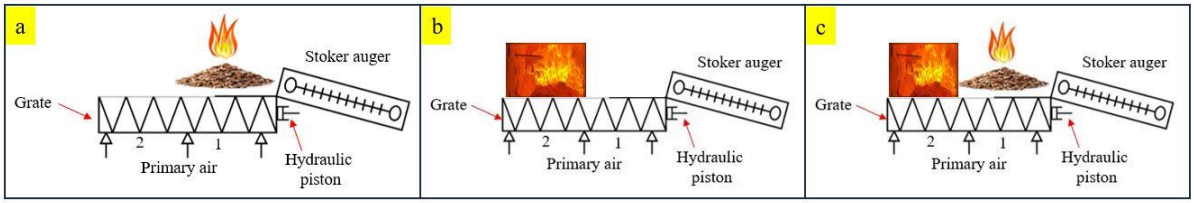

Figure 5-4 Working principle and mechanism of the grate movement system and the agglomeration formation on top of the bed of the grate boiler.

Figure 5-4 (a) illustrates the initial condition of the fuel firing on top of the grate where primary air is supplied from underneath the grate and consists of two main sections which are primary sections 1 and 2. The air will be used throughout the entire combustion process for

igniting and sustaining the combustion of the fuel. A hydraulic piston moves the grate to transport the fuels from the front to the back of the grate during combustion to ensure a continuous firing of the fuels with the support of air from the primary section 2. Additionally, this system also facilitates the even distribution of heat across the combustion chamber. In this phase, the fuel mixtures will be firing, and the temperature will increase which results in the agglomeration of the fuels on top of the grate as presented in Figure 5-3. As a result, the temperature will drop due to the obstruction of primary airflow by the fuel piles, resulting in low air supply. Figure 5-4 (b) shows the condition where the hydraulic piston moved the grate which shifted the burning fuels from primary air section 1 to section 2. This process moved the agglomerated fuel from the front of the combustion chamber (section 1) to its back (section 2). Figure 5-4 (c) shows the introduction of a new batch of fuel mixtures by the stoker auger, leading to a temperature rise as the air supply in primary section 1 now effectively reaches the new batch of fuel. This cyclical process continues until a substantial pile of agglomerated fuel forms on the grate, as shown in Figure 5-5, necessitating a boiler shutdown. Overall, an understanding of the temperature profile behaviour is essential for optimizing the combustion efficiency in industrial processes, where precise temperature control is vital to minimize downtime due to the slag and agglomeration formation in the boiler. Furthermore, it must be noted that different fuels will have different temperature profiles due to their chemical compositions and physical characteristics.

5.2.2 Slagging tendency of the fuels

Table 5-1 shows the sintering category and slagging index, I_n of the pure woody biomass feedstocks and mixtures of kaolin. The sintering category is a qualitative assessment of the degree to which the fuel mixtures contribute to the process by which particles fuse and lead to the formation of slag. The sintering category classification is based on the explanation in Section 2.6.1 (Figure 2-7). The I_n index is a quantitative measure developed in Chapter 3 which aims to predict the severity of slagging within the boiler at the high-temperature region. The virgin wood was observed as low slagging with a category 2 sintering degree with an I_n index of 0.34 compared to the recycled wood fuel, which was identified as moderate slagging at the sintering level of 3 and an I_n index of 0.40. However, VWK1.55, VWK2.5, RWK1.55, and RWK2.5 were categorized as severe slagging, and this is due to the grate boiler needing to be shut down due to severe slagging and agglomeration on the bed of the grate furnace, as shown in Figure 5-5, after running for ~7 hours. Figure 5-5 illustrates two conditions on the bed of the grate boiler, (left side: without kaolin injection, right side: with kaolin addition) for

Table 5-1 Sintering degree 2-4 of the feedstocks blended with kaolin at two different dosages.

Fuel mixture	Sintering category	I_n index [163]
Virgin wood (VW)	2	0.34
VWK1.55	4	0.74
VWK2.5	4	1.04
Recycled wood (RW)	3	0.40
RWK1.55	4	0.77
RWK2.5	4	1.07

Figure 5-5 Severe agglomeration of the recycled woods with addition of kaolin during firing. Left: without kaolin, right: with kaolin.

the recycled wood case study. It was clearly shown that severe agglomeration was formed with kaolin addition on the bed of the grate boiler compared to without kaolin injection. This has resulted in the boiler needing to stop feeding the fuel to the combustion chamber due to severe agglomeration on the bed of the grate boiler might potentially block the primary air.

The slagging index, I_n of the VWK1.55, VWK2.5, RWK1.55, and RWK2.5 show that the I_n value is increasing with the increase of the mixture ratio of kaolin from 1.55% to 2.5% for both feedstocks blended with kaolin. The trend clearly shows that when adding kaolin to both virgin and recycled wood increases the sintering category and the I_n index value,indicating an overall increase in the severity of slag formation. This Table 5-1 demonstrates that while kaolin is added to mitigate ash-related issues in the combustion processes, such as the reduction of the fly ash deposits, it can also enhance the agglomeration of ash deposits on the bed of the

moving grate, thereby increasing the potential for slagging within the combustion system. This is a significant finding for operational considerations in biomass combustion as it emphasizes the need to balance the benefits of kaolin against their potential to exacerbate slagging.

Figure 5-6 illustrates the post-firing condition inside of a grate boiler of virgin wood, VWK1.55 and VWK2.5. The virgin wood without kaolin addition shows a certain amount of ash deposition on the bed of the grate. There is a visible increase in the accumulation of ash on top of the grate from the VW to the VWK1.55 and VWK2.5. This suggests that the addition of kaolin has a noticeable effect on ash agglomeration. It is evident that with a higher percentage of kaolin, the ash appears more agglomerated, potentially indicating an enhanced slagging tendency. This is in line with the prediction of the slagging indices, I_n which show the index number increases as the increase in the ratios of kaolin in the virgin wood mixture. Moreover, the observation of the ash deposits in the VW appears looser and less fused while the ash deposition becomes denser and appears to adhere more strongly to the boiler surfaces in the VWK1.55 and VWK2.5. This is also in agreement with the sintering test which indicated the VW as category 2 while VWK1.55 and VWK2.5 were both in category 4. Additionally, this could imply that kaolin influences the ash chemistry and melting behaviour leading to a clinker formation on top of the bed of the grate boiler. The fuel with kaolin mixture appears to have a lighter ash colour and a more cohesive texture compared to the darker and more granular ash seen in the VW case.

Figure 5-6 The post-firing condition on top of the bed of the moving grate for virgin wood (VW) with kaolin addition at 1.55% (VWK1.55) and 2.5% (VWK2.5).

Figure 5-7 shows three different samples of slag by-products of the virgin wood combustion with the addition of kaolin. The first sample labelled VW, which is from the combustion of virgin wood without kaolin, displays a slag that has multiple colours, indicating

regions of varying temperatures and compositions. The structure appears to be more heterogeneous with distinct layers and textures, which could suggest a less uniform combustion process. For the VWK1.55 sample, we observe a transformation in the slag structure. The colour appears more uniform, and the slag appears to have a more cohesive and clumpy formation. This could be attributed to the intermediate level of kaolin addition, which may have started to change the ash fusion characteristics resulting in a different slag formation. The VWK2.5 sample shows a further progression with an even lighter colour and a very cohesive structure which suggests more significant changes in the ash chemistry due to the higher kaolin content. The slag here appears denser and more uniform, indicating that the higher percentage of kaolin has significantly influenced the melting behaviour of the ash which promotes the formation of slag. It suggests that the ash particles have fused more thoroughly, possibly due to the changes in the melting temperature and viscosity caused by the kaolin.

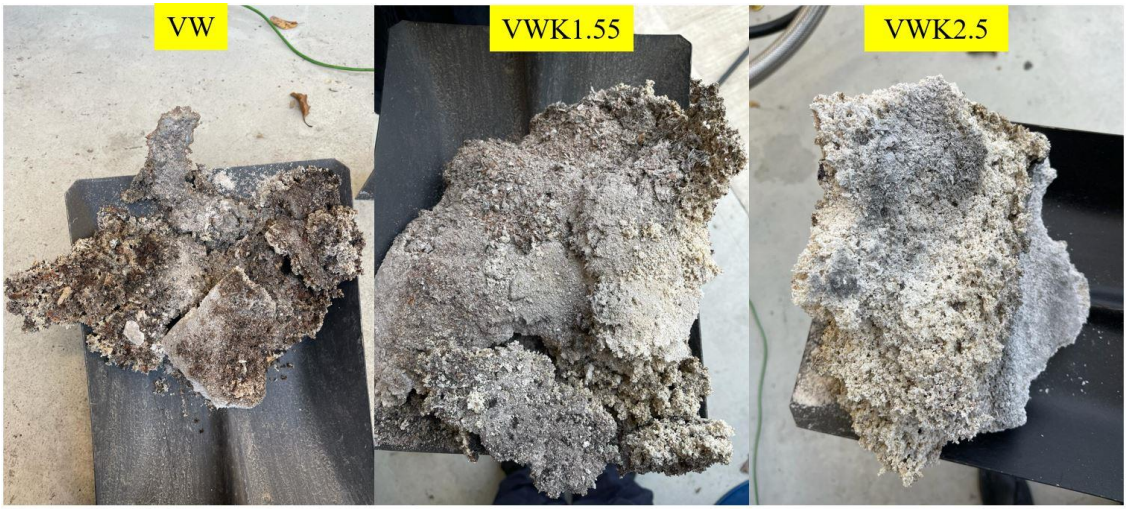

Figure 5-7 Slag formation byproducts of firing for virgin wood and mixtures of kaolin.

Figure 5-8 The post-firing condition on top of the bed of the moving grate for recycled wood (RW) with kaolin addition at 1.55% (RWK1.55) and 2.5% (RWK2.5).

Figure 5-8 demonstrates post-firing condition on top of the bed of the moving grate for recycled wood (RW) with kaolin addition at 1.55% (RWK1.55) and 2.5% (RWK2.5). The formation of ash deposition in RW maintains a certain level of fragmentation which is indicative of less extensive sintering or agglomeration. There is a visible change in RWK1.55. The addition of 1.55% kaolin appears to have influenced the ash deposition, which appears more agglomerated. The ash is denser and appears to coalesce more significantly, suggesting that the kaolin is affecting the ash fusion characteristics, potentially causing an increase in the sintering degree from 3 in RW to 4 in RWK1.55. Furthermore, RWK2.5 shows an even greater level of ash deposition. The RWK2.5 correlates with an even higher degree of agglomeration, resulting in a severe agglomeration of ash deposits observed on the bed of the grate boiler. This cohesive structure of ash deposits suggests that increasing kaolin content further enhances the slagging tendency as also indicated by a higher sintering category and higher slagging index, I_n as explained in the Table 5-1.

Figure 5-9 Slag formation byproducts of firing for recycled wood and mixtures of kaolin.

Figure 5-9 shows the formation of slag from recycled wood firing with kaolin addition at two different ratios of 1.55% and 2.5%. The differences between the samples suggest that kaolin affects the slag's physical structure which was identical to the virgin wood case study with kaolin addition. The slag from recycled wood without kaolin shows a rough, heterogeneous appearance with distinct layers, which could be indicative of various combustion phases. The structure of RWK1.55 appears more cohesive and clumped together, with less distinct stratification, implying that the addition of kaolin is influencing the ash's fusion and sintering properties. For the RWK2.5, the slag was found even denser and exhibited a uniform colour and surface, pointing to an even greater influence of the kaolin on the ash

behaviour, resulting in a slag that's less stratified, as the higher kaolin content likely facilitates a more complete fusion of ash particles during combustion.

Full-scale ash collection was carried out to determine the weight of the ash obtained after the combustion. The regions involved in the grate boiler for the full-scale ash collection were the bottom ash bin, underneath of the grate and the ash on the bed of the grate boiler. Table 5-2 presents the full-scale data of the ash collection in the grate boiler after the firing for the recycled wood case study. The percentage of bottom ash and slag shown in the Table 5-2 indicated the fraction of the total ash collected in the grate boiler. In general, it clearly shows that the total ash collected is increasing rapidly from 7.56±0.01 kg to 10.41±0.07 kg and 13.43±0.07 kg after the addition of the kaolin to the recycled wood at ratios 1.55% and 2.5%, respectively. The increased total ash collected with the addition of kaolin suggests that kaolin affects the ash characteristics. The K_2O is probably held within the bottom ash and slag in the form of silicate compounds due to the high ratio of Si/K in the pure recycled wood [110]. This can be supported by Valmari et al. [261] who stated that the non-volatile ash species were typically enriched in the bottom ash. The error percentage is to show the absence of the ash collected in the grate boiler. The highest error percentage is 6.86±0.47% for the RWK2.5

Table 5-2 Summary of the full-scale ash collection in the grate boiler after combustion.

Type of fuel	Fuel input (kg)	Time (min)	Total ash collected (Kg)	Bottom ash (%)	Slag (%)	Error (%)
RW	495-505	600	7.56±0.01	49.1±0.2	50.9±0.2	3.05±0.14
RWK1.55	345-355	420	10.41±0.07	45.9±0.9	54.1±0.9	5.92±0.64
RWK2.5	345-355	420	13.43±0.07	42.2±1.7	57.8±1.8	6.86±0.47

** The bottom ash (< 3 mm) was collected from the bottom ash bin, area on top and underneath of the grate while slag (> 3 mm) was collected from the bottom ash bin, area on top of the grate as outlined in Section 2.6.*

followed by 5.92±0.64% for the RWK1.55 and 3.05±0.14% for the RW. Overall, approximately 90% input of the ash is collected, which is fairly considered to be mass-balanced. However, given the complex and large setup of the grate boiler used in this experiment, it is difficult to get 100% mass balanced due to some of the ash potentially being vaporised, and some of the ash will be lost to the refractory wall, and carried away with the flue gas which ends up being captured by the electrostatic precipitator (ESP).

Overall, the kaolin's influence on the slag's physical properties is critical to understanding the application of the additives to control slagging in biomass combustion. By affecting the melting temperature and the viscosity of the ash, kaolin was found to have a marked effect on the agglomeration and adhesion properties of the slag. The visual of the bed

condition and slag formation in the grate boiler align with the expected outcomes of kaolin addition, which is known to change the melting behaviour of ash and thus its deposition and slagging tendencies in biomass-fired boilers. Moreover, the ash content for all of the 4 fuel mixtures (VWK1.55, VWK2.5, RWK1.55, and RWK2.5) were considered as high as shown in the Table 2-7 after the increase of the kaolin dosages. This also proves that adding kaolin will increase the formation of ash deposits. In addition, data collected in Table 5-2 is useful for future reference for the researchers or users to observe the trend of impact to the bottom ash and slag when adding kaolin to the fuel in grate combustor. A comprehensive analysis of laboratory results will be explained in detail in Sections 5.2.4 – 5.2.7 on the chemical and physical properties of the samples collected from these bottom ash and slag.

5.2.3 Fly ash depositions

5.2.3.1 Ash deposits morphology

The images of the ash deposits on the ceramic coupon were captured after each test. As outlined in Section 2.6, the duration of 19 tests ranged between 80 to 500 minutes to determine the deposition propensity as well as to ensure the total quantity of ash fed into the system was consistent. The flow of the flue gas direction is indicated by a yellow arrow as shown in Figure 5-10 and Figure ***5-11***. Figure 5-10 shows two ceramic coupons from the top view with deposits of fly ash from the combustion of virgin wood labelled with VW and a mixture of virgin wood with 1.55% kaolin labelled with VWK1.55. Based on Figure 5-10, it appears that the VW coupon has a thicker layer of fly ash deposit which indicates a higher rate of fly ash

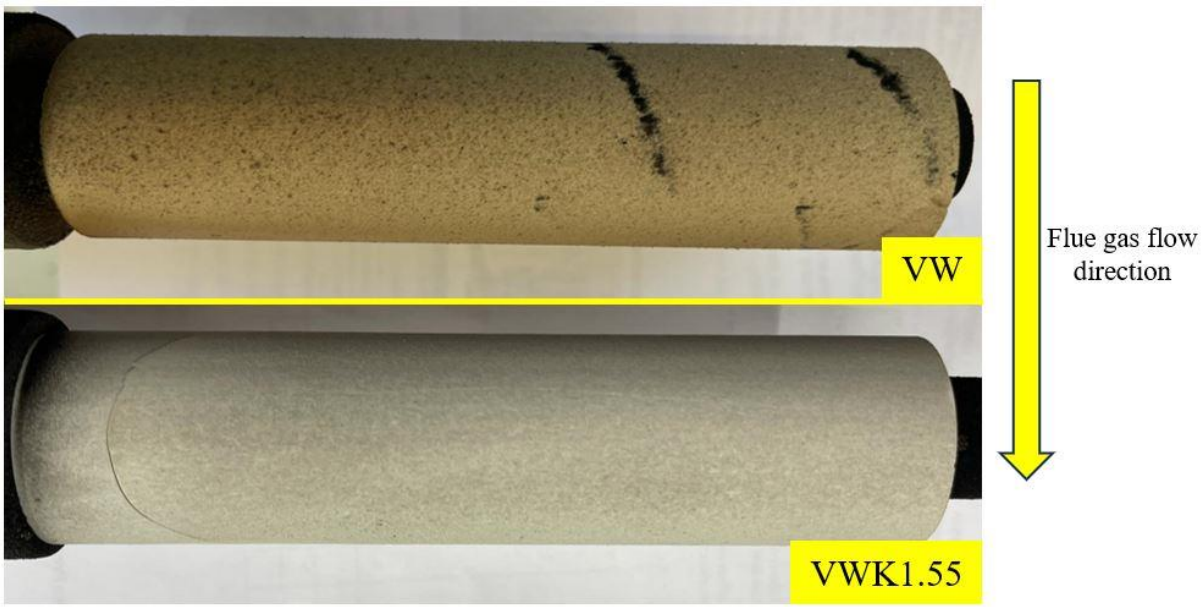

Figure 5-10 Fly ash deposits on the ceramic coupon for virgin wood and addition of kaolin at a ratio of 1.55%.

accumulation during combustion. The thicker layer was likely due to the formation of K-salt and K-silicate layers on the surface of the ceramic coupon for VW. In contrast, the VWK1.55 coupon has a visibly thinner layer of fly ash, suggesting that the addition of kaolin to the VW has resulted in less fly ash being deposited onto the coupon. This can be seen clearly in the rate of deposition, mg/m^2·min and ash deposition propensity in Section 5.2.3.2. Additionally, the structure of the ash deposits for VWK1.55 is porous and greyish compared to the VW. The reduction in fly ash deposition with the VWK1.55 mixture could be due to several factors influenced by the kaolin addition. Kaolin may change the thermal profile of the combustion process, chemical composition of the ash, and affect the ash melting point and stickiness, which reduce the tendency of the ash particles to adhere to surfaces such as the ceramic coupon [82].

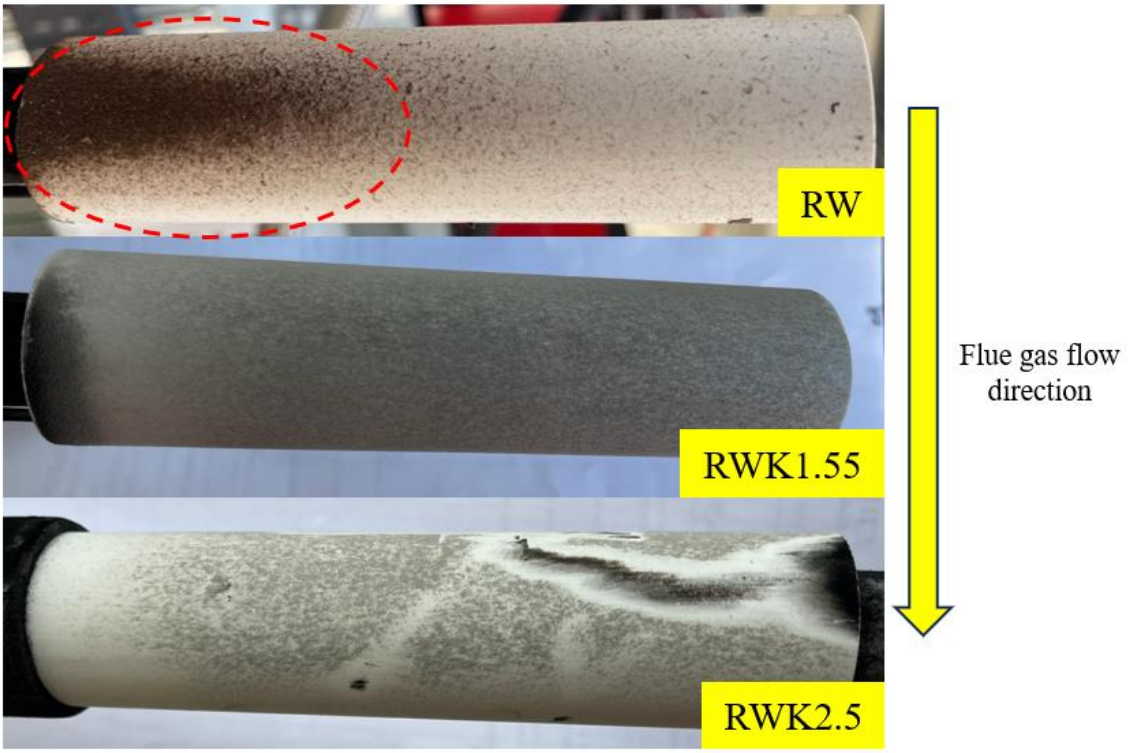

Figure 5-11 Fly ash deposits on the ceramic coupon for recycled wood and the addition of kaolin at ratios of 1.55% and 2.5%.

For the recycled wood, the red highlighted areas on the ceramic coupon show noticeable accumulations of ash deposits, as shown in Figure 5-11. The accumulation of the ash deposits is potentially formed partly by the condensation of K-salt vapour, which was produced during the firing of K-rich recycled wood. Moreover, eddy diffusion and thermophoresis can significantly influence the distribution and deposition patterns of submicron particles, such as fly ash whichcontributes to the formation of fly ash accumulation on the ceramic coupon [262, 263]. This fly ash accumulated on the ceramic coupon formed by the inertial impaction. For

RWK1.55 (recycled wood with 1.55% kaolin), the main body of the ceramic coupon appears finer, more uniform and greyish compared to the RW. The structure of the ash layer has much less ash deposition, indicating that reduction in the K-salt layer formation on the coupon. The ash deposit observed on the RWK1.55 coupon has a porous structure fand is very loose which can be removed easily by rotating the coupon upside down. This confirmed the effectiveness of a 1.55% kaolin addition in reducing fly ash depositions in the recycled wood fuel.

Moreover, the bottom coupon, labelled RWK2.5, shows the least ash deposition among the three, with even lower adhesion than the RWK1.55 coupon. This suggests that increasing the kaolin content to 2.5% further reduces the propensity for ash to deposit. The ash that has been deposited appears to have a distinct stratification with clear layers that are extremely loose and fragile. This can be seen in Figure 5-11 for RWK2.5, even with a light touch on the wall and slight vibration, for example, when pulling out the probe with a ceramic coupon attached to it from the combustion chamber caused the ash deposits to detach and fall. Generally, the ash deposit structure for RWK2.5 is identical to RWK1.55. The variation in ash deposition and structure across these coupons can be attributed to the impact of kaolin on the properties of the ash. Kaolin can change the melting temperature, physical and chemical properties of the ash compositions [260, 264]. In summary, these experiments reveal that kaolin addition to virgin wood and recycled wood fuels significantly reduces fly ash deposition in a combustion environment.

5.2.3.2 Deposition propensity

The deposition propensity, D_p was determined to understand how much fly ash will adhere to the surface of a ceramic coupon when firing the different biomass fuels with kaolin addition [190]. This is comparing the ratio of ash built up on the coupon and the maximum potential of deposits that could build up if every single fly ash particle in the flue gas around the coupon adheres to it. The deposition propensity equation 5-1 [190] can be referred to as follows:

$$D_p = \frac{m_{msd}}{m_{th}} \times 100\% \quad (5\text{-}1)$$

where m_{msd} is the weight measured of ash deposits formed on the ceramic coupon and m_{th} is the maximum value of possible build-up of ash deposits if every single ash particle in the flue gas around the coupon adheres to it. By applying the deposit propensity, D_p there is a tendency to compare the effects of various types of fuels with different ash chemistry and ash content on the process of deposit formation. The m_{th} is defined in the equation 5-2 [190] as follows:

$$m_{th} = m_{feed} \times \frac{A_{coupon}}{A_{region}} \quad (5\text{-}2)$$

where m_{feed} is the total feeding amount mixture of fuel ash with kaolin, while A_{coupon} and A_{region} are the projected area of the ash deposit on the ceramic coupon and the surface area of the primary overpass region in a 250 kW grate boiler, respectively as illustrated in Figure 5-12

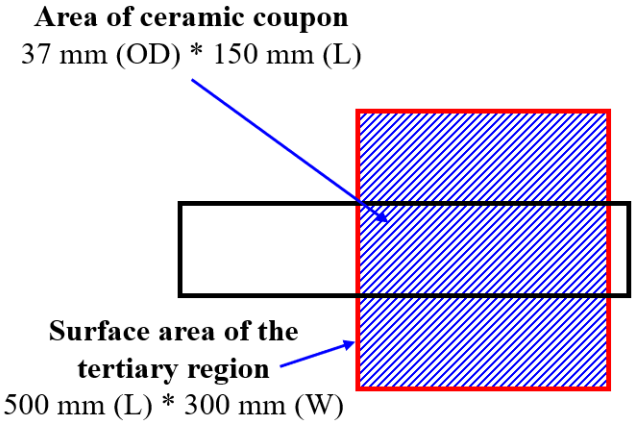

Figure 5-12 The projected area of deposited ceramic coupon and the surface area of the primary overpass region in the 250 kW grate combustor.

Table 5-3 Experimental reproducibility checking results (Num. represents the experimental matrix number based on Table 2-6).

Fuel mixtures	Num.	Deposition propensity, D_p (%)	Rate of ash deposition, mg/m^2·min
VW	2	6.27	5.57
	4	6.35	5.64
VWK1.55	9	1.25	2.56
	11	1.34	2.74
RW	19	9.68	11.48
	22	10.24	12.14
RWK1.55	28	2.35	5.50
	30	2.78	6.50

prior to the analysis of ash deposition, the author carried out experimental reproducibility to ensure the consistency of the results. 4 different types of case studies were carried out to duplicate the experiment under the same conditions as shown in Table 5-3. As listed in the experimental matrix in Table 2-6, experimental nums. 2 and 4, 9 and 11, 19 and 22, and 28 and 30 for VW, VWK1.55, RW and RWK1.55, respectively. Based on Table 5-3, the deposition propensity varied by 0.08 %, 0.09 %, 0.56 %, and 0.43 % between experiments nums. 2 and 4, 9 and 11, 19 and 22, and 28 and 30, respectively. Therefore, the experiment is reliably reproducible. For the rate of ash deposition, the error varied by 1.3 %, 6.7 %, 5.5% and 15.5%.

The error in experiment nums 28 and 30 were a bit higher compared to other experiments, However, according to Figure 5-14, it is observed that the deposit mass uptake for RWK1.55 has a comparable and good fit on the graph, which is reasonably accepted to determine the trend of the rate of fly ash deposits on the ceramic coupon.

The deposition propensity of the five mixture fuels including VW, VWK1.55, RW, RWK1.55 and RWK2.5 were calculated according to equation 5-1, and the results are presented in Figure 5-13. RW has the highest deposition propensity (10.4±0.7 %), meaning that 10.4 % of the fly ash collides with the ceramic coupon when firing the recycled wood. The virgin wood shows lower deposition propensity compared to the recycled wood which is 6.9±0.7 %. These findings align with the images taken as presented in Figure 5-10 and 5-11 for VW and RW, respectively. The images reveal that RW experienced a significantly higher accumulation of ash deposits compared to VW. This is potentially due to a high concentration of K-salt layer formation in the RW. Such observations are consistent with the deposition propensity and are highly linked to the fuel ash compositions as shown in Table 2-4 which shows that the potassium content level is about 1.7 times higher in RW compared to the VW.

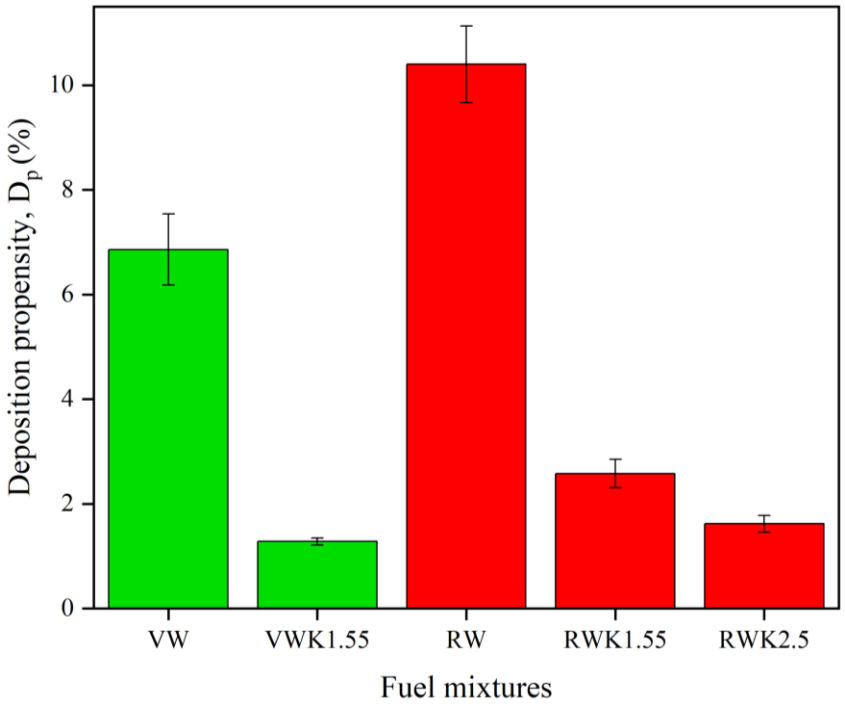

Figure 5-13 Deposition propensity of virgin wood (green bar) and recycled wood (red bar) with kaolin addition.

The deposition propensities of recycled wood firing with kaolin addition labelled with RWK1.55 and RWK2.5 are shown in Figure 5-13. The deposition propensity was observed to have a highly significant impact in the recycled wood after adding kaolin at ratios of 1.55 %. The deposition propensity of RWK1.55 firing reduces significantly by about 75 % from

10.4±0.7 % of RW to 2.6±0.3 % in RWK1.55. Furthermore, the use of 2.5% kaolin in recycled wood shows a reduction of about 85% in the deposition propensity. For the combustion of virgin wood with the kaolin at ratios of 1.55%. A similar phenomenon has been observed in virgin wood cases and recycled wood cases when blended with kaolin. The deposition propensity was decreased initially from 6.9±0.7 % in VW to 1.3±0.1 % in VWK1.55. This indicates that the reduction is approximately 81%. However, the study by Wang et al. [190] mentioned that there was no significant impact of deposition propensity when added kaolin in the K-rich woody biomass. Wang et al. [190] concluded that the formation deposits are primarily driven by inertial impaction and not significantly influenced by the kaolin addition. In the author's opinion, the study by Wang et al. [190] which investigated the impact of kaolin on biomass ash deposition in a lab scale-entrained flow reactor presented a contradicting argument based on their findings, the wheat straw was observed to have high deposition propensity compared to the milled wood. It was reported that the K value in wheat straw was 16.2 wt% while the milled wood was 0.7% higher than in wheat straw. Numerous studies have stated that high alkali metals in the fuel will lead to the formation of ash deposition [167, 265, 266]. However, this is not the case for the study by Wang et al. [190]. Hence, their findings observed insignificant results in deposition propensity when adding kaolin to the milled wood is questionable. Therefore, this is one of the research gaps that has been addressed in this study to show that the lab-scale reactor is not representative of the field and large scale. This is because, in field-scale combustors, biomass and mineral particles may experience different temperature profiles and more vigorous fragmentation compared to bench-scale reactors, leading to increased mineral matter released into the fly ash [120]. Moreover, the feed rate in the field scale will be much higher compared to the lab scale. As a result, more mineral matters are released from the biomass during combustion. Overall, the kaolin clearly shows a significant impact in reducing the deposition propensity in woody biomass by at least 75%. This is in agreement with the morphology of the images observed in Figure 5-10 and Figure ***5-11*** for VWK1.55, RWK1.55 and RWK2.5, respectively.

Figure 5-14 illustrates the deposit mass uptake over time for different fuel mixtures, consisting of VW, VWK1.55, RW, RWK1.55, and RWK2.5. This is another method to confirm the applicability of kaolin in reducing fly ash deposits. This is also to support the finding of deposition propensity to ensure the results are reliable. The RW shows the highest deposit mass uptake, with the line having the steepest slope, suggesting that the fly ash accumulates more quickly on the ceramic coupon over time compared to the other mixtures. VW has a lower deposit mass uptake than RW but still accumulates over time, as evidenced by the upward trend

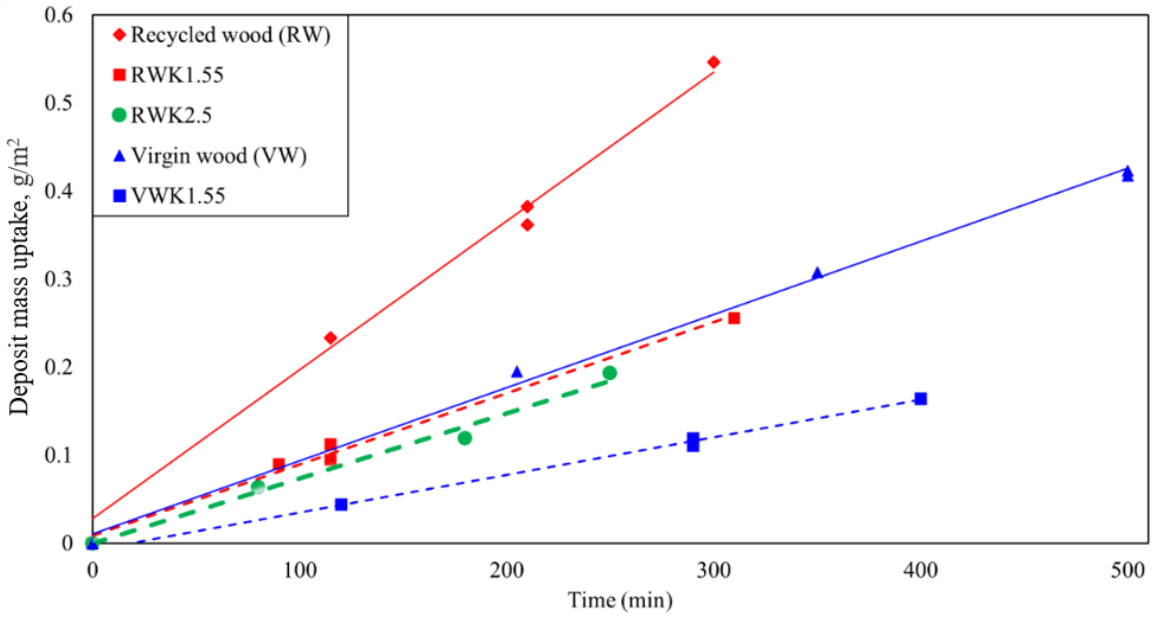

Figure 5-14 Deposit mass uptake for virgin wood and recycled wood blended with kaolin.

in its data points. These results agreed with the deposition propensity as shown in Figure 5-13 where the deposition propensity of RW is much higher compared to VW. RWK1.55 and RWK2.5 both display a reduction of about 57 % and 60 %, respectively in the deposit mass uptake compared to RW. This shows the kaolin's effectiveness in mitigating fly ash deposition issues in recycled wood firing in a 250 kW grate boiler. On the other hand, VWK1.55 also shows a reduction of approximately 51% in the deposit mass uptake which follows a similar trend as its recycled wood when blended with the kaolin. These trends suggest that kaolin when blended with wood biomass fuels tends to modify the ash characteristics, for example, increasing in melting temperature from alkali silicates to the formation of alkali-aluminium silicates which have higher melting points [260, 267]. However, it must be noted that earlier results in bottom ash and slag show that the addition of the kaolin to the woody biomass fuels has a negative impact which is a high slagging tendency observed on the grate. Additionally, Table 5-2 presented that the amount of bottom ash and slag collected were significantly increased in both woody biomass fuels after adding kaolin. This is highly related to the alkali metals enriched and trapped in the bottom ash. As a result, less fly ash was observed on the ceramic coupon as shown in Figure 5-10 and 5-11 for VWK1.55, RWK1.55, and RWK2.5. Moreover, the deposit mass uptake also validated the results in deposition propensity where the kaolin blending with the VW and RW significantly reduced the deposition propensity. In conclusion, the deposit mass uptake as illustrated in Figure 5-14 provides valuable information to the researchers and users in assessing the functionality of the kaolin impacts on the woody biomass fuels in the field scale grate boiler.

5.2.4 Ash partitioning: chemical composition analysis

a) Case 1: Virgin wood with kaolin addition

Figure 5-15 shows the ash partitioning of the chemical elements in the virgin wood fuel mixtures and in the post-firing samples, which consist of the bottom ash, slag and coarse fly ash. The chemical compositions were analysed by ICP-MS. The SiO_2 and Al_2O_3 increased rapidly in the bottom ash from 36% to 65% and 11% to 23%, respectively, after the added kaolin into the virgin wood. This was expected due to the high silica and aluminium content in line with the kaolin chemical compositions before the firing which are 48% and 36.5%, respectively. Figure 5-16 illustrates that based on the equilibrium model, potassium aluminium silicates compound formed for cases VWK1.55 and VWK2.5 at temperatures between 400°C – 1100 °C. This is in line with the study by Rebbling et al. [175, 179], which concluded the reduction of K in the bottom ash due to the formation of $KAlSiO_4$ (Kalsilite) and $KAlSi_2O_6$ (Leucite) after the addition of kaolin. The most dominant chemical composition in the melted ash (slag) of the virgin wood with kaolin addition was SiO_2. Also, Al_2O_3 shows the same trend

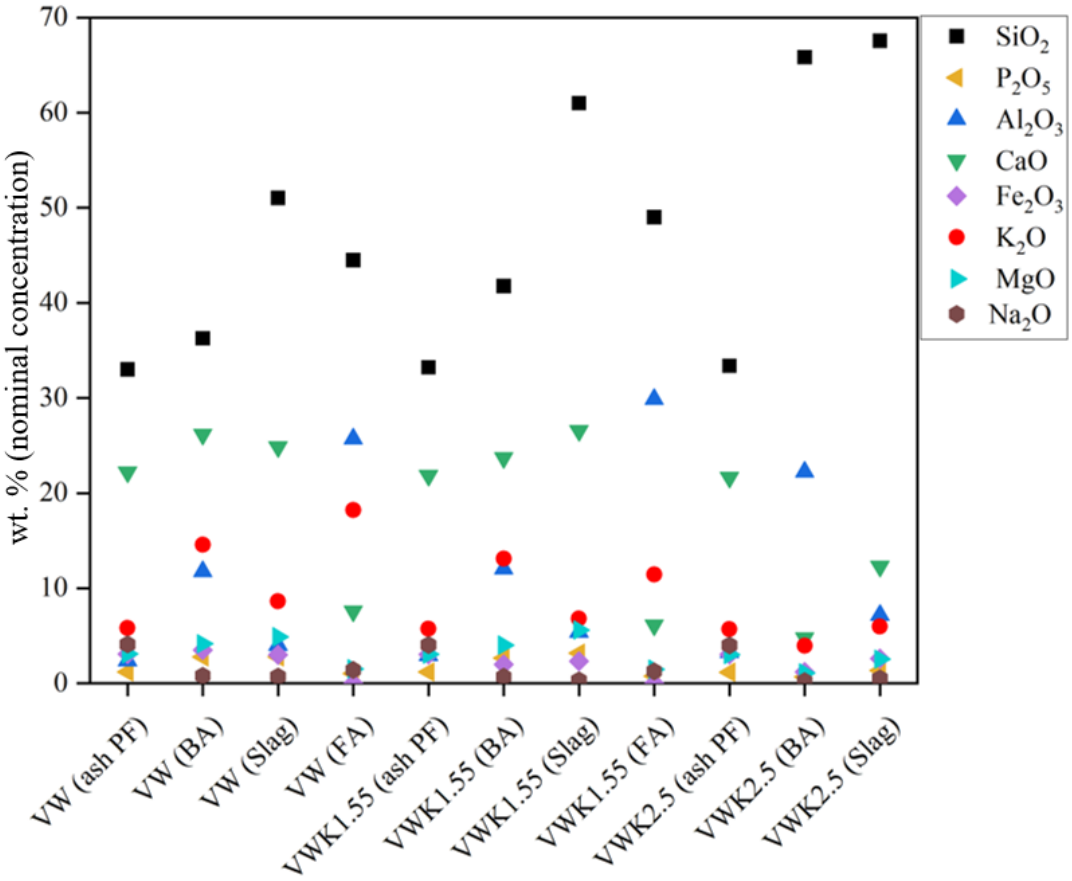

Figure 5-15 The relative distributions of the chemical elements on virgin wood ash pre-firing (PF) to post firing-bottom ash (BA), slag, and fly ash (FA). Ash PF for VWK1.55 and VWK2.5 are theoretical composition blends.

as its amount in the bottom ash was increased after the kaolin injection into the virgin wood. SiO_2 was the major constituent found in coarse fly ashes for the pure virgin wood and VWK1.55 cases, at concentrations of 44.5% and 49%, respectively.

The CaO increased in the bottom ash and slag after the firing compared to the amount of CaO before combustion for VW and VWK1.55. It was found that the amount of CaO was low in fly ash for all the fuel mixtures. This is potentially due to that most of the calcium formed a stable compound on the bed of the grate boiler, retaining it on the bed, which lowers the amount of calcium in the fly ash. According to the thermodynamic equilibrium model (Figure 5-16), about 40% of the $CaAl_2Si_2O_8$ (Anorthite) compound was formed during the combustion of the virgin wood mixed with kaolin and 18% wollastonite was formed in the pure virgin wood. The alkali metal, potassium, was reduced in the bottom ash after the addition of kaolin. The K_2O in slag was found to decrease from 8.6% (VW) to 6.8% and 5.9% for VWK1.55 and

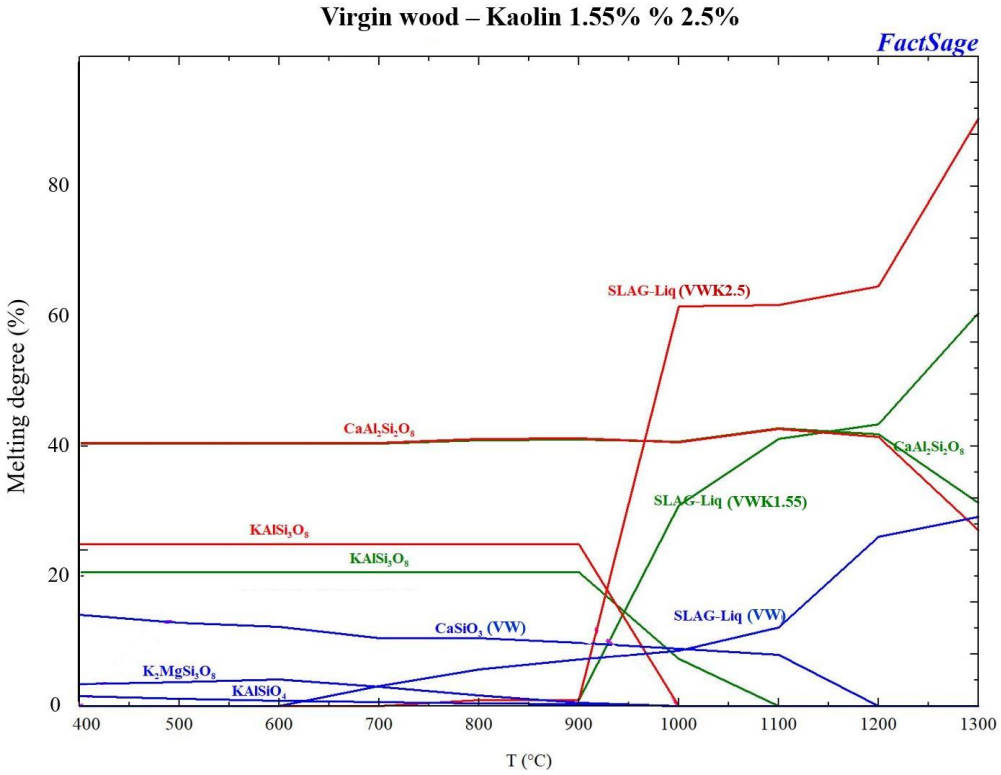

Figure 5-16 Solid-liquid phase for VW (blue line), VWK1.55 (green line) and VWK2.5 (red line) obtain by the thermodynamic equilibrium calculation.

VWK2.5, respectively. This is in line with the study by Öhman et al. [89] that also concluded the amount of calcium and K_2O decreased in the slag samples after adding kaolin. K_2O is higher in the post firing components compared to the pre-firing for VW and VWK1.55. This was suspected due to the potassium reacting with the additive to form potassium aluminium silicates as mentioned by Rebbling et al. [186]. There were no significant amount of changes in Na_2O,

P_2O_5, Fe_2O_3 and MgO in the chemical element distributions before and post-firing for VWK, VWK1.55 and VWK2.5. Figure 5-16 presents the prediction of the solid-liquid phase formation based on the TEM calculation. The VW was predicted to form the slag-liq at 600 °C while VWK1.55 and VWK2.5 start to form the slag-liq at 900 °C. This shows that the woody biomass blended with kaolin increased the slag-liq melting point from 600 °C to 900 °C. However, VWK2.5 was forecasted to form the highest amount of slag-liq followed by the VWK1.55 and VW. Overall, the SiO_2 shows similar trends for all 3 different fuel mixtures (VW, VWK1.55 and VWK2.5). It was found that there was an increasing concentration in the melted ash (slag) and a decrease in the coarse fly ash. SiO_2 and CaO are present in most significant quantities and should be considered besides potassium in the mitigation of the chemical elements to reduce ash related issues. In addition, previous research concluded that the silica is the predominant constituent in the formation of biomass slag [129, 131, 167, 268].

b) Case 2: Recycled wood with kaolin addition

Figure 5-17 presented the detailed relative distribution of element compositions prior to the firing and post firing (BA, slag, FA) of the blended recycled wood with kaolin. Both the bottom ash and slag in the recycled wood case study have the same phenomenon in the chemical composition analysis. The amount of SiO_2 and Al_2O_3 gradually increased, which is already expected due to the composition of kaolin being rich in silica and aluminium. Clery et al. [185] found that a high silica and aluminium content will lead to the retention of potassium in the bottom ash. Deng et al. [269] also confirmed that high calcium and magnesium to silica ratio will impede the retention of potassium in the solid phase. Moreover, it was observed that the trend between SiO_2 and CaO can be clearly seen in Figure 5-17, which is that the silica is increased and simultaneously the calcium decreases after being blended with kaolin. Figure 5-18 illustrates the solid-liquid phase for RW, RWK1.55 and RWK2.5 obtained by the TEM. RWK2.5 has the highest fraction of melting degree followed by RWK1.55 and RW. It was estimated that the addition of kaolin would accelerate the formation of slagging and this is in agreement with the experimental results that show severe agglomeration occurred after being mixed with kaolin as seen in Figure 5-5 and summarised in the sintering degree results in Table 5-1. In addition, this is also in line with the study by Nik Norizam et al. [167], who stated that the fuel which has a high silica-to-calcium ratio will be predicted as a high slagging index, I_n and categorized under severe slagging. In addition, the alkali metals, such as K_2O, Na_2O, and some other elements (P_2O_5, CaO, Fe_2O_3, MgO), were decreased in the bottom ash and slag after being blended with the kaolin compared to the fuel mixtures without kaolin. This is due

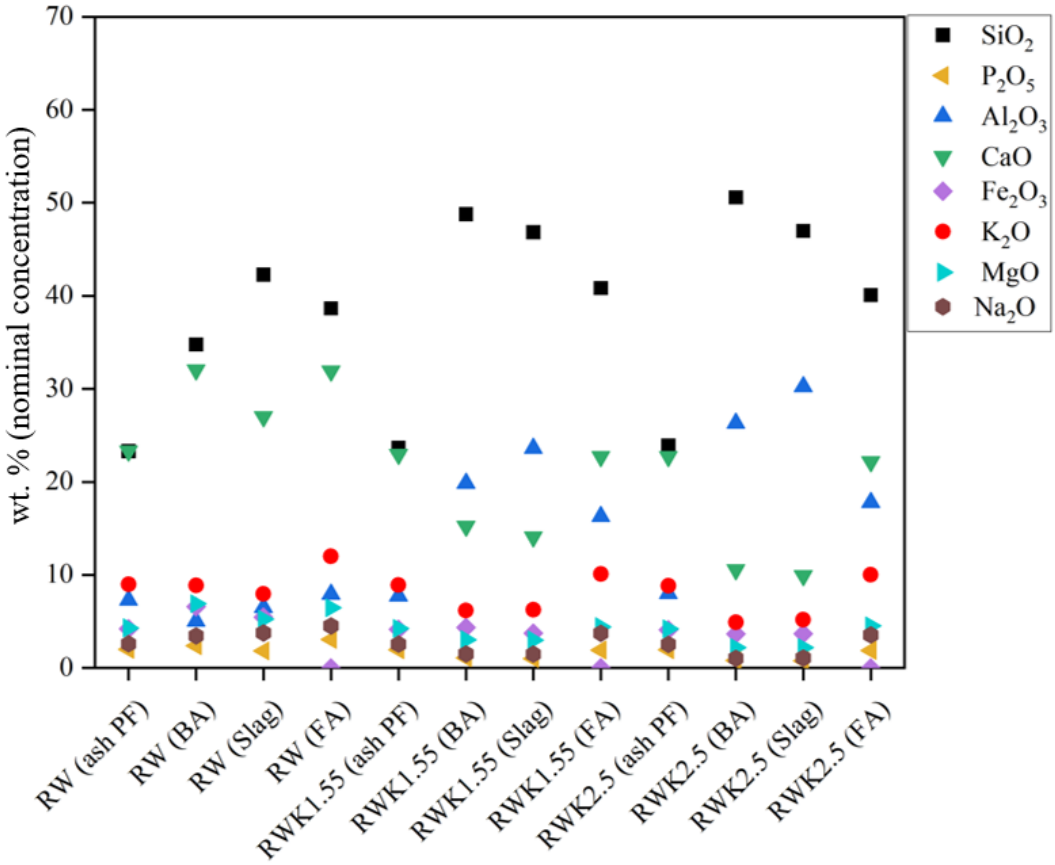

Figure 5-17 The relative distributions of the chemical elements on the recycled wood ash pre-firing (PF) to post-firing - bottom ash (BA), slag, and fly ash (FA). Ash PF for RWK1.55 and RWK2.5 are theoretical composition blends.

to the formation of crystalline aluminium silicates that reduce the release of the alkali metals after being added to the kaolin. This can be seen from the TEM calculation (Figure 5-18) that shows more than 25% formation of the $KAlSi_2O_6$ (Leucite), $KAlSi_3O_8$ (Sanidine), $CaAl_2Si_2O_8$ (Anorthite), and $Mg_2Al_4Si_5O_{18}$ at 10% crystalline observed after kaolin addition to the recycled wood. This is also in line with the study of co-fired straw with kaolin by Zhang et al. [270] which also found that the results of crystalline aluminium silicates detected by the XRD and FactSage models were identical.

The potassium level is increased in the coarse fly ash compared to the bottom ash and slag for all the fuel mixtures. This is suspected to be due to the potassium being a high volatile metal and can exist in the condition of coarse fly ash in the flue gas. In addition, the Cl content in recycled wood is low, namely 0.01%, and it can be assumed that the majority of the K-released during combustion is mainly from the evaporation of the KOH. The KOH has a lower melting temperature, which is 405°C compared to that of the KCl, hence the KOH exhibits a higher degree of mobility in the combustion system. According to Clery et al. [185] the evaporation of KOH will be competing with the reaction mechanism to fix the potassium in

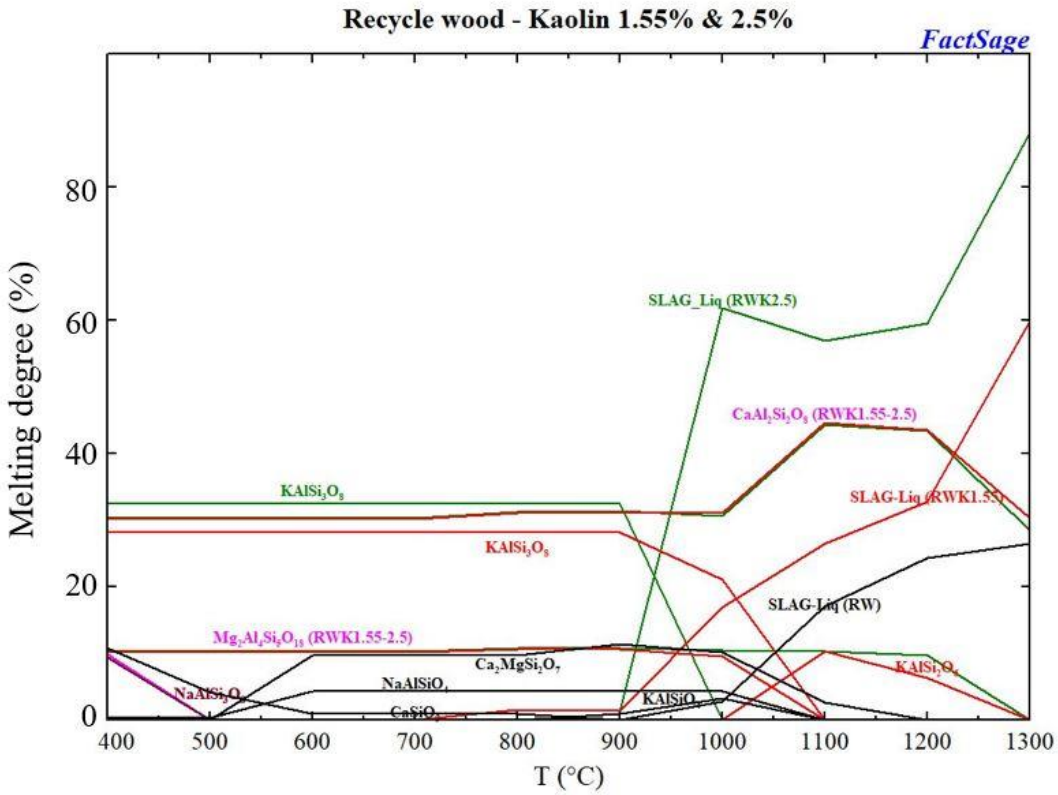

Figure 5-18 Solid-liquid phase for the RW (black line), RWK1.55 (red line) and RWK2.5 (green line) obtained by the thermodynamic equilibrium calculation.

the ash (e.g. potassium aluminium silicates), and this may assist in explaining the high mobility of potassium into the flue gas that carried the coarse fly ash. However, the element compositions analysis in coarse fly ash based, K_2O and Na_2O were found to have a small change after adding the kaolin. It was shown that the amount of alkali species was reduced about 16-17% from RW after adding 1.55% (RWK1.55) dosages of kaolin. However, only 0.5% K reduction and 4.5% Na reduction can be seen after dosage of kaolin increased from 1.55% (RWK1.55) to 2.5% (RWK2.5). On the other hand, the values of SiO_2 and Al_2O_3 were increased after mixing kaolin into the recycled wood. However, no substantial impact was observed when adding 2.5% of kaolin dosages towards the recycled wood in the coarse fly ash.

The Na_2O, P_2O_5, Fe_2O_3 and MgO were not in significant quantities to mitigate the ash-related issues, especially between post firing and before firing. This is because their elements are constantly low which is on average less than 5% in all the conditions of the fuel mixtures. It was suspected that these elements were not able to increase the melting temperature with a high amount of silica present in the fuel mixtures. Overall, SiO_2 again plays an important role and can be seen as a major component in all the stages (ash PF-BA-slag-FA). Previous studies concluded that silica is one of the main constituents found in slag samples derived from biomass fuels. These findings support the hypothesis that the melting properties of "sticky"

silicates escalate the ash-related issues, mainly the slagging in the boiler [132]. On the other hand, the CaO will have a complete reversal in behaviour compared to the SiO_2 when the biomass fuels are blended with the kaolin.

5.2.5 Crystallography of mineral phase compounds

Crystalline structure identification of the bottom ashes was determined by X-ray diffraction (XRD) analysis. Biomass contains a variety of inorganic components, such as potassium, calcium, magnesium, and silicon, which can form complex silicates, carbonates, and other compounds during combustion. XRD helps in understanding the interaction of these components at high temperatures which led to the formation of specific crystalline phases such as aluminosilicate compounds due to the addition of kaolin. In both analysis of VW and RW fuel mixtures with kaolin, calcium fluoride (CaF_2) was used as an internal standard for XRD analyses by blended with ash during sample preparation to enhance the accuracy and reliability of the measurements [271]. CaF_2 was selected in this study because it is chemically and thermally stable. This is to ensure that the CaF_2 does not react with the sample or decompose under the conditions during XRD analysis. Moreover, the diffraction peaks of CaF_2 are sharp which allows for precise calibration of the diffraction angles. This precision is important for accurate determination of lattice parameters and identification of crystalline phases in the sample. In addition, the diffraction peaks of CaF_2 does not overlap with the compounds or materials formed in this study as there is no fluorine observed in both fuel mixtures before combustion. This non-interference ensures that the peaks from the ash samples can be clearly distinguished and analysed without overlap which enhancing the analysis's accuracy.

Figure 5-19 illustrates the pattern of the XRD analysis for VW fuel mixtures. The CaF_2 (A) was identified during the phase identification. The incorporation of CaF_2 in the analysis enhance the clarity of the graph by amplifying the intensity of the detected signals as shown in Figure 5-19. This improvement effectively reduced the amorphous background leading to a more distinct and interpretable pattern. The CaF_2 peak's intensity were identical for all VW fuel mixtures which confirmed that the CaF_2 does not interfere with other compound materials. The phase identification of crystalline compounds in sample from VW and RW fuel mixtures are summarized in Table 5-4. VWK1.55 and VWK2.5 shows significantly increasing in the Quartz (C) after adding kaolin which is already expected due to the silica-rich composition in kaolin. It was observed that the formation of Cristobalite in VWK2.5 due to the excess of silica in the kaolin when adding 2.5% of kaolin compared to the ratio at 1.55% which has less silica. Kaolin primarily consists of kaolinite ($Al_2Si_2O_5(OH)_4$). The decomposition of kaolinite begins at 450

°C to 600 °C, resulting in the formation of metakaolin which is an amorphous alumina-silicate [187-189]. As the temperature increases, metakaolin reacts further to form mullite ($3Al_2O_3 \cdot 2SiO_2$) and silica (SiO_2) [187-189]. This reaction releases additional silica into the system, which can further participate in the transformation to cristobalite, especially in a condition that rich in silica from the quartz. In addition, the Kalsilite ($KAlSiO_4$) and Leucite ($KAlSi_2O_6$) were observed after added kaolin to the virgin wood in both ratios. Konsomboon et al. [272] also confirmed that the formation of Kalsilite and Leucite is due to the reaction between kaolin and potassium gas species at 1500 °C. This is also consistent with the finding by Rebbling et al. [175, 179] who observed the formation of Kalsilite and Leucite after the addition of kaolin to the woody biomass in 40 kW moving grate combustor. The chemical reactions involved can be described by the following reactions:

$$Al_2Si_2O_5(OH)_4 + 2KCl \rightarrow 2KAlSiO_4\ (Kalsilite) + H_2O + 2HCl \quad (5\text{-}3)$$

$$Al_2Si_2O_5(OH)_4 + 2KCl + 2SiO_2 \rightarrow 2KAlSi_2O_6\ (Leucite) + H_2O + 2HCl \quad (5\text{-}4)$$

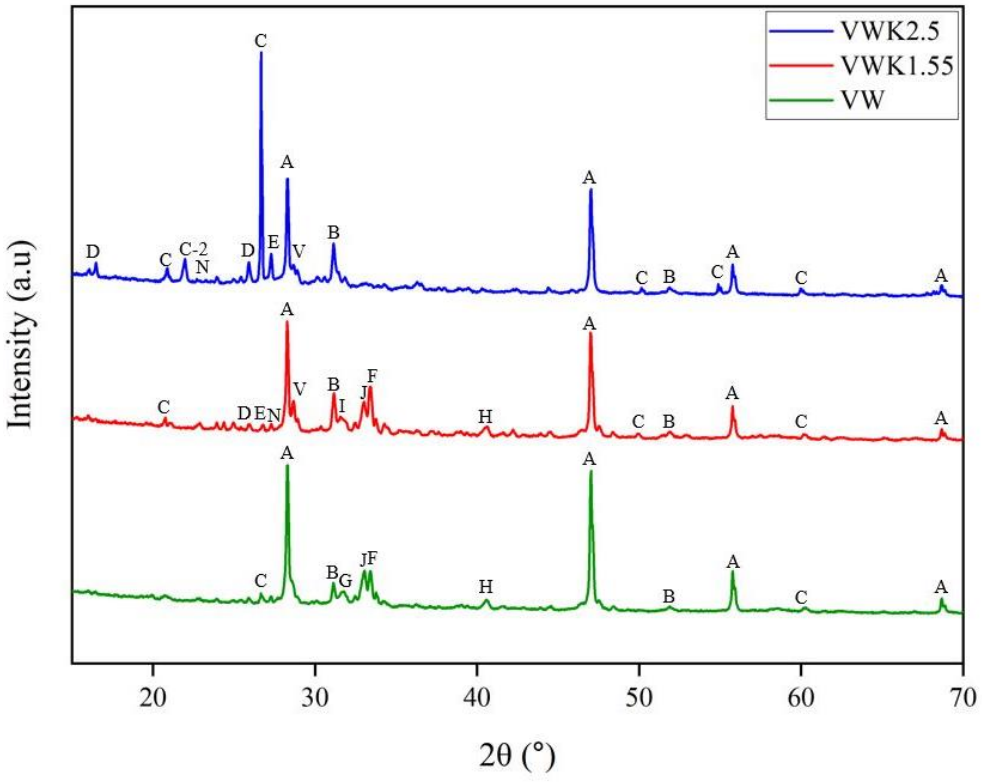

Figure 5-19 XRD pattern for VW fuel mixtures ashes.

Table 5-4 Phase identification of crystalline compounds in VW and RW fuel mixtures.

Indicator	Chemical formula	Description
A	CaF_2	Calcium fluoride
B	$Ca_2MgSi_2O_7$	Akermanite
C	SiO_2	Quartz
C-2	SiO_2	Cristobalite

D	$KAlSi_2O_6$	Leucite
E	$KAlSi_3O_8$	Sanidine
F	$Ca_3MgO_8Si_2$	Merwinite
G	$Ca_2Fe_2O_5$	Srebrodolskite
H	KCl	Potassium chloride
I	$Al_2K_3O_{13}Si_4$	Lithosite
J	$Mn_7O_{12}Si$	Braunite
K	Mn_2O_4Ti	Ulvospinel
L	$Al_{0.735}Ca_{0.24}Na_{0.26}O_4Si_{1.265}$	Andesine
M	$Al_{7.76}Ca_{3.44}Na_{0.56}O_{32}Si_{8.24}$	Bytownite
N	$CaAl_2Si_2O_8$	Anorthite
O	$CaMgO_6Si_2$	Diopside
P	$NaAlSi_3O_8$	Albite
Q	n/a	Pyroxene
R	$3Al_2O_3{\cdot}2SiO_2$	Mullite
S	n/a	Garnet
T	Fe_2O_3	Hematite
U	MgO_3Si	Enstatite
V	$KAlSiO_4$	Kalsilite

On the other hand, the KCl was found in the VW and VWK1.55 but absent in the VWK2.5. This is highly related to the formation of Kalsilite and Leucite explained earlier. Metakaolin has active Al_2O_3 components that can adsorb potassium K from KCl [186]. The adsorbed K can then react with silica and alumina in kaolin to form Kalsilite and Leucite [186]. This reaction effectively traps potassium in a stable mineral form, reducing the amount of free KCl. This can also be consistent with the formation of Leucite in VWK2.5 has a higher intensity compared to VWK1.55, which suggests that most of the potassium reacts with the excess silica in VWK2.5 to form stable mineral compounds, thus reducing the KCl formation. Lastly, the formation of Anorthite ($CaAl_2Si_2O_8$) was observed after added kaolin in VWK1.55 and VWK2.5. This finding is aligned with the equilibrium model in Figure 5-16 that predicted the formation of Anorthite after mixing the virgin wood with kaolin at 2 different ratios.

For RW cases (Figure 5-20), the quartz formation has the same trend as VW cases after kaolin addition. High intensity of Leucite was observed in RWK1.55 and RWK2.5 compared to the RW, which the explanation of chemical reaction already explained earlier. The Akermanite was detected in RW case, however, its intensity is reduced in RWK1.55 and RWK2.5 due to the kaolin addition which introduces extra of silica and alumina. The phenomenon promotes the formation of other alternative silicate minerals that do not contain magnesium, such as anorthite, which can reduce the relative abundance of Akermanite in the

bottom ash. According to Myat-Htun et al. [273], Akermanite ($Ca_2MgSi_2O_7$) is formed at 800 °C, yet kaolin was used to increase the melting temperature of compounds, leading to Anorthite formation over Akermanite. Moreover, the formation of Sanidine ($KAlSi_3O_8$) in RWK1.55 and RWK2.5 confirmed the result of the equilibrium model as shown in Figure 5-18. The presence of kaolin addition to the recycled wood also reduced the formation of Merwinite which is originally formed in RW. This is because the excess alumina in the kaolin can react with CaO present in the ash, this reaction will lead to the formation of calcium aluminate phases such as Bytownite which can be seen in RWK1.55 in Figure 5-20, therefore reducing the availability of CaO for merwinite formation. Furthermore, the presence of Andesine (sodium aluminium silicates) in RWK1.55 and RWK2.5 can be explained by the high-temperature reactions that occur between the kaolin composition and other inorganic materials present in the biomass ash. This phenomenon can be attributed to several factors: 1) Melting and solidification: As the temperature increases during the biomass firing process, some compositions of RW with kaolin addition may reach their melting points and begin to liquefy.

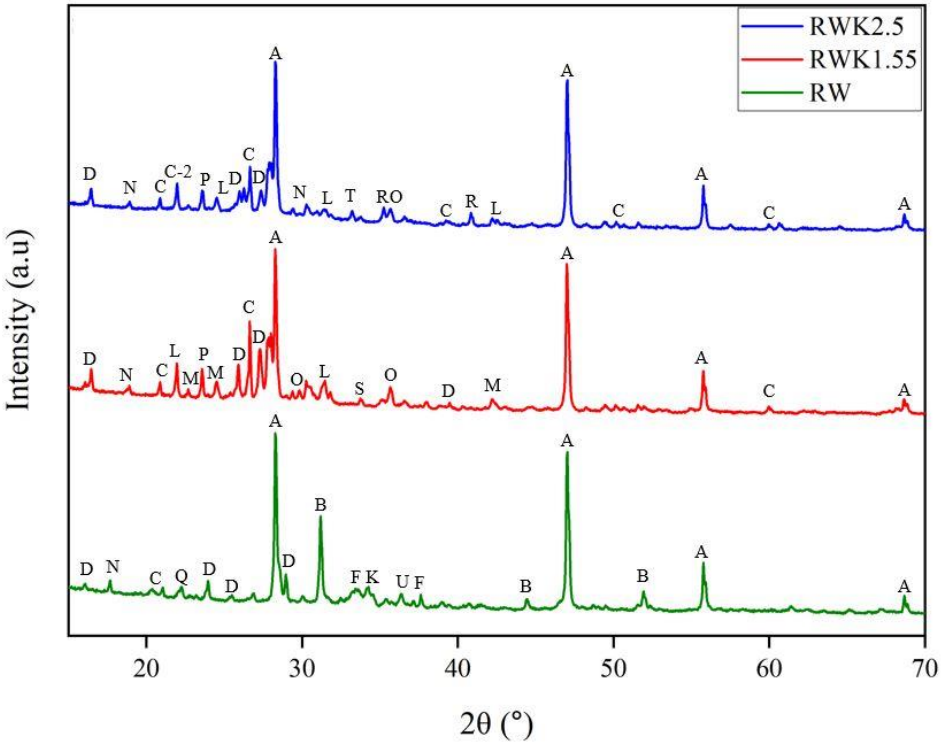

Figure 5-20 XRD pattern for RW fuel mixtures ashes.

This melting is mostly partial than complete, meaning only some of compositions of the mixture melt. The molten portion creates a liquid phase within the mixture, which can facilitate the movement and interaction of ions and molecules. This liquid phase is crucial for the chemical reactions necessary to form new compounds. In the liquid phase, the mobility of ions

(Al, Si, Na, and Ca) is significantly increased compared to solid state due to the decreased in viscosity and increased in space between ions in the liquid state. The ions can easily move and come into contact with each other, leading to reactions that would be slower in the solid state. For example, Si and Al from kaolin can react with Na and Ca present in the biomass ash. As the firing process completes and the temperature starts to decrease, the molten parts of the mixture begin to solidify. The first step in solidification is nucleation, where small, stable centres called nuclei form. These nuclei act as the foundation for crystal growth. Around these nuclei, ions arrange themselves into an Andesine which grow the initial crystals into larger grains. 2) Fluxing agents: Elements such as Na and K found in biomass ash will act as fluxing agents which decrease the melting temperature needed for subsequent reactions to occur [274]. These fluxing agents will promote the formation of Andesine at lower temperatures compared to the absence of Na and K. Overall, 23 crystal phases were identified in the study of the VW and RW cases, offering a comprehensive information into the compound's transformation through chemical reactions during combustion. The XRD analysis distinctly illustrates the differences in the crystalline structures of pure feedstocks, both without and with kaolin addition. Consistent with equilibrium models and previous research, adding kaolin to the feedstocks significantly influences the crystalline structure formation in the bottom ash such as the formation of Kalsilite, Leucite, Sanidine and many more. It is important to monitor these changes to ensure the crystalline structures do not adversely affect the boiler operation.

5.2.6 Morphology of bottom ash and slag

The bottom ash and slag were investigated to observe the impact of the kaolin addition on the morphology and structure of the ash by scanning electron microscope (SEM). Figure 5-21 shows the bottom ash for the virgin wood with the kaolin mixtures. The VW sample displays a comparatively homogeneous morphology, lacking agglomerations or significant porosity. In contrast, for both VWK1.55 and VWK2.5, the highlighted areas within the red circles reveal the presence of larger agglomerations. This suggests that the ash structure in these samples is more cohesive and exhibits a tendency to fuse which is influenced by the presence of kaolin.

In the RW cases as illustrated in Figure 5-22, the bottom ash morphology is identical to the microstructure observed in the bottom ash from the VW case. Figure 5-23 illustrates the

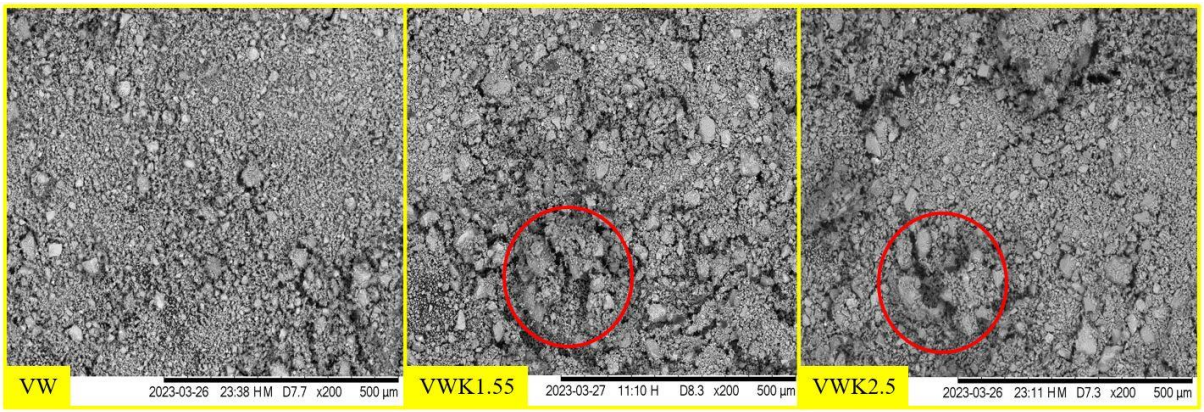

Figure 5-21 SEM morphology of the virgin wood with kaolin addition for bottom ash.

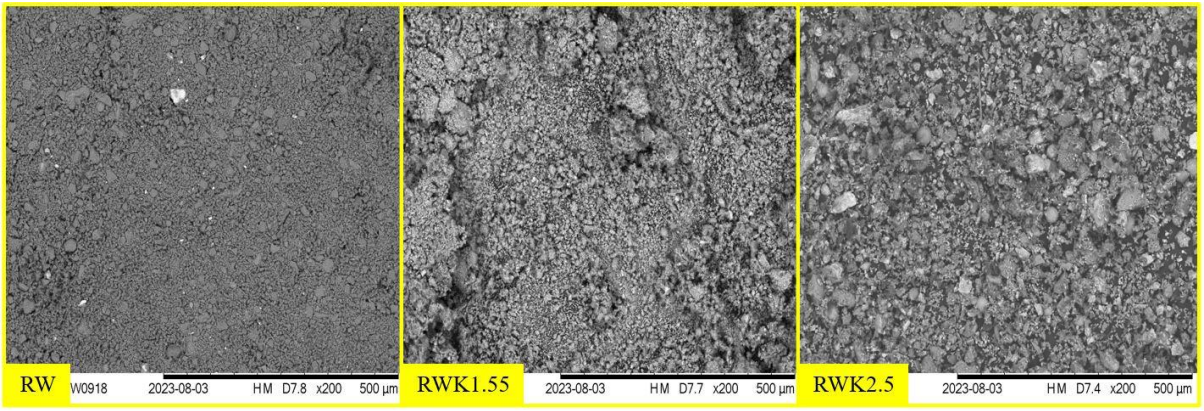

Figure 5-22 SEM morphology of the recycled wood with kaolin addition for bottom ash.

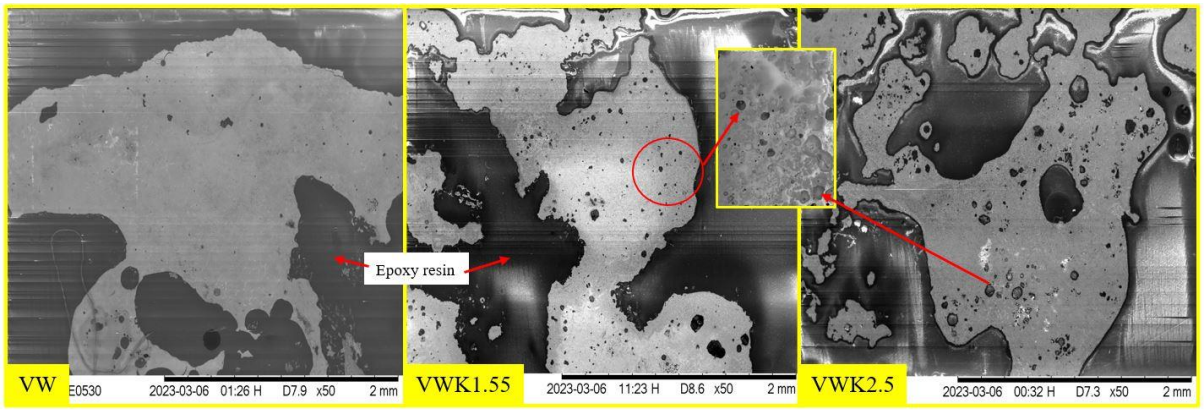

Figure 5-23 SEM morphology by cold mounting with the epoxy resin of the virgin wood with kaolin addition for slag.

SEM morphology of solid slag samples for VW fuel mixtures by cold mounting with epoxy resin. The slag from the VW presents a smooth surface in contrast to the fuel mixtures with the kaolin addition. The slag from both VWK1.55 and VWK2.5 were porous, as evident from the morphology observed on their surfaces by SEM. The presence of kaolin affects the ash's microstructure, which could be correlated to the increased porosity. Kaolin is composed primarily of kaolinite ($Al_2Si_2O_5(OH)_4$), which has a high melting point and acts as a refractory

material. During combustion, kaolin doesn't melt but instead undergoes dehydroxylation, forming metakaolin [255]. This phase transformation can create a porous structure due to the release of water vapour and other volatile substances such as alkali metals. Kaolin may act as a catalyst for the breakdown of other minerals and organic components within the biomass ash. This catalytic action can lead to the formation of additional porous structures as the components decompose and gases are released. Furthermore, kaolin contributes to the formation of aluminosilicate compounds which have high melting temperatures. At high temperatures, kaolin transforms into mullite ($3Al_2O_3 \cdot 2SiO_2$) and silica (SiO_2), which are stable phases. The transformation process can induce porosity due to volume changes and the expulsion of gases. Mullite formation can create a skeletal structure that increases porosity in the ash samples as shown in Figure 5-23. Moreover, the calcination of kaolin during combustion can create an active surface area that is capable of absorbing volatile components released from the combustion of biomass. This absorption can create a porous network as the absorbed substances are burned off as gases. By introducing kaolin into biomass during combustion, the ash produced is more porous compared to ash from biomass without kaolin.

5.2.7 Thermal stability of biomass ash

Figure 5-24 illustrates the thermal stability and weight loss of the six-biomass ash that were analysed by Thermogravimetric analysis (TGA). TGA is a thermal analysis where changes in physical and chemical properties of ash are measured by increasing temperature from 25 °C to 1000 °C with a constant heating rate at 20 °C/10 mins. Some of the inorganic elements such as Ca, Si, Fe, and Al, are vaporized at high temperatures (>1400 °C). The TGA curves obtained from the thermal stability test were categorised into three phases. The initial phase for the removal of moisture which occurs at temperatures below 200 °C. During the second phase, a notable weight reduction occurs between 200 and 600 °C which indicates the oxidation of organic materials. The final phase ranges between 600 and 1000 °C which mostly involves the transformation and reactions of inorganic substances [275]. For VW, the total weight loss was approximately 14.5 %. The moisture content was removed at a temperature below 200 °C while the weight loss observed from 200 °C to 780 °C indicated the oxidation of unburnt particles in the VW ash sample. The weight loss observed between 200 °C to 780 °C is attributed to the abundance of unburnt particles [275, 276]. For the RW case, the weight loss was observed between 400 °C to 700 °C as shown in Figure 5-24, which explains the oxidation of organic materials and their transformation into other phases such as Ca, Fe, and Si [277]. The total weight loss in RW was around 4 %. This suggests that the RW exhibit less weight

loss compared to the VW sample, suggesting that the RW have less volatile matter than the VW sample, which is 69.70 % and 74.60 %, respectively as presented in Table 2-4.

The thermal stability and weight loss for all the fuels with the addition of kaolin were stable. The mass reduction is approximately reduced to only 0.3 % for all fuel mixtures with kaolin. This is expected due to the kaolin stabilising the thermal characteristics of the fuel, for example, kaolin is a good absorbent for the moisture content in the fuel. This can be proven by the moisture content analysed earlier in Table 2-7 which concludes that the moisture content was decreased when added kaolin into the fuels. Hence it is aligned with the observation for all fuel mixtures with the kaolin addition that shows no changes in weight loss under 200 °C. Additionally, there is a high potential that particles have been coated or covered by the kaolin which prevents the weight loss. Overall, this TGA analysis provides an understanding of the impact of kaolin blending with virgin wood and recycled wood on the thermal degradation profile of the ash, which is crucial for optimizing the process to achieve the highest energy output while minimizing emissions.

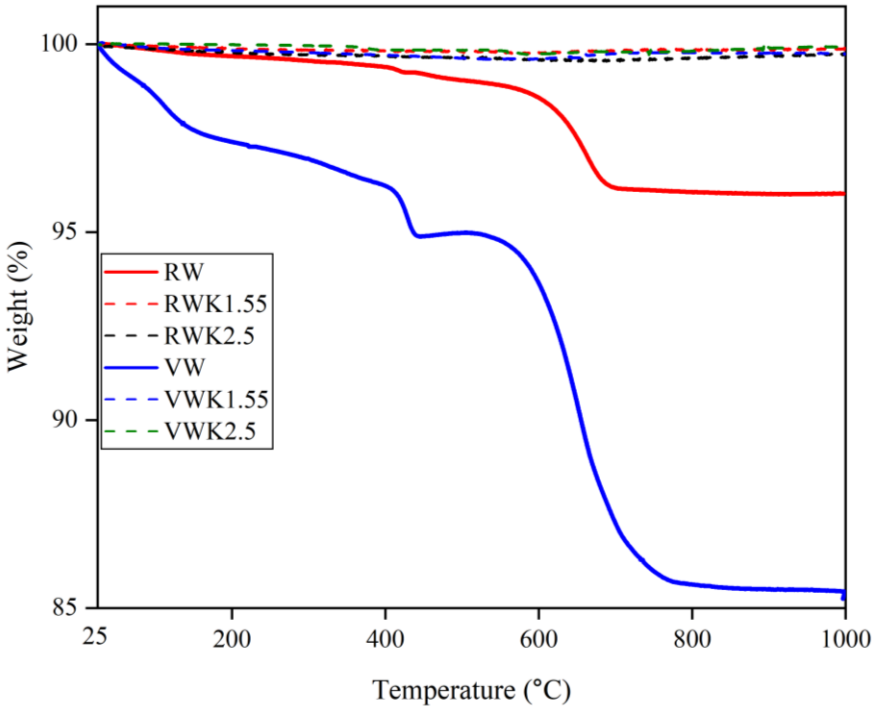

Figure 5-24 Thermal stability and weight loss profile for the six ash samples.

5.3 Conclusion

This study has successfully presented the impacts of blending kaolin at two different dosages into the woody biomass fuels in a 250 kW grate boiler. Kaolin was effective as an absorbent, but at the same time, it increased the ash content in the fuel mixture. High sintering

was observed for the virgin wood and the recycled wood fuel blended with the kaolin at any dosages in the grate boiler. This is due to the severe agglomerations that occurred during the combustion after the addition of kaolin. The thermodynamic equilibrium model successfully predicted the melting degree of the slag-liq where the RWK2.5 is the highest percentage of slag-liq compared to the RWK1.55 and RW. This is in relation to the ICP-MS analysis, which concluded that a high amount of silica was detected in the bottom ash and the slag compared to other elements. The alkali metals were reduced when kaolin was added. The TEM forecasted approximately 22% and 32% of potassium aluminium silicates were formed in the virgin wood and the recycled woods for cases of kaolin addition, respectively. Previous studies [186] indicated that the amount of the K-released was reduced due to the formation of potassium aluminium silicates in the bottom ash when adding the kaolin into the woody biomass.

The ash partitioning on the relative distributions of ash-forming elements in the fuel (pre-firing), bottom ash, slag and coarse fly ash concluded that the most dominant elements throughout the combustion process is silica. The Si/Ca ratio was seen to be very high after adding the kaolin into the woody biomass, and this resulted in the acceleration of the agglomeration and slagging formation in the boiler. On the other hand, the potassium level is increased in the coarse fly ash for the recycled wood fuel mixtures. This can be explained by the majority of K released during the firing is mainly from the evaporation of the KOH due to the low Cl content in the recycled wood. The KOH evaporation will affect the reaction mechanism to fix the potassium in the ash, as a result the potassium will be high mobility in the coarse fly ash carried by the flue gas.

Finally, the biomass compositions are complex, it varies between different types of the woody biomass, hence all the elements, including the non-volatile elements and alkali elements require careful examination in the future to mitigate the ash related issues in the utility's boiler. It must be noted that this study has focussed only on the chemical compositions of the ash, however the combustion parametric study of the boilers, such as the process parameter, boiler technologies, temperature profile of the boiler, etc. need to be considered as well in the future works to mitigate the ash related issues in the utility's boiler.

6 Impact of the blending of kaolin on particulate matter (PM) emissions in a biomass field-scale 250kW grate boiler.

6.1 Introduction

Previous studies in this field evaluated the performance of kaolin addition to various types of fuels on the PM emissions in laboratory, pilot and commercial scale furnaces. For example, Xu et al. [120] reported that there was a reduction in the PM2.5 emission when coal was co-fired with kaolin in a 1000 MW coal-fired power station. Furthermore, the addition of kaolin will lead to the formation of alkali aluminosilicates which enhance the capture of the PM through aggregation and collisions [120]. Tissari et al. [265] found that the addition of 5 wt% kaolin to oat grains reduced the emissions of alkali metals but increased the PM emissions of incomplete combustion in a 20 kW pellet burner. A recent study by Wang et al. [190] observed that the aerosol fraction of the total ash shows a slight reduction when kaolin or coal fly ash was introduced. Rebbling et al. [186] concluded that the addition of kaolin into the woody biomass reduced the concentration of alkali metals (K and Na) in PM emissions in a 40 kW grate boiler. Cheng et al. [278] attempted to modify the kaolin by phosphoric acid treatment to enhance the chemical reactivity of the kaolin in a small scale vertical fixed-bed boiler. According to their findings, a substantial decrease in the $PM_{0.2}$ emissions was observed when cornstalk was co-fired with kaolin treated with phosphoric acid. However, most of the studies done in the past were based on laboratory scale equipment. It is not certain whether the small scale rigs are able to mimic the same combustion behaviour in a field scale 250 kW. This is because larger equipment will require larger fuel feeding input, thus resulting in larger energy output. Small scale furnaces have simpler combustion processes, which might lead to less efficient fuel combustion. As a result, the flue gas may contain higher proportions of unburned hydrocarbons and particulate matter (PM).

To address the gaps in the literature, kaolin was blended at two different dosages (1.55 wt% and 2.5 wt%) into a virgin and a waste type woody biomass, which were virgin wood and grade A recycled wood in a 250 kW grate boiler. The aim of the present work is to investigate the impact of kaolin addition to woody biomass fuels on the partitioning of chemical elements (Si, K, Na, Al, Ca, Mg) within particulate matter (PM) emission. In addition, the impact of two dosages of kaolin on reducing alkali and non-volatile species in PM emissions from the combustion of these fuels was investigated. A comprehensive analysis of mass concentration based on particle size distribution (PSDs), elemental compositions and morphology of the PM has been conducted. The detailed discussion on this topic enabled an understanding to be

provided that will benefit industrial users and researchers in optimizing and improving the performance of biomass-fired boilers. Moreover, this research provided further insights into optimising kaolin dosage for the reduction of alkali and non-volatile species in PM emissions from these fuels, paving the way for future studies.

6.2 Results and Discussion

6.2.1 Effect of the addition of kaolin on the PM emissions in the grate boiler.

The effect of kaolin blending on particulate emissions, specifically, PM_{10}, PM_1 and $PM_{0.1}$ were measured in all the experiments. The mass of particle size distributions (PSDs) for virgin wood and grade A recycled wood cases are shown in Figure 6-1 (a). The reduction efficiencies of kaolin on size-fractionated PM were computed using the formula suggested by Xu et al. [120], with the results being illustrated in Figure 6-1 (b). Most of the mass concentrations of the aerosols captured between 1-10 μm with kaolin has lowered the emissions levels for both fuel blends. The addition of the kaolin significantly decreased the amount of PM in the virgin wood cases. The mass concentrations of $PM_{7.33-10}$ decreased from 3,039±90 mg/Nm^3 to 1,010±27 mg/Nm^3 and 694±33 mg/Nm^3 under the experimental conditions, resulting in a 66.7% and 77.2% of PM reduction efficiency for the VWK1.55 and VWK2.5 cases, respectively. On the other hand, the yield of the PM was also found to be significantly reduced in the grade A recycled wood when adding kaolin. As can be seen from Figure 6-1 (a), the mass concentrations of $PM_{7.33-10}$ decreased from 4,380±103 mg/Nm^3 to 2,123±60 mg/Nm^3 and 1,803±57 mg/Nm^3, corresponding to a 51.5% and 58.9% in the reduction efficiency after addition of kaolin ratio at 1.55 wt% and 2.5 wt%, respectively. Overall, the addition of kaolin into the VW and RW were able to reduce the PM emissions by at least ~60%.

The number of particle size distributions of the PM emissions for virgin wood and recycled wood cases are shown in Figure 6-2. It is clear that the number of particles captured at these submicron regions (1-10 μm) are low at ranges around 130-590 cm^{-3} as shown in Figure 6-2. This is suspected to be due to the fewer number of big particles existing in these submicron regions. Furthermore, the addition of kaolin resulted in a large reduction in the number of particles between 0.02-0.3 μm, e,g. ~2.2 million number of particles in VW were reduced to 446,000 cm^{-3} and 315,000 cm^{-3} at size distributions of $PM_{0.1}$ in VWK1.55 and VWK2.5, respectively. However, these amounts were not significant when compared to the mass-based size distributions. It was observed that the highest mass of particle size distributions was 11 mg/Nm^3 at ranges of $PM_{0.1}$. This means that the large number of very tiny particles were present

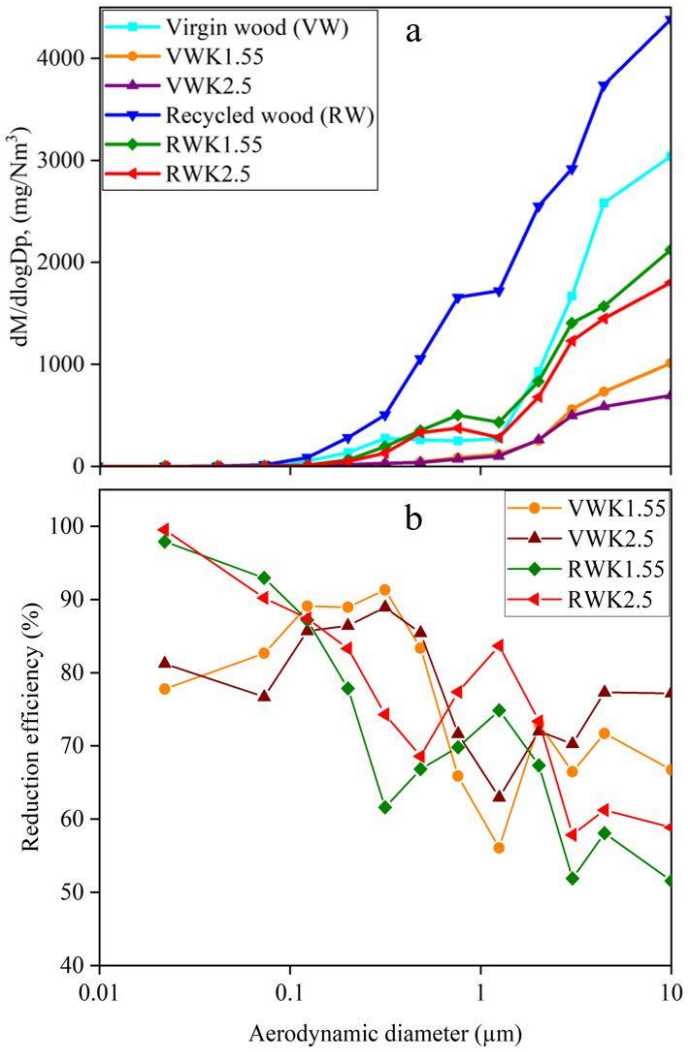

Figure 6-1 (a) PSDs of mass concentrations of the virgin wood and recycled wood cases in fine fly ash by Dekati ELPI+; (b) PM reduction efficiency of kaolin at two different dosages for virgin wood and recycled woods.

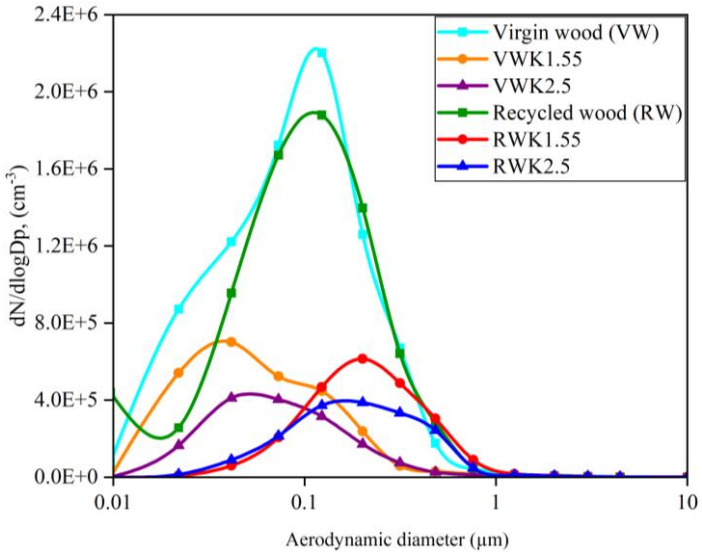

Figure 6-2 Particle number size distributions of virgin wood and recycled wood cases in fine fly ash (aerosols) by Dekati ELPI+.

in these submicron regions. The number of particles observed was 1.8 million cm^{-3} after 2 hours collection by using the Dekati ELPI+. The number of particles was reduced about 4 times from 1.8 million for the RW mixture to 467,000 cm^{-3} for the RWK1.55. The particulates later were observed to reduce again to 372,000 cm^{-3} after adding 2.5% dosages of kaolin. These values have been observed at the submicron region $PM_{0.1}$. However, in the context of the mass-based size distribution of particles at $PM_{0.1}$, the amount was relatively small. which is 1.8 mg/Nm^3 for RW and 0.44 mg/Nm^3 for both RWK1.55 and RWK2.5. The ultra-fine particles were present evenly on the surface of the plate collections and it can be confirmed that high volumes of ultra fine particles were existed in the submicron region $PM_{0.1}$ for all the fuel mixtures tested.

6.2.2 Effect of the addition of kaolin on the chemical element partitioning of the PM

The element concentration analysis of the PM emissions are illustrated in Figures 6-3 and 6-4 for the virgin wood and grade A recycled wood case studies, respectively. The motivation is to investigate the partitioning of alkali species and non-volatile elements concentrations in the submicron region by ICP-MS analysis. Results presented in Figure 6-3 illustrated that the fine and ultrafine PM had a high content of non-volatile elements species, such as SiO_2 and Al_2O_3 in the virgin wood case studies. The SiO_2 and Al_2O_3 were increased in $PM_{0.1,}$ PM_1 and PM_{10} after blending with kaolin for both dosages tested. These observations are suggested to be associated with the adhesion, aggregation or agglomerated of airborne kaolin with the ultrafine PM, as the kaolin used comprised of 48 wt% SiO_2 and 36.5 wt% Al_2O_3. Potassium was found at 20.1±0.2 wt% in the VW ash samples and this amount reduced significantly after the addition of kaolin at 1.55 wt% and 2.5 wt%. The use of kaolin also reduced the release of sodium by ~65% for virgin wood when adding kaolin. This is in agreement with the study by Rebbling et al. [186], who found that the addition of kaolin reduced the release of potassium and sodium by ~46% and ~80%, respectively. CaO and MgO were also observed in all fuel mixtures of PM samples, which indicated a contribution from heterogeneous condensation, agglomeration and coalescence to particles growth during the PM formation [279]. The magnesium level was found to slightly increase after blending the virgin wood with the kaolin. The amount of magnesium present in all the size-fractioned PM was below 4 wt% for all the VW mixtures. The CaO was found to decrease in PM_{10} from 4.9±0.1 wt% (VW), to 0.82±0.01 wt% and 0.67±0.01 wt% for VWK1.55 and VWK2.5, respectively. According to Ninomiya et al. [280] and Wei et al. [281], kaolin at specific addition ratios, would interact with calcium and promote the formation of a molten phase which potentially remain on the bed to form slag.

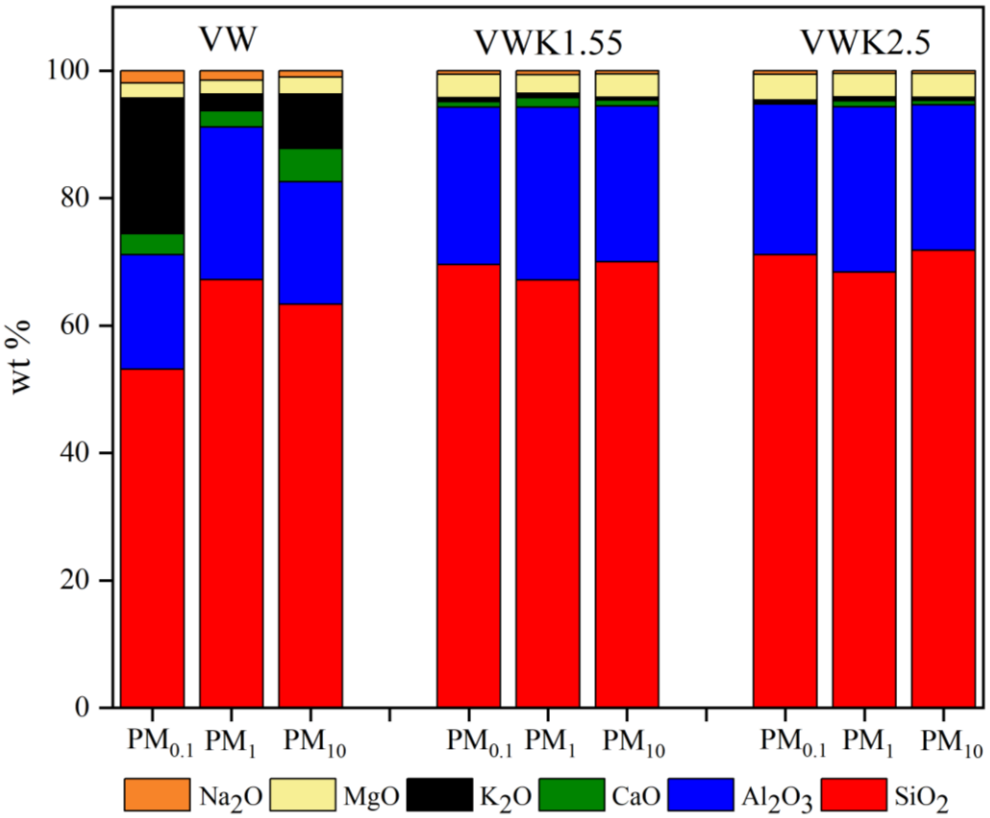

Figure 6-3 Chemical compositions of the PM (normalized to 100%) when kaolin was added to virgin wood by ICP-MS analysis.

For the recycled wood, SiO_2 was found to increase from 24.6±0.8 wt% in RW to 64.7±0.8 wt% and 66.4±0.6 wt% in the PM_{10} size fraction, after being added with kaolin at dosages of 1.55 wt% and 2.5 wt%, respectively. In addition, there are no significant change in SiO_2 after the addition of kaolin for both dosages in PM_1 and $PM_{0.1}$. The high amount of CaO was found in the PM_1 at 30.6±0.4 wt%, potentially due to the following reasons. First, CaO in the RW blends, primarily formed as organic-bound, was exposed to reducing atmosphere and high combustion temperatures. It is crucial to monitor the bed condition due to the primary air being supplied from underneath of the bed as shown in Figure 2-6. Any ash related issues such as agglomeration, clinkers and slagging formed on the bed will result in localised spots with limited oxygen available for the combustion (strong reducing atmosphere). Second, in an actual furnace, biomass and mineral particles may undergo significantly higher temperatures and more vigorous fragmentation compared to bench-scale reactors, leading to increased mineral matter release into the fly ash. However, CaO was remarkably reduced to 1.96±0.03 wt% and 0.71±0.01 wt% for the 1.55 wt% and 2.5 wt% cases, respectively.

These observations show that kaolin and meta-kaolin, reacted with calcium-containing compounds, effectively binding these elements to the additive's particles [282, 283]. The MgO was increased from $PM_{0.1}$ to PM_1 and then to PM_{10} in the RW case. The MgO increased in

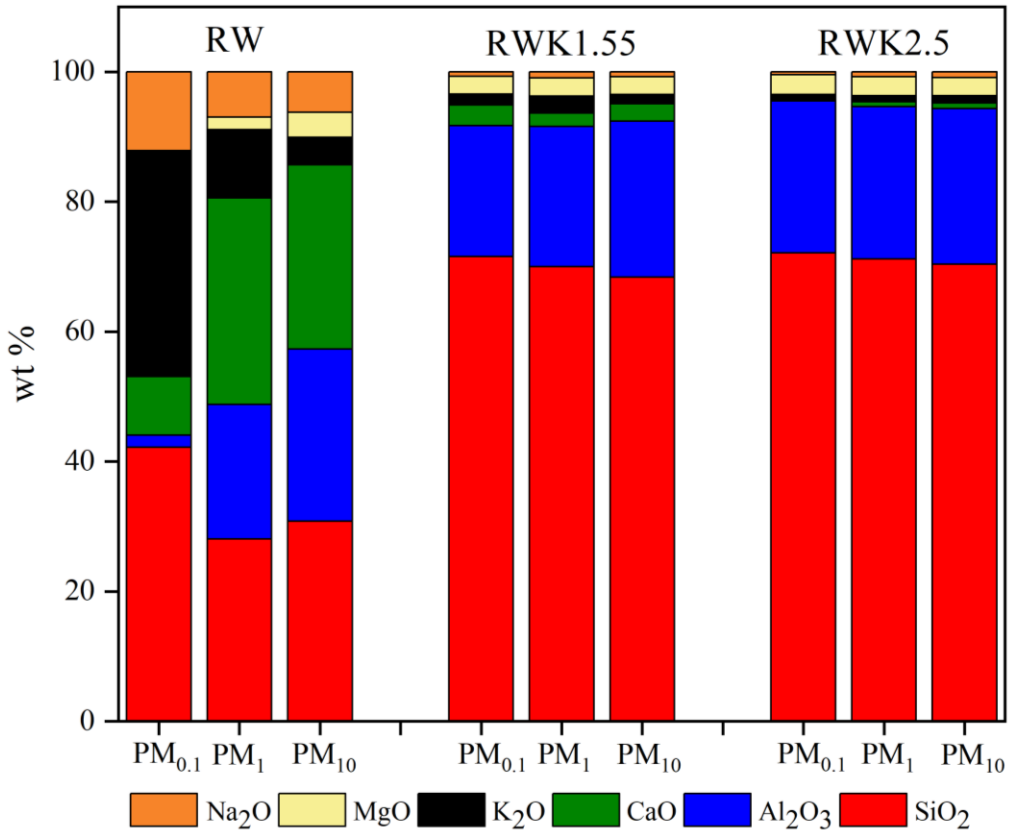

Figure 6-4 Chemical compositions of the PM (normalized to 100%) when kaolin was added to grade A recycled woods by ICP-MS analysis.

$PM_{0.1}$ and PM_1 after the addition of kaolin while the amount of magnesium in PM_{10} is slightly lower compared to without kaolin in RW cases. The utilization of kaolin resulted in a reduction of approximately 90% in the release of sodium, as determined by a weighted average, when kaolin was added to grade A recycled wood at 1.55 wt% dosage. However, no difference has been observed when adding 2.5 wt% dosages of the kaolin. This is speculated to be due to the increases in the alkaline dosages from 1.55 wt% to 2.5 wt% becoming inefficient in the chemisorption of the sodium.

Moreover, the amount of K_2O was found to be the highest which was 33.6±0.4 wt% in the aerosols from the RW case. This is a very interesting and important finding where the amount of potassium was considered high at particle sizes <0.1 μm. This observation aligns with the Energy Dispersive Spectroscopy (EDS) results presented in Figure 6-5 for $PM_{0.48}$, where it revealed high concentrations of K and Cl. Fernandes and Costa [284] suggested that these particulate matters predominantly consist of potassium chlorides which have a low melting temperature of 770 °C and the presence of sodium would further decrease the melting point [285]. According to Yang et al. [285], the alkali metal compounds that melted are prone to form gas phase in the form of chloride and alkali metal vapor during the combustion process.

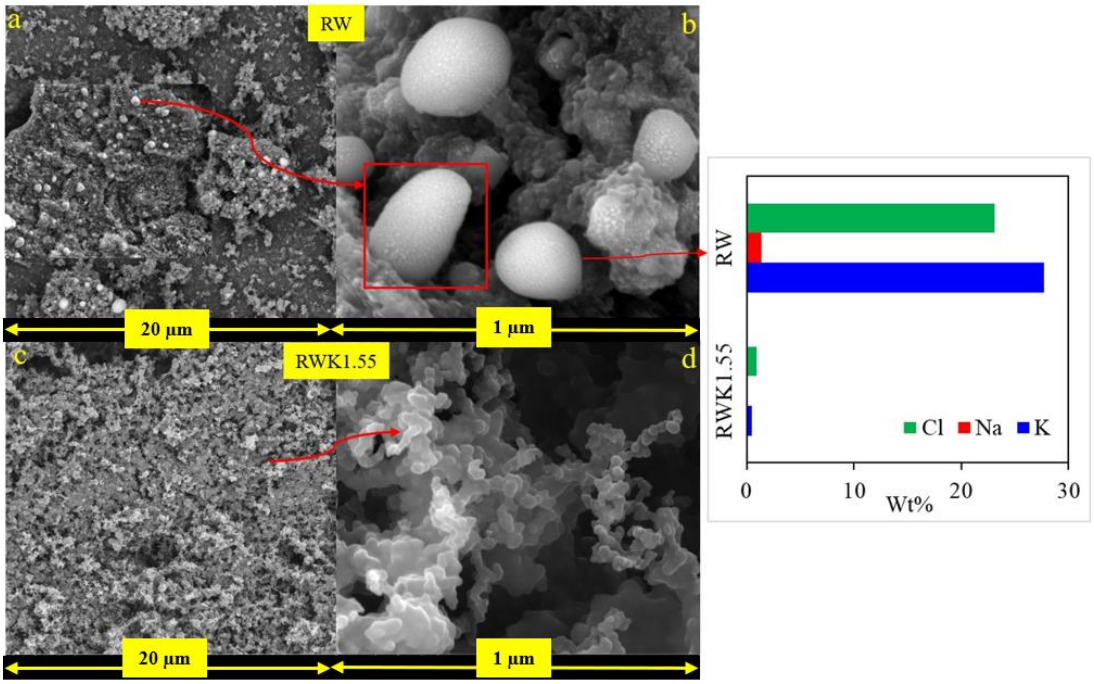

Figure 6-5 (a-d) Micromorphology of the $PM_{0.48}$ (particles collected on the 7th stage of ELPI+) observed by SEM-EDS.

These alkali salts in a gaseous state can condense on cooler surfaces when the ambient temperature is lower than their melting point and this results in the formation of submicron particles via heterogeneous condensation and homogeneous nucleation [258, 279]. Furthermore, the K_2O was significantly reduced in the PM emissions after the addition of kaolin, as shown in Figure 6-4. This shows the good capability of the kaolin to adsorb alkali metals in the flue gas. Also, this is supported by the studies of Sommersacher et al. [83] where the K-release has been successfully reduced by about 18% in the experiment blending kaolin and spruce in a small reactor. The EDS analysis in Figure 6-5 also proves that the kaolin reduced the formation of fine particles by trapping gaseous alkali substances, primarily potassium salts such as KCl.

On the other hand, from Figure 6-5 (a-b), illustrating the morphology images of RW samples at $PM_{0.48}$, it can be clearly seen that KCl salts (white cylindrical shape) were formed during the combustion of RW. However, the KCl salts were significantly reduced and their visibility in Figure 6-5 (c-d) is diminished after added kaolin to RW at 1.55 wt% dosages. This direct morphology confirmed that the introduction of kaolin could enhance the capture of the ultrafine PM by the molten coarse PM [120]. A significant portion of the PM appeared to be agglomerated, as indicated in Figure 6-5 (b and d). The formation of the large structures may have arisen through processes such as agglomeration on the particles, interactions with the grease, as well as instances of particles rebounding (bounce-off) or undergoing re-entrainment

from higher ELPI+ cascade stages [286]. Agglomerates frequently exhibit porosity and possess a low effective density, leading to size of aerodynamic diameter smaller than apparent [286]. Moreover, Hindsgaul et al. [287] studied particles generated from biomass gasification through SEM and concluded that sizable agglomerates had reached to the lower stages of the cascade impactor. Thus, these explained our finding on the agglomerated particles appeared in $PM_{0.48}$ morphology as shown in the Figure 6-5 (b and d).

6.3 Conclusions

Overall, this study aimed to provide a better understanding to the industrial users and researchers on the impact of kaolin addition to woody biomass fuels on the partitioning of the chemical elements of fine and ultrafine particulate matter (PM) emissions. The highest particle mass concentrations were observed at $PM_{7.33\text{-}10}$ for both fuel mixture cases with kaolin. Kaolin demonstrated an effective reduction in the formation of fine and ultrafine PM through vapor and liquidus capture, achieving a minimum of 60% PM reduction when injected to VW and RW fuels. The addition of kaolin resulted in reduced alkali species in PM emissions for both fuel mixtures, indicating kaolin's efficacy as a gaseous substance adsorbent in flue gas. The presence of CaO and MgO in all fuel blend samples suggested contributions from heterogeneous condensation, agglomeration, and coalescence to particle growth during PM formation. Moreover, the concentration of non-volatile elements significantly increased after adding kaolin, attributed to the high SiO_2 and Al_2O_3 content in the ultrafine kaolin powder. This result implies the importance of future works to explore the influence of kaolin particle size on PM emissions, encompassing both non-volatile components and alkali elements.

In addition, the influence of kaolin on alkali species reduction and the increase in non-volatile elements demonstrated comparable effects at concentrations of both 1.55 wt% and 2.5 wt%. Consequently, it is strongly advised that future studies explore into the impact of kaolin concentrations below 1.55 wt% to understand the influence of additive concentration on PM emissions. This research underlined the effective mitigation of PM emissions in a field-scale grate boiler through the injection of kaolin with woody biomass fuels. Future investigations could explore the incorporation of kaolin into other types of biomass fuels to prevent the introduction of excessive aluminosilicate additives, thereby preserving optimal boiler conditions. The findings from this study lay the groundwork for subsequent research aimed at determining optimal dosages for kaolin addition to wood-based biomass fuels.

7 Conclusions and Future Work

7.1 Summary

In the near future, biomass firing in boilers for electricity generation will still play a significant role in a sustainable energy practice that uses organic materials such as wood, agricultural residues, or waste for fuel. This has become increasingly more popular in the power generation industry as this sector increasingly relies on biomass as a renewable energy source to reduce carbon emissions and dependence on fossil fuels. However, the process of biomass combustion in boilers presents several challenges, especially the formation of ash deposition, such as slagging and bed agglomeration in fixed bed and fluidized bed combustors, respectively. During combustion, the inorganic constituents of biomass form ash deposits that can accumulate on heat exchanger surfaces. This deposition not only hinders efficient heat transfer but also leads to potential corrosion and decreased overall boiler efficiency. As a result, the boiler requires frequent shutdowns for cleaning and maintenance which affects the sustainability of biomass as a fuel source for power generation. Addressing these challenges is crucial for improving the reliability and efficiency of biomass-fired power plants. Thus, the reliable tools to predict the ash deposition issues in the utility boiler is needed to assist the power plant operators in determining the characteristics and behaviours of biomass during firing in the utility's boiler.

For power plant operators, the ability to accurately predict the ash deposition issues is invaluable. It allows for better fuel selection and boiler design modifications, aiming to minimize the impacts of slagging in a fixed bed combustor and bed agglomeration in a fluidized bed boiler. This proactive approach can lead to improve boiler efficiency, reduced downtime, and lower operational costs. Moreover, understanding the ash deposition issues and the potential of various biomass fuels helps in adjusting operational parameters such as combustion temperature and air supply, which are critical for optimizing the combustion processes and reducing the maintenance intervals. By mitigating one of the primary technical challenges of biomass combustion, power generation facilities can more reliably integrate biomass as a key component of their fuel mix. This integration supports the shift towards sustainable energy practices, aligning with global carbon reduction targets and contributing to environmental sustainability. The melt fraction concept is currently a reliable indicator for determining the formation of biomass ash deposition in the boiler by using the thermodynamic equilibrium model. FactSage 8.1 serves as a precise tool for predicting the melt fraction behavior of various

types of biomass ash in boilers. Accurate prediction of the melt fraction is the prerequisite step to predict the ash depositions such as slagging and bed agglomeration in fixed bed and fluidised bed combustors, respectively. Moreover, the development of the ash deposition indices is an easy and simple tool for the users without much knowledge in FactSage application model.

The introduction of an improved slagging index, I_n and bed agglomeration index, I_a developed through thermodynamic equilibrium modelling and partial least squares regression (PLSR) are a breakthrough for the power generation industry. These indices enhance the prediction accuracy of slagging and bed agglomeration tendencies in biomass combustion in fixed bed boilers and fluidised bed combustors, respectively, by an extensive analysis of ash compositions and melting behaviours, which are crucial for managing and optimizing boiler operations. The findings suggest that the slagging index, I_n can reliably predict slagging propensities across various woody biomass types, including blends with peat under different combustion conditions. Additionally, the bed agglomeration index, I_a also allows for a reliable categorization of bed agglomeration propensities and shows superior performance compared to the existing indices available in the literature. It is effective in identifying the roles of K_2O and CaO in influencing agglomeration tendencies, proving crucial for operational strategies in biomass combustion. Furthermore, these indices are validated with comprehensive experimental data with thermodynamic modelling to enhance the reliability and consistency of their prediction to determine the slagging and bed agglomeration tendency in the utility boiler.

Ultimately, the implication of this research extends beyond individual plant operations, influencing the entire field of energy production. By providing a robust method to predict the ash deposition issues, the study not only supports the operational efficiency of power plants but also plays a role in the strategic planning and development of future biomass-based energy systems. This ensures that as the industry moves towards greener alternatives, it does so with greater confidence in the reliability and efficiency of biomass technologies. This predictive study underscores the importance of detailed chemical analysis of biomass ash in developing effective predictive tools for managing slagging in biomass-fired boilers, thereby supporting operational efficiency and longevity in biomass energy production. In addition, this study successfully advances our understanding of ash depositions behaviours in biomass combustion within utility boilers in the power generation industry.

Regarding the experimental approach to mitigate the ash deposition issues in the utility boiler, the study employs an aluminosilicate additive to investigate and enhance the understanding of kaolin injection's effects on virgin wood and grade A recycled wood in a field-scale 250 kW grate combustor. The author concentrates on the impact of ash behavior in two

principal areas: (i) ash partitioning in the main combustion chambers, where issues such as slagging, agglomeration, and fly ash deposition occur (Chapter 5); and (ii) the formation of particulate emissions, where a PM_{10} cyclone captures all ultrafine fly ash (Chapter 6). The significance of this research to observe the transformation and partitioning of chemical ash compositions from the pre-firing stage to the post-firing stages, with a specific focus on the critical chemical elements that are prone to ash deposition formation in the boiler. To achieve these tasks, the methods described in Section 2.4 – 2.7 have been conducted.

The results indicate that the propensity for fly ash deposition significantly decreases when kaolin is blended with biomass feedstocks. This reduction is attributed to the kaolin's effectiveness in capturing alkali metals in the fly ash. Metal analysis by ICP-MS demonstrates a substantial decrease in alkali metals with the presence of kaolin in the fuel mixtures. However, while integrating kaolin significantly reduces ash fusion temperatures, thus lowering the temperature at which ash becomes viscous and problematic, it also means that the ash can become sticky at lower temperatures, potentially leading to the formation of clinkers and slag. This stickiness can impair the movement and effectiveness of the grate, necessitating more frequent shutdowns for cleaning. This occurs because kaolin modifies the chemical reactions within the combustion process, thus affecting slagging behaviors. Slagging, primarily noted with higher doses of kaolin, can obstruct air flows and interfere with heat transfer, leading to efficiency losses and increased operational costs. It was observed that the addition of kaolin accelerates the agglomeration of fuel mixtures on the grate, requiring the boiler to shut down after a certain period of operation. It was found that silica, abundant in the kaolin itself, is the major element contributing to the formation of agglomeration and slagging. Furthermore, as concluded in Chapter 3, silica accelerates slagging in fixed-bed boilers. Additionally, there was reasonable agreement between the predicted results using the slagging index, I_n, and the experimental observations of virgin wood and grade A recycled wood with kaolin addition during firing. Moreover, the predictions of crystalline phases by the TEM model show consistent results with the XRD analysis in the bottom ash, identifying crystalline structures such as Kalsilite, Leucite, and Sanidine. Understanding these transformations of crystalline structures due to kaolin addition is crucial to ensure smooth boiler operation. Overall, this chapter provides a clearer understanding and concrete evidence of the impacts of blending kaolin with biomass feedstocks at two different ratios, aiding researchers in future evaluations of kaolin's applicability in biomass firing for safe power generation.

Chapter 6 discusses the impacts of adding kaolin to woody biomass on the formation of particulate matter (PM) emissions in grate boilers. The results indicate that the addition of

kaolin leads to a 60% reduction in PM emissions for both virgin wood and grade A recycled wood. This reduction is expected and aligns with the findings in Chapter 5, which noted that most alkali elements were trapped in the bottom ash, forming alkali aluminium silicates. However, it was also found that PM emissions are rich in SiO_2 and Al_2O_3, which poses challenges for meeting environmental regulations concerning emissions. This is attributed to the adhesion and aggregation of particulates between airborne kaolin and fine and ultrafine PM particles. Additionally, since kaolin is rich in silica and alumina, there is a potential for an abundance of these elements in the flue gas. Therefore, it is crucial for researchers and power plant operators to closely monitor and understand the impacts of kaolin addition to fuel mixtures. By controlling kaolin injection, they can reduce the risk of corrosion and wear within the boiler system, thereby prolonging the life of the combustor and ensuring compliance with environmental emissions regulations.

7.2 Recommendations for future work

The current slagging index, I_n has been applied to woody biomass in fixed bed combustion technology. While this index demonstrates good predictive accuracy for woody biomass, it should be validated with larger datasets from large-scale experiments to enhance its accuracy and applicability across a broader range of woody biomass types, including various grades of waste biomass. This need for further validation arises because each type of biomass possesses unique chemical ash composition characteristics that can influence combustion behavior in distinct ways. Expanding the dataset will allow researchers to refine the index by accounting for these variations, potentially leading to improved predictive models that are more universally applicable. Additionally, expanding the scope of the research to include diverse types of woody and waste biomass can help in developing tailored approaches for managing slagging and fouling, which are critical for optimizing combustion efficiency and reducing maintenance requirements in biomass boilers. Moreover, understanding the variability among different biomass types can help in the formulation of more effective additives or treatments to enhance combustion performance and meet environmental standards. Ultimately, refining this index could lead to broader technological improvements in biomass combustion systems, fostering more sustainable and efficient energy production.

To further enhance the predictive capabilities of bed agglomeration, it is essential to conduct additional industrial tests to gather a broader dataset. This will refine the accuracy and reliability of the I_a index across a wider range of biomass types and combustion conditions. Furthermore, investigating the performance of the I_a index with alternative bed materials other

than quartz could broaden its applicability in various fluidized bed combustion (FBC) technologies. Currently, quartz is the predominant bed material used in the industry due to its low cost; however, materials such as olivine might become potential replacements due to their higher efficiency and less associated problems. Therefore, extending the applicability of the I_a index to different bed materials is crucial. These advancements could further solidify the role of the I_a index as a critical tool in the biomass combustion industry, enhancing both the efficiency and sustainability of biomass utilization in power generation. These recommendations aim to not only improve the predictability of slagging and bed agglomeration in fixed bed and fluidised bed combustors, respectively, but also contribute to the overall efficiency and sustainability of biomass combustion systems.

For the experimental approach, several topics could be investigated to understand the impact trends of kaolin when blended with woody biomass. In this study, the author faced a limitation in investigating kaolin dosages lower than 1.55 wt%, which might provide cost savings or efficiency improvements without compromising PM reduction effectiveness. This limitation is due to the screw feeder, which can only operate with kaolin concentrations of 1.55% and above. Future studies should focus on determining the optimal kaolin dosages that balance emission control with minimal impacts on slagging and agglomeration. This involves experimenting with varying concentrations and assessing their effects under different operational conditions.

In this study, it was concluded that the addition of kaolin to the feedstocks reduced the presence of alkali metals. However, an abundance of silica compound were observed in the bottom ash, slag, coarse fly ash, and PM emissions, attributable to the high silica content in the kaolin itself. Furthermore, the kaolin used in this study was very fine, with 70% of the particles smaller than 1µm. It was determined that the high silica content in PM emissions is due to the aggregation and cohesion of airborne kaolin within the flue gas. This occurs because the kaolin particles are very light, thus having a high potential to enrich the flue gas with silica. Future research should investigate the impacts of kaolin's particle size on combustion behaviour in the boiler by using coarser kaolin particles or pelletized kaolin. By doing so, researchers will be able to observe and monitor the trends and impacts of kaolin particle size on biomass combustion behaviour in boilers. This will allow for conclusions on the applicability of kaolin additions to field-scale combustors. By addressing these recommendations, future research can enhance the understanding and application of additives in biomass combustion, aiming to optimize both environmental performance and operational efficiency.

Bibliography

1. *GB Fuel type power generation production*. 2024 [cited 2024 28 April]; Available from: https://gridwatch.co.uk/.
2. Zero, D.f.E.S.N., *Digest of UK Energy Statistics Annual data for UK, 2023*. 2024.
3. Zhou, Y., N. Zhao, B. Li, T. Bahargul, D. Chen, and R. Dong, *Application of Biomass Co-combustion in Rural Daily Energy Supply.* Nongye Jixie Xuebao/Transactions of the Chinese Society for Agricultural Machinery, 2018. **49**: p. 407-412.
4. Yuan, L., Y. Niu, L. Yang, S. Liu, D. Wang, and H. Suo, *Experiment and Kinetics Studies on Ash Fusion Characteristics of Biomass/Coal Mixtures During Combustion.* Energy & Fuels, 2019.
5. García, R., M.V. Gil, F. Rubiera, and C. Pevida, *Pelletization of Wood and Alternative Residual Biomass Blends for Producing Industrial Quality Pellets.* Fuel, 2019.
6. Кокшарев, O.M. and A.V. Gil, *Study of in-Furnace Gas-Dynamic Processes With Different Design of Vortex Burners.* Matec Web of Conferences, 2018. **194**: p. 01027.
7. Carroll, J.P. and J. Finnan, *Physical and chemical properties of pellets from energy crops and cereal straws.* Biosystems engineering, 2012. **112**(2): p. 151-159.
8. DRAX. *DRAX Power Station*. 2021 March 1, 2021; Available from: https://www.drax.com/about-us/drax-power-station/.
9. EUROPE, E.P. *Lynemouth Power*. March 1, 2021]; Available from: https://www.eppowereurope.cz/en/companies/lynemouth-power/#siteMapSection.
10. Mason, P.E., *Investigations on the combustion behaviour of single particles of pulverised biomass fuel* 2016, The University of Leeds.
11. Environment, R.E., *Analysing the potential of bioenergy with carbon capture in the UK to 2050*2020.
12. Sugiyono, A., I. Febijanto, and E. Hilmawan. *Potential of biomass and coal co-firing power plants in Indonesia: a PESTEL analysis*. in *IOP Conference Series: Earth and Environmental Science*. 2022. IOP Publishing.
13. Roni, M.S., S. Chowdhury, S. Mamun, M. Marufuzzaman, W. Lein, and S. Johnson, *Biomass co-firing technology with policies, challenges, and opportunities: A global review.* Renewable and Sustainable Energy Reviews, 2017. **78**: p. 1089-1101.
14. Tillman, D.A., *Solid fuel blending [electronic resource] : principles, practices, and problems*. 1st ed. ed, ed. D. Duong and N.S. Harding. 2012, Amsterdam: Amsterdam : Elsevier, Butterworth-Heinemann, c2012.
15. McKendry, P., *Energy production from biomass (part 1): overview of biomass.* Bioresour Technol, 2002. **83**(1): p. 37-46.
16. Roni, M.S., S. Chowdhury, S. Mamun, M. Marufuzzaman, W. Lein, and S. Johnson, *Biomass co-firing technology with policies, challenges, and opportunities: A global review.* Renewable & sustainable energy reviews, 2017. **78**(C): p. 1089-1101.
17. Riaza, J., R. Khatami, Y.A. Levendis, L. Álvarez, M.V. Gil, C. Pevida, F. Rubiera, and J.J. Pís, *Combustion of Single Biomass Particles in Air and in Oxy-Fuel Conditions.* Biomass and Bioenergy, 2014. **64**: p. 162-174.
18. Kleinhans, U., C. Wieland, F.J. Frandsen, and H. Spliethoff, *Ash formation and deposition in coal and biomass fired combustion systems: Progress and challenges in the field of ash particle sticking and rebound behavior.* Progress in energy and combustion science, 2018. **68**: p. 65-168.
19. Weber, R., M. Mancini, N. Schaffel-Mancini, and T. Kupka, *On predicting the ash behaviour using Computational Fluid Dynamics.* Fuel processing technology, 2013. **105**: p. 113-128.

20. Lachman, J., M. Baláš, M. Lisý, H. Lisá, P. Milčák, and P. Elbl, *An overview of slagging and fouling indicators and their applicability to biomass fuels.* Fuel processing technology, 2021. **217**.
21. Ma, W., T. Wenga, F.J. Frandsen, B. Yan, and G. Chen, *The fate of chlorine during MSW incineration: Vaporization, transformation, deposition, corrosion and remedies.* Progress in energy and combustion science, 2020. **76**: p. 100789.
22. Yang, X., *Development of Ash Deposition Prediction Models through the CFD Methods and the Ash Deposition Indice*, in *Department of Mechanical Engineering* 2016, University of Sheffield.
23. Lapuerta, M.n., A. Acosta, and A. Pazo, *Fouling Deposits From Residual Biomass With High Sodium Content in Power Plants.* Energy & Fuels, 2015. **29**(8): p. 5007-5017.
24. Laxminarayan, Y., P.A. Jensen, H. Wu, F.J. Frandsen, B. Sander, and P. Glarborg, *Deposit Shedding in Biomass-Fired Boilers: Shear Adhesion Strength Measurements.* Energy and Fuels, 2017. **31**(8): p. 8733-8741.
25. Idris, M.H.B.M., *Experimental Investigation into the Effects of Co-firing with Empty Fruit Bunch (EFB) on the Formation of Slagging and Fouling in Solid Fuel Combustion Test Rig*, in *College of Engineering*. 2018, Universiti Tenaga Nasional.
26. Dai, B.-Q., X. Wu, A. De Girolamo, and L. Zhang, *Inhibition of lignite ash slagging and fouling upon the use of a silica-based additive in an industrial pulverised coal-fired boiler. Part 1. Changes on the properties of ash deposits along the furnace.* Fuel, 2015. **139**: p. 720-732.
27. Pang, L., Y. Shao, W. Zhong, and H. Liu, *Experimental study of SO2 emissions and desulfurization of oxy-coal combustion in a 30 kWth pressurized fluidized bed combustor.* Fuel, 2020. **264**: p. 116795.
28. Moradian, F., *Ash Behavior in Fluidized-Bed Combustion and Gasification of Biomass and Waste Fuels*. 2016, University of Borås: Sweden.
29. Singh, A., V. Sharma, S. Mittal, G. Pandey, D. Mudgal, and P. Gupta, *An overview of problems and solutions for components subjected to fireside of boilers.* International Journal of Industrial Chemistry, 2018. **9**(1).
30. Abdelhady, S., D. Borello, and A. Shaban, *Techno-economic assessment of biomass power plant fed with rice straw: Sensitivity and parametric analysis of the performance and the LCOE.* Renewable Energy, 2018. **115**: p. 1026-1034.
31. Bermúdez, C.A., J. Porteiro, L.G. Varela, S. Chapela, and D. Patiño, *Three-dimensional CFD simulation of a large-scale grate-fired biomass furnace.* Fuel Processing Technology, 2020. **198**: p. 106219.
32. Öhman, M., C. Boman, H. Hedman, A. Nordin, and D. Boström, *Slagging tendencies of wood pellet ash during combustion in residential pellet burners.* Biomass and Bioenergy, 2004. **27**(6): p. 585-596.
33. Fagerstrom, J., I.-L. Nazelius, C. Gilbe, D. Bostrom, M. Ohman, and C. Boman, *Influence of peat ash composition on particle emissions and slag formation in biomass grate co-combustion.* Energy & Fuels, 2014. **28**(5): p. 3403-3411.
34. Fagerström, J., E. Steinvall, D. Boström, and C. Boman, *Alkali transformation during single pellet combustion of soft wood and wheat straw.* Fuel processing technology, 2016. **143**: p. 204-212.
35. Bäfver, L.S., M. Rönnbäck, B. Leckner, F. Claesson, and C. Tullin, *Particle emission from combustion of oat grain and its potential reduction by addition of limestone or kaolin.* Fuel Processing Technology, 2009. **90**(3): p. 353-359.
36. Boström, D., N. Skoglund, A. Grimm, C. Boman, M. Öhman, M. Broström, and R. Backman, *Ash Transformation Chemistry during Combustion of Biomass.* Energy & Fuels, 2012. **26**(1): p. 85-93.

37. Singh, A., V. Sharma, S. Mittal, G. Pandey, D. Mudgal, and P. Gupta, *An overview of problems and solutions for components subjected to fireside of boilers.* International Journal of Industrial Chemistry, 2018. **9**(1): p. 1-15.
38. Yin, C., L.A. Rosendahl, and S.K. Kær, *Grate-firing of biomass for heat and power production.* Progress in energy and combustion science, 2008. **34**(6): p. 725-754.
39. Wu, D., Z. Yuan, S. Liu, J. Zheng, X. Wei, and C. Zhang, *Recent Development of Corrosion Factors and Coating Applications in Biomass Firing Plants.* Coatings, 2020. **10**(10): p. 1001.
40. Rebbling, A., P. Sundberg, J. Fagerström, M. Carlborg, C. Tullin, D. Boström, M. Öhman, C. Boman, and N. Skoglund, *Demonstrating Fuel Design To Reduce Particulate Emissions and Control Slagging in Industrial-Scale Grate Combustion of Woody Biomass.* Energy Fuels, 2020. **34**(2): p. 2574-2583.
41. Kær, S.K., L.A. Rosendahl, and L.L. Baxter, *Towards a CFD-based mechanistic deposit formation model for straw-fired boilers.* Fuel (Guildford), 2006. **85**(5): p. 833-848.
42. Abioye, K.J., N.Y. Harun, S. Sufian, M. Yusuf, A.H. Jagaba, B.C. Ekeoma, H. Kamyab, S. Sikiru, S. Waqas, and H. Ibrahim, *A review of biomass ash related problems: Mechanism, solution, and outlook.* Journal of the Energy Institute, 2024. **112**: p. 101490.
43. Wang, L., G. Skjevrak, J.E. Hustad, and Ø. Skreiberg, *Investigation of biomass ash sintering characteristics and the effect of additives.* Energy & Fuels, 2014. **28**(1): p. 208-218.
44. Piotrowska, P., M. Zevenhoven, M. Hupa, J. Giuntoli, and W. de Jong, *Residues from the production of biofuels for transportation: Characterization and ash sintering tendency.* Fuel processing technology, 2013. **105**: p. 37-45.
45. Wang, L., J.E. Hustad, Ø. Skreiberg, G. Skjevrak, and M. Grønli, *A Critical Review on Additives to Reduce Ash Related Operation Problems in Biomass Combustion Applications.* Energy procedia, 2012. **20**: p. 20-29.
46. Wang, L., G. Skjevrak, Ø. Skreiberg, H. Wu, H.K. Nielsen, and J.E. Hustad, *Investigation on Ash Slagging Characteristics During Combustion of Biomass Pellets and Effect of Additives.* Energy & Fuels, 2017. **32**(4): p. 4442-4452.
47. PŁAZA, P.P., *The Development of a Slagging and Fouling Predictive Methodology for Large Scale Pulverised Boilers Fired with Coal/Biomass Blends*, in *Mechanical Engineering*. 2013, Cardiff University.
48. Yang, X., *Development of Ash Deposition Prediction Models through the CFD Methods and the Ash Deposition Indice*. 2017, University of Sheffield.
49. Jing, N., Q. Wang, L. Cheng, Z. Luo, and K. Cen, *The sintering behavior of coal ash under pressurized conditions.* Fuel (Guildford), 2013. **103**: p. 87-93.
50. Li, J., M. Zhu, Z. Zhang, and D. Zhang, *A new criterion for determination of coal ash sintering temperature using the pressure-drop technique and the effect of ash mineralogy and geochemistry.* Fuel (Guildford), 2016. **179**: p. 71-78.
51. Haiying, Z., Z. Youcai, and Q. Jingyu, *Utilization of municipal solid waste incineration (MSWI) fly ash in ceramic brick: Product characterization and environmental toxicity.* Waste Manag, 2011. **31**(2): p. 331-341.
52. Haykiri-Acma, H., S. Yaman, and S. Kucukbayrak, *Effect of biomass on temperatures of sintering and initial deformation of lignite ash.* Fuel (Guildford), 2010. **89**(10): p. 3063-3068.
53. Great Britain. Department of, E., *The efficient use of energy*. 1975, Guildford: Guildford : IPC Science and Technology Press for the Institute of Fuel acting on behalf of the UK Department of Energy, 1975.

54. Zhu, Y., H. Su, T. Qiu, Y. Zhai, H. Mikulčić, X. Wang, L. Zhang, J. Xie, and T. Yang, *Modelling of fly ash viscous deposition and slagging prediction of biomass-fired boiler.* Renewable Energy, 2024. **227**: p. 120605.
55. Roberts, L.J., *Additives to Mitigate Against Slagging and Fouling in Biomass Combustion* in *School of Chemical and Process Engineering, Faculty of Engineering*. 2018, University of Leeds.
56. Sefidari, H., H. Wiinikka, B. Lindblom, L.O. Nordin, G. Wu, E. Yazhenskikh, M. Müller, C. Ma, and M. Öhman, *Comparison of high-rank coals with respect to slagging/deposition tendency at the transfer-chute of iron-ore pelletizing grate-kiln plants: A pilot-scale experimental study accompanied by thermochemical equilibrium modeling and viscosity estimations.* Fuel processing technology, 2019. **193**: p. 244-262.
57. Cai, Y., K. Tay, Z. Zheng, W. Yang, H. Wang, G. Zeng, Z. Li, S. Keng Boon, and P. Subbaiah, *Modeling of ash formation and deposition processes in coal and biomass fired boilers: A comprehensive review.* Applied Energy, 2018. **230**: p. 1447-1544.
58. Kær, S.K., *Numerical investigation of ash deposition in straw-fired boilers: using CFD as the framework for slagging and fouling predictions*. 2001: Institut for Energiteknik, Aalborg Universitet.
59. Baxter, L.L., *Ash deposition during biomass and coal combustion: A mechanistic approach.* Biomass & bioenergy, 1993. **4**(2): p. 85-102.
60. MASIÁ, T., *Characterisation and prediction of deposits in biomass co-combustion* 2010, Universidad de Sevilla, España.
61. Baxter, L.L., T.R. Miles, T.R. Miles Jr, B.M. Jenkins, T. Milne, D. Dayton, R.W. Bryers, and L.L. Oden, *The behavior of inorganic material in biomass-fired power boilers: field and laboratory experiences.* Fuel processing technology, 1998. **54**(1-3): p. 47-78.
62. Masiá, A.T., *Characterisation and prediction of deposits in biomass co-combustion.* 2011.
63. Vega-Nieva, D.J., L. Ortiz Torres, J.L. Míguez Tabares, and J. Morán, *Measuring and Predicting the Slagging of Woody and Herbaceous Mediterranean Biomass Fuels on a Domestic Pellet Boiler.* Energy Fuels, 2016. **30**(2): p. 1085-1095.
64. McCaffrey, Z., P. Thy, M.E. Long, M.C.J.d. Oliveira, L. Wang, L. Torres, T. Aktaş, B.S. Chiou, W.J. Orts, and B.M. Jenkins, *Air and Steam Gasification of Almond Biomass.* Frontiers in Energy Research, 2019. **7**.
65. Wang, H. and J.N. Harb, *Modeling of ash deposition in large-scale combustion facilities burning pulverized coal.* Progress in energy and combustion science, 1997. **23**(3): p. 267-282.
66. Míguez, J.L., J. Porteiro, F. Behrendt, D. Blanco, D. Patiño, and A. Dieguez-Alonso, *Review of the use of additives to mitigate operational problems associated with the combustion of biomass with high content in ash-forming species.* Renewable and Sustainable Energy Reviews, 2021. **141**: p. 110502.
67. Jappe Frandsen, F., *Utilizing biomass and waste for power production—a decade of contributing to the understanding, interpretation and analysis of deposits and corrosion products.* Fuel (Guildford), 2005. **84**(10): p. 1277-1294.
68. Werther, J., M. Saenger, E.U. Hartge, T. Ogada, and Z. Siagi, *Combustion of agricultural residues.* Progress in energy and combustion science, 2000. **26**(1): p. 1-27.
69. Thy, P., C. Yu, B.M. Jenkins, and C.E. Lesher, *Inorganic Composition and Environmental Impact of Biomass Feedstock.* Energy & Fuels, 2013. **27**(7): p. 3969-3987.
70. Sefidari, H., B. Lindblom, L.O. Nordin, and H. Wiinikka, *The feasibility of replacing coal with biomass in iron-ore pelletizing plants with respect to melt-induced slagging.* Energies, 2020. **13**(20).

71. Steenari, B.-M., A. Lundberg, H. Pettersson, M. Wilewska-Bien, and D. Andersson, *Investigation of Ash Sintering during Combustion of Agricultural Residues and the Effect of Additives.* Energy Fuels, 2009. **23**(11): p. 5655-5662.
72. Gilbe, C., M. Öhman, E. Lindström, D. Boström, R. Backman, R. Samuelsson, and J. Burvall, *Slagging Characteristics during Residential Combustion of Biomass Pellets.* Energy Fuels, 2008. **22**(5): p. 3536-3543.
73. Lindstrom, E., M. Sandstrom, D. Bostrom, and M. Ohman, *Slagging Characteristics during Combustion of Cereal Grains Rich in Phosphorus.* Energy Fuels, 2007. **21**(2): p. 710-717.
74. Wang, L., G. Skjevrak, J.E. Hustad, and M.G. Grønli, *Effects of Sewage Sludge and Marble Sludge Addition on Slag Characteristics during Wood Waste Pellets Combustion.* Energy Fuels, 2011. **25**(12): p. 5775-5785.
75. Teixeira, P., H. Lopes, I. Gulyurtlu, N. Lapa, and P. Abelha, *Slagging and fouling during coal and biomass cofiring: Chemical equilibrium model applied to FBC.* Energy and Fuels, 2014. **28**(1): p. 697-713.
76. Yao, X., K. Xu, F. Yan, and Y. Liang, *The influence of ashing temperature on ash fouling and slagging characteristics during combustion of biomass fuels.* BioResources, 2017. **12**(1): p. 1593-1610.
77. Vassilev, S.V., D. Baxter, L.K. Andersen, and C.G. Vassileva, *An overview of the composition and application of biomass ash. Part 1. Phase–mineral and chemical composition and classification.* Fuel, 2013. **105**: p. 40-76.
78. Li, F., X. Wang, C. Zhao, Y. Li, M. Guo, H. Fan, Q. Guo, and Y. Fang, *Influence of additives on potassium retention behaviors during straw combustion: A mechanism study.* Bioresource technology, 2020. **299**: p. 122515.
79. Link, S., P. Yrjas, and L. Hupa, *Ash melting behaviour of wheat straw blends with wood and reed.* Renewable Energy, 2018. **124**: p. 11-20.
80. Regueiro, A., D. Patiño, E. Granada, and J. Porteiro, *Experimental study on the fouling behaviour of an underfeed fixed-bed biomass combustor.* Applied Thermal Engineering, 2017. **112**: p. 523-533.
81. Li, F., Y. Li, H. Fan, T. Wang, M. Guo, and Y. Fang, *Investigation on fusion characteristics of deposition from biomass vibrating grate furnace combustion and its modification.* Energy, 2019. **174**: p. 724-734.
82. Davidsson, K.O., B.M. Steenari, and D. Eskilsson, *Kaolin Addition during Biomass Combustion in a 35 MW Circulating Fluidized-Bed Boiler.* Energy Fuels, 2007. **21**(4): p. 1959-1966.
83. Sommersacher, P., T. Brunner, I. Obernberger, N. Kienzl, and W. Kanzian, *Application of Novel and Advanced Fuel Characterization Tools for the Combustion Related Characterization of Different Wood/Kaolin and Straw/Kaolin Mixtures.* Energy Fuels, 2013. **27**(9): p. 5192-5206.
84. Li, H., Z. Zhang, A. Ji, R. Zhao, and P. Yang, *Behavior of slagging and corrosion of biomass ash.* J. Environ. Eng. Technol., 2017. **7**(1): p. 107-113.
85. Ruan, R., B. Long, Z. Liu, and A. Xu, *Study of the index for discriminating the slagging of ash produced from combustion of biomass.* J. Eng. Therm. Energy Power, 2013. **28**: p. 650-666.
86. Yuan, Y., R. Wieczorek, D.L. Green, P. Cook, H. Ballard, and D.J. Araten, *Multiple myeloma involving skin and pulmonary parenchyma after autologous stem cell transplantation.* J Hematol Oncol, 2009. **2**(1): p. 48-48.
87. Lai, X., Z. Zhou, H. Liu, Y. Huang, X. Yin, and C. Wu, *Experiment study of biomass ash sintering and melting.* Transactions of the Chinese Society for Agricultural Machinery, 2016. **47**: p. 158-166.

88. Chen, C., S. Qin, and Z. Lu, *Application of fuzzy grey clustering method in discrimination of bagasse combustion tendency.* Journal of Guangxi University: Natural Science Edition, 2017(5): p. 1707-1714.
89. Öhman, M., D. Boström, A. Nordin, and H. Hedman, *Effect of Kaolin and Limestone Addition on Slag Formation during Combustion of Wood Fuels.* Energy Fuels, 2004. **18**(5): p. 1370-1376.
90. Roberts, L.J., P.E. Mason, J.M. Jones, W.F. Gale, A. Williams, A. Hunt, and J. Ashman, *The impact of aluminosilicate-based additives upon the sintering and melting behaviour of biomass ash.* Biomass and Bioenergy, 2019. **127**.
91. Grimm, A., N. Skoglund, D. Boström, and M. Öhman, *Bed Agglomeration Characteristics in Fluidized Quartz Bed Combustion of Phosphorus-Rich Biomass Fuels.* Energy Fuels, 2011. **25**(3): p. 937-947.
92. Visser, H.J.M., S.C. van Lith, and J.H.A. Kiel, *Biomass Ash-Bed Material Interactions Leading to Agglomeration in FBC.* Journal of energy resources technology, 2008. **130**(1): p. 0118011-0118016.
93. Davidsson, K.O., L.E. Åmand, B.M. Steenari, A.L. Elled, D. Eskilsson, and B. Leckner, *Countermeasures against alkali-related problems during combustion of biomass in a circulating fluidized bed boiler.* Chemical engineering science, 2008. **63**(21): p. 5314-5329.
94. Bartels, M., W. Lin, J. Nijenhuis, F. Kapteijn, and J.R. van Ommen, *Agglomeration in fluidized beds at high temperatures: Mechanisms, detection and prevention.* Progress in energy and combustion science, 2008. **34**(5): p. 633-666.
95. Grimm, A., M. Öhman, T.s. Lindberg, A. Fredriksson, and D. Boström, *Bed Agglomeration Characteristics in Fluidized-Bed Combustion of Biomass Fuels Using Olivine as Bed Material.* Energy Fuels, 2012. **26**(7): p. 4550-4559.
96. Morris, J.D., S.S. Daood, S. Chilton, and W. Nimmo, *Mechanisms and mitigation of agglomeration during fluidized bed combustion of biomass: A review.* Fuel, 2018. **230**: p. 452-473.
97. Hupa, M., *Ash-Related Issues in Fluidized-Bed Combustion of Biomasses: Recent Research Highlights.* Energy Fuels, 2012. **26**(1): p. 4-14.
98. Zevenhoven, M., P. Yrjas, B.-J. Skrifvars, and M. Hupa, *Characterization of Ash-Forming Matter in Various Solid Fuels by Selective Leaching and Its Implications for Fluidized-Bed Combustion.* Energy & fuels, 2012. **26**(SEPOCT): p. 6366-6386.
99. Boström, D., G. Eriksson, C. Boman, and M. Öhman, *Ash Transformations in Fluidized-bed Combustion of Rapeseed Meal.* Energy Fuels, 2009. **23**(5): p. 2700-2706.
100. Ninduangdee, P. and V.I. Kuprianov, *Combustion of an oil palm residue with elevated potassium content in a fluidized-bed combustor using alternative bed materials for preventing bed agglomeration.* Bioresource Technology, 2015. **182**: p. 272-281.
101. Olofsson, G., Z. Ye, I. Bjerle, and A. Andersson, *Bed agglomeration problems in fluidized-bed biomass combustion.* Industrial and Engineering Chemistry Research, 2002. **41**(12): p. 2888-2894.
102. Oka, S., *Fluidized bed combustion*. 2003: CRC press.
103. Scala, F. and R. Chirone, *Characterization and Early Detection of Bed Agglomeration during the Fluidized Bed Combustion of Olive Husk.* Energy & Fuels, 2006. **20**(1): p. 120-132.
104. Chirone, R., F. Miccio, and F. Scala, *Mechanism and prediction of bed agglomeration during fluidized bed combustion of a biomass fuel: Effect of the reactor scale.* Chemical Engineering Journal, 2006. **123**(3): p. 71-80.

105. Lin, W., K. Dam-Johansen, and F. Frandsen, *Agglomeration in bio-fuel fired fluidized bed combustors.* Chemical engineering journal (Lausanne, Switzerland : 1996), 2003. **96**(1): p. 171-185.
106. Skrifvars, B.-J., M. Hupa, R. Backman, and M. Hiltunen, *Sintering mechanisms of FBC ashes.* Fuel (Guildford), 1994. **73**(2): p. 171-176.
107. Öhman, M., L. Pommer, and A. Nordin, *Bed Agglomeration Characteristics and Mechanisms during Gasification and Combustion of Biomass Fuels.* Energy Fuels, 2005. **19**(4): p. 1742-1748.
108. Price-Allison, A., P.E. Mason, J.M. Jones, E.K. Barimah, G. Jose, A. Brown, A.B. Ross, and A. Williams, *The Impact of Fuelwood Moisture Content on the Emission of Gaseous and Particulate Pollutants From a Wood Stove.* Combustion Science and Technology, 2021. **195**(1): p. 133-152.
109. Lamberg, H., J. Tissari, J. Jokiniemi, and O. Sippula, *Fine Particle and Gaseous Emissions from a Small-Scale Boiler Fueled by Pellets of Various Raw Materials.* Energy & Fuels, 2013. **27**(11): p. 7044-7053.
110. Kortelainen, M., J. Jokiniemi, I. Nuutinen, T. Torvela, H. Lamberg, T. Karhunen, J. Tissari, and O. Sippula, *Ash behaviour and emission formation in a small-scale reciprocating-grate combustion reactor operated with wood chips, reed canary grass and barley straw.* Fuel (Guildford), 2015. **143**: p. 80-88.
111. Szemmelveisz, K., I. Szűcs, Á. Palotás, L. Winkler, and E. Eddings, *Examination of the combustion conditions of herbaceous biomass.* Fuel Processing Technology, 2009. **90**(6): p. 839-847.
112. Becidan, M., D. Todorovic, Ø. Skreiberg, R.A. Khalil, R. Backman, F. Goile, A. Skreiberg, A. Jovovic, and L. Sørum, *Ash related behaviour in staged and non-staged combustion of biomass fuels and fuel mixtures.* Biomass & Bioenergy, 2012. **41**: p. 86-93.
113. Xu, M., D. Yu, H. Yao, X. Liu, and Y. Qiao, *Coal combustion-generated aerosols: Formation and properties.* Proceedings of the Combustion Institute, 2011. **33**(1): p. 1681-1697.
114. Yao, Q., S.-Q. Li, H.-W. Xu, J.-K. Zhuo, and Q. Song, *Studies on formation and control of combustion particulate matter in China: A review.* Energy, 2009. **34**(9): p. 1296-1309.
115. Liu, X., Y. Xu, X. Zeng, Y. Zhang, M. Xu, S. Pan, K. Zhang, L. Li, and X. Gao, *Field Measurements on the Emission and Removal of PM2.5 from Coal-Fired Power Stations: 1. Case Study for a 1000 MW Ultrasupercritical Utility Boiler.* Energy & Fuels, 2016. **30**(8): p. 6547-6554.
116. Jaworek, A., A. Krupa, and T. Czech, *Modern electrostatic devices and methods for exhaust gas cleaning: A brief review.* Journal of Electrostatics, 2007. **65**(3): p. 133-155.
117. Jena, M.C., S.k. Mishra, and H.S. Moharana, *Effect of Particle Size on Collection Efficiency of ESP and RABH: A Case Study.* Aerosol Science and Engineering, 2019. **3**(3): p. 75-87.
118. Wang, C., X. Liu, D. Li, J. Si, B. Zhao, and M. Xu, *Measurement of particulate matter and trace elements from a coal-fired power plant with electrostatic precipitators equipped the low temperature economizer.* Proceedings of the Combustion Institute, 2015. **35**(3): p. 2793-2800.
119. Xu, Y., X. Liu, J. Cui, D. Chen, M. Xu, S. Pan, K. Zhang, and X. Gao, *Field measurements on the emission and removal of PM2. 5 from coal-fired power stations: 4. PM removal performance of wet electrostatic precipitators.* Energy & Fuels, 2016. **30**(9): p. 7465-7473.

120. Xu, Y., X. Liu, H. Wang, X. Zeng, Y. Zhang, J. Han, M. Xu, and S. Pan, *Influences of In-Furnace Kaolin Addition on the Formation and Emission Characteristics of PM2.5 in a 1000 MW Coal-Fired Power Station.* Environmental Science & Technology, 2018. **52**(15): p. 8718-8724.
121. Rahman, A.A., *Studies of Co-firing Coal with Biomass on a Two Stage Simulator for Utility Boilers*, in *Division of Mechanical Engineering and Energy Studies Cardiff School of Engineering* 2006, Cardiff University.
122. *Biomass pelletization : standards and production / edited by A. Garcia-Maraver & J.A. Pérez-Jiménez*, ed. A. Garcia-Maraver and J.A. Pérez-Jiménez. 2015. 180-180 pages.
123. Yu, L.Y., L.W. Wang, and P.S. Li, *Study on prediction models of biomass ash softening temperature based on ash composition.* Journal of the Energy Institute, 2014. **87**(3): p. 215-219.
124. Ganapathy, V., *Industrial boilers and heat recovery steam generators: design, applications, and calculations*. 2002: CRC Press.
125. Rayaprolu, K., *Boilers: A practical reference*. 2012: CRC press.
126. *95/00598 Understanding slagging and fouling during pf combustion.* Fuel and energy abstracts, 1995. **36**(1): p. 35-35.
127. Skrifvars, B.-J., M. Öhman, A. Nordin, and M. Hupa, *Predicting bed agglomeration tendencies for biomass fuels fired in FBC boilers: a comparison of three different prediction methods.* Energy & fuels, 1999. **13**(2): p. 359-363.
128. Öhman, M., A. Nordin, H. Hedman, and R. Jirjis, *Reasons for slagging during stemwood pellet combustion and some measures for prevention.* Biomass and Bioenergy, 2004. **27**(6): p. 597-605.
129. Vega-Nieva, D., C. Alvarez, and L. Ortiz. *Results of new laboratory methods and slagging classification systems for the prediction and quantification of ash slagging in woody and herbaceous biomass fuels*. in *Central European Biomass Conference*. 2014.
130. Vega-Nieva, D., R. Dopazo, and L. Ortiz, *Strategies for minimizing ash slagging in combustion of mediterranean biomasses.* World Bioenergy, 2012. **2012**.
131. Somoza, L., D. Vega-Nieva, and L. Ortiz, *Quality control of wood chips and wood pellet from the biomass logistic center of Biopalas.* FEADER-Xunta Project Report, 2014.
132. Garcia-Maraver, A., J. Mata-Sanchez, M. Carpio, and J.A. Perez-Jimenez, *Critical review of predictive coefficients for biomass ash deposition tendency.* Journal of the Energy Institute, 2017. **90**(2): p. 214-228.
133. Moilanen, A., *Thermogravimetric characterisations of biomass and waste for gasification processes*. 2006, VTT Technical Research Centre of Finland.
134. Zevenhoven-Onderwater, M., R. Backman, B.-J. Skrifvars, and M. Hupa, *The ash chemistry in fluidised bed gasification of biomass fuels. Part I: predicting the chemistry of melting ashes and ash–bed material interaction.* Fuel (Guildford), 2001. **80**(10): p. 1489-1502.
135. Jenkins, B.M., L.L. Baxter, T.R. Miles, and T.R. Miles, *Combustion properties of biomass.* Fuel processing technology, 1998. **54**(1): p. 17-46.
136. Baxter, L.L., T.R. Miles, T.R. Miles, B.M. Jenkins, T. Milne, D. Dayton, R.W. Bryers, and L.L. Oden, *The behavior of inorganic material in biomass-fired power boilers: field and laboratory experiences.* Fuel processing technology, 1998. **54**(1): p. 47-78.
137. Bryers, R.W., *Fireside slagging, fouling, and high-temperature corrosion of heat-transfer surface due to impurities in steam-raising fuels.* Progress in energy and combustion science, 1996. **22**(1): p. 29-120.
138. Olanders, B. and B.-M. Steenari, *Characterization of ashes from wood and straw.* Biomass and Bioenergy, 1995. **8**(2): p. 105-115.

139. Jenkins, B.M., R.R. Bakker, and J.B. Wei, *On the properties of washed straw.* Biomass & bioenergy, 1996. **10**(4): p. 177-200.
140. Llorente, M.J.F., J.M.M. Laplaza, R.E. Cuadrado, and J.E.C. García, *Ash behaviour of lignocellulosic biomass in bubbling fluidised bed combustion.* Fuel (Guildford), 2006. **85**(9): p. 1157-1165.
141. Nutalapati, D., R. Gupta, B. Moghtaderi, and T.F. Wall, *Assessing slagging and fouling during biomass combustion: A thermodynamic approach allowing for alkali/ash reactions.* Fuel processing technology, 2007. **88**(11-12): p. 1044-1052.
142. Miles, T.R., T.R. Miles, L.L. Baxter, R.W. Bryers, B.M. Jenkins, and L.L. Oden, *Boiler deposits from firing biomass fuels.* Biomass & bioenergy, 1996. **10**(2): p. 125-138.
143. Nielsen, H.P., L.L. Baxter, G. Sclippab, C. Morey, F.J. Frandsen, and K. Dam-Johansen, *Deposition of potassium salts on heat transfer surfaces in straw-fired boilers: a pilot-scale study.* Fuel, 2000. **79**(2): p. 131-139.
144. HRN, E., *14961-5: 2011 Solidbiofuels–Fuel specifications and classes–Part 5: Firewood for non-industrial use.* Hrvatski zavod za norme, Zagreb: p. 1-12.
145. Obernberger, I., T. Brunner, and G. Bärnthaler, *Chemical properties of solid biofuels—significance and impact.* Biomass and Bioenergy, 2006. **30**(11): p. 973-982.
146. Obernberger, I. and G. Thek, *Physical characterisation and chemical composition of densified biomass fuels with regard to their combustion behaviour.* Biomass and Bioenergy, 2004. **27**(6): p. 653-669.
147. Vamvuka, D. and D. Zografos, *Predicting the behaviour of ash from agricultural wastes during combustion.* Fuel (Guildford), 2004. **83**(14): p. 2051-2057.
148. Miles, T.R., T.R. Miles, L.L. Baxter, R.W. Bryers, B.M. Jenkins, and L.L. Oden, *Boiler deposits from firing biomass fuels.* Biomass and Bioenergy, 1996. **10**(2): p. 125-138.
149. Teixeira, P., H. Lopes, I. Gulyurtlu, N. Lapa, and P. Abelha, *Evaluation of slagging and fouling tendency during biomass co-firing with coal in a fluidized bed.* Biomass and bioenergy, 2012. **39**: p. 192-203.
150. Pronobis, M., *Evaluation of the influence of biomass co-combustion on boiler furnace slagging by means of fusibility correlations.* Biomass & bioenergy, 2005. **28**(4): p. 375-383.
151. Tortosa Masiá, A.A., B.J.P. Buhre, R.P. Gupta, and T.F. Wall, *Characterising ash of biomass and waste.* Fuel processing technology, 2007. **88**(11-12): p. 1071-1081.
152. Niu, Y., Y. Zhu, H. Tan, X. Wang, S.e. Hui, and W. Du, *Experimental study on the coexistent dual slagging in biomass-fired furnaces: Alkali- and silicate melt-induced slagging.* Proceedings of the Combustion Institute, 2015. **35**(2): p. 2405-2413.
153. Dunnu, G., J. Maier, and G. Scheffknecht, *Ash fusibility and compositional data of solid recovered fuels.* Fuel (Guildford), 2010. **89**(7): p. 1534-1540.
154. Gray, R. and G. Moore. *BURNING SUB-BITUMINOUS COALS OF MONTANA AND WYOMING IN LARGE UTILITY BOILERS*. in *Mechanical Engineering*. 1975. ASME-AMER SOC MECHANICAL ENG 345 E 47TH ST, NEW YORK, NY 10017.
155. Raask, E., *Mineral Impurities in Coal Combustion: Behavior, Problems, and Remedial Measures*. 1985: Hemisphere Publishing Corporation.
156. Huggins, F.E., D.A. Kosmack, and G.P. Huffman, *Correlation between ash-fusion temperatures and ternary equilibrium phase diagrams.* Fuel (Guildford), 1981. **60**(7): p. 577-584.
157. Cummer, K.R. and R.C. Brown, *Ancillary equipment for biomass gasification.* Biomass and Bioenergy, 2002. **23**(2): p. 113-128.
158. Niu, Y., Y. Zhu, H. Tan, S. Hui, Z. Jing, and W. Xu, *Investigations on biomass slagging in utility boiler: Criterion numbers and slagging growth mechanisms.* Fuel processing technology, 2014. **128**: p. 499-508.

159. Vamvuka, D., D. Zografos, and G. Alevizos, *Control methods for mitigating biomass ash-related problems in fluidized beds.* Bioresour Technol, 2008. **99**(9): p. 3534-3544.
160. Oleschko, H. and M. Müller, *Influence of Coal Composition and Operating Conditions on the Release of Alkali Species During Combustion of Hard Coal.* Energy Fuels, 2007. **21**(6): p. 3240-3248.
161. Díaz-Ramírez, M., C. Boman, F. Sebastián, J. Royo, S. Xiong, and D. Boström, *Ash Characterization and Transformation Behavior of the Fixed-Bed Combustion of Novel Crops: Poplar, Brassica, and Cassava Fuels.* Energy & Fuels, 2012. **26**(6): p. 3218-3229.
162. Wang, S., X.M. Jiang, X.X. Han, and H. Wang, *Fusion Characteristic Study on Seaweed Biomass Ash.* Energy Fuels, 2008. **22**(4): p. 2229-2235.
163. Hu, Y., S. Cheng, P. Sun, J. Xie, and H. Zhang, *Research on fusion behavior of ash from mixedly burning biomass with coal.* Thermal Power Generation, 2011. **40**(10): p. 8-12.
164. Ye, Y., *Research on the Characteristics of Biomass Ash and Agglomeration Mechanism*. 2007, Phd thesis) Huazhong University of science & technology.
165. Raask, E., *Mineral impurities in coal combustion : behavior, problems, and remedial measures*. 1984, Washington: Washington : Hemisphere Pub. Corp., c1984.
166. Teixeira, P., H. Lopes, I. Gulyurtlu, N. Lapa, and P. Abelha, *Evaluation of slagging and fouling tendency during biomass co-firing with coal in a fluidized bed.* Biomass & bioenergy, 2012. **39**: p. 192-203.
167. Nik Norizam, N.N.A., X. Yang, D. Ingham, J. Szuhánszki, W. Yang, J. Rezende, L. Ma, and M. Pourkashanian, *An improved index to predict the slagging propensity of woody biomass on high-temperature regions in utility boilers.* Journal of the Energy Institute, 2023. **109**: p. 101272.
168. Scala, F., *Particle agglomeration during fluidized bed combustion: Mechanisms, early detection and possible countermeasures.* Fuel Processing Technology, 2018. **171**: p. 31-38.
169. Vamvuka, D., D. Zografos, and G. Alevizos, *Control methods for mitigating biomass ash-related problems in fluidized beds.* Bioresource Technology, 2008. **99**(9): p. 3534-3544.
170. Dayton, D., B. Jenkins, S. Turn, R. Bakker, R. Williams, D. Belle-Oudry, and L. Hill, *Release of inorganic constituents from leached biomass during thermal conversion.* Energy & Fuels, 1999. **13**(4): p. 860-870.
171. Fernández Llorente, M.J. and J.E. Carrasco García, *Comparing methods for predicting the sintering of biomass ash in combustion.* Fuel, 2005. **84**(14): p. 1893-1900.
172. Vamvuka, D. and D. Zografos, *Predicting the behaviour of ash from agricultural wastes during combustion.* Fuel, 2004. **83**(14-15): p. 2051-2057.
173. Rizeq, R. and F. Shadman, *Alkali-induced agglomeration of solid particles in coal combustors and gasifiers.* Chemical Engineering Communications, 1989. **81**(1): p. 83-96.
174. Öhman, M. and A. Nordin, *The Role of Kaolin in Prevention of Bed Agglomeration during Fluidized Bed Combustion of Biomass Fuels.* Energy Fuels, 2000. **14**(3): p. 618-624.
175. Steenari, B.-M. and O. Lindqvist, *High-temperature reactions of straw ash and the anti-sintering additives kaolin and dolomite.* Biomass and Bioenergy, 1998. **14**(1): p. 67-76.
176. Aho, M. and J. Silvennoinen, *Preventing chlorine deposition on heat transfer surfaces with aluminium–silicon rich biomass residue and additive.* Fuel (Guildford), 2004. **83**(10): p. 1299-1305.

177. Barišić, V., K. Peltola, and E. Coda Zabetta, *Role of Pulverized Coal Ash against Agglomeration, Fouling, and Corrosion in Circulating Fluidized-Bed Boilers Firing Challenging Biomass.* Energy Fuels, 2013. **27**(10): p. 5706-5713.
178. Shao, Y., J. Wang, F. Preto, J. Zhu, and C. Xu, *Ash deposition in biomass combustion or co-firing for power/heat generation.* Energies, 2012. **5**(12): p. 5171-5189.
179. Nowak Delgado, R., T. de Riese, P. Johne, S. Fendt, and H. Spliethoff, *Impact of Coal Fly Ash Addition on Combustion Aerosols (PM2.5) in Pilot- and Full-Scale Pulverized Wood Combustion: A Comparative Study.* Energy Fuels, 2022. **36**(22): p. 13665-13677.
180. Parshetti, G.K., A. Quek, R. Betha, and R. Balasubramanian, *TGA–FTIR investigation of co-combustion characteristics of blends of hydrothermally carbonized oil palm biomass (EFB) and coal.* Fuel processing technology, 2014. **118**: p. 228-234.
181. Kær, S.K., L.A. Rosendahl, and L. Baxter, *Towards a CFD-based mechanistic deposit formation model for straw-fired boilers.* Fuel, 2006. **85**(5-6): p. 833-848.
182. Shadman, F. and W. Punjak, *Thermochemistry of alkali interactions with refractory adsorbents.* Thermochimica acta, 1988. **131**: p. 141-152.
183. Tran, Q.K., B.-M. Steenari, K. Iisa, and O. Lindqvist, *Capture of potassium and cadmium by kaolin in oxidizing and reducing atmospheres.* Energy & fuels, 2004. **18**(6): p. 1870-1876.
184. Tran, K.-Q., K. Iisa, B.-M. Steenari, and O. Lindqvist, *A kinetic study of gaseous alkali capture by kaolin in the fixed bed reactor equipped with an alkali detector.* Fuel, 2005. **84**(2-3): p. 169-175.
185. Clery, D.S., P.E. Mason, C.M. Rayner, and J.M. Jones, *The effects of an additive on the release of potassium in biomass combustion.* Fuel, 2018. **214**: p. 647-655.
186. Rebbling, A., J. Fagerström, E. Steinvall, M. Carlborg, M. Öhman, and C. Boman, *Reduction of Alkali Release by Two Fuel Additives at Different Bed Temperatures during Grate Combustion of Woody Biomass.* Energy Fuels, 2019. **33**(11): p. 11041-11048.
187. Wang, G., P.A. Jensen, H. Wu, F.J. Frandsen, B. Sander, and P. Glarborg, *Potassium capture by kaolin, part 2: K2CO3, KCl, and K2SO4.* Energy & fuels, 2018. **32**(3): p. 3566-3578.
188. Wang, G., P.A. Jensen, H. Wu, F.J. Frandsen, B. Sander, and P. Glarborg, *Potassium capture by kaolin, part 1: KOH.* Energy & fuels, 2018. **32**(2): p. 1851-1862.
189. Chen, C., G. Lan, and W. Tuan, *Microstructural evolution of mullite during the sintering of kaolin powder compacts.* Ceramics international, 2000. **26**(7): p. 715-720.
190. Wang, G., J.N.F. Poulsen, S.N.F. Poulsen, P.A. Jensen, and F.J. Frandsen, *Influence of kaolin and coal fly ash addition on biomass ash deposition in an entrained flow reactor.* Fuel (Guildford), 2022. **313**: p. 123041.
191. Bøjer, M., P.A. Jensen, F. Frandsen, K. Dam-Johansen, O.H. Madsen, and K. Lundtorp, *Alkali/Chloride release during refuse incineration on a grate: Full-scale experimental findings.* Fuel processing technology, 2008. **89**(5): p. 528-539.
192. James Thomas, S.C.a.I.S., *Measurement of the in-situ performance of solid biomass boilers*. 2018.
193. Sippula, O., H. Lamberg, J. Leskinen, J. Tissari, and J. Jokiniemi, *Emissions and ash behavior in a 500kW pellet boiler operated with various blends of woody biomass and peat.* Fuel, 2017. **202**: p. 144-153.
194. Gehrig, M., M. Wöhler, S. Pelz, J. Steinbrink, and H. Thorwarth, *Kaolin as additive in wood pellet combustion with several mixtures of spruce and short-rotation-coppice willow and its influence on emissions and ashes.* Fuel, 2019. **235**: p. 610-616.

195. Nowak Delgado, R., P. Bieli, T. de Riese, S. Fendt, and H. Spliethoff, *Influence of additive surface area degradation on fine particle formation during biomass pulverised-fuel combustion.* Fuel (Guildford), 2023. **338**: p. 127247.
196. Höfer, I., T. Huelsmann, and M. Kaltschmitt, *Influence of Ca- and Al-additives on the pollutant emissions from blends of wood and straw in small-scale combustion.* Biomass and Bioenergy, 2021. **150**: p. 106135.
197. Moradian, F., A. Pettersson, and T. Richards, *Thermodynamic equilibrium model applied to predict the fouling tendency in a commercial fluidized-bed boiler, combusting solid waste.* Energy & fuels, 2015. **29**(5): p. 3483-3494.
198. Lindberg, D., R. Backman, P. Chartrand, and M. Hupa, *Towards a comprehensive thermodynamic database for ash-forming elements in biomass and waste combustion — Current situation and future developments.* Fuel processing technology, 2013. **105**: p. 129-141.
199. **李寒旭**, **二宮善彦**, **董众兵**, and 张明旭, *Application of the FactSage to Predict the Ash Melting Behavior in Reducing Conditions.* Chinese Journal of Chemical Engineering, 2006. **14**(6): p. 784-789.
200. Jak, E., *Prediction of coal ash fusion temperatures with the F ∗A ∗C ∗T thermodynamic computer package.* Fuel (Guildford), 2002. **81**(13): p. 1655-1668.
201. Abdi, H., *Partial least squares regression and projection on latent structure regression (PLS Regression).* WIREs Comp Stat, 2010. **2**(1): p. 97-106.
202. Seggiani, M. and G. Pannocchia, *Prediction of Coal Ash Thermal Properties Using Partial Least-Squares Regression.* Ind. Eng. Chem. Res, 2003. **42**(20): p. 4919-4926.
203. UnscramblerX, *Introduction to Partial Least Squares Regression (PLSR)*. 2021.
204. Zhang, M., H. Mu, G. Li, and Y. Ning, *Forecasting the transport energy demand based on PLSR method in China.* Energy (Oxford), 2009. **34**(9): p. 1396-1400.
205. Yang, X., D. Ingham, L. Ma, N. Srinivasan, and M. Pourkashanian, *Ash deposition propensity of coals/blends combustion in boilers: a modeling analysis based on multi-slagging routes.* Proceedings of the Combustion Institute, 2017. **36**(3): p. 3341-3350.
206. Wold, S., M. Sjöström, and L. Eriksson, *PLS-regression: a basic tool of chemometrics.* Chemometrics and intelligent laboratory systems, 2001. **58**(2): p. 109-130.
207. Wen, X.Q., *Study on the Methods of Predicting the Fouling Characteristics of Plate Heat Exchanger Based on Water Quality Parameters.* Applied mechanics and materials, 2013. **459**: p. 153-158.
208. Lorber, A., L.E. Wangen, and B.R. Kowalski, *A theoretical foundation for the PLS algorithm.* Journal of Chemometrics, 1987. **1**(1): p. 19-31.
209. Lindström, E., S.H. Larsson, D. Boström, and M. Öhman, *Slagging Characteristics during Combustion of Woody Biomass Pellets Made from a Range of Different Forestry Assortments.* Energy Fuels, 2010. **24**(6): p. 3456-3461.
210. Gilbe, C., E. Lindström, R. Backman, R. Samuelsson, J. Burvall, and M. Öhman, *Predicting Slagging Tendencies for Biomass Pellets Fired in Residential Appliances: A Comparison of Different Prediction Methods.* Energy Fuels, 2008. **22**(6): p. 3680-3686.
211. Öhman, M., C. Boman, H. Hedman, A. Nordin, and D. Boström, *Slagging tendencies of wood pellet ash during combustion in residential pellet burners.* Biomass & bioenergy, 2004. **27**(6): p. 585-596.
212. Näzelius, I.-L., D. Boström, C. Boman, H. Hedman, R. Samuelsson, and M. Öhman, *Influence of Peat Addition to Woody Biomass Pellets on Slagging Characteristics during Combustion.* Energy Fuels, 2013. **27**(7): p. 3997-4006.
213. Regueiro, A., L. Jezerská, R. Pérez-Orozco, D. Patiño, J. Zegzulka, and J. Nečas, *Viability Evaluation of Three Grass Biofuels: Experimental Study in a Small-Scale Combustor.* Energies (Basel), 2019. **12**(7): p. 1352.

214. Näzelius, I.-L., D. Boström, A. Rebbling, C. Boman, and M. Öhman, *Fuel Indices for Estimation of Slagging of Phosphorus-Poor Biomass in Fixed Bed Combustion.* Energy Fuels, 2017. **31**(1): p. 904-915.
215. Lin, W., K. Dam-Johansen, and F. Frandsen, *Agglomeration in bio-fuel fired fluidized bed combustors.* Chemical Engineering Journal, 2003. **96**(1-3): p. 171-185.
216. Yu, C., Z. Tang, L. Zeng, C. Chen, and B. Gong, *Experimental determination of agglomeration tendency in fluidized bed combustion of biomass by measuring slip resistance.* Fuel, 2014. **128**: p. 14-20.
217. Llorente, M.F., R.E. Cuadrado, J.M. Laplaza, and J.C. García, *Combustion in bubbling fluidised bed with bed material of limestone to reduce the biomass ash agglomeration and sintering.* Fuel, 2006. **85**(14-15): p. 2081-2092.
218. Liu, R., B. Jin, Z. Zhong, and J. Zhao, *Reduction of bed agglomeration in CFB combustion biomass with aluminium-contain bed material.* Process Safety and Environmental Protection, 2007. **85**(5): p. 441-445.
219. Grimm, A., N. Skoglund, D. Boström, and M. Ohman, *Bed agglomeration characteristics in fluidized quartz bed combustion of phosphorus-rich biomass fuels.* Energy & Fuels, 2011. **25**(3): p. 937-947.
220. Piotrowska, P., A. Grimm, N. Skoglund, C. Boman, M. Öhman, M. Zevenhoven, D. Boström, and M. Hupa, *Fluidized-bed combustion of mixtures of rapeseed cake and bark: the resulting bed agglomeration characteristics.* Energy & fuels, 2012. **26**(4): p. 2028-2037.
221. Moradian, F., P.A. Tchoffor, K.O. Davidsson, A. Pettersson, and R. Backman, *Thermodynamic equilibrium prediction of bed agglomeration tendency in dual fluidized-bed gasification of forest residues.* Fuel processing technology, 2016. **154**: p. 82-90.
222. GesmbH, H. *Magno VR 250-550 kW, Forward grate firing technology driven by hydraulic drive*. 2022 [cited 2024 01 May]; Available from: https://www.hargassner.com/at-en/boilers/industrial-boiler/magno-vr-250-550-kw/.
223. Schnabel, K., F. Brück, S. Pohl, and H. Weigand, *Development and Test of a Rotating Drum Reactor for the Simultaneous Hydration and Carbonation of Dry Biomass Bottom Ash.* Waste and Biomass Valorization, 2022. **13**(10): p. 4319-4330.
224. Dalkhsuren, D., K. Iwabuchi, T. Itoh, T. Narita, M.I. Piash, B. Nachin, and G. Sukhbaatar, *Effects of ash composition and combustion temperature on reduced particulate matter emission by biomass carbonization.* BioEnergy Research, 2023. **16**(3): p. 1629-1638.
225. Chen, Y., G. Tian, M. Zhou, Z. Huang, C. Lu, P. Hu, J. Gao, Z. Zhang, and X. Tang, *Catalytic control of typical particulate matters and volatile organic compounds emissions from simulated biomass burning.* Environmental Science & Technology, 2016. **50**(11): p. 5825-5831.
226. Shen, G., S. Tao, Y. Chen, Y. Zhang, S. Wei, M. Xue, B. Wang, R. Wang, Y. Lu, and W. Li, *Emission characteristics for polycyclic aromatic hydrocarbons from solid fuels burned in domestic stoves in rural China.* Environmental science & technology, 2013. **47**(24): p. 14485-14494.
227. Ammann, A.A., *Inductively Coupled Plasma Mass Spectrometry (ICP MS): A Versatile Tool.* Biological Mass Spectrometry, 2007.
228. Sommersacher, P., N. Kienzl, T. Brunner, and I. Obernberger, *Simultaneous Online Determination of S, Cl, K, Na, Zn, and Pb Release From a Single Particle During Biomass Combustion. Part 2: Results From Test Runs With Spruce and Straw Pellets.* Energy & Fuels, 2016.

229. Wilczyńska-Michalik, W., R. Gasek, M. Michalík, J. Dańko, and T. Plaskota, *Mineralogy, Chemical Composition and Leachability of Ash From Biomass Combustion and Biomass–coal Co-Combustion.* Mineralogia, 2018.
230. Ali, A., Y.W. Chiang, and R.M. Santos, *X-ray diffraction techniques for mineral characterization: A review for engineers of the fundamentals, applications, and research directions.* Minerals, 2022. **12**(2): p. 205.
231. Khan, H., A.S. Yerramilli, A. D'Oliveira, T.L. Alford, D.C. Boffito, and G.S. Patience, *Experimental methods in chemical engineering: X-ray diffraction spectroscopy—XRD.* The Canadian journal of chemical engineering, 2020. **98**(6): p. 1255-1266.
232. Zhou, W., R. Apkarian, Z.L. Wang, and D. Joy, *Fundamentals of scanning electron microscopy (SEM).* Scanning microscopy for nanotechnology: techniques and applications, 2007: p. 1-40.
233. Akhtar, K., S.A. Khan, S.B. Khan, and A.M. Asiri, *Scanning electron microscopy: Principle and applications in nanomaterials characterization*. 2018: Springer.
234. Leslie, S.A. and J.C. Mitchell, *Removing gold coating from SEM samples.* palaeontology, 2007. **50**(6): p. 1459-1461.
235. Kijo-Kleczkowska, A., M. Szumera, A. Gnatowski, and D. Sadkowski, *Comparative thermal analysis of coal fuels, biomass, fly ash and polyamide.* Energy, 2022. **258**: p. 124840.
236. Jak, E., *Prediction of coal ash fusion temperatures with the F∗A∗C∗T thermodynamic computer package.* Fuel, 2002. **81**(13): p. 1655-1668.
237. Isaak, P., H. Tran, D. Barham, and D. Reeve, *Stickiness of fireside deposits in kraft recovery units.* Journal of pulp and paper science, 1986. **12**(3): p. 84-88.
238. Zhou, H., P.A. Jensen, and F.J. Frandsen, *Dynamic mechanistic model of superheater deposit growth and shedding in a biomass fired grate boiler.* Fuel, 2007. **86**(10): p. 1519-1533.
239. Mueller, C., M. Selenius, M. Theis, B.-J. Skrifvars, R. Backman, M. Hupa, and H. Tran, *Deposition behaviour of molten alkali-rich fly ashes—development of a submodel for CFD applications.* Proceedings of the Combustion Institute, 2005. **30**(2): p. 2991-2998.
240. Beckmann, A.M., M. Mancini, R. Weber, S. Seebold, and M. Müller, *Measurements and CFD modeling of a pulverized coal flame with emphasis on ash deposition.* Fuel, 2016. **167**: p. 168-179.
241. Schermelleh-Engel, K., H. Moosbrugger, and H. Müller, *Evaluating the Fit of Structural Equation Models: Tests of Significance and Descriptive Goodness-of-Fit Measures.* Methods of Psychological Research Online, 2003. **8**: p. 23–74.
242. Weber, R., Y. Poyraz, M. Mancini, and A. Schwabauer, *Biomass fly-ash deposition: Dependence of deposition rate on probe/particle temperature in 115–1200 °C range.* Fuel (Guildford), 2021. **290**: p. 120033.
243. Weber, R., Y. Poyraz, A.M. Beckmann, and S. Brinker, *Combustion of biomass in jet flames.* Proceedings of the Combustion Institute, 2015. **35**(3): p. 2749-2758.
244. Kirnbauer, F. and H. Hofbauer, *Investigations on bed material changes in a dual fluidized bed steam gasification plant in Güssing, Austria.* Energy & fuels, 2011. **25**(8): p. 3793-3798.
245. Hupa, M., *Ash-related issues in fluidized-bed combustion of biomasses: recent research highlights.* Energy & Fuels, 2012. **26**(1): p. 4-14.
246. Schermelleh-Engel, K., H. Moosbrugger, and H. Müller, *Evaluating the fit of structural equation models: Tests of significance and descriptive goodness-of-fit measures.* Methods of psychological research online, 2003. **8**(2): p. 23-74.

247. Visser, H.J.M., J. Kiel, and H. Veringa, *The influence of fuel composition on agglomeration behaviour in fluidised-bed combustion*. 2004: Energy research Centre of the Netherlands ECN Delft.
248. Zabetta, E.C., V. Barišić, K. Peltola, and A. Hotta. *Foster Wheeler Experience with biomass and waste in CFBs*. in *Proceedings of the 33rd international technical conference on coal utilization and fuel systems*. 2008.
249. Barišić, V., L.-E. Åmand, and E. Coda Zabetta, *The role of limestone in preventing agglomeration and slagging during CFB combustion of high phosphorus fuels.* World Bioenergy, Jönköping (Sweden), 2008.
250. Piotrowska, P., M. Zevenhoven, K. Davidsson, M. Hupa, L.-E. Åmand, V. Barišić, and E. Coda Zabetta, *Fate of alkali metals and phosphorus of rapeseed cake in circulating fluidized bed boiler part 1: cocombustion with wood.* Energy & fuels, 2010. **24**(1): p. 333-345.
251. Liu, H., Y. Feng, S. Wu, and D. Liu, *The role of ash particles in the bed agglomeration during the fluidized bed combustion of rice straw.* Bioresource Technology, 2009. **100**(24): p. 6505-6513.
252. Bain, R.L., R.P. Overend, and K.R. Craig, *Biomass-fired power generation.* Fuel processing technology, 1998. **54**(1-3): p. 1-16.
253. Wang, Q., K.-H. Han, H. Li, J.-H. Qi, and C.-M. Lu, *Influence of ammonium dihydrogen phosphates additive on potassium fixation capacity and ash fusibility for rice straw combustion in an O2/CO2 atmosphere.* Journal of fuel chemistry and technology, 2015. **43**(8): p. 955-960.
254. Deng, Y., G.N. White, and J.B. Dixon, *Effect of Structural Stress on the Intercalation Rate of Kaolinite.* Journal of Colloid and Interface Science, 2002. **250**(2): p. 379-393.
255. Sperinck, S., P. Raiteri, N. Marks, and K. Wright, *Dehydroxylation of kaolinite to metakaolin—a molecular dynamics study.* Journal of Materials Chemistry, 2011. **21**(7): p. 2118-2125.
256. Chen, Y.-H. and D.-L. Lu, *CO2 capture by kaolinite and its adsorption mechanism.* Applied Clay Science, 2015. **104**: p. 221-228.
257. Blomberg, T., *A thermodynamic study of the gaseous potassium chemistry in the convection sections of biomass fired boilers.* Materials and Corrosion, 2011. **62**(7): p. 635-641.
258. Niu, Y., H. Tan, and S.e. Hui, *Ash-related issues during biomass combustion: Alkali-induced slagging, silicate melt-induced slagging (ash fusion), agglomeration, corrosion, ash utilization, and related countermeasures.* Progress in Energy and Combustion Science, 2016. **52**: p. 1-61.
259. Nguyen, H.K., J.H. Moon, S.H. Jo, S.J. Park, D.H. Bae, M.W. Seo, H.W. Ra, S.-J. Yoon, S.-M. Yoon, and J.G. Lee, *Ash characteristics of oxy-biomass combustion in a circulating fluidized bed with kaolin addition.* Energy, 2021. **230**: p. 120871.
260. Boström, D., A. Grimm, C. Boman, E. Björnbom, and M. Öhman, *Influence of Kaolin and Calcite Additives on Ash Transformations in Small-Scale Combustion of Oat.* Energy & Fuels, 2009.
261. Valmari, T., E.I. Kauppinen, J. Kurkela, J.K. Jokiniemi, G. Sfiris, and H. Revitzer, *Fly ash formation and deposition during fluidized bed combustion of willow.* Journal of aerosol science, 1998. **29**(4): p. 445-459.
262. Laxminarayan, Y., P.A. Jensen, H. Wu, F.J. Frandsen, B. Sander, and P. Glarborg, *Biomass fly ash deposition in an entrained flow reactor.* Proceedings of the Combustion Institute, 2019. **37**(3): p. 2689-2696.

263. Warey, A., S. Balestrino, P. Szymkowicz, and M.R. Malayeri, *A One-Dimensional Model for Particulate Deposition and Hydrocarbon Condensation in Exhaust Gas Recirculation Coolers.* Aerosol Science and Technology, 2012.
264. Xiong, S., J. Burvall, H. Örberg, G. Kalen, M. Thyrel, M. Öhman, and D. Boström, *Slagging Characteristics during Combustion of Corn Stovers with and without Kaolin and Calcite.* Energy Fuels, 2008. **22**(5): p. 3465-3470.
265. Tissari, J., O. Sippula, J. Kouki, K. Vuorio, and J. Jokiniemi, *Fine Particle and Gas Emissions from the Combustion of Agricultural Fuels Fired in a 20 kW Burner.* Energy Fuels, 2008. **22**(3): p. 2033-2042.
266. Capablo, J., P.A. Jensen, K.H. Pedersen, K. Hjuler, L. Nikolaisen, R. Backman, and F. Frandsen, *Ash Properties of Alternative Biomass.* Energy & Fuels, 2009.
267. Wang, L., M. Becidan, and Ø. Skreiberg, *Sintering Behavior of Agricultural Residues Ashes and Effects of Additives.* Energy & Fuels, 2012.
268. Vega-Nieva, D., R. Dopazo, and L. Ortiz, *Strategies for minimizing ash slagging in combustion of mediterranean biomasses.* World Bioenergy, 2012. **2012**: p. 29-31.
269. Deng, L., J. Ye, X. Jin, and D. Che, *Transformation and release of potassium during fixed-bed pyrolysis of biomass.* Journal of the Energy Institute, 2018. **91**(4): p. 630-637.
270. Zhang, H., J. Li, X. Yang, S. Guo, H. Zhan, Y. Zhang, and Y. Fang, *Influence of coal ash on potassium retention and ash melting characteristics during gasification of corn stalk coke.* Bioresource technology, 2018. **270**: p. 416-421.
271. Wu, P., J. Li, X. Zhuang, X. Querol, N. Moreno, B. Li, D. Ge, Z. Shuang, X. Ma, P. Córdoba, and Y. Shangguan, *Mineralogical and Environmental Geochemistry of Coal Combustion Products From Shenhuo and Yihua Power Plants in Xinjiang Autonomous Region, Northwest China.* Minerals, 2019.
272. Konsomboon, S., S. Pipatmanomai, T. Madhiyanon, and S. Tia, *Effect of kaolin addition on ash characteristics of palm empty fruit bunch (EFB) upon combustion.* Applied Energy, 2011. **88**(1): p. 298-305.
273. Myat-Htun, M., H. Mohammadi, A.-F.M. Noor, M. Kawashita, and Y.M.B. Ismail, *COMPREHENSIVE INVESTIGATION OF PHASE FORMATION MECHANISM AND PHYSICO-MECHANICAL PROPERTIES OF Ca-Mg-Silicate.* Asean Engineering Journal, 2021.
274. Horiguchi, G., R. Fujii, Y. Beppu, H. Kamiya, and Y. Okada, *Understanding the Mechanism of Particle Adhesion in High-Temperature Combustion Induced by Sodium and Potassium: Use of a Synthetic Ash Strategy.* Industrial & Engineering Chemistry Research, 2020.
275. Arias-Duque, N., O. Giraldo, and A. Rosales-Rivera, *Synthesis and characterization of magnesium-doped layered manganese oxides.* Revista Mexicana de Física, 2012. **58**(2): p. 151-154.
276. dos Santos, R.P., J. Martins, C. Gadelha, B. Cavada, A.V. Albertini, F. Arruda, M. Vasconcelos, E. Teixeira, F. Alves, and J. Lima Filho, *Coal fly ash ceramics: preparation, characterization, and use in the hydrolysis of sucrose.* The Scientific World Journal, 2014. **2014**.
277. Munawar, M.A., A.H. Khoja, M. Hassan, R. Liaquat, S.R. Naqvi, M.T. Mehran, A. Abdullah, and F. Saleem, *Biomass ash characterization, fusion analysis and its application in catalytic decomposition of methane.* Fuel, 2021. **285**: p. 119107.
278. Cheng, W., Y. Zhu, J.a. Shao, W. Zhang, G. Wu, H. Jiang, J. Hu, Z. Huang, H. Yang, and H. Chen, *Mitigation of ultrafine particulate matter emission from agricultural biomass pellet combustion by the additive of phosphoric acid modified kaolin.* Renewable Energy, 2021. **172**: p. 177-187.

279. Yang, W., Y. Zhu, W. Cheng, H. Sang, H. Yang, and H. Chen, *Characteristics of Particulate Matter Emitted from Agricultural Biomass Combustion.* Energy & Fuels, 2017. **31**(7): p. 7493-7501.
280. Ninomiya, Y., Q. Wang, S. Xu, K. Mizuno, and I. Awaya, *Effect of additives on the reduction of PM2. 5 emissions during pulverized coal combustion.* Energy & Fuels, 2009. **23**(7): p. 3412-3417.
281. Wei, B., X. Wang, H. Tan, L. Zhang, Y. Wang, and Z. Wang, *Effect of silicon–aluminum additives on ash fusion and ash mineral conversion of Xinjiang high-sodium coal.* Fuel, 2016. **181**: p. 1224-1229.
282. Gale, T.K. and J.O. Wendt, *In-furnace capture of cadmium and other semi-volatile metals by sorbents.* Proceedings of the Combustion Institute, 2005. **30**(2): p. 2999-3007.
283. Chen, D., X. Liu, C. Wang, Y. Xu, W. Sun, J. Cui, Y. Zhang, and M. Xu, *Effects of H2O and HCl on particulate matter reduction by kaolin under oxy-coal combustion.* Energy & Fuels, 2017. **31**(6): p. 6455-6462.
284. Fernandes, U. and M. Costa, *Particle emissions from a domestic pellets-fired boiler.* Fuel Processing Technology, 2012. **103**: p. 51-56.
285. Yang, W., Y. Zhu, W. Cheng, H. Sang, H. Xu, H. Yang, and H. Chen, *Effect of minerals and binders on particulate matter emission from biomass pellets combustion.* Applied Energy, 2018. **215**: p. 106-115.
286. Gustafsson, E., M. Strand, and M. Sanati, *Physical and chemical characterization of aerosol particles formed during the thermochemical conversion of wood pellets using a bubbling fluidized bed gasifier.* Energy & Fuels, 2007. **21**(6): p. 3660-3667.
287. Hindsgaul, C., J. Schramm, L. Gratz, U. Henriksen, and J.D. Bentzen, *Physical and chemical characterization of particles in producer gas from wood chips.* Bioresource Technology, 2000. **73**(2): p. 147-155.

8 Appendix

Calibration was performed daily. A 5-point calibration curve was used for each element of interest (see Table 8-1 for concentrations). Commercially available certified reference standards (Sigma-Aldrich/Supelco TraceCERT Standard for ICP; FisherScientific Spex Certiprep standards; VWR/BDH inorganic reference standard) were used to make the calibration standards which were made up in 10.9% nitric acid (Primar Plus - Trace Analysis Grade, FisherScientific). An internal standard of Y and Sc (1ppm) was used. A validation standard containing 0.05-1ppm of the elements of interest was run during analysis to check the recovery.

Table 8-1 Standard concentrations in ppm.

	Level 1	Level 2	Level 3	Level 4	Level 5	Level 6	Level 7	Level 8	Level 9	Level 10	Level 11	Level 12	Level 13	Level 14	Level 15	Level 16
Al	0	0.3125	0.625	1.25	2.5	5										
Mg	0	0.03125	0.0625	0.125	0.25	0.5										
Ni	0	0.0625	0.125	0.25	0.5	1										
K	0	0.0625	0.125	0.25	0.5	1										
P	0	0.03125	0.0625	0.125	0.25	0.5										
Ca	0						0.03125	0.0625	0.125	0.25	0.5					
Si	0						0.625	1.25	2.5	5	10					
Na	0						0.03125	0.0625	0.125	0.25	0.5					
S	0						0.3125	0.625	1.25	2.5	5					
Fe	0											0.0625	0.125	0.25	0.5	1
Mn	0											0.03125	0.0625	0.125	0.25	0.5
Ti	0											0.03125	0.0625	0.125	0.25	0.5